

University of Nevada, Reno

**Functional Role Of Non-selective Cation Channels On Colonic Excitability
In Physiological And Pathological Conditions**

A dissertation submitted in partial fulfillment of the requirements for the degree of
Doctor of Philosophy in Cellular and Molecular Pharmacology and Physiology

By Laura Dwyer

Dr. Sang Don Koh/Dissertation Advisor

December, 2009



University of Nevada, Reno
Statewide • Worldwide

THE GRADUATE SCHOOL

We recommend that the dissertation
prepared under our supervision by

LAURA DWYER

entitled

**Functional Role Of Non-Selective Cation Channels On Colonic Excitability In
Physiological And Pathological Conditions**

be accepted in partial fulfillment of the
requirements for the degree of

DOCTOR OF PHILOSOPHY

Sang Don Koh, M.D., Ph.D., Advisor

Fiona Britton, Ph.D., Committee Member

Kenton Sanders, Ph.D., Committee Member

Sean Ward, Ph.D., Committee Member

Hanna Damke, Ph.D., Graduate School Representative

Marsha H. Read, Ph. D., Associate Dean, Graduate School

December, 2009

Abstract

Aims:

Integrity of smooth muscle mechanisms is essential for maintaining colonic excitability. This excitability is regulated in part, by the activity of specific ion channels that can affect the resting membrane potential. The experiments performed in this thesis investigated multiple aspects of colonic excitability in various species (human, monkey and mouse) including activity of specific ion channels, their molecular candidates and the regulation of these ion channels in physiological and pathological conditions. Since the resting membrane potential is generally more positive than E_k in gastrointestinal smooth muscle, firstly we hypothesized that non-selective cation channels are involved in setting the resting membrane potential. Secondly we examined intracellular signaling mechanisms of non-selective cation channels that contribute to membrane excitability. Since smooth muscle excitability can be changed in pathological conditions, we also examined the effects of histamine to mimic the acute effects of inflammation in two different species (monkey and mouse). Finally we investigated the functional role of non-selective cation channels in an animal model of colitis.

Results:

Patch clamp techniques, conventional microelectrode recordings, isometric force measurements and molecular studies were employed to examine colonic excitability. Firstly, we found that basally activated non-selective cation channels contribute to the resting membrane potential in human and monkey

colonic smooth muscle cells. Basal influx of Na^+ and Ca^{2+} ions through these channels were responsible for generating relatively positive membrane potentials thus increasing the excitability of colonic smooth muscle cells. Among Transient Receptor Potential subfamily members, molecular candidates for basally activated non-selective cation channels were different in human and monkey colonic smooth muscle cells.

Initial plans to examine phospholipase C (PLC)-dependent regulation of basally activated non-selective cation channels were changed on discovery of unexpected effects of a PLC-activator on colonic contractility. To understand the decreased contractility by this drug, we tested the effects of this PLC-activator on various ionic conductances. Both the PLC activator and its inactive analog decreased colonic contractile amplitude, suppressed delayed rectifier K^+ and L-type Ca^{2+} currents and also transiently increased intracellular Ca^{2+} . These multiple PLC-independent effects suggest that extreme caution must be employed when using these drugs to decipher PLC-related pathways.

Since several reports have suggested a possible link between Rho-kinase and ion channel activity, we investigated the involvement of Rho-kinase in colonic excitability at both the tissue and cellular level. Nerve-evoked and CCh-induced contractions were significantly decreased independent of neuronal influences suggesting that the Rho-kinase inhibitor acts directly on smooth muscle. In addition, CCh-induced depolarization was significantly reduced by Rho-kinase inhibitors suggesting that Rho-kinase may be involved in regulating agonist stimulated non-selective cation channels. Patch-clamp experiments

revealed that Rho-kinase inhibition did not affect basally activated non-selective cation currents but GTP γ S-activated currents were inhibited by a Rho-kinase inhibitor. Thus Rho-kinase may play a role in regulation of receptor-activated non-selective cation channels in colonic smooth muscle.

In order to examine the functional role of non-selective cation channels in pathological conditions, we examined the effects of the inflammatory mediator, histamine, on colonic excitability in monkey and murine colonic smooth muscle tissue and cells. In monkey colonic tissue, histamine induced significant depolarization and contraction. A similar effect was observed with application of either H1 or H4 receptor agonists. A 5pS non-selective cation channel was activated by histamine in monkey colonic smooth muscle cells. In contrast, in murine colonic tissue, histamine caused hyperpolarization and decreased contractility. This hyperpolarization was prevented by pretreatment with the ATP-sensitive K⁺ channel blocker, glibenclamide, suggesting activation of these channels through the H2/G_s/cAMP/PKA pathway. Patch clamp experiments also revealed that glibenclamide inhibited an ATP-sensitive K⁺ current activated by histamine. These different contractile responses were proposed to be due to differential expression of specific histamine receptors in the colons from these two species.

Finally, inflammation induced by treatment with dextran sulphate sodium in mice caused a significant shift in the resting membrane potential of inflamed colonic smooth muscle to more negative values. Furthermore, carbachol-induced depolarization and contractile amplitude were significantly attenuated in the

inflamed smooth muscle suggesting that there may be changes in expression of specific Transient Receptor Potential channels in smooth muscle cells during inflammation.

Conclusions:

The studies in this dissertation addressed for the first time 1) the contribution of non-selective cation channels to the resting membrane potential, 2) potential molecular candidates for non-selective cation channels and 3) contribution of non-selective cation channels to colonic excitability in physiological and inflammatory conditions.

Dedication

I dedicate this dissertation to my fantastic parents. They have supported me with everything I have ever done in my life. They motivated me as a child to always work hard and do the best I can at anything I set my mind to. No words can describe how much I appreciate everything you have done for me. Thank you both for your never ending love and support.

Acknowledgements

Firstly I would like to thank my supervisor and good friend Professor Sang Don Koh for all of his help and support over the years. He has been an exceptional supervisor who has helped me from the very beginning when I started my Ph.D. He has made research interesting and challenging for me over the years and has always been there to discuss any ideas or problems. His enthusiasm and love for science and many discussions in the pub have made my Ph.D. a very enjoyable experience. In addition I am extremely grateful to him for giving me opportunities to attend not only international meetings but also carry out research in other countries such as Japan and Korea. I am deeply indebted to him for everything he has done for me and feel lucky to have had such a great boss.

I would also like thank Professor Sean Ward for not only all of his help and support over the years but also for starting the exchange program for the Irish students in the first place. Without you, I (and a lot of other fellow Irish folk) would not be here.

I would like to acknowledge my other committee members, Professor Kenton Sanders, Dr Fiona Britton and Dr Hanna Damke for all of their help and advice. They have always been very supportive and I appreciate them all giving up their valuable time to help me through my Ph.D. I would also like to thank a true angel, Nancy Horowitz for all of her help with the dreaded LI90 cells, sorting out my mice, making solutions etc. In addition I offer my sincere thanks to the many other people who have helped or contributed to my Ph.D. including Hyun-

Jin Kim, Lauren Peri, Seungil Ro, Orline and Yulia Bayguinov, Byoung Koh, my chicken curry (Yukari)....the list is endless. Thanks everyone.

Table of contents

Chapter 1: Introduction

1.1 Smooth muscle excitability in the gastrointestinal tract.....	1
1.2. Effects of inflammation on colonic excitation and contraction.....	4
1.2.1. <i>Pathophysiology of IBD.....</i>	<i>4</i>
1.2.2. <i>Animal models of IBD.....</i>	<i>10</i>
1.2.3. <i>Disturbances in excitation and contraction.....</i>	<i>16</i>
1.3. Effects of the inflammatory mediator histamine on colonic function...29	
1.3.1. <i>Sources and actions of histamine.....</i>	<i>29</i>
1.3.2. <i>H1 receptor.....</i>	<i>30</i>
1.3.3. <i>H2 receptor.....</i>	<i>32</i>
1.3.4. <i>H3 receptor.....</i>	<i>33</i>
1.3.5. <i>H4 receptor.....</i>	<i>33</i>
1.3.6. <i>H receptor distribution in the GI tract.....</i>	<i>34</i>
1.3.7. <i>Histamine involvement in IBD.....</i>	<i>36</i>
1.3.8. <i>Histamine and GI contractility.....</i>	<i>37</i>
1.4. Role of NSCC in smooth muscle depolarization and contraction and their molecular candidates.....	39
1.4.1. <i>Muscarinic receptor-activated NSCC in the GI tract.....</i>	<i>39</i>
1.4.2. <i>Molecular candidates for NSCC.....</i>	<i>41</i>
1.4.3. <i>Molecular candidates for smooth muscle NSCC.....</i>	<i>59</i>
1.5. Contribution of ion channels to smooth muscle excitability.....	62
1.5.1. <i>Contribution of K⁺ channels to RMP.....</i>	<i>62</i>

1.5.2. Contribution of Ca^{2+} -activated Cl currents and NSCC to RMP.....	66
1.6. PLC-dependent regulation of ion channels.....	69
1.6.1. PLC-pathway and associated downstream mediators.....	69
1.6.2. PLC regulation of cellular activities.....	70
1.7. Rho-kinase and colonic excitability.....	74
1.7.1. Ca^{2+} sensitization mechanism and Rho-kinase.....	74
1.7.2. Involvement of Ca^{2+} sensitization in basal tone and agonist-induced contractions.....	76
1.7.3. Rho-kinase pathway and ion channel regulation.....	77
<u>Chapter 2: Basal activation of non-selective cation currents regulate the resting membrane potential in human and monkey colonic smooth muscle cells</u>.....	79
2.1. Summary.....	79
2.2. Background and Aims.....	81
2.3. Materials and methods.....	83
2.3.1. Human tissue.....	83
2.3.2. Animal tissues.....	83
2.3.3. Preparation of isolated colonic SMC.....	84
2.3.4. Voltage-clamp and current-clamp methods.....	84
2.3.5. Solutions and reagents.....	85
2.3.6. RNA isolation, reverse transcription PCR (RT-PCR) and quantitative PCR (qPCR).....	86
2.3.7. Statistical analysis.....	88

2.4. Results	89
2.4.1. <i>Basally activated NSCC recorded in human and monkey colonic SMC</i>	89
2.4.2. <i>Na⁺ contributed to bl_{NSCC} and membrane potential</i>	90
2.4.3. <i>NSCC blockers inhibited bl_{NSCC}</i>	91
2.4.4. <i>Ca²⁺ contributed to bl_{NSCC}</i>	91
2.4.5. <i>Single channel conductances recorded in monkey colonic SMC</i>	92
2.4.6. <i>TRP channels expressed in human and monkey colonic SMC</i>	92
2.5. Figures and figure legends	94
2.6. Discussion	107
<u>Chapter 3:</u> <u>Phospholipase C-independent effects of the phospholipase C agonist, m-3M3FBS, in murine colon</u>	111
3.1. Summary	111
3.2. Background and Aims	113
3.3. Materials and methods	116
3.3.1. <i>Animals</i>	116
3.3.2. <i>Mechanical responses</i>	116
3.3.3. <i>Intracellular microelectrode recordings</i>	117
3.3.4. <i>Preparation of isolated colonic SMC</i>	118
3.3.5. <i>Voltage-clamp methods</i>	119
3.3.6. <i>Solutions</i>	119
3.3.7. <i>Calcium imaging analysis</i>	120

3.3.8. Statistical analysis.....	121
3.3.9. Chemicals.....	121
3.4. Results.....	123
3.4.1. <i>m</i> -3M3FBS inhibited contractility of murine colonic smooth muscle.....	123
3.4.2. <i>m</i> -3M3FBS inhibited delayed rectifier K^+ currents in a PLC-independent manner.....	124
3.4.3. <i>m</i> -3M3FBS and <i>o</i> -3M3FBS inhibited inward currents.....	127
3.4.4. The effect of <i>m</i> -3M3FBS on I_L was PLC-independent	129
3.4.5. <i>m</i> -3M3FBS and <i>o</i> -3M3FBS stimulated $[Ca^{2+}]_i$	129
3.5. Figures and figure legends.....	131
3.6. Discussion.....	147
<u>Chapter 4: Contribution of Rho-kinase to colonic excitability in murine colonic smooth muscle</u>	153
4.1. Summary.....	153
4.2. Background and Aims.....	155
4.3. Materials and methods.....	157
4.3.1. <i>Animals</i>	157
4.3.2. <i>Mechanical responses and nerve stimulation</i>	157
4.3.3. <i>Intracellular microelectrode recordings</i>	158
4.3.4. <i>Preparation of isolated colonic SMC</i>	159
4.3.5. <i>Voltage-clamp methods</i>	160
4.3.6. <i>Solutions</i>	160

4.3.7. Chemicals.....	161
4.3.8. Statistical analysis.....	161
4.4. Results.....	162
4.4.1. Y-27632 reduced nerve-stimulated and CCh-induced contractions in colonic smooth muscle.....	162
4.4.2. H-1152 reduced nerve-stimulated and CCh-induced contractions in colonic smooth muscle.....	164
4.4.3. Y27632 did not significantly effect KCl-induced contractions and L-type Ca ²⁺ currents.....	165
4.4.4. Y27632 reduced GTPγS evoked currents.....	166
4.5. Figures and figure legends.....	168
4.6. Discussion.....	184
<u>Chapter 5.....</u>	188
<u>5.1. Identification of histamine receptors and effects of histamine on murine and monkey colonic excitability.....</u>	189
5.1.1. Summary.....	189
5.1.2. Background and Aims.....	191
5.1.3. Materials and methods.....	194
5.1.3.1. Animals.....	194
5.1.3.2. Inducing dextran sulphate sodium (DSS)-colitis in C57BL/6 mice.....	194
5.1.3.3. Immunohistochemical studies of mast cell infiltration.....	195
5.1.3.4. Molecular Studies.....	196
5.1.3.5. Isometric Force Measurements.....	197
5.1.3.6. Intracellular Microelectrode Recordings.....	198

5.1.3.7. Isolation of SMC.....	198
5.1.3.8. Patch Clamp Experiments.....	199
5.1.3.9. Solutions and Drugs.....	200
5.1.3.10. Statistical Analysis.....	201
5.1.4. Results.....	202
5.1.4.1. Mast cells were located in monkey and inflamed murine colonic smooth muscle	202
5.1.4.2. Transcriptional expression of histamine receptors was different in murine and monkey colonic tissue.....	203
5.1.4.3. Histamine had opposite effects on spontaneous contractility in monkey and murine colonic smooth muscle.....	203
5.1.4.4. Effects of histamine on monkey and murine colonic contractility were TTX-insensitive.....	204
5.1.4.5. Histamine had opposite effects on membrane potential in monkey and murine colonic smooth muscle.....	204
5.1.4.6. Histamine receptor agonists affected monkey colonic contractility.....	205
5.1.4.7. Histamine receptor agonists affected monkey colonic membrane potential.....	206
5.1.4.8. Histamine increased the open probability of 5pS NSCC in monkey colonic SMC.....	206
5.1.4.9. Histamine activated K_{ATP} whole-cell currents in murine colonic SMC.....	207
5.1.5. Figures and figure legends.....	209
5.1.6. Discussion.....	227
<u>5.2. Effect of DSS-induced colitis on RMP and contractility in murine colonic tissue.....</u>	231

5.2.1. Summary	231
5.2.2. Background and Aims	232
5.2.3. Materials and methods	234
5.2.3.1. <i>Inducing dextran sulphate-sodium (DSS) colitis in C57BL/6 mice</i>	234
5.2.3.2. <i>Isometric Force Measurements</i>	234
5.2.3.3. <i>Intracellular Microelectrode Recordings</i>	235
5.2.3.4. <i>Chemicals and solutions</i>	236
5.2.3.5. <i>Statistical Analysis</i>	236
5.2.4. Results	237
5.2.4.1. <i>Clinical symptoms</i>	237
5.2.4.2. <i>RMP and electrical responses to CCh in inflamed colonic smooth muscle were different compared to controls</i>	237
5.2.4.3. <i>Contractile responses to CCh were decreased in inflamed colonic smooth muscle compared with controls</i>	238
5.2.5. Figures and figure legends	239
5.2.6. Discussion	243
<u>Chapter 6: Summary, Discussion and Future Work</u>	246
6.1. Smooth muscle excitability in colonic SMC	246
6.2. PLC regulation	248
6.2.1. <i>Drug non-specificity</i>	249
6.2.2. <i>m-3M3FBS and o-3M3FBS</i>	250
6.3. Rho-kinase regulation of colonic excitability and ion channel activity	251

6.4. Histamine effects on monkey and murine colonic excitability.....	252
6.5. DSS-induced colitis results in alterations in colonic excitability.....	254
6.6. Overall conclusion.....	255
<u>References</u>.....	256

List of figures

Chapter 1

Figure 1	Th1 mediated response in Crohn's disease.....	8
Figure 2	Th2-type response in Ulcerative Colitis.....	10
Figure 3	Major effects of histamine via specific H receptors.....	29
Figure 4	H1 receptor signaling pathway.....	31
Figure 5	H2 receptor signaling pathway.....	32
Figure 6	H4 receptor signaling pathway.....	33
Figure 7	TRP superfamily.....	41
Figure 8	TRPC channel structure.....	43
Figure 9	Current-voltage relationship of TRPC7 expressed in HEK293 cells.....	49
Figure 10	TRPM channel structure.....	50
Figure 11	TRPV channel structure.....	55
Figure 12	Constitutively active NSCC in rabbit mesenteric artery myocytes.....	59
Figure 13	PLC-dependent intracellular signaling pathway.....	69
Figure 14	Structures of <i>m</i> -3M3FBS and <i>o</i> -3M3FBS.....	70
Figure 15	Ca ²⁺ sensitization pathway.....	75

Chapter 2

Figure 1	Spontaneous transient inward currents recorded in colonic SMC.....	94
Figure 2	Na ⁺ contributed to bI_{NSCC} and membrane potential.....	96
Figure 3	NSCC blockers inhibited bI_{NSCC}	98

Figure 4	Ca ²⁺ contributed to bI_{NSCC}	100
Figure 5	Single channel conductances recorded in monkey colonic SMC.....	102
Figure 6	TRP channels expressed in human and monkey colonic tissue and SMC	104

Chapter 3

Figure 1	<i>m</i> -3M3FBS and <i>o</i> -3M3FBS decreased colonic smooth muscle contractility.....	131
Figure 2	<i>m</i> -3M3FBS caused a PLC-independent decrease in I_{DR}	133
Figure 3	<i>m</i> -3M3FBS inhibited I_A	135
Figure 4	<i>m</i> -3M3FBS decreased I_{DRS}	137
Figure 5	<i>m</i> -3M3FBS decreased I_L	139
Figure 6	<i>o</i> -3M3FBS decreased I_L	141
Figure 7	<i>m</i> -3M3FBS caused PLC-independent inhibition of I_L	143
Figure 8	<i>m</i> -3M3FBS and <i>o</i> -3M3FBS increased $[Ca^{2+}]_i$ and simultaneously decreased I_L	145

Chapter 4

Figure 1	Y-27632 reduced the amplitude of nerve-stimulated on- and off- contractions.....	168
Figure 2	Y-27632 reduced the amplitude of nerve-stimulated on- and off- contractions evoked at increasing durations.....	170
Figure 3	Y27632 reduced colonic contractility independent of neuronal influences	172
Figure 4	Y-27632 pretreatment reduced CCh-induced	

	depolarization in murine colonic smooth muscle.....	174
Figure 5	H-1152 reduced the amplitude of nerve-stimulated on- and off- contractions	176
Figure 6	HA-1077 pretreatment inhibited CCh-induced depolarization in murine colonic smooth muscle.....	178
Figure 7	Y-27632 did not effect KCl evoked contractions in colonic smooth muscle.....	180
Figure 8	Y-27632 reduced GTP γ S activated NSCC.....	182

Chapter 5.1.

Figure 1	Mast cells were located in monkey and inflamed murine colonic smooth muscle.....	209
Figure 2	H receptor expression was different in monkey and murine colonic tissue.....	211
Figure 3	Histamine altered contractility in monkey and murine colonic smooth muscle.....	213
Figure 4	Histamine-evoked changes in contractility in monkey and murine colonic smooth muscle were TTX-insensitive.....	215
Figure 5	Histamine altered membrane potential in monkey and murine colonic smooth muscle.....	217
Figure 6	Specific H receptor agonists had different effects on contractility in monkey colonic smooth muscle.....	219
Figure 7	Specific H receptor agonists changed membrane potential in monkey colonic smooth muscle.....	221
Figure 8	Histamine increased the open probability of a 5pS NSCC in monkey colonic SMC.....	223
Figure 9	Histamine activated K _{ATP} currents in murine colonic SMC.....	225

Chapter 5.2.

- Figure 1 RMP and CCh-induced depolarization were significantly changed in inflamed colonic smooth muscle239
- Figure 2 Spontaneous and CCh-induced contractility were suppressed in inflamed colonic smooth muscle.....241

List of tables

Chapter 1

Table 1	Models of chemically- and nematode-induced colitis.....	12
Table 2	Transgenic inflammatory-related models.....	15
Table 3	Evidence supporting <i>increased</i> contraction in IBD.....	24
Table 4	Evidence supporting <i>decreased</i> contraction in IBD.....	24-26
Table 5	Alterations in Ca ²⁺ sensitization mechanisms in IBD.....	27
Table 6	Alterations in ion channel activity and/or expression in IBD.....	27
Table 7	Alterations in RMP in IBD.....	28
Table 8	Summary of H receptor distribution in human GI tract.....	35

Chapter 2

Table 1	Oligonucleotides used in the TRP channel study.....	106
---------	---	-----

Abbreviations

ACh	Acetylcholine
ADP-ribose	adenosine diphosphoribose
4-AP	4-aminopyridine
AUC	area under the curve
bI_{NSCC}	basally activated non-selective cation currents
B2M	beta-2 macroglobulin
BK	large conductance Ca^{2+} -activated K^+ channel
$[Ca^{2+}]_i$	intracellular Ca^{2+}
CAM	calmodulin
CAMKII	calmodulin-dependent protein kinase II
cAMP	cyclic adenosine monophosphate
CaPSS	Ca^{2+} -containing physiological salt solution
CCh	carbachol
CD	Crohns disease
CPI-17	PKC-potentiated phosphatase inhibitor
DSS	dextran sulphate sodium
DAG	diacylglycerol
EFS	electrical field stimulation
EGTA	ethylene glycol tetraacetic acid
E_K	equilibrium potential for K^+ ions
ENS	enteric nervous system
ERK	Extracellular-regulated kinase
Gd^{3+}	gadolinium
GEF	guanine nucleotide exchange factors
GFP	green fluorescent protein
GI	gastrointestinal
GPCR	G-protein coupled receptor
GTP γ S	guanosine 5'-3-O-(thio)triphosphate
H-1152	[(S)-(+)-(2-methyl-5-isoquinoliny) sulfonylhomopiperazine, 2HCl]
HA-1077	[(5-isoquinolinesulfonyl)homopiperazine, 2HCl]
HC	holding current
HDC $^{-/-}$	histamine-deficient, histidine decarboxylase knockout mice
HEPES	4-(2-hydroxyethyl)-1-piperazineethanesulfonic acid
HK	K^+ -rich (140mM) solution
HTMT	histamine-trifluoromethyl-toluidine
I_A	A-type K^+ currents
IAS	internal anal sphincter
IBD	inflammatory bowel disease
ICC	Interstitial Cells of Cajal
I_{DR}	delayed rectifier K^+ currents
I_{DRS}	slowly-activating delayed rectifier K^+ currents
IFN- γ	interferon- γ
IK	intermediate conductance
IK $_{Ca}$	intermediate-conductance Ca^{2+} -activated K^+ channels

IL	interleukin
I_L / L-type	high threshold voltage-activated Ca^{2+} current
IJP	inhibitory junction potential
I_{LVA}	low threshold voltage-activated Ca^{2+} -current
IP3	inositol trisphosphate
I-V	current-voltage
La^{3+}	lanthanum
LKbg	large conductance background-type potassium channel
LPC	lysophosphatidylcholine
K2P	two pore K^+ channel
K_{ATP}	ATP-sensitive K^+ channel
Kir	inwardly rectifying K^+
KO	knockout
KRB	Krebs-Ringer bicarbonate solution
K_v	voltage-gated, Ca^{2+} independent
MLC_{20}	20-kDa myosin regulatory light chain
MLCK	myosin light chain kinase
MLCP	myosin light chain phosphatase
<i>m</i> -3M3FBS	2, 4, 6-trimethyl-N-(meta-3-trifluoromethyl-phenyl)-benzenesulfonamide
M	muscarinic
MAPK	p38 mitogen-activated protein kinase
MHDC	4-Methylhistamine dihydrochloride
mI_{CAT}	muscarinic receptor-induced NSCC activated current
MnPSS	Mn^{2+} (Ca^{2+} -free) containing physiological salt solution
NMDG	N-methyl-D-glucamine
NSCC	non-selective cation channels
NF- $\kappa\beta$	nuclear factor-kappa beta
<i>o</i> -3M3FBS	2, 4, 6-trimethyl-N-(ortho-3-trifluoromethyl-phenyl)-benzenesulfonamide
PIP_2	phosphatidylinositol 4,5-bisphosphate
PI 3-kinase	Phosphatidylinositol-3-kinase
PLC	Phospholipase C
PKA	protein kinase A
PKC	protein kinase C
qPCR	quantitative polymerase chain reaction
RMP	resting membrane potential
ROC	receptor-operated channels
RT-PCR	real time-polymerase chain reaction
SCID	Severe combined immunodeficient
SOC	store-operated channels
SK	small conductance
sNSCC	small conductance non-selective cation channels
SMC	smooth muscle cells
smMHC/Cre/eGFP	smooth muscle myosin heavy chain, Cre recombinase

	enhanced fluorescent protein
STICs	spontaneous transient inward currents
STOCs	spontaneous transient outward currents
TEA	tetraethylammonium chloride
TNBS	trinitro-benzene sulphonic acid
TNF- α	tumor necrosis factor- α
Th1	CD4+ T helper 1
Th2	CD4+ T helper 2
TM	transmembrane
TRP	transient receptor potential
TTX	tetrodotoxin
TGF- β	tumor necrosis factor- β
U73122	1-(6-((17 β -3-methoxyestra-1,3,5(10)-trien-17-yl)amino)hexyl)-1H-pyrrole-2,5-dione
UC	ulcerative colitis
VDCC	voltage-dependent Ca ²⁺ channels
Y-27632	(R)-(+)-trans- <i>N</i> -(4-pyridyl)-4-(1-aminoethyl) cyclohexane carboxanecarb-oxamide, 2HCl

Chapter 1: Introduction

1.1 Smooth muscle excitability in the gastrointestinal tract

The gastrointestinal tract (GI) tract is required for the ingestion and digestion of food, absorption of vital nutrients and elimination of waste. Coordinated movements of the *tunica muscularis* are essential for the movement of ingested material through the different organs of the GI tract. Several different extrinsic systems contribute to the final effect of contraction seen in smooth muscle including the enteric nervous system (ENS) and specialized pacemaking cells called Interstitial Cells of Cajal (ICC). In the colon, the ENS modulates spontaneous contractions in smooth muscle through enteric motor neurons. The nerve blocking agent, tetrodotoxin (TTX), increases the amplitude of spontaneous contractions suggesting that tonically driven, inhibitory motor neurons play a key role in controlling colonic motility patterns (Borjesson *et al.*, 1999; Wood *et al.*, 1999). In the small intestine, ICC generate cyclic depolarizations called electrical slow waves that spread electrical signals through gap junctions to smooth muscle resulting in rhythmical contractions (Farrugia, 2008). However despite the importance of these extrinsic systems in smooth muscle motility, if contractile mechanisms in smooth muscle are not intact, the extrinsic regulatory signals will not have their desired effects.

The mechanisms that underlie smooth muscle excitability are of unequivocal importance since they ultimately determine contractile behavior. The

resting membrane potential (RMP) is a major determinant of smooth muscle excitability and ranges widely in the GI tract, from -85mV to -40mV (Sanders, 2008). In those regions where RMP is near the equilibrium potential for K⁺ ions (E_K), approximately -90mV, K⁺ still dominate here. Conversely, in those regions where RMP is substantially more positive than E_K , other ionic conductances such as Na⁺/Ca²⁺ are thought to contribute to these more depolarized potentials. Differences in ion channel expression are thought to underlie these regional variations in RMP in the GI tract.

Excitation-contraction coupling is an important phenomenon in GI motility as it refers to the dynamic coupling between membrane potential and muscle contraction (Carl *et al.*, 1996). Ca²⁺ plays a fundamental role in this coupling since, when bound to calmodulin, it can activate myosin light chain kinase (MLCK) which phosphorylates 20kDa myosin light chain subunits of myosin and initiates cross-bridge cycling (Murthy *et al.*, 2000; Camello-Almaraz *et al.*, 2009). The RMP is a critical factor that contributes to the excitability of smooth muscle because Ca²⁺ influx and intracellular Ca²⁺ ($[Ca^{2+}]_i$) are significantly influenced by membrane depolarization. When RMP is close to E_K , smooth muscle tissue is in a quiescent state until a major stimulus causes activation of non-selective cation channels (NSCC). Influx of Na⁺ and Ca²⁺ ions through these channels depolarizes smooth muscle cells (SMC) to membrane potentials where voltage-dependent Ca²⁺ channels (VDCC) are activated i.e. there is an increase in their open probability. Ca²⁺ entry through VDCC then activates the contractile

apparatus. When RMP is considerably less negative than E_K , it is closer to the window current of VDCC. In these cases only a small depolarization is required to increase the open probability of VDCC resulting in contraction and therefore these tissues are considered more excitable.

It is now well recognized that a process called Ca^{2+} -sensitization plays an important role in the contractile response of smooth muscle (Al-Jarallah *et al.*, 2008; Fernandes *et al.*, 2006). This is based on the discovery that following increases in $[Ca^{2+}]_i$ by muscarinic stimulation, the force of contractions is greater than from equivalent $[Ca^{2+}]_i$ increases caused by membrane depolarization following elevation of external K^+ . This process is modulated by changing the activity of myosin light chain phosphatase (MLCP). Inhibition of MLCP increases phosphorylation of myosin by MLCK which facilitates cross-bridge cycling (Somlyo & Somlyo, 2003). More details concerning the Ca^{2+} -sensitization mechanism are described in section 1.7.

The ionic mechanisms that regulate the membrane potential and Ca^{2+} entry in smooth muscle are of utmost importance in maintaining normal GI excitability and hence contractility. Therefore any disturbances in these ionic mechanisms can prove detrimental to normal colonic excitability and motility. For example, in pathophysiological states such inflammatory bowel disease (IBD), intestinal dysmotility has often been reported (Vermillion *et al.*, 1993; Galeazzi *et al.*, 2000; Vrees *et al.*, 2002). Alterations in ENS, ICC and smooth muscle function have been suggested to contribute to this dysmotility. Several studies

have also reported changes in ion channel expression and/ or activity that may underlie altered colonic excitability and motility in inflammatory conditions.

The following section will address the pathophysiology of two inflammatory diseases that are known to alter colonic motility. The animal models that are currently used to investigate pathophysiological mechanisms and immunological processes underlying human IBD will be briefly described. Finally, changes in smooth muscle function and underlying reasons relating to ion channel activity, membrane potential and Ca^{2+} sensitization will be summarized.

1.2. Effects of inflammation on colonic excitation and contraction

1.2.1. Pathophysiology of IBD

IBD can be divided into two diseases called Crohn's disease (CD) and ulcerative colitis (UC) which result from abnormal immune responses to infection of the intestinal epithelium (Kennedy *et al.*, 2000 Ozaki *et al.*, 2005; Kawada *et al.*, 2007; Ohama *et al.*, 2007). CD is a transmural inflammatory disease of the mucosa that can affect any part of the GI tract where clinical symptoms include abdominal pain and diarrhea. Patients develop many intestinal complications including ulcers, strictures and fistulas (Baumgart, 2009). UC is a non-transmural inflammatory disease that is constrained to the colon. Characteristic symptoms of UC include abdominal pain, fever, diarrhea and passage of blood and mucus in stool (Baumgart, 2009). This disease is marked by abnormalities of

the epithelium. In particular, ulcers, abscesses and apoptosis of epithelial cells with an increase in mucosal leakiness are hallmark signs of UC (Heller *et al.*, 2005). It is estimated that one to two million Americans suffer from IBD (Boismenu & Chen, 2000). Treatment of IBD generally consists of administration of anti-inflammatory agents and immunosuppressants. One of the main agents used is Infliximab which is a IgG1 antibody that forms stable complexes with a major proinflammatory cytokine called tumor necrosis factor- α (TNF- α) which results in loss of activity of TNF- α (Owczarek *et al.*, 2009). Although the pathogenesis of these disorders has not been clearly defined, recent studies suggest that a complex interplay between genetic, environmental and immunological factors contribute to the pathogenesis of these diseases (Kawada *et al.*, 2007).

Genetic factors: Epidemiological studies within families and between monozygotic and dizygotic twins have indicated that genetic factors are important in IBD, especially CD (Hibi & Ogata, 2006). A genetic mutation in the gene NOD2, which encodes for caspase recruitment domain-containing protein, CARD15, was found to be associated with CD (Ogura *et al.*, 2001). In addition, genetic variation in an autophagy gene called ATG16L1 was also found to be related to CD. Interestingly both genes are involved in the immune system's response to bacterial components and therefore these genetic variations could render the mucosa more susceptible to bacterial invasion (Cho, 2003; Cho, 2008). Both UC and CD are associated with variations in the gene encoding the

interleukin (IL) -23 receptor subunit and also IL12B, signal transducer and activator of transcription 3, and transcription factor NKX2-3 gene regions (Cho, 2008). Further studies are needed to identify specific gene mutations that render individuals more susceptible to IBD.

Environmental factors: Consumption of specific food stuffs is associated with increased risk of IBD (Guarner & Malagelada, 2003). For example a high intake of animal fat and/or sugar-rich foods can accelerate the development of CD (Sakamoto *et al.*, 2005). Conversely, intake of prebiotics, which are non-digestible food constituents such as dietary fibre and some types of oligosaccharides, have been used to treat IBD (Kanauchi *et al.*, 2003). Prebiotics can increase the population of certain bacteria and in turn significantly change the composition of the microflora. This may cause an increase in short-chain fatty acids that are a source of nutrients for the intestine and inducers of an acidic environment (Hibi & Ogata, 2006).

Strong evidence for the role of luminal bacteria in IBD has been obtained using experimental animal models of IBD (see section 1.2.2. on animal models). Intestinal inflammation induced by dextran sulphate sodium (DSS) and trinitrobenzene sulphonic acid (TNBS) was alleviated by pretreatment with antibiotics (Okayasu *et al.*, 1990; Videla *et al.*, 1994). HLA-B27 transgenic rats, that develop chronic colitis spontaneously, did not develop intestinal inflammation in a germ free/sterile environment (Guarner & Malagelada, 2003). These studies support

the important function of normal enteric bacteria in initiating and sustaining inflammation.

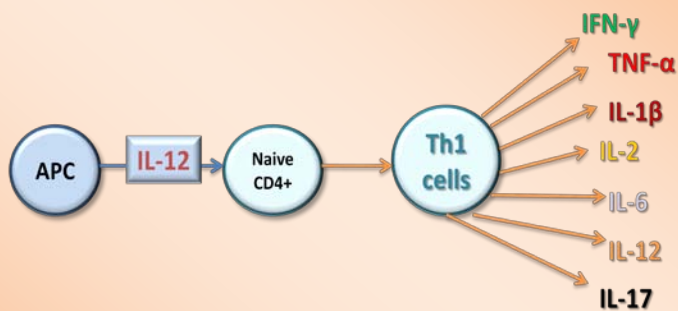
Immunological factors: Normally, there is a delicate balance between cytokine synthesis and activation of cytokine-dependent pathways within the lumen of the intestine. This balance is highly dependent on regulatory T cells and intricate feedback mechanisms (Ihle, 1995; O'Shea & Murray, 2008). Following an injury insult, specific T-helper cell dependent immune responses are activated. They are commonly divided into two types of responses called CD4+ T helper 1 (Th1) and CD4+ T helper 2 (Th2) responses. The balance and change in the overall cytokine production profile is dependent on the Th1/Th2 polarization pattern (Alex *et al.*, 2009).

The Th1 response is characterized by the release of IL-12 from antigen-presenting cells (mainly macrophages and B cells) which in turn stimulate differentiation of CD4+ T cells to produce IL-2 and interferon- γ (IFN- γ) leading to cell-mediated responses. IFN- γ activates macrophages and granulocytes which in turn release IL-16 and TNF- α (Heller *et al.*, 2005). TNF- α can stimulate the production of other inflammatory cytokines such as IL-6, IL-12 and IL-18 (Kinoshita *et al.*, 2006). Generally the Th1 response is thought to protect against invasive bacterial and viral infection but can also cause autoimmune diseases (Rosloneic *et al.*, 2002). On the other hand, the Th2 mediated response is associated with the secretion of IL-4, IL-5, IL-6, IL-10 and IL-13 from CD4+ Th2 cells and mediates humoral responses as well as promoting allergic responses

(O’Gara & Murphy, 1994; Oosterhout & Motta, 2005). The Th2 response is often considered anti-inflammatory since some of the Th2-type cytokines suppress the development of Th1 T cells (Fort *et al.*, 2001). For instance, IL-4 can enhance T-cell proliferation and differentiation of naïve CD4+ T cells towards a Th2 phenotype and suppress the production of IFN- γ from Th2 cells (Chomarat & Banchereu, 1998). In TNBS-induced colitis in rats, which stimulates the Th1 response, inflammation could be ameliorated by IL-4 gene transfer (Hogaboam *et al.*, 1997).

Recently, a distinct lineage of Th-cells was identified termed Th-17 cells that contribute to tissue damage and remodeling in IBD. These cells produce IL-17A, IL-21 and IL-22 that can enhance the expression of chemo-attractants by epithelial cells and adhesion molecules such as intercellular adhesion molecule by endothelial cells (Caprioli *et al.*, 2008). Adhesion molecules can increase the number of lymphocytes, macrophages,

Figure 1: Th1 mediated response in Crohn’s disease



In Crohn’s disease, antigen presenting cells (APC) release IL-12 which in turn stimulates differentiation of CD4+ T cells into Th1 T cells. These cells produce specific Th1 associated cytokines and inflammatory mediators such as TNF- α and IFN- γ .

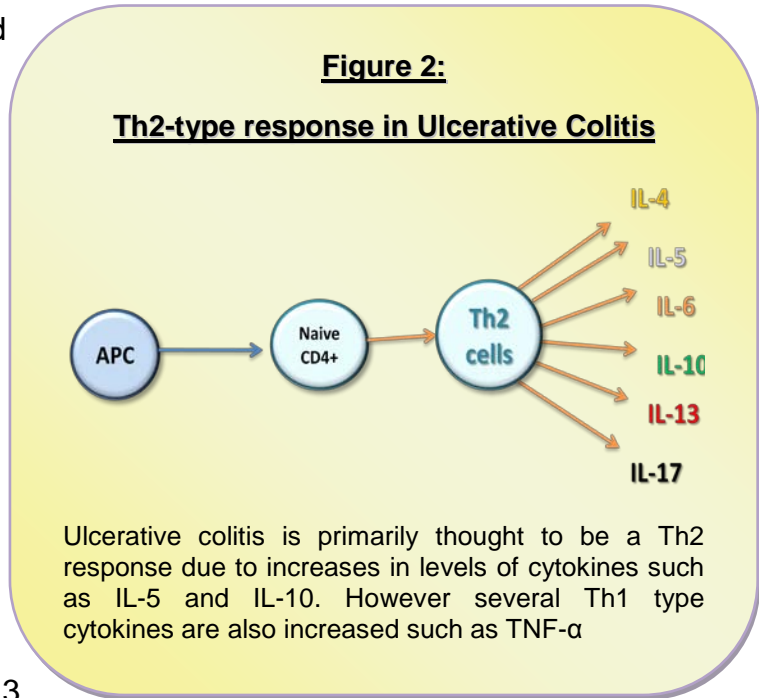
neutrophils and plasmocytes in inflamed tissue (Owczarek *et al.*, 2009).

In IBD, there is a dramatic shift in the cytokine profile, where dysregulation of Th1 and/or Th2 cell populations results in uncontrolled immunological responses to naturally occurring bacterial antigens (Boismenu & Chen, 2000; Alex *et al.*, 2009).

Crohn's disease: CD is associated with the differentiation of CD4+ T helper cells into a Th1 subpopulation where predominant cytokines secreted include TNF- α , IFN- γ and interleukins-1 β , IL-2, IL-6, IL-8, IL-12 and IL-17 (see Fig. 1) (Fujino *et al.*, 2003; Owczarek *et al.*, 2009). These proinflammatory cytokines activate the transcription factor nuclear factor-kappa beta (NF- κ β) pathway that enhances production of other inflammatory mediators which therefore exacerbates the inflammation (Kinoshita *et al.*, 2006). Evidence of this dominating Th1 response comes from studies where T cells from the colons of patients suffering from CD produce vast amounts of the Th1 cytokines IFN- γ and TNF- α but few of the Th2 cytokines IL-4 or IL-10 (Fort *et al.*, 2001). However reports are beginning to reveal that Th2 cells are also involved in the pathogenesis of CD. For example, the Th2 interleukin, IL-5, was reported to be up-regulated in CD (Gor *et al.*, 2003).

Ulcerative colitis: Unlike CD disease, the immunological basis of UC has not been clearly defined. Secretion of IFN- γ and IL-12 are not increased in patients with UC which suggests it is not through a Th1 response. Conversely, the major proinflammatory and Th1 cytokine, TNF- α , was reported to be up-regulated in UC

(Fort *et al.*, 2001; Gor *et al.*, 2003). As in CD, the proinflammatory cytokine, IL-17 is significantly up-regulated in UC (Fujino *et al.*, 2003). Despite these findings, UC is primarily associated with a Th2-like response since there is an increase in the production of Th2 cytokines, IL-5, IL-6 and IL-10 cytokines (see Fig. 2) (Alex *et al.*, 2009). IL-13,



produced by NK T cells and found in the lamina propria, is regarded as one of the most important Th2 cytokines in patients with UC as it can severely effect epithelial cell function including apoptosis, tight junctions and permeability (Heller *et al.*, 2005).

1.2.2. Animal models of IBD

Several animal models of inflammation have been developed in order to investigate pathophysiological mechanisms and immunological processes underlying human IBD. Although the models do not completely mimic pathological features of human IBD, they do resemble several important immunological and histopathological aspects. These animal models are summarized in Table 1.

Chemical and nematode induced models of IBD: The most commonly used models of intestinal inflammation are chemically-induced as the commencement and duration of inflammation can be controlled easily (Alex *et al.*, 2009). Oral administration of DSS for approximately five days results in disruption of the epithelial lining and subsequent translocation of luminal bacteria. In particular, extensive crypt and epithelial cell damage, tissue edema and infiltration of macrophages and neutrophils within damaged segments have been reported. Reasons for the deleterious effects of DSS are not clearly understood although epithelial cell toxicity, activation of macrophages and increased intestinal permeability have been suggested as potential mechanisms (Kitajima *et al.*, 1999; Boismenu & Chen, 2000). Several studies have reported that mice treated with DSS exhibit a Th2 profile with increased secretion of the Th2 cytokines IL-4, IL-5 and IL-6 (Fuss *et al.*, 1996; Ihara *et al.*, 2009). However a recent study showed that acute colitis (7 days treatment with 3% DSS) was associated with a Th1 pattern where there are elevated levels of IL-17, TNF- α and keratinocyte-derived chemokine (Alex *et al.*, 2009).

However administration of several cycles of DSS (usually 3-5), can cause chronic inflammation characterized by severe T-lymphocyte infiltration and regenerative changes in the epithelium (Okayasu *et al.*, 1990). In a recent study, change in treatment from acute to chronic DSS-induced colitis (consisting of 4 cycles of DSS (5%) for 7days/cycle and 10 days normal drinking water), resulted

in conversion from a Th1 pattern in acute DSS to a Th2-based (IL-4, IL-10) profile in chronic DSS (Alex *et al.*, 2009).

The macrophage-derived, proinflammatory cytokine IL-18 is an important mediator in DSS colitis as administration of anti-IL-18 antibodies attenuated colitis damage in this model of colitis (Sivakumar *et al.*, 2002). Successful inducement of DSS-colitis is also dependent on the strain of mouse. It was reported that C57/BL6

mice developed chronic colitis after 4 weeks following removal of DSS treatment.

However, BALB/c mice recovered after this period following DSS-treatment for 7 days (Melgar *et al.*, 2005).

Table 1: Models of chemically- and nematode-induced colitis

Model	Area affected	TH-response	Cytokine profile
DSS (UC-like)	colon	Th1/Th2	Acute:IL-1 β , TNF- α , IL6, IL17 Chronic:IL-4,IL10
TNBS (CD-like)	colon	Th1	Th1-Th17 response IL-1 β , TNF- α , IL6, IL17
Acetic acid	Distal colon	Th1/Th2	TNF- α , IL-6
Oxazolone (UC-like)	Distal colon	Th2	IL4/IL5
<i>Trichinella spiralis</i> (UC-like)	Prox Small intestine	Th2	IL-4, IL-5, IL-9, IL-13

Rectal

administration of TNBS dissolved in ethanol causes a severe inflammatory

response with many characteristic features of human CD including transmural infiltration of inflammatory cells especially macrophages, necrosis, and IL-12-mediated Th1-immune response (Strober *et al.*, 1997). Administration of anti-IL-12 antibodies in TNBS-induced colitis can prevent the commencement of the disease (Neurath *et al.*, 1995). TNBS-induced colitis is mediated by not only IL-12 but also IL-18 as TNBS treatment failed to induce significant colitis in IL-18 KO mice. In addition, application of anti-IL-18 antibodies significantly attenuated mucosal inflammation in TNBS-induced colitis (Kanai *et al.*, 2001). As with the DSS-model, the susceptibility of different strains of mice to TNBS varies. For example C57/B1 mice are resistant while BALB/c and SJL are susceptible to TNBS treatment (Yamamoto-Furusho, 2007).

Intrarectal administration of 3-5% acetic acid produces acute inflammation in the distal colon of rats (MacPherson and Pfeiffer, 1978). Organic acids in particular cause epithelial necrosis and edema that extends from the *lamina propria* into the submucosa and external muscle layers (Yamada *et al.*, 1992). This method of inducing inflammation has been reported to increase levels of both Th1 and Th2 cytokines (Hagar *et al.*, 2007).

Rectal administration of the haptening agent oxazolone suspended in a chemical vehicle leads to colitis in the distal region of the colon. A Th2 type response is induced with a significant increase in IL-4/IL-5 while co-administration of an anti-IL-4 antibody can attenuate the inflammation (Boirivant *et al.*, 1998).

Many intestinal nematode infections including *Trichinella spiralis* preferentially reside in the proximal small intestine of mammals. In *Trichinella spiralis*-induced colitis, a strong Th2 response is activated and is characterized by expression of cytokines such as IL-4, IL-5, IL-9 and IL-13 (Khan & Collins, 2004). Increased mucus secretion, hypercontractility and thickening of the smooth muscle layers are characteristic changes in nematode infections (Blennerhassett *et al.*, 1992; Khan *et al.*, 2002; Khan & Collins, 2004). Table 1 is a summary of these animal models of IBD and the specific cytokine responses they activate.

Knockout mice: When IL-10 deficient mice are kept in germ-free conditions, they appear healthy and there is no immunologic activation. When housed in a specific pathogen-free environment, these mice develop chronic transmural enterocolitis with mucosal hyperplasia, endotoxemia, pseudopolyp formation, granulomas and Th1-mediated intestinal inflammation (Berg *et al.*, 1996; Kennedy *et al.*, 2000; Mizoguchi *et al.*, 2003). Transfer of these mice to conventional conditions results in development of lethal small and large intestinal inflammation (Kuhn *et al.*, 1993). These studies revealed that IL-10 plays a vital role in regulating the mucosal immune system by suppressing the production of many pro-inflammatory cytokines and chemokines including IL-12, TNF- α and IL-1 β (Buelens *et al.*, 1997; Moore *et al.*, 2001). IL-10 administration via *Lactococcus lastis* in DSS-treated mice or via adenoviral vectors in TNBS-treated mice, significantly reduced disease severity in both these models of IBD (Steidler

et al., 2000; Lindsay *et al.*, 2002). In mice where the IL-2 gene is disrupted, they develop spontaneous colitis and approximately 50% die within 4-9 weeks of age (Sadlack *et al.*, 1993). The role of TNF- α in initiating and amplifying the immune response in IBD was

illustrated through a TNF- α knockout (KO) mouse, where characteristic effects of TNBS treatment such as increases in IL-1 β and IL-6 did not occur in the TNF- α KO mice treated with TNBS (Kinoshita *et al.*, 2006).

Severe combined immunodeficient

(SCID) mice are a specific

mouse strain that lack T- and B- cell adaptive immunity (Bosma *et al.*, 1983).

Transfer of CD4⁺ T cells into these SCID mice induces IBD with infiltration of macrophages, neutrophils and plasma cells into the *lamina propria* (Morrissey *et*

Table 2: Transgenic inflammatory-related models

Model	Result	Concluded role
IL-10 KO	Lethal when housed in conventional (dirty) conditions	Vital role in suppressing pro-inflammatory cytokines e.g. TNF α , IL-1 β , IL-12
IL-18 KO	TNBS failed to induce significant colitis	essential cytokine in Th1 mediated response in TNBS
TNF- α	Normal TNBS-induced changes were prevented	Initiates and amplifies immune response in CD
SCID + CD45RB ^h _i CD4 ⁺ T	Th1 response activated	Th1-subpopulation of cells can induce colitis
IL-2	Develop spontaneous colitis	Major anti-inflammatory role

al., 1993; Powrie *et al.*, 1994; Claesson *et al.*, 2003). Table 2 summarizes the findings of the some of the most important transgenic models of IBD. Clearly genetic models are helpful tools for determining the contribution of a specific gene to IBD.

1.2.3. Disturbances in excitation and contraction

In intestinal inflammation, both hypo- and hyper-contractility have been observed and are thought to reflect alterations in enteric, endocrine and myogenic systems (Vermillion *et al.*, 1993; Galeazzi *et al.*, 2000; Vrees *et al.*, 2002).

Enteric dysfunction: Changes in neuron dependent mechanisms have been reported in IBD and thought to contribute to changes in motility (Khan & Collins, 1994; Galeazzi *et al.*, 2000; Aulí & Fernández, 2007; Boissé *et al.*, 2009). Neurotransmitter release (such as acetylcholine (ACh) and norepinephrine) from enteric nerves was suppressed in *Trichinella spiralis* infection in rodents thus contributing to dysmotility (Khan & Collins, 1994). Studies suggest that IL-1 β , TNF- α , and IL-6 released from macrophages are responsible for this disruption in neurotransmitter release from longitudinal muscle-myenteric plexus (Main *et al.*, 1993; Hurst & Collins, 1994; Ruhl *et al.*, 1994). Another study using *Trichinella spiralis*-induced colitis revealed reduced spontaneous colonic motility associated with an increase in the expression of inducible nitric oxide synthase in the epithelium and lamina propria (Aulí & Fernández, 2007).

ICC damage: In the gut, ICC generate pacemaker activity and are essential for maintaining normal motility patterns (Ward *et al.*, 1994). Disruptions in ICC networks have been linked with altered intestinal contractility following inflammation (Lu *et al.*, 1997; Der *et al.*, 2000; Fausone-Pellegrini *et al.*, 2002). Suppression in phasic contractions of inflamed distal canine smooth muscle strips by acetic acid treatment was suggested to be in part, due to damage to ICC (Lu *et al.*, 1997).

Smooth muscle changes: Several inflammatory studies have reported an increase in smooth muscle contractility. For example in *Trichinella spiralis* infection-induced gut inflammation, smooth muscle contractility was increased in the jejunum 6 days post infection (Vermillion & Collins, 1988; Blennerhassett *et al.*, 1992). In one recent report, carbachol (CCh)-induced contractions were increased in circular smooth muscle strips from BALB/c mice treated with DSS for 7 days (Ihara *et al.*, 2009).

However, the majority of reports from human studies and using various models of IBD have reported a decrease in the contractile activity of smooth muscle in the inflamed colon and/or intestine in response to neurotransmitters (Reddy *et al.*, 1991; Snape *et al.*, 1991; Grossi *et al.*, 1993; Myers *et al.*, 1997a; Shi & Sarna., 2000; Vrees *et al.*, 2002; Khan *et al.*, 2005; Kinoshita *et al.*, 2006; Al-Jarallah *et al.*, 2008). In patients with UC, sigmoid circular smooth muscle contractions were significantly reduced and suggested to be in part due to hydrogen peroxide produced by increased levels of IL-1 β in the muscle layer

(Vrees *et al.*, 2002). In TNBS and acetic acid-induced colitis in rats, reduced contractile activity was recorded in response to CCh (Grossi *et al.*, 1993; Kinoshita *et al.*, 2003; Khan *et al.*, 2005; Kinoshita *et al.*, 2006; Al-Jarallah *et al.*, 2008). Canine colonic circular SMC contractility was suppressed in response to ACh, KCl and Bay K8644 following acetic acid treatment (Shi & Sarna, 2000). Tables 3 and 4 summarize findings from studies examining contractility using various models of IBD. These studies suggest that normal smooth muscle structure and function may be disturbed in inflammatory conditions. Recently researchers have focused their efforts on determining the underlying mechanism(s) that may account for the decrease in smooth muscle contractility and excitability seen in IBD.

Rho-kinase, Ca²⁺ sensitization: Ca²⁺ sensitization is an important mechanism that can regulate MLC phosphorylation and hence contractility in a Ca²⁺-independent manner. Changes in Ca²⁺ sensitization mechanisms have been linked with altered colonic motility in inflammatory models of IBD. For example in TNBS-induced colitis in rats, TNF- α reduced the expression of CPI-17, which is a PKC-potentiated phosphatase inhibitor that can inactivate MLCP. Hence increased MLCP activity and dephosphorylation of MLC was suggested to underlie the decreased amplitude of longitudinal and circular smooth muscle contractions induced by CCh (Ohama *et al.*, 2007). A study by Al-Jarallah and colleagues using colonic smooth muscle from TNBS-treated rats found that reduced CCh-induced contractions were due to changes in Ca²⁺ sensitization

involving the protein kinase C (PKC) pathway. In particular, they found a reduced expression of total PKC in inflamed colonic smooth muscle and decreased CCh-induced phosphorylation of CPI-17. In addition a higher basal smooth muscle tone was observed in inflamed colonic segments which correlated with an increase in the expression of an isoform of Rho-kinase called ROCK1 (Al-Jarallah *et al.*, 2008).

Extracellular-regulated kinase (ERK) and p38 mitogen-activated protein kinase (MAPK) also play important roles in Ca^{2+} sensitization in intestinal smooth muscle (Ohama *et al.*, 2007). A recent report demonstrated that increased expression of ERK and p38MAPK contributed to hypercontractility and increased Ca^{2+} sensitization seen in murine DSS-induced colitis (Ihara *et al.*, 2009) (see Table 5 for summary).

Cytokines and other contributors to dysmotility: Smooth muscle excitability and motility can be altered by pro/anti inflammatory cytokines e.g. IL-1 β and mediators e.g. histamine, trypsin, PAR activator and substance P (Kawabata *et al.*, 1999; Coruzzi *et al.*, 2001; De Schepper *et al.*, 2008). The pro-inflammatory cytokine, IL-1 β is considered an important mediator in dysmotility seen in IBD. IL-1 β treatment of ileal smooth muscle significantly reduced CPI-17 expression. In addition constitutively phosphorylated MLCP was also decreased. These two effects were proposed to increase MLCP activity and hence reduce contractility (Ohama *et al.*, 2003). Hypercontractility reported in *Trichinella spiralis* was suggested to be due to Th2 cytokine-induced expression of TGF- β 1 and

subsequent up-regulation of cyclooxygenase and prostaglandin E₂ at the smooth muscle level (Akiho *et al.*, 2005).

Ion channels and dysmotility: Recent evidence has revealed that changes in the activity and/or expression of specific ion channels may be important factors contributing to decreased motility seen in intestinal smooth muscle in IBD (Ozaki *et al.*, 2005; Ohama *et al.*, 2007;). In GI smooth muscle, L-type voltage-dependent Ca²⁺ channels (Ca_v1.2/ α_{1C}) play fundamental roles in excitation-contraction coupling by mediating the influx of Ca²⁺ required for contraction. Whole-cell patch clamp experiments using inflamed colonic SMC from DSS-treated mice revealed significant suppression in L-type Ca²⁺ currents (Akbarali *et al.*, 2000; Liu *et al.*, 2001a). In intestinal inflammation induced by ethanol and acetic acid, Ca²⁺ currents were also suppressed in SMC. A decrease in the expression of the α_{1C} subunit of L-type Ca²⁺ channels was proposed to account for this suppression in current (Liu *et al.*, 2001a). In 2003, Kinoshita and colleagues reported that decreased contractility and current density of L-type Ca²⁺ channels in smooth muscle tissue and cells from TNBS-treated rat colon could be partially recovered by pretreatment of NF-κβ inhibitors. However, mRNA and protein levels of L-type Ca²⁺ channels remained unchanged in the inflamed colon. Therefore it was suggested that L-type Ca²⁺ channel function may be altered via NF-κβ-dependent pathways (Kinoshita *et al.*, 2003). Kang's group also reported a decrease in L-type Ca²⁺ channel currents in murine SMC following DSS-induced inflammation but reported no decrease in the expression

of the two isoforms of $\text{Ca}_v1.2$ (encoded by either exon 1a or 1b). This group suggested that altered regulation of the Ca^{2+} channels may be via the intracellular tyrosine kinase, c-src (since modulation of Ca^{2+} currents by c-src kinase was down-regulated in inflamed SMC) (Kang *et al.*, 2004). A study in 2005 revealed that treatment of cultured human colonic smooth muscle cells with TNF- α resulted in activation of NF- $\kappa\beta$ subunits p50 and p65 which in turn suppressed mRNA expression of the $\text{Ca}_v1.2$ subunit (Shi *et al.*, 2005). Inconsistencies relating to the expression levels of $\text{Ca}_v1.2$ in inflamed tissue may be due to different methods employed to induce inflammation and/or the different species used.

K_{ATP} channels are important in modulating cell excitability and are composed of pore forming subunits (either Kir6.1 or 6.2) and a sulfonylurea receptor (SUR1 or SUR2 (splice variants SUR2A and SUR2B)) (see section 1.5.1. for more information). Whole cell recordings revealed increases in the size of K_{ATP} -sensitive currents in colonic SMC isolated from DSS-treated mice. In addition, cell-attached recordings demonstrated that the bursting activity of inflamed cells was increased with the application of the K_{ATP} activator levcromakalim. These findings correlated with up-regulation of the Kir6.1 subunit by almost 22-fold after inflammation. Since K_{ATP} channels are known to be basally active and contribute to the membrane potential, an increase in activity could possibly reduce the excitability of the colonic smooth muscle (Jin *et al.*, 2004).

To date, two types of ion channels have been identified that may be involved in the reduced smooth muscle excitability and contractility seen in inflamed intestine. Further studies are required to examine if there are disturbances in the activity and/ or expression of other types of ion channels that may contribute to altered motility in human IBD and animal models of IBD (see Table 6 for summary).

RMP: Despite the well documented alterations in agonist-induced contraction of smooth muscle, few studies have examined the effects of colitis on RMP of smooth muscle. In Transient Receptor Potential (TRP) cation channel, subfamily V, member 1 (TRPV1) KO mice treated with DSS, membrane potential measurements revealed spontaneous atropine insensitive rhythmic action potentials in circular smooth muscle. These changes in membrane excitability were attributed to alterations in the myocytes themselves rather than neurons since they were unaltered in the presence of tetrodotoxin. The investigators suggested that TRPV1 may provide a protective mechanism for maintaining membrane stability during inflammation (Sibaev *et al.*, 2006). Analysis of the RMP in inflamed smooth muscle from the distal colon of formaldehyde treated rabbits revealed a decreased (more depolarized) RMP which was suggested to be due to alterations in electrogenic pump mechanisms (Cohen *et al.*, 1986). Conversely in a rat model of colitis using *Trichinella spiralis*, RMP was more hyperpolarized in inflamed circular SMC (-57mV) compared with control (-46mV) and suggested to be associated with the decreased contractility seen in inflamed

tissue. However the investigators stated that the mechanisms underlying the generation of the RMP are not completely understood and could only speculate underlying reasons for the change in RMP ($\text{Na}^+\text{-K}^+$ pump or ICC) (Aulí & Fernández, 2007). One study found no changes in RMP, slow wave frequency or amplitude in circular smooth muscle from sigmoid colon of UC patients (Koch *et al.*, 1988).

These studies suggest that changes in RMP may be correlated with alterations in colonic excitability and contractility. However, as stated by Aulí and Fernandez in 2007, the mechanisms involved in modulating RMP have not been clearly defined (see Table 7 for a summary of these studies).

Clearly many cellular mechanisms critical for maintaining normal colonic excitability are affected in inflammatory conditions. In chapter 5.2., the DSS model of colitis was used to examine changes in colonic excitability with particular emphasis on RMP since this parameter has not been examined in this model of IBD.

Effect of inflammation on colonic excitability:

• **Table 3: Evidence supporting increased contraction in IBD**

Model	Species	Effect	Proposed reasons &/or conclusion	Reference
DSS	Mouse BALB/c	•Increased contractile response to carbachol	• extracellular-regulated kinase) & p38 mitogen-activated protein kinase expression increase & thus increased contribution to contractile dysfunction	Ihara <i>et al.</i> , 2009
<i>Trichinella spiralis</i>	Rat	•Increased SM contractility by day 6 post infection	• Changes in excitation contraction coupling	Vermillion & Collins, 1988

• **Table 4: Evidence supporting decreased contraction in IBD**

Disease/ Model	Species	Effect	Proposed reasons &/or conclusion	Reference
TNBS	Rat	•Decreased contractile response to carbachol	•Decreased Ca ²⁺ sensitization	Al-Jarallah <i>et al.</i> , 2008
<i>Trichinella spiralis</i>	Rat	•Decreased contractile response to ACh and KCl	•increase in the expression of inducible nitric oxide synthase in the epithelium and lamina propria	Aulí & Fernandez, 2007
TNBS	Rat	•Decreased carbachol-induced contractions in circular & longitudinal smooth muscle	•Decreased CPI-17 expression via TNF- α	Ohama <i>et al.</i> , 2007
TNBS	Rat	•Decreased contractile response to carbachol in tissue	•Not given but Na-H exchanger 1 inhibitor (amiloride) reversed reduced contractile response	Khan <i>et al.</i> , 2005

TNBS	Rat	<ul style="list-style-type: none"> •Decreased contractile response to KCl, carbachol and Bay K8644 in circular SMC 	<ul style="list-style-type: none"> •Decreased activity of L-type Ca^{2+} channels. Dysfunction may be mediated via NF-κB-dependent pathways (as decreased contractility & L-type current density were partially recovered by pretreatment with NF-kappaB inhibitors. (NOT due to decrease in α1c) 	Kinoshita <i>et al.</i> , 2003
UC	Human	<ul style="list-style-type: none"> •contractions of circular SMC significantly reduced in response to NK and thapsigargin 	<ul style="list-style-type: none"> •Increased IL-1β in circular SMC produced hydrogen peroxide which contributed to motor dysfunction 	Vrees <i>et al.</i> , 2002
UC	Human	<ul style="list-style-type: none"> •Decreased force in muscle contraction in response to betanechol, increased $[K^+]_e$ and EFS-stimulated off-contractions 	<ul style="list-style-type: none"> •Suggested to be due to altered Ca^{2+}-calmodulin dependent regulation of actin-myosin cross-bridge formation 	Snape <i>et al.</i> , 1991
UC	Human	<ul style="list-style-type: none"> •Decreased contractility, increased low-amplitude propagating contractions, variable transit 	N/A	Reddy <i>et al.</i> , 1991
Acetic acid(distal)	Rat	<ul style="list-style-type: none"> •proximal colon circular smooth muscle contractility increased and decreased distal colon circular smooth muscle contractility to ACh and K^+ 	<ul style="list-style-type: none"> •suggested alterations in excitation-contraction coupling 	Myers <i>et al.</i> , 1997b
TNBS	Rat	<ul style="list-style-type: none"> •Acute: Increased tension response to Substance P & ACh. Decreased response to neurokinin A •Reduced contractility in latter stage (reduced tension) 	<ul style="list-style-type: none"> •a reduction in inhibitory neural input to smooth muscle originating via ACh acting at nicotinic receptors in the myenteric ganglia •associated with SMC thickening. May be due to combined loss of contractile proteins and increase in resistive forces 	Hosseini <i>et al.</i> , 1999
TNBS control & TNF-α-KO	Mouse	<ul style="list-style-type: none"> •Decreased contractile responses to KCl, carbachol, BayK8644. However contractions were scarcely affected in KO mouse •Organ culture of SM tissue: SM function disturbed 	<ul style="list-style-type: none"> •TNF-α plays essential role in both mucosal and muscularis inflammation in colon •TNF-α directly induces motor dysfunctions by acting on smooth muscle 	Kinoshita <i>et al.</i> , 2006

TNBS, Trichinella spiralis, acetic acid & mitomycin C	Rat	<ul style="list-style-type: none"> •Reduced carbachol-induced contraction of longitudinal muscle (also used KCl & Substance P) 	<ul style="list-style-type: none"> •Decreased contractility is independent in manner in which colitis is induced and is mediated at a receptor-independent locus on muscle cell 	Grossi <i>et al.</i> , 1993
Ethanol & acetic acid	Dog	<ul style="list-style-type: none"> •Decreased contractile response to ACh, KCl & Bay K8644 significantly decreased in circular SMC 	<ul style="list-style-type: none"> •Impairment of Ca²⁺ influx through L-type Ca²⁺ channels 	Shi & Sarna, 2000
Acetic acid Distal region	Rat	<ul style="list-style-type: none"> •ACh-induced contraction in circular smooth muscle was decreased 	<ul style="list-style-type: none"> •Proposed impaired utilization of intracellular Ca²⁺ 	Myers <i>et al.</i> , 1997a
IL-1β & IL-6 treatment	Rat	<ul style="list-style-type: none"> •Reduction in direct contractile response 	<ul style="list-style-type: none"> •ILs caused changes in mucosal ionic transport parameters and altered neurotransmission 	Natale <i>et al.</i> , 2003

Table 5: Alterations in Ca²⁺ sensitization mechanisms in IBD

Disease/ Model	Species	Effect	Proposed reason	Reference
TNBS	Rat	<ul style="list-style-type: none"> •Higher basal tone as Rho-kinase inhibitor caused significantly greater relaxation •reduced carbachol-induced contraction & phosphorylation of CPI-17 	<ul style="list-style-type: none"> •Increased Rho-kinase (ROCK I) expression •reduced expression of PKC, therefore decreased CPI-17 phosphorylation of MLCP 	Al-Jarallah <i>et al.</i> , 2008
TNBS	Rat	•Decreased carbachol-induced contractions in circular & longitudinal SM	•Decreased CPI-17 expression via TNF- α	Ohama <i>et al.</i> , 2007

Table 6: Alterations in ion channel activity and/or expression in IBD

Disease/ Model	Species	Effect	Proposed reasons &/or conclusion	Reference
TNF- α	Human	•decreased expression of Cav1.2 mRNA	•activation of NF- κ B subunits p50 & p65	Shi <i>et al.</i> , 2005
DSS	Mouse	•Decreased L-type Ca ²⁺ channel activity	•NOT due to decrease in α 1c expression. May be result from altered regulation by the non-receptor cellular tyrosine kinase, c-src kinase	Kang <i>et al.</i> , 2004
DSS	Mouse	•Reduced motility of colonic smooth muscle	•Increased Kir6.1 pore-forming subunit of K _{ATP} channel	Jin <i>et al.</i> , 2004
TNBS	Rat	•Decreased L-type Ca ²⁺ current density	• L-type Ca ²⁺ channel function directly altered via NF- κ B-pathways	Kinoshita <i>et al.</i> , 2003
Acetic acid	Dog	•Ca ²⁺ currents suppressed	• α 1c subunit of L-type Ca ²⁺ channels significantly reduced in intestine	Liu <i>et al.</i> , 2001a

Table 7: Alterations in RMP in IBD

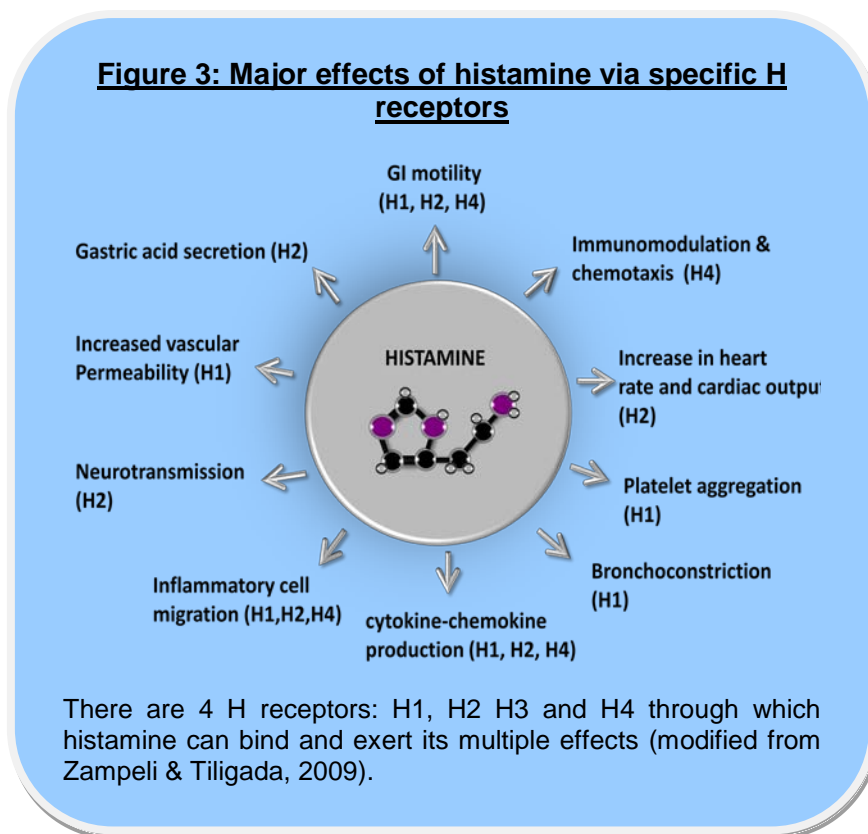
Disease/ Model	Species	Effect	Proposed reason	Reference
Acetic acid	Rat	•Depolarized RMP in inflamed muscle strips	•Proposed through ICC damage	Lu <i>et al.</i> , 1997
TRPV1 ^{-/-}	mouse	•disturbances in membrane potential in circular smooth muscle in the form of spontaneous action potential spikes. Inhibitory junction potential (IJP) prolonged	•TRPV1 may provide a protective mechanism for maintaining membrane stability during inflammation	Sibaev <i>et al.</i> , 2006
<i>Trichinella spiralis</i> induced colitis	Rat	•Circular muscle: lower resting membrane potential and decreased duration of IJP •In controls, the RMP in circular muscle cells was 45.9 ± 2.04 mV whereas inflamed muscle cells RMP was -56.5 ± 2.42 mV	•Stated that mechanisms determining RMP are not fully understood. Therefore they speculated that may be due alterations in electrogenic pump or ICC	Aulí & Fernández, 2007
UC	Human	•circular SM from sigmoid: No effect on RMP, slow wave amplitude or frequency, or IJP amplitude. Wider range in frequency of summation of contractions	N/A	Koch <i>et al.</i> , 1988
Formaldehyde	Rabbit	•Smooth muscle tissue from distal region: Control -55mV to -44mV in colitis	•Suggested alterations in electrogenic pump mechanisms (not Na ⁺ -K ⁺ -ATPase as was intact) could be responsible for depolarization	Cohen <i>et al.</i> , 1986

1.3. Effects of the inflammatory mediator histamine on colonic function

Inflammatory mediators released in different pathophysiological conditions such as UC may also contribute to disturbances in colonic excitability. For this thesis we examined the effect of histamine, one of the major inflammatory mediators, on colonic excitability.

1.3.1. Sources and actions of histamine

One of the main pathophysiological characteristics of allergic diseases such as food allergy, asthma and atopic eczema is inflammation. Histamine is a biological amine that is synthesized from the basic amino acid histidine and is a major mediator in many of these inflammatory and allergic reactions (Dy and Schneider, 2004).



The main sources

of histamine in humans are mast cells, basophils, gastric enterochromaffin-like cells and histaminergic neurons in the brain (MacGlashan, 2003). Mast cells are

derived from hematopoietic progenitor cells in the bone marrow and are a key source of powerful mediators of allergic inflammation including not only histamine but proteinases, cytokines, leukotrienes and prostaglandins. Mast cell activation is a major process in allergic reactions since it can result in the development of microvascular leakage and edema (Xie & He, 2005). Histamine can be released from mast cells via exocytosis by various immunological and non-immunological stimuli such as allergens, drugs, cold and endogenous peptides (e.g. bradykinin or substance P). Upon its release it can modulate many critical functions such as cell migration, GI motility and cytokine release (see Fig. 3) (Zampeli & Tiligada, 2009). Histamine is neither expressed by enteric neurons nor acts as a neurotransmitter in the ENS. Instead it acts in a paracrine manner (Wood, 2006)

Four types of Histamine (H) receptors have been identified: H1, H2, H3 and H4 receptors and are differentially expressed in assorted cell types (Akdis & Simons, 2006). These receptors exert various effects upon binding of histamine since they are coupled to different G-proteins that activate different signaling pathways.

1.3.2. H1 receptor

H1 receptors are found throughout the body and are coupled predominantly to $G_{q/11}$ proteins. Binding of histamine to this receptor type results in stimulation of phospholipase C (PLC) which promotes inositol trisphosphate (IP_3)- dependent Ca^{2+} release from intracellular stores, diacylglycerol (DAG) production and subsequent activation of PKC (Fig. 4). Hence H1 receptor

stimulation can affect cellular activities that are sensitive to these signaling by-products. For example in human glioblastoma cells, histamine application causes hyperpolarization through stimulation of the H1 receptor pathway resulting in an increase in $[Ca^{2+}]_i$ and activation of

intermediate-conductance Ca^{2+} -activated K^+ channels (IK_{Ca})

(Fioretti *et al.*, 2009). H1

receptors are also coupled to $G_{i/o}$ proteins and thus can decrease cAMP levels by inhibiting adenylate cyclase. In tracheal myocytes, application of

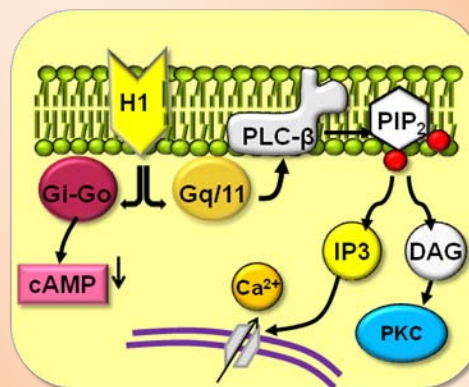
histamine resulted in H1 receptor-dependent activation of NSCC

through coupling to $G_{i/o}$ proteins and increased $[Ca^{2+}]_i$ by $G_{q/11}$ proteins (Wang *et al.*, 2000a). Another study using tracheal myocytes found that histamine application activated a Ca^{2+} -activated Cl^- conductance through an increase in $[Ca^{2+}]_i$ brought about by the H1 pathway (Janssen & Sims, 1993). Histamine can also activate the transcription factor $NF-\kappa\beta$ which can regulate the expression of many pro-inflammatory mediators (Roumestan *et al.*, 2008).

A study examining the contribution of H1 receptors to asthma found that when H1 receptor KO mice were treated with ovalbumin, allergic responses in

Figure 4:

H1 receptor signaling pathway



H1 receptors are mainly coupled to $G_{q/11}$ proteins. Upon stimulation, $G_{q/11}$ activates PLC- β which produces IP₃ and DAG through hydrolysis of PIP₂

the airway were suppressed (i.e. decreased levels of IL-4, IL-5 and TGF- β). This study concluded that activation of H1 receptors by histamine plays an important role in enhancing the Th2 response in airway inflammation (Miyamoto *et al.*, 2006).

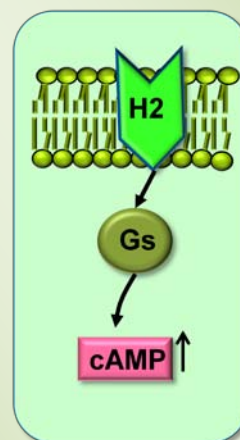
1.3.3. H2 receptor

H2 receptors are coupled to G_s proteins and therefore can increase cyclic adenosine monophosphate (cAMP) concentration via activation of adenylate cyclase (Fig. 5). cAMP in turn can

activate protein kinase A (PKA) and the transcription factor, cAMP Receptor Element Binding protein which modulates many physiological processes (Haas *et al.*, 2008). When histamine binds to H2 receptors located on the membranes of parietal cells in the stomach, the increase in PKA stimulates the proton pump H⁺/K⁺ATPase resulting in gastric acid secretion (Prinz & Gratzl, 2003). Mice

that are deficient in H2 receptors exhibit marked hypertrophy in gastric mucosa but acid secretion is surprisingly normal due to compensation by cholinergic mechanisms (Kobayashi *et al.*, 2000).

Figure 5:
H2 receptor signaling pathway



H2 receptors are coupled to G_s proteins. Upon binding of histamine to H2 receptor, G_s activates adenylate cyclase which increases the levels of the secondary messenger cAMP.

1.3.4. H3 receptor

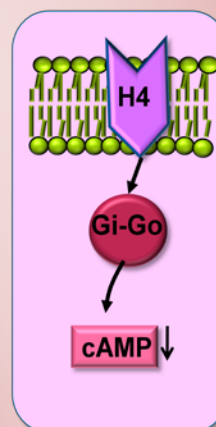
Studies have revealed that H3 receptors are predominantly found on neurons and mainly act to negatively regulate neurotransmitter release in the brain, airways and digestive system (Arrang *et al.*, 1983; Schlicker *et al.*, 1989; Schlicker *et al.*, 1993; Blandizzi *et al.*, 2001). Experiments in guinea pig intestine found that contractility is modulated by H3 receptors acting on transmitter release from enteric neurons (Blandizzi *et al.*, 2001). This study also revealed that this action was via H3/ $G_{i/o}$ coupling since application of pertussis toxin ($G_{i/o}$ inhibitor) could attenuate the inhibitory effect of histamine on acetylcholine release from cholinergic nerve endings (Brandizzi *et al.*, 2001). However the relevance of this receptor in human gastrointestinal motility is called into question due to the lack of H3 receptor expression throughout the GI tract (Sander *et al.*, 2006).

1.3.5. H4 receptor

The H4 receptor is most closely related to the H3 receptor sharing 35% homology. It is pertussis-toxin-sensitive and expressed predominantly in cells of the immune system such as mast cells, monocytes, eosinophils, T cells, natural killer cells and also peripheral tissues

Figure 6:

H4 receptor signaling pathway



H4 receptors are coupled to $G_{i/o}$ proteins. Stimulation of this receptor activates $G_{i/o}$ which inhibits adenylyl cyclase and therefore decreases cAMP levels.

such as the spleen, thymus, colon and bone marrow (Damaj *et al.*, 2007). The H4 receptor can enhance leucocyte migration and recruitment from bone marrow to sites of inflammation via the $G_{i/o}$ pathway (see Fig. 6) therefore implicating it in chemotaxis. In addition, it increases $[Ca^{2+}]_i$ and augments the expression of adhesion molecules such as CD54 (Barnard *et al.*, 2008). Pathologically, H4 receptors play a significant role in not only the initial inflammatory signal by increasing immune cell numbers in conditions such as asthma and allergic disorders, but also in the maintenance of inflammation (Zampelli & Tiligada, 2009).

1.3.6. H receptor distribution in the GI tract

In the human GI tract, immunohistochemical and molecular studies have revealed the presence of H1, H2 and H4 receptors but interestingly not the H3 receptor. H1 receptors are widely expressed in enterocytes, muscle layers, blood vessels, immune cells and ganglion cells of the myenteric plexus in the human GI tract (Sander *et al.* 2006). H2 receptors are located on parietal cells in the mucosa of the fundus, intestinal epithelium, immune cells and myenteric ganglia (Diaz *et al.*, 1994; Sander *et al.*, 2006). H3 receptors have not been detected in the human GI tract though it has been reported in the rat and guinea-pig GI tract (Blandizzi *et al.*, 2001; Héron *et al.*, 2001; Sander *et al.*, 2006). Transcriptional expression of the H4 receptor was reported in the human stomach, small intestine and colon though at lower levels than H1 and H2. H4 receptors were expressed predominantly in leucocytes inside mucosa and submucosal blood

vessels in the colon (Oda *et al.*, 2000; Sander *et al.*, 2006). Table 8 is a summary of the distribution of H receptors in tissue and cells in the human GI tract.

Properties	H1	H2	H3	H4
G-protein	G _{q/11}	Gα _s	G _{i/o}	G _{i/o}
Signal transduction	PLC, IP ₃ , Ca ²⁺ , DAG, PKC,	AC, cAMP, PKA, CREB	↓AC, ↓cAMP, MAPK, Akt/GSK3	↓AC, ↓cAMP, MAPK, ↑[Ca ²⁺]
GI expression	Ubiquitously expressed throughout gut wall Mucosa and muscular layer, enteric nerves	Ubiquitously expressed throughout gut wall Mucosa & muscular layer	Generally absent	Mucosa and muscular layer (though lower than H1 and H2)
GI cell expression	Ganglion cells of myenteric plexus, intestinal fibroblasts (exclusively), epithelial & immune cells, enterocytes, connective tissue cells	Epithelial cells, immune cells, enterocytes	N/A	Only few cells. Mainly leucocytes inside mucosal and submucosal blood vessels, epithelial cells, enterocytes
Expression change in IBS & FA patients	Significantly increased in mRNA (though did not state where specifically)	Significantly increased in mRNA (though did not state where specifically)	N/A	No change

Table 8:

Summary of H receptor distribution in human GI tract
Summarized from Sander *et al.*, 2006

1.3.7. Histamine involvement in IBD

In IBD, there is an increase in the number of mast cells and their cellular contents such as IL-16, TNF- α and substance P (Rijnierse *et al.*, 2007). In patients with CD, degranulation of mast cells and histamine secretion were significantly increased from controls and correlated with increased disease activity (Knutson *et al.*, 1990). Elevated levels of histamine in the mucosa were observed in patients with allergic enteropathy and UC (Raithel *et al.*, 1995). In TNBS-induced colitis in rats, release of histamine from mast cells was found to contribute to tissue damage in this model (Zhao *et al.*, 2009). These studies therefore suggest a link between mast cell numbers, histamine and inflammatory conditions.

Histamine can also influence the cytokine profile in inflammatory diseases such as IBD through altering the Th1-Th2 balance. In particular, it causes an elevation in the production of Th2 type cytokines (e.g. IL-10 and IL-13) and suppresses Th1 type cytokines such as IFN γ (Bene *et al.*, 2004). In histamine-deficient, histidine decarboxylase KO mice (HDC^{-/-}), clinical and histological activity caused by DSS treatment was not as severe. This suggests that histamine is an important contributor to damage incurred in DSS-induced colitis. In addition there were significantly fewer IL-10 positive lymphocytes in HDC^{-/-} mice and increased Th1 cytokines such IL-1, TNF- α and IFN- γ (Bene *et al.*, 2004). The H4 receptor has also been implicated in contributing to IBD as oral

administration of H4 receptor antagonists significantly decreased TNBS-induced colon damage and influx of neutrophils (Varga *et al.*, 2005).

In IBD, there are major alterations in mucosal secretion that result in symptoms such as diarrhea. Application of histamine can stimulate Cl⁻ secretion via activation of H1 receptors and subsequent eicosanoid synthesis and release of prostaglandins across the human and guinea-pig colonic epithelium (Wang *et al.*, 1990; Kelly *et al.*, 1995).

1.3.8. Histamine and GI contractility

Several studies have examined the effect of histamine on contractility. In longitudinal muscle of guinea-pig ileum, histamine caused depolarization of the membrane potential (Bolton *et al.*, 1981). In another study using guinea-pig intestine, exogenous application of histamine caused contraction through H1-receptor activation. This contraction was not via histamine-induced ACh release as pretreatment with atropine did not affect the contractile response to histamine (Leurs *et al.*, 1991). In a study performed on human small intestine and colon, histamine had variable effects on contractility though pro-contractile effects predominated. Application of the ganglion blocker, hyoscine or anti-adrenaline drugs did not prevent the histamine effects suggesting its actions are independent of neurons. The authors proposed that during inflammatory conditions, histamine levels increase and upon their release act directly on smooth muscle (Bennett & Whitney, 1966).

All of the mentioned studies suggest that histamine contributes significantly to altered gut function seen in inflammatory conditions such as UC. However it is surprising that so few studies have examined its role in colonic motility. Therefore in chapter 5.1., H receptor expression and responses to histamine and histamine specific-agonists were examined and compared in monkey and murine colon.

1.4. Role of NSCC in smooth muscle depolarization and contraction and their molecular candidates

As mentioned in section 1.1, the ionic mechanisms that underlie basal colonic excitability have not been clearly defined. Since pathophysiological conditions such as IBD can disturb colonic excitability, it is essential to identify the ionic conductances that regulate excitability in order to explain changes evoked in inflammatory conditions. In the GI tract, NSCC have been shown to play an essential role in depolarization and hence contraction. In this section the contribution of NSCC in agonist-induced depolarization and contraction in the GI tract will be introduced as well as a brief summary of molecular candidates for NSCC.

1.4.1. Muscarinic receptor-activated NSCC in the GI tract

Muscarinic (M) receptors play essential roles in linking parasympathetic neurotransmitter release with smooth muscle excitation and contraction. The muscarinic receptor subtypes, M2 and M3 are reported to mediate enteric excitatory motor neurotransmission in the GI tract (Unno *et al.*, 2006). M2 receptors are coupled to $G_{i/o}$ proteins, and their activation results in a decrease in intracellular cAMP levels through inhibition of adenylate cyclase (Okamoto *al.*, 2004). Activation of M3 receptors, which are coupled to $G_{q/11}$ proteins, stimulates PLC resulting in the production of IP_3 and DAG via hydrolysis of phosphatidylinositol 4,5-bisphosphate (PIP_2) (Unno *et al.*, 2006). In the GI tract,

stimulation of M receptors results in activation of non-selective cation channels (NSCC) which cause membrane depolarization to values within the window current of voltage-dependent Ca^{2+} channels (VDCC). This increase in Ca^{2+} influx results in smooth muscle contraction and promotes intestinal motility. Muscarinic receptor-induced NSCC activated current (mI_{CAT}) was first recorded in rabbit jejunal myocytes. Activation of mI_{CAT} results in membrane depolarization and opening of VDCC (Brading & Sneddon, 1980; Benham *et al.*, 1985). Acetylcholine (ACh) is a major excitatory neurotransmitter that can activate several NSCC with conductances of 10-140pS in different species depending on experimental conditions (Zholos & Bolton, 1995; Dresviannikov *et al.*, 2006). Channels carrying mI_{CAT} are more or less equally permeable to monovalent cations (Kang *et al.*, 2001). However their Ca^{2+} permeability is relatively low (Inoue & Isenberg, 1990; Zholos & Bolton, 1995). A rise in $[\text{Ca}^{2+}]_i$ is insufficient to activate mI_{CAT} whereas when this current is activated by stimulation of G-proteins, a further rise in $[\text{Ca}^{2+}]_i$ via IP_3 receptor-mediated release by flash photolysis can greatly potentiate this current (Gordienko *et al.*, 2004). Unusually low levels of $[\text{Ca}^{2+}]_i$ abolish mI_{CAT} (Komori *et al.*, 1993; Gordienko *et al.*, 2003). There are no specific blockers for native NSCC thus making it difficult to classify their functional and molecular identities.

Transient receptor potential (TRP) channel members are considered molecular candidates for NSCC recorded in GI smooth muscle cells (as well as other cell types). Difficulties however have arisen in the identification of TRP

channel candidates in native cells since there are few blockers and agonists that are specific for a particular subtype. However the recent development of specific TRP-KO mice and anti-sense technology has begun to unravel molecular identities of NSCC in smooth muscle. The following sub-section is a brief summary outlining some main facts currently known about the three major subfamilies of TRP channels.

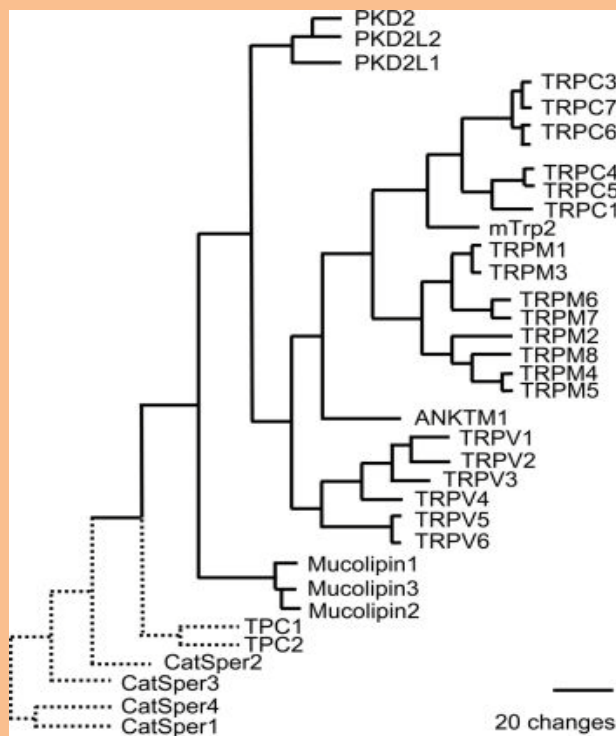
1.4.2. Molecular candidates for NSCC

The TRP superfamily of channel proteins is expressed in many cell types from a great variety of multicellular organisms (Venkatachalam & Montell, 2007). This superfamily is unified by their relative homology to the product of the *Drosophila trp* gene. Seven main subfamilies make up this superfamily on the basis of structural homology:

TRPC (Canonical),

TRPV

Figure 7:
TRP superfamily



The three main subfamilies of the TRP superfamily are TRPC (canonical), TRPV (Vanilloid) & TRPM (Melastatin). (From IUPHAR database)

(Vanilloid), TRPM (Melastatin), TRPP (Polycystin), TRPML (Mucophilin), TRPA (Ankyrin) and TRPN (no mechanoreceptor potential C, NOMPC) (see Fig. 7) (Ramsey *et al.*, 2006). Functional TRP channels are either composed of homo- or heteromultimers of four TRP subunits and the short hydrophobic stretch between transmembrane (TM) 5 and 6 is thought to form a cation-permeable pore region. TRP channels are deficient in a conserved series of arginine residues in segment 4 that form the sensor for TM potential in classical 6-TM voltage-gated cation channels (Montell, 2005). TRP channels are a highly unusual family of channels as they display a remarkable diversity of cation selectivity and specific activation mechanisms. They are involved in many processes such as vasoregulation (TRPC3/4/5), temperature sensing (TRPV family), signaling in the central nervous system (TRPC1/3/4) and the regulation of contraction in SMC. Also TRP superfamily members are essential components of store-operated, receptor-operated, stretch & temperature-activated and tonically active channels (Clapham, 2003; Vriens *et al.*, 2004; Owsianik *et al.* 2006). Their multiple functions and properties are further complicated by the fact that many TRP channels can assemble as heteromeric complexes (Strübing *et al.*, 2003; Poteser *et al.*, 2006). The following section is a very brief summary of known properties of the members belonging to the three main subfamilies, TRPC, TRPM and TRPV.

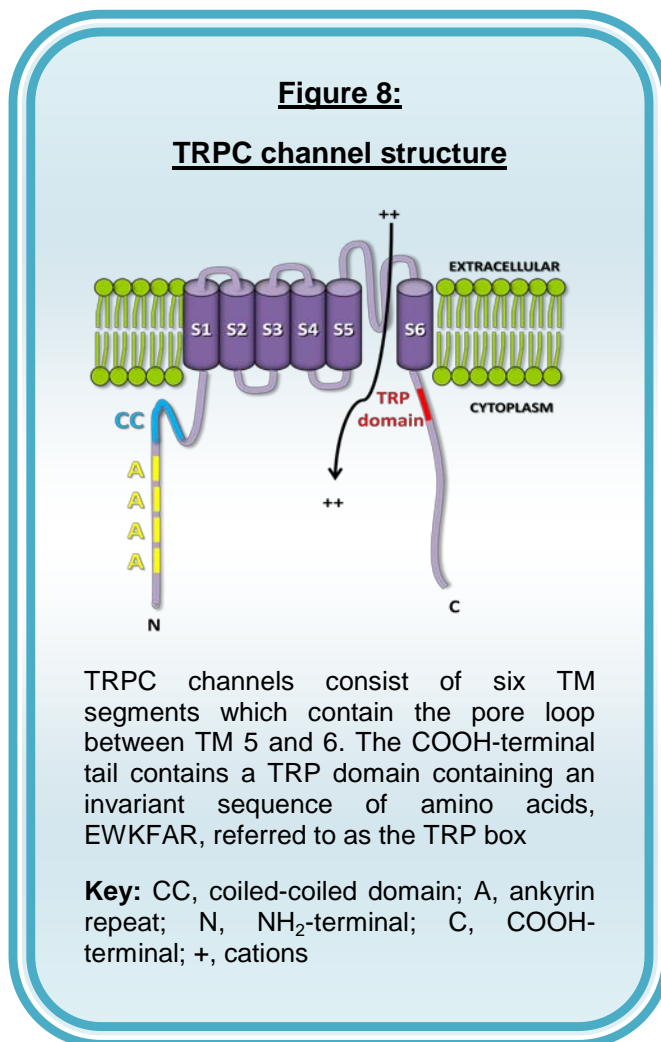
TRPC subfamily: There are seven mammalian TRPC proteins which are most closely related to *Drosophila* TRPs (Nilius *et al.*, 2007). The members of this

subfamily share $\geq 30\%$ amino acid identity with each other (Venkatachalam & Montell, 2007). The largest region of homology spans the six TM segments which contain the pore loop (see Fig. 8) Their common structural motif consists of a COOH-terminal tail and a TRP

domain containing an invariant sequence of amino acids, EWKFAR, referred to as the TRP box which has been shown to be necessary for PIP_2 binding and regulation of channel gating (Ramsey *et al.*, 2006). There are also three or four NH_2 -terminal ankyrin repeats (which are 33 amino acid sequences that participate in protein-protein interactions and cytoskeleton anchorage) (Nilius *et al.*, 2007).

All TRPC members are activated via pathways coupled to

stimulation of PLC. However, there is still controversy over the mechanisms that lead to activation of TRPC (as well as other TRP subfamily members) following PLC activation. TRPC members are often divided into 4 groups: (1) TRPC1, (2)



TRPC2, (3) TRPC3, 6 and 7 and (4) TRPC4 and 5 based on their sequence similarity.

TRPC1: This was the first mammalian TRP channel identified and its single channel conductance is estimated at around 16pS and is non-selective (Vazquez *et al.*, 2004a). This channel is widely expressed such as in the central nervous system, epithelia, cardiovascular system, liver and uterine myometrium (Abramowitz & Birnbaumer, 2009). It is generally accepted that when TRPC1 is expressed in heteromeric complexes with TRPC3, C4 or C5, it functions as part of a $G_{q/11}$ receptor-operated cation channel (Strübing *et al.*, 2001). For example in glomerular mesangial cells, TRPC1 forms a complex with TRPC4 (Sours-Brothers *et al.*, 2009). It has also been suggested that TRPC1 forms a stretch-activated cation channel in vertebrate cells (Maroto *et al.*, 2005). However this remains controversial as a later report found no significant role for TRPC1 in stretch-activated channels when expressed alone in either COS or CHO cells (Gottlieb *et al.*, 2008). In addition mechano-sensation was normal in TRPC1 KO mice. Surprisingly these KO mice show no apparent phenotype with no detectable up-regulation in other TRPC channel members (Dietrich *et al.*, 2007). This is unexpected since TRPC1 is the most widely expressed TRPC subunit and has been implicated in many different cellular functions such as vascular smooth muscle cell proliferation (and hence pulmonary vascular resistance), regulating skeletal muscle $[Ca^{2+}]_i$ and lymphocyte activation (Golovina *et al.*, 2001; Mori *et al.*, 2002; Vandebrouck *et al.*, 2002).

TRPC2: This complete gene was lost in the Old World monkey and humans and the remaining nonfunctional truncated protein is considered a pseudogene (Yildirim & Birnbaumer, 2007; Vannier *et al.*, 1999). Nevertheless, a number of studies have been performed in rodents to identify its function. These have revealed that TRPC2 is involved in the detection of pheromonal signals by the mammalian vomeronasal organ and TRPC2 KO exhibit irregular sexual and social behaviors (Zufall, 2005).

TRPC3: These channels have a single channel conductance of 60-66pS, display double rectification and are weakly Ca^{2+} selective (Clapham *et al.*, 2001; Dietrich *et al.*, 2005b; Owsianik *et al.*, 2006). TRPC3 channels exhibit high basal activity which can be increased by G-protein coupled receptor (GPCR) stimulation or receptor tyrosine kinases (Vasquez *et al.*, 2004a; Dietrich *et al.*, 2005b). Application of exogenous DAG reflects the mechanism of action upon PLC-linked GPCR stimulation, independent of IP_3 and store depletion (Hofmann *et al.*, 1999; Beck *et al.*, 2006). A study in 2004 revealed that TRPC3 activation by synthetic DAGs and receptor stimulation was dependent on src kinases, as pharmacological inhibition of these kinases abolished muscarinic receptor stimulation and DAG activation. They suggested that DAG was not acting directly on these channels to induce activation (Vazquez *et al.*, 2004b). PKC has also been shown to negatively regulate these channels (Venkatachalam *et al.*, 2003). The importance of this channel in regulating the RMP was revealed in TRPC6^{-/-} where TRPC3 expression was significantly increased in SMC. This resulted in higher basal cation entry, and hence, more depolarized membranes.

Consequently these mice exhibited an elevated blood pressure and enhanced myogenic contractility in cerebral arteries (Dietrich *et al.*, 2005a).

TRPC4: They are most closely related to TRPC1 and are activated by $G_{q/11}$ and receptor tyrosine kinases. When expressed alone, TRPC4 channels exhibit an unusual double rectifying I-V relationship (Schaefer *et al.*, 2000; Strübing *et al.*, 2001) with a single channel conductance of ~40-55pS (Schaefer *et al.*, 2000; Clapham *et al.*, 2001; Tsvilovskyy *et al.*, 2009) and are weakly Ca^{2+} selective (Owsianik *et al.*, 2006). TRPC4 is a candidate for store-operated Ca^{2+} (SOC) channels activated by depletion of Ca^{2+} stores in aortic endothelial cells (Freichel *et al.*, 2001). It is also a candidate for receptor-operated channels (ROC) activated by muscarinic stimulation in gastric SMC since it is virtually absent in TRPC4 KO mice (Lee *et al.*, 2005; Kim *et al.*, 2006). In TRPC4 expressing HEK cells, neither Rho-kinase inhibitor nor MLCK inhibitors could decrease GTP γ S-induced currents (Sung *et al.*, 2009). Recently it was revealed that this channel is the major component of mI_{CAT} in ileal smooth muscle (Tsvilovskyy *et al.*, 2009). The two primary products of PLC enzyme activity, IP_3 and DAG, cannot directly activate this channel (Schaefer *et al.*, 2000; Clapham *et al.*, 2001). There are two TRPC4 variants: TRPC4 α (full length) and TRPC4 β (lacks stretch of 84 amino acid residues in the C-terminus). PIP_2 inhibited TRPC4 α activity but not TRPC4 β suggesting that this region of 84 amino acids is an important site for PIP_2 interaction (Otsuguro *et al.*, 2008). Intracellular Ca^{2+} can potentiate TRPC4 β channels expressed in HEK cells (Blair *et al.*, 2009).

TRPC5: This channel is highly homologous to TRPC4 (70% sequence similarity) and shares many similar properties such as neither IP₃ nor DAG are sufficient to activate this channel. It has a single channel conductance of ~40pS and like TRPC4, receptor-mediated activation of these channels can be potentiated by trivalent lanthanide cations La³⁺ and Gd³⁺. The mechanism of this effect is thought to be through interaction of these lanthanides at an extracellular Ca²⁺ binding site (Jung *et al.*, 2003). Increases in [Ca²⁺]_i are necessary for potentiation of TRPC5 current as dialysis with the Ca²⁺ chelator, BAPTA can effectively prevent this current potentiation (Blair *et al.*, 2009). Heteromeric TRPC1+C5 channels exhibit a much simpler current-voltage relationship than homomeric TRPC5 with little rectification and the single channel conductance is much smaller than that of homomeric TRPC5 (5pS for TRPC1+C5) (Strubing *et al.*, 2001).

TRPC6: Unlike TRPC3 and 7, TRPC6 exhibits low basal activity (Dietrich *et al.*, 2005b). Studies have demonstrated that these channels can form ROC in the aorta, where activation of TRPC6 underlies the vasopressin-activated cation channel in an aortic smooth muscle cell line (Jung *et al.*, 2002) and the α1-adrenoceptor-activated NSCC in vascular portal vein SMC (Inoue *et al.*, 2001). As with TRPC3, DAG activates these channels independently of PKC in different cell types such as mesenteric artery and portal vein. Recently TRPC6 was reported to be activated by PIP₂ in excised patches in HEK cells (Lemonnier *et al.*, 2008). However Albert and colleagues found that constitutively produced

PIP₂ tonically inhibits the activity of native TRPC6 channels in freshly dispersed rabbit mesenteric artery myocytes. They concluded that PIP₂ has a dual role in regulating TRPC6 channel activity by being a precursor for DAG production for activation and also a direct inhibitor of channel activity (Albert *et al.*, 2008). A study by Boulay implicated calmodulin (CaM) in activation of this channel as the CaM inhibitor calmidazolium could abolish agonist-activated entry through TRPC6 channels (Boulay *et al.*, 2002). Expression studies have shown that TRPC6 is not potentiated by IP₃ (Shi *et al.*, 2004).

The TRPC6^{-/-} mice exhibited an unexpected phenotype as mentioned previously. They had elevated blood pressure, enhanced myogenic contractility in cerebral arteries and enhanced agonist-induced contractility of isolated aortic rings. Further investigation revealed that the RMP in cerebral arteries was more depolarized, accounted for by increased TRPC3 expression (Dietrich *et al.*, 2005a)

TRPC7: Like TRPC3, TRPC7 exhibits high basal activity and rectification at positive and negative voltages (see Fig. 9) (Okada *et al.*, 1999; Clapham *et al.*, 2001; Dietrich *et al.*, 2005b). It has a single channel conductance of 25-50pS (Owsianik *et al.*, 2006) (75pS in DT40 cel' ;) and has relatively low selectivity for Ca²⁺ over Na⁺ (Clapham *et al.*, 2001). Studies have revealed that TRPC7 channels can form ROC and are activated by PLC-derived DAG (Hofmann *et al.*, 1999; Beck *et al.*, 2006; Vazquez *et al.*, 2006; Lemonnier *et al.*, 2008). In human keratinocytes, TRPC7-specific knockdown by antisense oligonucleotides caused

a significant decrease in ATP- and CCh- Ca^{2+} entry and also DAG-activated currents (Beck *et al.*, 2006). Another study found that when TRPC7 channels were expressed at low levels (suggested to correspond to native levels) in DT40 B lymphocytes, DAG-activated currents required IP_3 receptors as DT40 cells lacking IP_3 receptors showed no

OAG-evoked single channel activity (Vasquez *et al.*, 2006).

PKC negatively regulates these channels (Vazquez *et al.*, 2006; Venkatachalam & Montell,

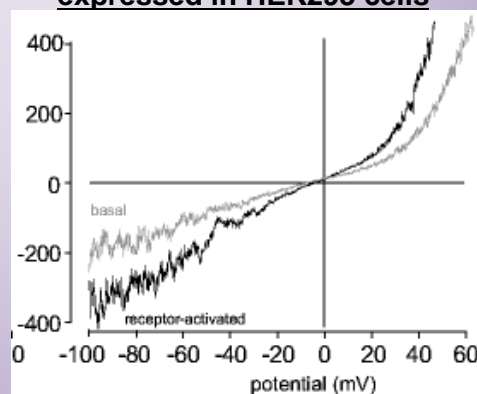
2007). Ca^{2+} entering through these channels upon activation by OAG, has been demonstrated to inhibit these

channels if it is not sequestered by

closely associated SERCA pumps (Lemonnier *et al.*, 2006).

Recently, it has been demonstrated that TRPC7 can be activated by application of PIP_2 and ATP but not IP_3 in excised patches from HEK cells. Surprisingly application of OAG, which activated TRPC7 channels in the cell-attached configuration, failed to do so in excised patches. The investigators suggested that an unknown factor or factors are lost in the excised patch that are necessary for DAG activation therefore suggesting that DAG does not simply directly activate these channels (Lemonnier *et al.*, 2008).

Figure 9:
Current-voltage relationship of TRPC7
expressed in HEK293 cells



TRPC7 exhibits basal activity which is augmented upon receptor stimulation (Dietrich *et al.*, 2005)

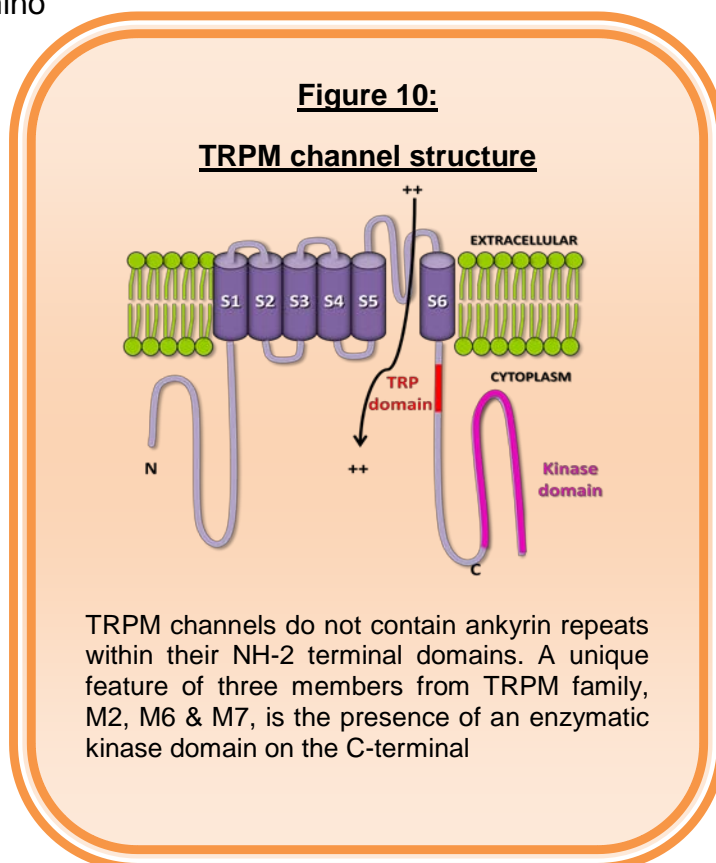
TRPM subfamily: This subfamily comprises of 8 members that have structurally similar N-terminal tails containing four amino acid sequences that have sequence similarity (Fig. 10). The similarity between this subfamily and other TRP channels lies in a stretch of ~250 amino

acids containing the 6TM spanning region (Perraud *et al.*, 2004). The C-terminal tails differ in length and structure between the different TRPM family members and in particular TRPM2, TRPM6 and TRPM7 contain enzymatic domains. Splice variants of all TRPM members have been reported

that can change some of their

functional properties (Vázquez & Valverde, 2006). TRPM members are involved in regulating many physiological processes including Mg^{2+} homeostasis, modulation of membrane potential and taste sensation (Devi *et al.*, 2009).

TRPM1: This channel was first identified by its reduced expression in a metastatic melanoma cell line and therefore thought to act as a melanoma metastasis suppressor. In humans, TRPM1 is now used as a predictor of melanoma progression since its expression is decreased in aggressive forms of



melanoma (Oancea *et al.*, 2009). A recent report suggests that TRPM1 plays a role in Ca^{2+} homeostasis in human melanocytes and changes in its expression correlate with changes in proliferation and differentiation *in vitro* (Devi *et al.*, 2009).

TRPM2: This channel is widely expressed such as in neurons, blood cells and the endocrine pancreas. Channel activation at the plasma membrane can be induced by elevated intracellular levels of adenosine diphosphoribose (ADP-ribose), which bind to part of the Nudix enzymatic domain on the C-terminal, and results in Ca^{2+} influx (Fleig & Penner, 2004; Eisfeld & Lückhoff, 2007). In addition reactive oxygen species, in particular hydrogen peroxide, can lead to activation of these channels which in turn activates a signaling cascade resulting in chemokine production and neutrophil infiltration. Therefore they have been implicated in inflammatory conditions such as UC (Yamamoto *et al.*, 2008; Lange *et al.*, 2009).

TRPM3: This protein is found mainly in the kidney and brain (though not in the kidney of mice) and has received little attention in comparison with its other subfamily members. It exhibits constitutive activity with conductance states ranging from 80-120pS, and it is permeable to both monovalent and divalent cations. The physiological role of this channel still remains poorly defined, though it was proposed to be involved in renal Ca^{2+} homeostasis (Grimm *et al.*, 2003). A recent study found that TRPM3 acts as an ionotropic steroid receptor that when

activated, enhances insulin secretion from pancreatic β cells (Wagner *et al.*, 2008).

TRPM4: This channel is found in excitable and non-excitable cells and so far, two splice variants have been identified (short form, TRPM4a and the long form, TRPM4b). Unlike most of the other TRP channels, it is essentially impermeable to Ca^{2+} ions but conducts Na^+ and K^+ with a single channel conductance of $\sim 25\text{pS}$. This channel is directly activated by Ca^{2+} and is therefore thought to provide a mechanism for depolarization to occur in a Ca^{2+} dependent manner (Launay *et al.*, 2002; Marigo *et al.*, 2009). Recently it was revealed that depolarizing currents generated by TRPM4 are important for insulin secretion in β -cells (Marigo *et al.*, 2009). In immune cells, TRPM4 is vital for Ca^{2+} oscillations and cytokine production (Vennekens *et al.*, 2007). This TRP channel is also involved in mast cell migration (Shimizu *et al.*, 2009).

TRPM5: Like TRPM4, this channel is a Ca^{2+} - and voltage-activated Ca^{2+} -impermeable channel, with a single channel conductance of 25pS (Fleig & Penner, 2004; Damann *et al.*, 2008). TRPM5 differs from TRPM4 in its activation and inactivation kinetics and responsiveness to Ca^{2+} release from intracellular stores (Fleig & Penner, 2004). Recent findings have identified this channel in playing a vital role in the signal transduction pathway following activation of sweet, bitter and umami receptors found on the tongue (Damann *et al.*, 2008). In addition studies have implicated a role for this channel in insulin release (Pérez *et al.*, 2002; Zhang *et al.*, 2003).

TRPM6: This channel is found mainly in the colon and kidney where it plays a critical role in Mg^{2+} (re)absorption (Fleig & Penner, 2004). Mutations in the gene encoding for TRPM6 result in familial hypomagnesaemia with secondary hypocalcaemia therefore highlighting its important role in Mg^{2+} homeostasis (Cao *et al.*, 2009). Studies have revealed that TRPM6 exhibits constitutive activity with a 40pS single channel conductance which can be inhibited by $[Mg^{2+}]_i$ (Voets *et al.*, 2004; Cao *et al.*, 2009). TRPM6 contains a C-terminal α -kinase domain but the function of this enzymatic domain in relation to channel activity remains elusive although a recent study did show that modulation of TRPM6 activity by intracellular ATP requires an ATP binding motif in the kinase domain (Thebault *et al.*, 2008).

TRPM7: Like TRPM2 and TRPM6, TRPM7 is a bifunctional molecule consisting of an ion channel fused to an α -kinase domain (Montell, 2003; Langeslag *et al.*, 2007). It is constitutively active and has a single channel conductance of 40pS (Nadler *et al.*, 2001; Fleig & Penner, 2004). Strong outward rectification of TRPM7 currents reflects the permeation properties of the channel where, at negative potentials, there is selective inward flux of divalent cations. At positive potentials, there is outward movement of monovalent cations such as K^+ and Cs^+ but not Na^+ (Fleig & Penner., 2004). It is involved in Mg^{2+} homeostasis and is essential for cell viability and proliferation (Nadler *et al.*, 2001; Runnels *et al.*, 2001; Hanano *et al.*, 2004; He *et al.*, 2005;). The high constitutive activity of this channel can be suppressed by high intracellular concentrations of MgATP and

free Mg^{2+} (Nadler *et al.*, 2001). Controversy surrounds the mechanism of PIP_2 regulation in TRPM7 channels. Runnels and colleagues suggested that receptor-mediated activation of PLC in HEK cells inhibits TRPM7 by hydrolyzing and reducing the local PIP_2 concentration (Runnels *et al.*, 2001). Conversely, another report suggested that opening of TRPM7 channels in N1E-115 cells closely correlated with PLC activation (Langeslag *et al.*, 2007).

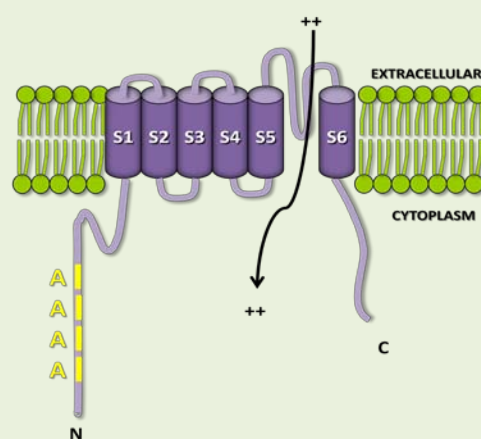
TRPM8: Studies have shown that TRPM8 is expressed in neurons and prostate cells. Temperatures below 24°C and cooling agents such as menthol can activate this 83pS single channel conductance. In addition, intracellular pH can regulate channel activity with acidification inhibiting responses to cold but not menthol (Andersson *et al.*, 2004). This member is regulated in part by androgens through androgen response elements in the promoter region of TRPM8. Its expression is significantly increased in androgen-dependent prostate cancer cells and therefore may be a useful prognostic marker for predicting prostate cancer development. It is also involved in modulation of cell proliferation and apoptosis (Prevarskaya *et al.*, 2007; Gkika & Prevarskaya, 2009).

TRPV subfamily: This family of TRP channels comprises of 6 members, four of which are involved in nociception and thermosensing (TRPV1-4) (Clapham, 2003; Vriens *et al.*, 2004). TRPV5 and 6 contribute to renal absorption/reabsorption processes. TRPV proteins share ~25% homology with TRPC channels over a region spanning TM domains 5 and 6 (Ventkatachalam & Montell, 2007). They

contain 3-5 ankyrin repeats in their cytosolic N-termini (see Fig. 11) (Nilius *et al.*, 2007).

TRPV1: This was the first mammalian TRPV identified when it was found to be activated by the inflammatory vanilloid compound, capsaicin. It has a single channel conductance ranging from 35 to 80pS and it's Ca^{2+} selectivity differs depending on activation mechanism (e.g. $P_{\text{Ca}}:P_{\text{Na}}= 10:1$ for capsaicin activated current whereas 4:1 for heat-activated current). In addition, it responds to heat $\sim >45^\circ\text{C}$ and also low pH ($\sim < 5.5$) as well as many other chemicals, including endocannabinoid and anandamide (Conway, 2008). It is highly expressed in trigeminal nerves, dorsal root ganglion and neurons (Venkatachalam & Montell, 2007).

Figure 11:
TRPV channel structure



TRPV channels contain 3-5 ankyrin repeats on their N termini and share 25% homology with TRPC channels in the region spanning TM domains 5 and 6. TRPV1-4 are involved in nociception whereas V5 & 6 are important in Ca^{2+} absorption

Studies performed in the colon found that TRPV1 is expressed predominantly in the rectum and distal colon and is located in mucosa, submucosa, smooth muscle layers and myenteric plexus. Addition of capsaicin,

the TRPV1 activator, results in transient contraction in the proximal colon and transient followed by long-lasting contraction in the distal colon. The different contractile effects of capsaicin are due to activation of different pathways i.e. intrinsic cholinergic and extrinsic sensory pathways involving release of tachykinins such as substance P and neurokinin A (Matsumoto *et al.*, 2009).

TRPV2: TRPV2 is 50% identical to TRPV1 and forms a weakly Ca^{2+} -selective channel whose single channel conductance remains to be determined (Clapham *et al.*, 2001). TRPV2 has been proposed to be involved in nociception and mechano-sensation which is supported by the fact that they are expressed in A δ mechano- and sensory- neurons in the dorsal root ganglion (Lewinter *et al.*, 2004). However TRPV2 is also found in non-neuronal tissues suggesting alternative roles for this channel other than pain sensation (Caterina *et al.*, 1999).

The properties of TRPV2 activation also exhibit species specificity. When rat and mouse TRPV2 are expressed in HEK cells, they can be activated by noxious heat (up to 53°C) and 2-APB. However human TRPV2 channels are not affected by these stimuli (Neeper *et al.*, 2007). Unlike TRPV1, these channels are not sensitive to capsaicin or changes in pH (Caterina *et al.*, 1999; Neeper *et al.*, 2007). Phosphatidylinositol-3-kinase (PI 3-kinase) promotes TRPV2 activity in CHO cells and in the same cells, TRPV2 was shown to be constitutively active under resting conditions that resulted in increased basal $[\text{Ca}^{2+}]_i$ levels (Penna *et al.*, 2006). In TRPV2 KO mice, mechanical and thermal pain behavioral assays detected no differences from normal mice (Park *et al.*, 2008).

TRPV3: This channel is highly expressed in the distal colon mucosa, skin, tongue and nose but in very low amounts in sensory neurons (Ueda *et al.*, 2009; Vriens *et al.*, 2009). It is activated by warm temperatures ranging between 34-39°C and exogenous chemical ligands. TRPV3 shares 40% structural similarity with TRPV1 and has a single channel conductance of ~190pS (Nilius *et al.*, 2007). Its involvement in cutaneous thermosensation was revealed in TRPV3 KO mice, where they exhibited abnormal behavioral responses to innocuous and noxious heat (Moqrich *et al.*, 2005).

TRPV4: Both physical and chemical stimuli including moderate heat (>27°C), hypotonic swelling, shear stress and the synthetic phorbol derivative 4 α -phorbol-12,13-didecanoate can activate this channel. Interestingly TRPV4 is not activated by cell swelling via mechanosensing itself, rather through cell swelling activated phospholipase A2 and formation of epoxyeicosatrienoic acids (Vriens *et al.*, 2009). This channel is moderately Ca²⁺ selective and has a single channel conductance of 90pS (Nilius *et al.*, 2007). It is expressed in sensory ganglia, free nerve endings and DRG. A recent study revealed that intracolonic administration of the TRPV4 activator 4 α -PDD caused visceral hypersensitivity, which is a major clinical feature of patients suffering from irritable bowel syndrome (Cenac *et al.*, 2008).

TRPV5: This TRP protein is distinct from the first four members of the TRPV family, as it is not activated by heat and is highly Ca²⁺ selective ($P_{Ca}: P_{Na} >100$). Removal of extracellular Ca²⁺ results in the influx of monovalent cations and a

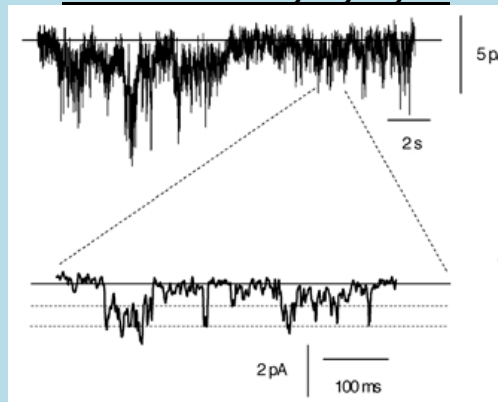
single channel conductance of 75pS under these conditions (Vennekens *et al.*, 2000). Ca^{2+} is the sole ion transported through this channel in physiological conditions and therefore it plays an essential role in organs that mediate transcellular Ca^{2+} transport such as the duodenum, jejunum, colon but predominantly the kidney (Van Abel *et al.*, 2005; Mensenkamp *et al.*, 2007; Venkatachalam & Montell, 2007). This important role was made apparent from studies of TRPV5 KO mice which exhibited impaired Ca^{2+} reabsorption in the kidney, reduced bone thickness and intestinal Ca^{2+} hyperabsorption (Hoenderop *et al.*, 2003).

TRPV6: This channel shares 75% homology with TRPV5 and exhibits similar characteristics including no response to heat and high Ca^{2+} selectivity. A single aspartic residue at position number 542 was found to be crucial for this Ca^{2+} permeation (Nilius *et al.*, 2001). This channel has a single channel conductance between 40-70pS when only monovalent cations are present externally (Nilius *et al.*, 2007). Like TRPV5, TRPV6 plays an important role in Ca^{2+} absorption especially in the small intestine and prostate where it is predominantly expressed (Hoenderop *et al.*, 2000). This is evident from TRPV6 KO mice that display defective intestinal Ca^{2+} absorption, decreased bone marrow density and increased urinary Ca^{2+} excretion (Bianco *et al.*, 2007). In addition this channel appears to play a role in tumor development and progression as expression levels are up-regulated in tissue samples from breast, prostate, colon, thyroid, ovary and pancreatic tumors (Zhuang *et al.*, 2002; Prevarskaya *et al.*, 2007).

1.4.3. Molecular candidates for smooth muscle NSCC

Studies in vascular SMC suggested that TRPC1 cation currents were activated in response to hypo-osmotic swelling and store depletion (Maroto *et al.*, 2005). However in TRPC1 KO mice, stretch-activated and store-operated currents in vascular SMC from cerebral arteries were similar to wild-type therefore suggesting these channels are not mechanosensitive or activated by store-depletion (Dietrich *et al.*, 2007).

Figure 12:
Constitutively active NSCC in rabbit mesenteric artery myocytes



Single channel currents resolved with whole cell recordings. TRPC3 is the proposed molecular candidate for these constitutively active NSCC (Albert *et al.*, 2003).

In rabbit ear artery myocytes, TRPC3 is the proposed molecular candidate for constitutively active Ca^{2+} -permeable NSCC (Fig. 12) (Albert *et al.*, 2006). This basal activity is suggested to reside in constitutive $G_{i/o}$ proteins that are coupled to phospholipase D. This phospholipase D hydrolyses phosphatidylcholine into phosphatidic acid which is subsequently converted to DAG which induces channel opening via a PKC-independent mechanism (Albert *et al.*, 2005).

As mentioned previously TRPC6 is the proposed molecular candidate for $\alpha 1$ -adrenoceptor-activated NSCC in vascular SMC (Inoue *et al.*, 2001) and the vasopressin-activated cation channel in an aortic A7r5 cell line (Jung *et al.*,

2002). Welsh and colleagues reported that antisense oligodeoxynucleotides to TRPC6 greatly suppressed arterial smooth muscle depolarization and constriction caused by elevated pressure in cerebral arteries (Welsh *et al.*, 2002). These studies strongly suggested that TRPC6 plays an important role in receptor-operated and pressure-induced NSCC activated in vascular SMC. Therefore it was expected that TRPC6 KO mice would exhibit a loss of vascular tone and suffer from hypotension. However, these mice showed an elevated blood pressure, higher basal cation entry, and more membrane depolarization through compensation by increased TRPC3 expression (Dietrich *et al.*, 2005a).

As mentioned previously, mI_{CAT} plays an important role in initiating contraction in intestinal smooth muscle (Zholos & Bolton, 1995; Dresviannikov *et al.*, 2006). A number of studies proposed a definitive link between TRPC4/TRPC5 and mI_{CAT} since these TRP channels and this native current exhibit similar properties in terms of regulation through the PLC pathway, involvement of IP_3 and intracellular Ca^{2+} regulation (Schaefer *et al.*, 2000; Kanki *et al.*, 2001; Okamoto *et al.*, 2004; Plant & Schaefer, 2005; Kim *et al.*, 2007). Examination of gastric SMC from TRPC4 KO mice revealed that CCh-induced NSCC were significantly reduced. Therefore TRPC4 appeared to form an essential component in NSCC activation in the murine stomach following muscarinic stimulation (Lee *et al.*, 2005). Slow waves were still present in these mice which ruled out TRPC4 as the NSCC responsible for regulating pacemaker activity in ICC (Lee *et al.*, 2005; Kim *et al.*, 2006).

A recent study revealed that 80% of mI_{CAT} stimulated by CCh in intestinal smooth muscle was through TRPC4 channels. A 55pS conductance recorded in wildtype SMC was absent in the TRPC4 KO mice and therefore identified as the TRPC4 conductance that contributes to the majority of mI_{CAT} . TRPC6 was identified as the other channel responsible for the remaining mI_{CAT} since it was completely abolished in SMC from TRPC4/6 KO mice. Furthermore, CCh-induced membrane depolarizations were significantly reduced in TRPC4-deficient ileal myocytes. Deletion of both TRPC4 and TRPC6 further decreased the response. Finally, TRPC4 and TRPC6 KO mice exhibited slower intestinal transit. This study clearly revealed for the first time the molecular identities of mI_{CAT} in intestinal SMC (Tsvilovskyy *et al.*, 2009).

In Chapter 2, we examined the molecular candidates of basally activated NSCC in smooth muscle and SMC from human and monkey colon.

1.5. Contribution of ion channels to smooth muscle excitability

RMP plays a critical role in determining the excitability of smooth muscle, because small changes can result in major alterations in Ca^{2+} entry and $[\text{Ca}^{2+}]_i$ levels. The ionic conductances that contribute to the RMP in different cell types determine their degree of excitability. This section gives a brief summary of the role of K^+ channels, Ca^{2+} activated Cl^- channels and NSCC to RMP.

1.5.1. Contribution of K^+ channels to RMP

K^+ channels play major roles in regulating the RMP. In certain cell types such as cardiac myocytes, the RMP lies very close to $E_K \sim -80\text{mV}$ thus indicating a high permeability to K^+ ions that maintain the cells in a quiescent state by decreasing their excitability. There is a huge molecular diversity within the K^+ channel family and therefore extensive studies have examined the contribution of different types of K^+ channels in regulating RMP. In keeping with the topic of this thesis, the contribution of specific K^+ channels to RMP in the GI tract will be addressed.

Ca^{2+} -activated K^+ channels: There are three types of Ca^{2+} activated K^+ channels which can be distinguished by their single channel conductance: small conductance (SK), intermediate conductance (IK) and large conductance (BK) Ca^{2+} -activated K^+ channels. SK and IK currents have been recorded in murine colonic smooth muscle and have single channel conductances of 5-10pS and 20-40pS respectively (Hille, 2001). These channels are Ca^{2+} -activated that require $[\text{Ca}^{2+}]_i$ levels to reach 50-100nM to cause activation but are not voltage

dependent. SK channels play a significant role in the fast component of inhibitory junction potentials (IJP) elicited by nerve stimulation which results in reduced excitability (Koh *et al.*, 1997). BK channels are both Ca^{2+} and voltage-dependent channels and have a single channel conductance of 200-250pS (Hille, 2001). Large outward currents through these channels can be recorded during step depolarizations to positive potentials using the patch-clamp technique. In addition, spontaneous transient outward currents (STOCs) have been recorded in murine colonic SMC which are activated by Ca^{2+} release from IP_3 receptor-operated intracellular stores. STOCs are composed of SK and BK channels (Kong *et al.*, 2000; Bayguinov *et al.*, 2001).

Voltage-gated, Ca^{2+} independent K^+ (Kv) channels: Kv currents can be divided into two categories: slowly-activating delayed rectifier K^+ currents and A-type K^+ currents based on their kinetics and pharmacological properties (Amberg *et al.*, 2003). Slowly-activating delayed rectifier K^+ channels exhibit a delayed onset of activation and slow inactivation. These currents are sensitive to tetraethylammonium (TEA). In the murine colon, inhibition of slowly-activating delayed rectifier K^+ channels increased the amplitude of spike action potentials though had no effect on RMP (Koh *et al.*, 1999b). A-type K^+ currents are distinguished from slowly-activating delayed rectifier K^+ currents by their rapid rates of activation and inactivation. Thresholds for activation are typically between -45 and -60mV and currents elicited are sensitive to 4-AP ($\leq 10\text{mM}$) but insensitive to external TEA. A-type K^+ currents have been recorded from different

smooth muscle from different tissues including genitourinary, GI and vascular. In relation to the GI tract, the molecular components of A-type K^+ channels were identified as Kv4.3 alpha-subunit associated with KCHIP1 in murine colonic smooth muscle (Amberg *et al.*, 2002). Since the RMP of GI smooth muscle lies between -50mV and -60mV, there is a fraction of A-type current that is continuously available i.e. lies within the window current, therefore implicating its involvement in RMP (Amberg *et al.*, 2003). In murine colon, the contribution of A-type K^+ currents to the RMP was revealed when addition of 4-AP caused depolarization and a loss of quiescent periods between phasic contractions (Koh *et al.*, 1999b).

Inwardly rectifying K^+ (Kir) channels: Kir channels exhibit an unusual I-V relationship compared with other K^+ channels. At potentials below E_k there is a substantial influx of K^+ ions, but at potentials positive to E_k , there is little outward current elicited. Kir channel members have been identified in colonic smooth muscle, including Kir2, Kir3 and Kir6 (Horowitz *et al.*, 1999). In canine colonic smooth muscle, high expression of Kir2.1 near the submucosal surface of the circular smooth muscle layer was suggested to be responsible for the more negative RMP recorded there in relation to other regions (Flynn *et al.*, 1999). Another group belonging to the Kir family is composed of K_{ATP} channels which have been identified in several tissues including rabbit portal vein, canine bronchial smooth muscle and murine colonic smooth muscle (Kamei *et al.*, 1994; Kamouchi & Kitamura, 1994; Koh *et al.*, 1998). When activated by a decrease in

ATP or agonists such as pinacidil, an inwardly rectifying K^+ current is evoked which can in turn can be inhibited by high concentrations of ATP or glibenclamide (Koh *et al.*, 1998). K_{ATP} channels are composed of an inward rectifier K^+ channel subunit of the Kir6 family (Kir6.1 or 6.2) and a sulfonylurea receptor (encoded by genes SUR1 and SUR2, of which there are two splice variants, SUR2A and SUR2B). The role of K_{ATP} in regulating RMP has been demonstrated in a number of tissues such as the heart and pancreatic- β cells (Noma, 1983; Ashcroft & Kakei, 1989). In murine colonic muscle, K_{ATP} channels were shown to contribute to RMP as addition of the K_{ATP} activator lemakalim caused hyperpolarization, an effect which could be inhibited by glibenclamide. Transcript analysis in single SMC revealed that Kir6.2/SUR2B subunits were likely candidates for K_{ATP} channels (Koh *et al.*, 1998).

Two pore K^+ channels (K2P): The family of two pore K^+ channels can be divided into 6 subfamilies (TWIK, TREK, TASK, TASK-2, THIK, TRESK) in accordance with their functional domains (Franks & Honore, 2004). Members of at least two of these subfamilies have been implicated in stabilization of the RMP. The proximal colon functions as a reservoir which allows sufficient absorption of water. Unlike other organs where stretch leads to a myogenic response of depolarization, in the proximal colon there is little change in the RMP. Activation of stretch-dependent K^+ channels (thought to be encoded by TREK-1) allow efflux of K^+ that may oppose the influx of Na^+ and Ca^{2+} through stretch-sensitive NSCC thus preventing any change in the RMP (Sanders & Koh, 2006).

TASK channels (TASK-1 and -2) are pH-sensitive K^{2P} channels that are expressed in murine intestinal smooth muscle. They have also been implicated in contributing to the RMP in GI muscles as reduction of extracellular pH and application of lidocaine inhibited a rapidly activating and inactivating K⁺ current and caused depolarization in colonic and ileal SMC. The properties of this K⁺ conductance are similar to those found in TASK channels when expressed in *Xenopus oocytes* (Cho *et al.*, 2005).

Clearly K⁺ channels are essential for maintaining the RMP near E_k. However, increased attention has been focused on the underlying conductances that cause RMP to be substantially less negative than E_k in certain tissues and cell types, thus increasing excitability.

1.5.2. Contribution of Ca²⁺-activated Cl⁻ currents and NSCC to RMP

In tissues where the RMP is less negative than E_k such as in the GI tract (~-50mV), it is reasonable to assume that conductances other than K⁺ must be contributing to it.

Spontaneous transient inward currents (STICs) have been reported in many cell types including cardiac muscle, smooth muscle and epithelium (Elble *et al.*, 2002). STICs are Cl⁻ currents that are activated by localized release of Ca²⁺ from intracellular stores and cause spontaneous depolarization to a range where VDCC open and thus increase Ca²⁺ influx (Wang *et al.*, 1992; Craven *et al.*, 2004). Therefore physiological evidence suggests they play an important role in

spontaneous electrical activity and excitation/contraction coupling in smooth muscle (Elbe *et al.*, 2002).

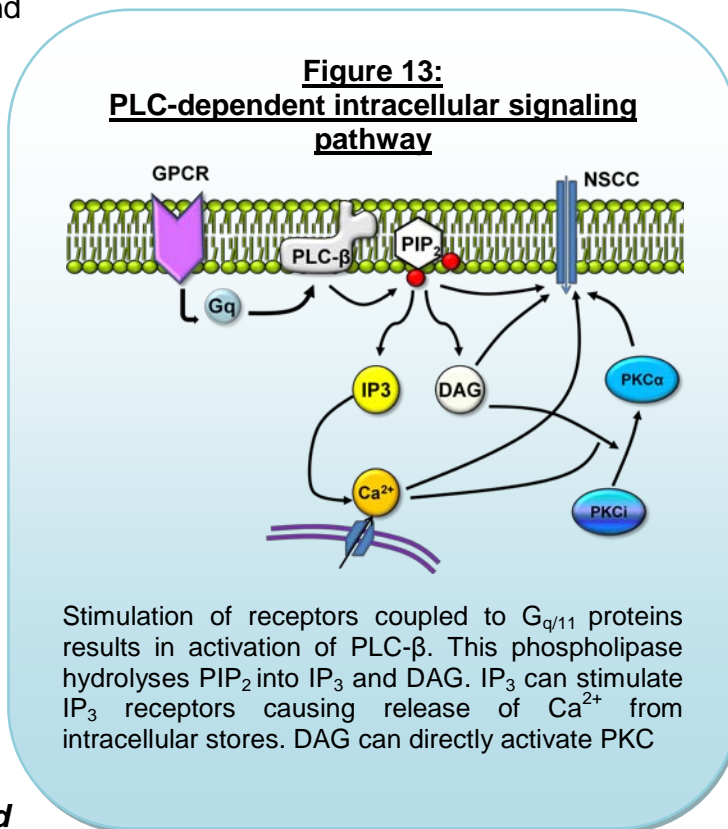
It has been proposed that the inward movement of ions such as Na^+ may shift the RMP to these more positive values. There is accumulating evidence that basally active NSCC play essential roles in regulating the RMP. In rabbit coronary artery SMC, the RMP is approximately -46mV. Background NSCC were found to contribute to this RMP as replacement of extracellular Na^+ with NMDG caused significant hyperpolarization in current-clamp experiments (Terasawa *et al.*, 2002). As described in section 1.4.2., spontaneous inward currents were recorded in rabbit ear artery myocytes and these constitutively active Ca^{2+} permeable NSCC (TRPC3, proposed molecular candidate) were suggested to contribute to the RMP (Albert *et al.*, 2003; Albert *et al.*, 2006). In rabbit pulmonary arterial SMC, a small background NSCC current was recorded and proposed to shift the RMP to positive values from E_K (Bae *et al.*, 1999). Similar findings were reported in murine urinary bladder SMC where inhibition of NSCC caused a substantial hyperpolarization from an initial RMP of approximately -40mV and a decrease in the amplitude of phasic contractions. These data strongly suggest that basal activation of NSCC cause tonic depolarization of bladder SMC (Thorneloe & Nelson, 2004).

RMP plays a fundamental role in determining the motility and excitability of GI smooth muscle. Less negative RMP values result in higher basal influx of Ca^{2+} ions as the window current of VDCC is approached. In human colonic smooth

muscle, RMP is approximately -50mV (Rae et al., 1998). However, no studies have examined the underlying ion channels that contribute to this value in colonic smooth muscle. Therefore, in Chapter 2, the potential contribution of basally activated NSCC to the RMP was examined in human and monkey colonic SMC.

1.6. PLC-dependent regulation of ion channels

Since excitation and contraction in GI smooth muscle have been linked with activation of the PLC pathway through stimulation of GPCR, we will introduce PLC-dependent pathways and PLC-regulation of cellular activities in this section.



1.6.1. PLC-pathway and associated downstream mediators

In order to understand the physiological functions of specific ion channels it is crucial to identify how they are regulated. PLC plays a crucial role in the signal transduction of various cellular events. The PLC-subfamily, PLC- β , is activated through agonists binding to $G_{q/11}$ coupled receptors or receptor tyrosine kinases (Trebak, 2006; Unno *et al.*, 2006; Zholos, 2006). The resultant activation of PLC causes hydrolysis of PIP_2 found on the cytoplasmic leaflet of the plasma membrane where it constitutes 1% of the lipid. This forms important signaling molecules such as IP_3 and DAG that activate further cellular events (see Fig. 13). For example, Ca^{2+} release often results from binding of IP_3 to their concomitant

receptors. This, in turn, may be followed by Ca^{2+} influx from the extracellular environment through store-operated Ca^{2+} channels. DAG can activate PKC which in turn can phosphorylate many types of ion channels such as L-type Ca^{2+} channels (Horowitz *et al.*, 2005; Trebak, 2006). These downstream signaling molecules of PLC may be involved in regulation of colonic excitability. However, it would be overly ambitious to cover all of these potential modulators for one thesis. Therefore we focused on direct activation of PLC using a currently available pharmacological tool (see next section).

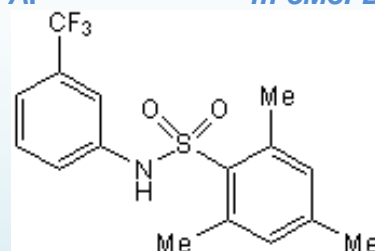
1.6.2. PLC regulation of cellular activities

Selective tools for activating and inhibiting PLC are important in determining its role in cellular pathways and physiological reactions. Bae *et al* reported that the compound 2, 4, 6-trimethyl-N-(meta-3-trifluoromethyl-phenyl)-benzenesulfonamide (*m*-3M3FBS) could directly activate PLC in human neutrophils and generate superoxide. A second compound called 2, 4, 6-trimethyl-N-(ortho-3-trifluoromethyl-phenyl)-benzenesulfonamide (*o*-3M3FBS), which differs from *m*-3M3FBS by the position of the trifluoromethyl-phenyl group (see Fig. 14) was

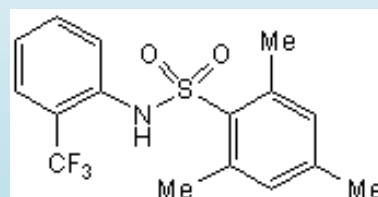
Figure 14:

Structures of *m*-3M3FBS and *o*-3M3FBS

A. *m*-3M3FBS



B. *o*-3M3FBS



o-3M3FBS differs from *m*-3M3FBS by the position of the trifluoromethyl-phenyl group

recognized as the inactive analog as it did not affect superoxide generation up to 50 μ M (Bae *et al.*, 2003). In the same study, *m*-3M3FBS exhibited no cell type specificity as it caused a transient increase in $[Ca^{2+}]_i$ in various cell lines including neutrophils, leukocytes and fibroblasts. This effect on $[Ca^{2+}]_i$ was abolished by the PLC inhibitor, 1-(6-((17 β -3-methoxyestra-1,3,5(10)-trien-17-yl)amino)hexyl)-1H-pyrrole-2,5-dione (U73122). In U937 cells, *m*-3M3FBS stimulated the formation of inositol phosphates which was indicative of PLC activation. It was also observed that purified forms of various PLC-subfamily members (β 2, β 3, γ 1, γ 2 and δ 1 were tested) were all activated by *m*-3M3FBS therefore indicating this compound exhibits no isoform-specificity. The inactive analog *o*-3M3FBS did not affect any of the mentioned parameters (Bae *et al.*, 2003). This was the first compound reported to specifically activate PLC and therefore was expected to be a useful tool for examining PLC-dependent mechanisms.

However, the specificity of *m*-3M3FBS was called into question by a study performed in SH-SY5Y human neuroblastoma cells by Krjukova and colleagues. Although they found that *m*-3M3FBS caused a slowly developing Ca^{2+} elevation which reached a plateau within 6 minutes, it did not coincide with PLC activity as it took more than 20 minutes for generation of IP_3 (Krjukova *et al.*, 2004). In addition, store-operated Ca^{2+} influx, which was evoked by application of external Ca^{2+} solution following pretreatment with thapsigargin and then perfusion with $0Ca^{2+}$ solution, was significantly decreased by *m*-3M3FBS. Furthermore, in SH-SY5Y cells, experiments were performed using plasma membrane GFP-PH-

PLC δ 1 fluorescent probe which, upon PIP₂ hydrolysis, translocates to the membrane. However exposure to *m*-3M3FBS for over 5 minutes did not cause any translocation of GFP-PH-PLC δ 1 fluorescence suggesting this compound was not activating PLC. From these studies the authors concluded that *m*-3M3FBS was not a selective PLC activator in these cells and its effects on Ca²⁺ signaling were via PLC-independent mechanism(s) (Krjukova *et al.*, 2004). In a recent study using canine renal tubular cells, *m*-3M3FBS was found to induce PLC-independent increases in [Ca²⁺]_i via release of Ca²⁺ from endoplasmic reticulum and Ca²⁺ entry through store-operated as well as other unidentified Ca²⁺ permeable channels (Fang *et al.*, 2009).

This compound has been used to study the role of PLC in the regulation of certain ion channels. For example one study hypothesized that KCNQ channels were positively regulated by PIP₂ and depletion of PIP₂ levels by receptor-activated PLC- β could suppress these currents. A fluorescent probe was used to track depletion of PIP₂ by *m*-3M3FBS in tsA cells transfected with KCNQ2/3 channels. However, unlike the study by Bae *et al.*, application of *m*-3M3FBS caused migration of the PH-EGFP probe suggesting that this compound activated PLC. In addition it caused a simultaneous decrease in KCNQ2 and 3 currents. Conversely, *o*-3M3FBS induced no migration of the probe or suppression of KCNQ currents. Though the authors did accept that the effects seen by *m*-3M3FBS were indicative of a PLC activator, they did detect some unusual activity. For example, unexpected for a PLC activator, this compound

was slow to act, had a long latency and also exhibited varied responses. It was suggested that *m*-3M3FBS may activate conflicting signaling mechanisms that would account for variability in responses (Horowitz *et al.*, 2005).

A voltage-independent, large conductance background-type K⁺ channel was identified in B lymphocytes and hypothesized to be tonically inhibited by PIP₂. Application of *m*-3M3FBS caused activation of this current in the inside-out configuration supporting this hypothesis. Further studies revealed that this channel was stretch-sensitive and depletion of PIP₂ by stretch-activated PLC released this channel from tonic inhibition by PIP₂ (Nam *et al.*, 2007).

Since excitation and contraction in GI smooth muscle has been linked with activation of the PLC pathway through stimulation of muscarinic receptors coupled to specific G proteins (Unno *et al.*, 2006; Zholos, 2006), this PLC activator was used to study the effects of direct PLC activation independent of receptor activation on colonic smooth muscle excitability. *Preliminary studies revealed unexpected effects of direct PLC-activation using m-3M3FBS on colonic contractility. Since this compound has been used in many studies, we thought it was essential to uncover the underlying mechanism(s) of action of this compound that could account for its reduction in contractility in Chapter 3.*

1.7. Rho-kinase and colonic excitability

1.7.1. Ca^{2+} sensitization mechanism and Rho-kinase

Agonist-induced smooth muscle contraction is a well documented process that involves activation of a PLC-mediated pathway. Hydrolysis of PIP_2 results in IP_3 -mediated release of Ca^{2+} from intracellular stores. This Ca^{2+} binds to calmodulin and activates MLCK. In turn, MLCK phosphorylates 20kDa myosin light chain subunits of myosin and initiates cross-bridge cycling leading to activation of actin-activated myosin ATPase, interaction of actin and myosin, and muscle contraction (Murthy *et al.*, 2000; Camello-Almaraz *et al.*, 2009). Conversely MLCP can return the smooth muscle to its precontracted state by dephosphorylation of the phosphorylated myosin light chain subunits of myosin.

It is now well established that Ca^{2+} sensitization can also contribute to smooth muscle contraction (Fernandes *et al.*, 2006; Al-Jarallah *et al.*, 2008). This process changes the sensitivity of the contractile machinery independent of changes in $[Ca^{2+}]_i$ through inhibition of MLCP and decreased MLC dephosphorylation. A main pathway that mediates Ca^{2+} sensitization is through Rho-kinase activation. Rho-kinase is a Rho-associated coiled-coil forming serine/threonine protein kinase with a molecular mass of ~160 kDa and belongs to the Ras family of GTPases. There are two isoforms of Rho-kinase, ROCK-I/p160ROCK and ROCK-II/ROK α (Ishizaki *et al.*, 2000). They are distributed in the cytoplasm and upon activation of the GTP-binding protein, Rho-A, they translocate to the membrane. Rho-kinase is involved in a variety of cellular

functions including proliferation, migration, gene expression and contraction (Yoshii *et al.*, 1999).

Activation of receptors coupled to certain trimeric G proteins (G_q , $G_{12/13}$)

and receptor

tyrosine

kinases

causes an

exchange

of GDP for

GTP on

RhoA by

guanine

nucleotide

exchange

factors

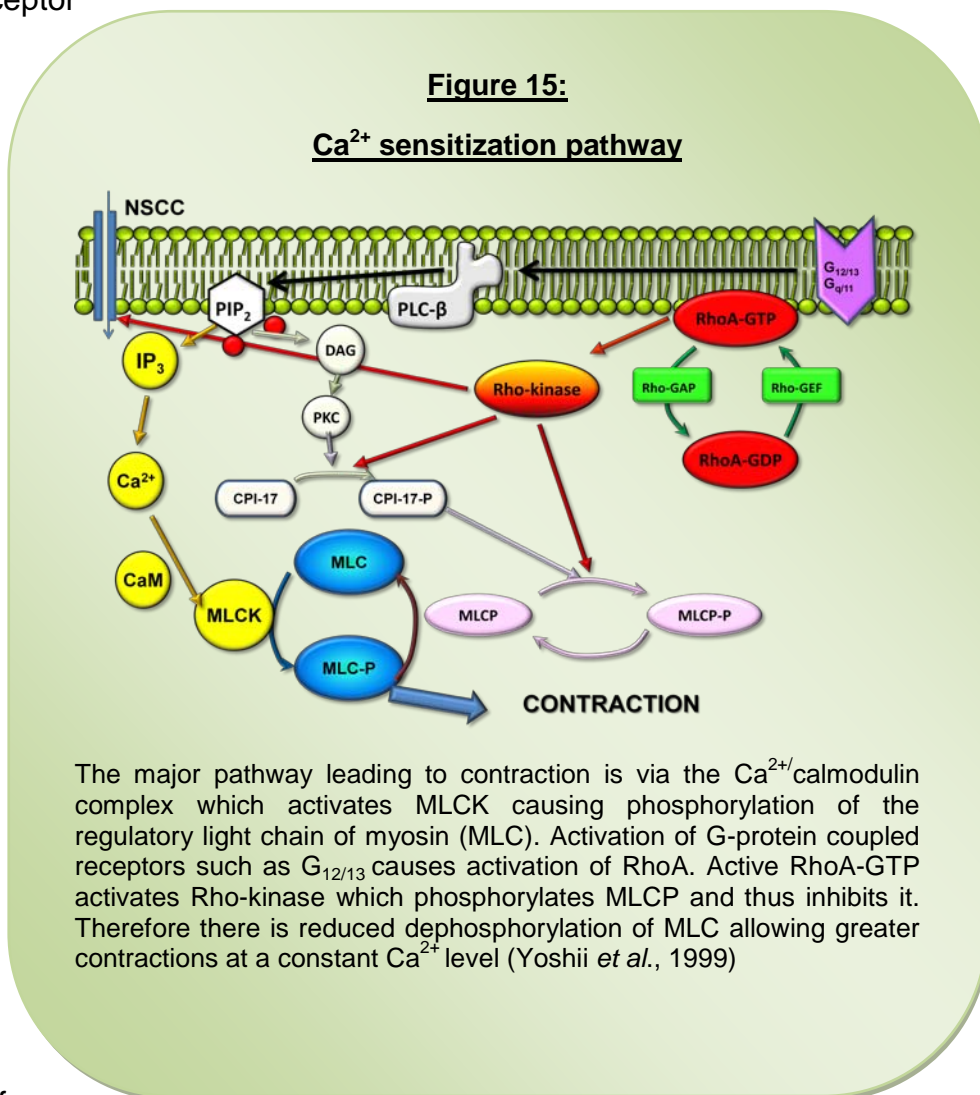
(GEF) (Fig.

15). RhoA

then

translocates from

the cytosol to the membrane where it associates with Rho-kinase to initiate a signaling cascade. In turn, Rho-kinase phosphorylates the regulatory subunit, MYPT1 at several sites including threonine 696 and 853 residues of MLCP



resulting in its inhibition. Consequently, there is an overall increase in the phosphorylation of MLC by MLCK and Ca^{2+} sensitization of the contractile filaments (Somlyo & Somlyo, 2003).

PKC can also contribute to decreased MLCP activity by contractile agonists (Fig. 15). Activation of PLC and subsequent creation of DAG from PIP_2 hydrolysis activates PKC. CPI-17, which is a PKC-potentiated phosphatase inhibitor, is activated by phosphorylation of Thr38 by PKC. In turn, CPI-17 phosphorylates the catalytic subunit of MLCP and inactivates it (Ohama *et al.*, 2007).

It is now established that activation of MLCK leads to the initial contraction of smooth muscle, whereas inhibition of MLCP via Rho-kinase and PKC contributes to sustained contractions (Murthy *et al.*, 2000; Somlyo & Somlyo, 2003). Studies have documented that contribution of Rho-kinase and PKC to Ca^{2+} sensitization varies between species and the type of smooth muscle (Takeuchi *et al.*, 2004; Durlu-Kandilci & Brading, 2006).

1.7.2. Involvement of Ca^{2+} sensitization in basal tone and agonist-induced contractions

There are several Rho-kinase inhibitors currently available that have been used to examine the contribution of Rho-kinase to smooth muscle tone and contraction including Y27632, H-1152 and HA1077. Raten and Patel reported that basal tone in rat internal anal sphincter (IAS) was significantly attenuated by

application of H-1152 and Y-27632. These findings directly correlated with decreases in Rho-kinase activity suggesting that Rho-kinase plays a critical role in maintenance of IAS tone (Rattan & Patel, 2008). In trabecular meshwork strips, Y-27632 significantly reduced CCh-induced contractions (Rosenthal *et al.*, 2005). Several studies in different species have revealed a crucial role for Rho-kinase in sustained contraction of airways therefore implicating its involvement in bronchoconstriction/asthma (Hashimoto *et al.*, 2002; Burdyga *et al.*, 2003; Gosens *et al.*, 2004). In rabbit tracheal smooth muscle, application of Y27632 suppressed CCh-induced contractions (Yoshii *et al.*, 1999).

Alterations in Ca^{2+} sensitization have been reported in animal models of IBD and associated with altered contractility as described in section 1.2.3. For example in colonic strips from TNBS-treated rats, application of Y-27632 caused a significantly greater relaxation from controls suggesting higher basal tone in these tissues. The same study found that expression of PKC was reduced in inflamed colonic muscle as well as CCh-induced phosphorylation of CPI-17. Therefore this study suggested that the decrease in contractility was through decreased MLCP inhibition and hence altered Ca^{2+} sensitization (Al-Jarallah *et al.*, 2008).

1.7.3. Rho-kinase pathway and ion channel regulation

Recently it has been recognized that Rho-GTPase signaling can regulate several different classes of ion channels including Kv1.2, NSCC and Ca^{2+} channels (Staruschenko *et al.*, 2004). RhoA activation of Rho-kinase can

increase PIP₂ levels through stimulation of phosphatidylinositol-4-phosphate 5-kinase. In turn this increase in PIP₂ promotes not only the insertion of epithelial Na⁺ channels into the plasma membrane but also channel gating (Staruschenko *et al.*, 2004; Pochynyuk *et al.*, 2006). In guinea pig ventricular myocytes, Rho-kinase was proposed to contribute to lysophosphatidylcholine (LPC) - induced NSCC. LPC, which is found in ischemic hearts, is considered to be one of the causes of Ca²⁺ overload during cardiac ischemia and reperfusion (Li *et al.*, 2002). In rat penile arteries, application of phenylalanine activated a Rho-kinase-sensitive Ca²⁺ influx that was resistant to nifedipine. It was suggested that this Ca²⁺ entry was via NSCC that were final effectors of Rho-kinase (Villalba *et al.*, 2008).

It is becoming increasingly evident that Rho-kinase is involved in the modulation of cellular activities other than Ca²⁺ sensitization. Therefore, in Chapter 4, the potential role of Rho-kinase in nerve-evoked and agonist-induced contractions in colonic smooth muscle was examined.

Chapter 2:

Basal activation of non-selective cation currents regulate the resting membrane potential in human and monkey colonic smooth muscle cells

2.1. Summary

Resting membrane potential (RMP) plays an important role in determining the basal excitability of gastrointestinal smooth muscle. In colonic smooth muscle, the RMP lies within -50 to -60mV. Since these values are significantly less negative than the equilibrium potential of K^+ (E_K), this suggests that the RMP is not solely regulated by K^+ conductances but by other conductances such as Na^+ and Ca^{2+} . We investigated the contribution of basally active non-selective cation channels (bI_{NSCC}) to the RMP in human and monkey colonic smooth muscle cells (SMC) and examined molecular candidates for these channels.

We used voltage- and current- clamp techniques to investigate the contribution of bI_{NSCC} to the RMP in human and monkey colonic SMC. In addition, qualitative PCR was performed to examine molecular candidates for the bI_{NSCC} among the Transient Receptor Potential (TRP) channel family.

Spontaneous transient inward currents (STICs) and holding currents (HC) were recorded in human and monkey SMC. When the equilibrium potential for Cl^- (E_{Cl}) was changed from 0mV to -40mV, the reversal potential of these currents was not effected (remained at 0mV) therefore demonstrating that these

currents were not due to a Cl^- conductance but NSCC. Under voltage clamp, replacement of either extracellular Na^+ with equimolar TEA or Ca^{2+} with Mn^{2+} inhibited bI_{NSCC} . Trivalent cations, La^{3+} and Gd^{3+} , inhibited bI_{NSCC} . Furthermore under current clamp, replacement of extracellular Na^+ with NMDG⁺ caused hyperpolarization of RMP. Molecular analysis for potential candidates for bI_{NSCC} revealed that TRPC7, V1 and V2 were expressed in human SMC whereas TRPC4 and 5 were found in monkey SMC.

These findings suggest that there is NSCC activity that is basally active under resting conditions in human and monkey colonic SMC. Furthermore current clamp data suggests that bI_{NSCC} contribute to the RMP which is significantly more positive than E_K in colonic SMC. Thus bI_{NSCC} may play a role in determining basal excitability of colonic smooth muscle by regulating the RMP.

2.2. Background and Aims

In the gastrointestinal tract (GI), the coordinated movement of luminal contents is regulated by a range of factors released from excitatory and inhibitory motor nerves as well as rhythmical electrical activity generated by specialized pacemaker cells known as interstitial cells of Cajal (ICC). Signals from enteric neurons and ICC are transmitted to SMC where they are translated into the final acts of excitation and contraction. Thus the specific ionic conductances that set RMP and initiate depolarization in SMC play essential roles in determining the basal pattern of contractile activity as well as modulating the muscle response to excitatory and inhibitory signals.

Since the RMP of SMC in certain parts of the GI tract is significantly less negative than the equilibrium potential for K^+ (E_K) ions, this suggests that there is an opposing influx of Na^+ and Ca^{2+} ions through NSCC which drive the RMP to more positive values. This in turn effects further Ca^{2+} influx since the amount of current entry through voltage-dependent Ca^{2+} channels (VDCC) is comparative to the length of time the channel is in the open state, which is highly dependent on RMP (Yuan, 1995).

Surprisingly a limited number of studies have actually examined the ionic mechanisms that are responsible for more positive RMP than E_K (e.g. -60 to -40mV) in certain cell types. In rabbit pulmonary arterial SMC, a small background NSCC current was recorded and suggested to be responsible for shifting the RMP from E_K (Bae *et al.*, 1999). In rabbit coronary artery SMC, current clamp

recordings clearly identified that background NSCC activated by lysophosphatidylcholine, contributed substantially to the RMP (Terasawa *et al.*, 2002). Constitutively active NSCC have also been recorded in rabbit ear artery myocytes and murine urinary bladder SMC that were suggested to contribute to the resting conductance (Albert *et al.*, 2003; Albert *et al.*, 2006; Thorneloe & Nelson, 2004).

In human colonic smooth muscle tissue, the RMP is approximately -50mV (Rae *et al.*, 1998). This is very similar to RMP in monkey colonic smooth muscle tissue (unpublished observation). Therefore we examined if there were basally active NSCC conductance(s) that significantly contributed to the RMP using voltage and current clamp techniques in freshly dispersed colonic SMC. Qualitative PCR was performed on human and monkey smooth muscle tissue and SMC in order to identify molecular candidates for basally active NSCC.

2.3. Materials and methods

2.3.1. Human tissue

Human colonic specimens were obtained and experimented under the guidelines of the ethical committee of Samsung medical centre. Patients of both sexes (21 male and 5 female) ranging in age from 43 to 76yrs underwent necessary surgery for mainly colon cancer. During surgery after anaesthetization, colonic tissue was removed (ascending 8, transverse 3, descending 7, sigmoid 9). The diseased tissue was removed along with a small region of healthy tissue. This healthy tissue was used for experimental studies.

2.3.2. Animal tissues

The animals used for these studies were maintained and experiments performed in accordance with the National Institutes of Health Guide for the Care and Use of Laboratory Animals, and the Institutional Animal Use and Care Committee at the University of Nevada approved all procedures used. *Cynomolgus monkeys* (Charles River Laboratories, Preclinical Services, Sparks, NV, USA) of either sex (22 monkeys, 2.5–7 years of age) were initially sedated with Ketamine (10 mg kg^{-1}), then administered 0.7 mL Beuthanasia-D[®] solution (Schering-Plough AH, Kenilworth, NJ, USA) (pentobarbital sodium and phenytoin sodium) followed by exsanguination.

2.3.3. Preparation of isolated colonic SMC

Human and monkey colon segments were placed in Krebs-Ringer bicarbonate solution (KRB) with the following composition (mM): 118.5 NaCl, 4.5 KCl, 1.2 MgCl₂, 23.8 NaHCO₃, 1.2 KH₂PO₄, 11.0 dextrose and 2.4 CaCl₂. Each segment was opened and pinned to the base of a dissecting dish coated with Sylgard elastomer (Dow Corning Corp., Miland, MI, USA) and the adhering mucosa and submucosa were removed. Freshly dispersed colonic SMC were prepared from colonic muscle strips using Ca²⁺-free Hank's solution containing (mM): 125 NaCl, 5.36 KCl, 15.5 NaOH, 0.336 Na₂HPO₄, 0.44 KH₂PO₄, 10 glucose, 2.9 sucrose and 11 Hepes, adjusted to pH 7.4 with Tris. Pieces of muscle were incubated for 50-55 minutes at 37°C in a Ca²⁺-free solution (2 ml) containing collagenase (4 mg/mL, Worthington Biochemical, Lakewood, NJ), trypsin inhibitor (8 mg/mL), fatty acid-free bovine serum albumin (8 mg/mL), papain (2 mg/mL), and L-dithiothreitol (LDTT, 0.3 mg/mL, Sigma-Aldrich, MO, USA). Tissue pieces were washed with Ca²⁺-free solution and then gently agitated to create a cell suspension. Dispersed SMC were stored at 4°C in Ca²⁺-free solution. Drops of the cell suspensions were placed on the bottom of a 300 µl chamber mounted on an inverted microscope and allowed to adhere to the bottom of the chamber for 5 minutes before recording.

2.3.4. Voltage-clamp and current-clamp methods

Whole cell voltage-clamp techniques were used to record membrane currents from dissociated SMC. Membrane currents were amplified by an Axopatch 200B (Axon Instruments, Foster City, CA) and digitized with an analog-to-digital converter (Digidata 1200, Axon Instruments). Data were collected at 5 kHz, filtered at 2 kHz via Bessel filter, and digitized online with pCLAMP software (version 8.1.0, Axon Instruments). The data were analyzed with the use of pCLAMP software (version 10, Axon Instruments). Pipette resistances were 1–4M Ω . Conventional and perforated whole cell (amphotericin B) patch-clamp techniques were used for recording ionic currents under voltage clamp. Experiments were performed at room temperature (between 22 and 25°C). The RMP was measured using the current-clamp configuration ($I=0$) of the whole-cell patch clamp technique at room temperature (between 22 and 25°C).

2.3.5. Solutions and reagents

In conventional dialyzed whole cell experiments, the internal solution contained (in mM): 135 KCl, 0.1 EGTA, 0.1 Na₂GTP, 3 MgATP, 10 glucose, 2.5 creatine phosphate disodium and 10 HEPES. The external solution was (in mM): 135 NaCl, 5 KCl, 2 CaCl₂, 1.2 MgCl₂, 10 glucose, 10 HEPES and adjusted to pH 7.4 with Tris (CaPSS). In some experiments, cells were perfused in 0 mM Ca²⁺ external solution (MnPSS; Ca²⁺ was replaced with Mn²⁺ (2 mM)). In Na⁺ replacement experiments, Na⁺ was replaced with equimolar tetraethylammonium (TEA) under voltage-clamp conditions. In order to isolate inward currents, the

pipette solution contained (in mM): 135 CsCl, 0.1 EGTA, 0.1 Na₂GTP, 3 MgATP, 10 glucose, 2.5 creatine phosphate disodium and 10 HEPES. This solution was adjusted to pH 7.2 with Tris. For low Cl⁻ solution (30 mM), CsCl was replaced with equimolar caesium aspartate (E_{Cl} was -40 mV). The calculated junction potential was 7 mV. For perforated patches, amphotericin B (60 mg/ml) was dissolved in DMSO, sonicated, and diluted in the pipette solution to give a final concentration of 270 µg/ml. The effects of gadolinium (Gd³⁺) and lanthanum (La³⁺) (Sigma, St Louis, MO, USA) were tested by bath perfusion. For current-clamp recordings ($I=0$), SMC were exposed to CaPSS and the internal solution contained (in mM): 135 KCl, 0.1 EGTA, 0.1 Na₂GTP, 3 MgATP, 10 glucose, 2.5 creatine phosphate disodium and 10 HEPES. In current-clamp ($I=0$) recordings, external Na⁺ was reduced to 5mM with the remaining 130mM Na⁺ replaced with N-methyl-D-glucamine (NMDG).

2.3.6. RNA isolation, reverse transcription PCR (RT-PCR) and quantitative PCR (qPCR)

Both colonic tissue and SMC were used for molecular studies. SMC were collected by applying suction to the pipette resulting in aspiration of the cells into the pipette. Total RNA was isolated from human and monkey colonic tissue and cells using TRIzol reagent (GIBCO, Gaithersburg, MD) according to the manufacturer's instructions. Eluted total RNA was treated with DNase I to remove genomic DNA, which might be isolated along with total RNAs. First-

strand cDNA was prepared from the total RNA with a Superscript Reverse Transcriptase kit (GIBCO). One microgram of total RNA was reverse transcribed with 200 U of reverse transcriptase in a 20- μ l reaction containing 25 ng of oligo(dT) primer, dNTPs each at 500 μ M, 75 mM KCl, 3 mM MgCl₂, 10 mM DTT, and 50 mM Tris-HCl (pH 8.3). All primers: beta-2 macroglobulin (B2M), transient receptor potential cation channel, subfamily C, M and V, were designed from a region spanning at least two exons in reference to cDNAs in the National Center for Biotechnology Information (NCBI) (see Table 1). Each gene cDNA was amplified by RT-PCR or qPCR with gene-specific primers (see Table 1). RT-PCR was carried out with AmpliTaq polymerase (PE Biosystems) in a 2300 thermal cycler (PE Biosystems), and PCR fragments were analyzed by gel electrophoresis (2% agarose). All amplicons were at the expected cDNA size, which showed that they were clean from genomic DNA contamination. To determine the relative expression levels of TRP subfamily members in human and monkey tissue and SMC, qPCR was performed with the use of SYBR Green chemistry as described previously (Amberg *et al.*, 2002). Standard curves were generated for each TRP subfamily member and the constitutively expressed GAPDH from regression analysis of the mean values of PCR amplifications for the log₁₀ diluted cDNA. Unknown quantities relative to the standard curve for TRP isoforms were calculated, yielding transcriptional quantitation of TRP cDNA relative to the endogenous standard (GAPDH). Each cDNA sample was tested in triplicate.

2.3.7. Statistical analysis

Data are reported as means \pm S.E.M. In describing the voltage-clamp results, n is the number of cells tested. Statistical significance was evaluated by Student's t test. P values less than 0.05 were considered significant.

2.4. Results

2.4.1. Basally activated NSCC recorded in human and monkey colonic SMC

Whole-cell voltage clamp experiments were performed on single colonic SMC isolated from human and monkey colon smooth muscle under physiological extracellular and intracellular ionic conditions ($E_{Cl} = 0\text{mV}$) (see methods section). We recorded basally activated inward currents that were composed of two types of inward currents. One was a basal 'holding current' (HC, see red dotted line, Fig. 1A and Aa) which was the measured current between 0pA and the red-dotted line as an average over a 60 second recording. The other type of inward current was spontaneous transient inward currents (STICs, blue arrow and asterisk, Fig. 1A and Aa). Figure 1Aa illustrates how STICs were measured by taking an average of peak currents (blue asterisk) over a period of 60 seconds from the red-dotted line (which represents 0mV for measuring STIC currents). At a holding potential of -80mV, the HC recorded from human colonic myocytes was $-46 \pm 3\text{pA}$ ($n=18$, Fig. 1A). In addition, the amplitude of STICs ranged from -8 to -60 pA, with an average of $-21 \pm 2\text{pA}$ (Fig. 1A). Similar STIC activity was recorded in monkey colonic SMC where the average amplitude was $-12 \pm 2\text{pA}$ ($n=19$, Fig. 1B). The average HC was $-30 \pm 4\text{pA}$ (Fig. 1B). In previous studies, STICs have been reported to be due to a Ca^{2+} -activated Cl^- conductance (see section 1.5.2.) (Janssen & Sims, 1993; Craven *et al.*, 2004; Bolton, 2006). Therefore, the internal Cl^- concentration was decreased (CsCl 30Mm, Cs-aspartate 110mM) to set $E_{Cl} = -40\text{mV}$. The holding potential was changed from -

60mV to +60mV in 20mV increments and held at each voltage for approximately 2 minutes. The STIC activity and HC reversed at approximately 0mV (Fig. 1C) indicating that a Cl⁻ conductance does not contribute to basally activated inward currents ($E_{Cl} = -40\text{mV}$). Therefore, we termed these basally activated inward currents as 'basally activated non-selective cation currents' or bI_{NSCC} .

2.4.2. Na⁺ contributed to bI_{NSCC} and membrane potential

Na⁺ is a major charge carrier in NSCC (Clapham *et al.*, 2001). Therefore we used high Cs⁺ internal solution to test Na⁺ permeability of bI_{NSCC} (see materials and methods section). In the external solution, Na⁺ (135mM) was replaced with equimolar TEA. Under these conditions, the HC was significantly reduced from -44 ± 5 to $-16 \pm 2\text{pA}$ ($n=5$, $P < 0.001$, Fig. 2A & C) and STIC activity was also decreased from -22 ± 0.1 to $-9 \pm 0.2\text{pA}$ at -80mV ($n=5$, $P < 0.001$, Fig. 2A & D) in human colonic SMC. In monkey colonic SMC, the HC was significantly reduced from -28 ± 8 to $-11 \pm 3\text{pA}$ ($n=6$, $P < 0.05$, Fig. 2B & C) and STIC activity was decreased from -11 ± 0.1 to $-4 \pm 0.04\text{pA}$ at -80mV ($n=5$, $P < 0.001$, Fig. 2B & D). Current clamp recordings ($I=0$) were performed to explore the significance of bI_{NSCC} in regulating the RMP in human and monkey colonic SMC. The pipette contained a high K⁺ solution (see materials and methods). Reduction in external Na⁺ from 135mM to 5mM (replaced with 130mM NMDG) induced hyperpolarization of human SMC from $-29 \pm 3\text{mV}$ to $-38 \pm 3\text{mV}$ ($n=4$, $P < 0.01$, Fig. 2E). A similar effect of reducing external Na⁺ was recorded in monkey colonic

SMC ($n=6$, $P<0.01$, Fig. 2F). These data suggest an important contribution of the Na^+ permeable conductance of bI_{NSCC} in regulating RMP in colonic SMC.

2.4.3. NSCC blockers inhibited bI_{NSCC}

The trivalent cations, Gd^{3+} and La^{3+} , are widely used as NSCC/TRP channel blockers (Vazquez *et al.*, 2004a). Therefore we tested their effects on bI_{NSCC} . Under voltage clamp conditions, La^{3+} ($10\mu\text{M}$) significantly decreased the HC from -45 ± 7 pA to -20 ± 2 pA ($n=5$, $P<0.001$, Fig. 3A & E) and also STIC activity from -17 ± 0.2 pA to -6 ± 0.1 pA ($n=5$, $P<0.001$, Fig. 3A & F) in human colonic SMC. Application of La^{3+} ($10\mu\text{M}$) significantly inhibited bI_{NSCC} in monkey colonic SMC (HC: $n=4$, $P<0.05$, and STICs: $n=4$, $P<0.001$, Fig. 3B, E & F). Gd^{3+} ($10\mu\text{M}$) also significantly decreased STICs and HC in both human and monkey colonic SMC (Fig. 3C-F). These inhibitory effects were not reversible as has previously been reported (Halaszovich *et al.*, 2000; Raingo *et al.*, 2004).

2.4.4. Ca^{2+} contributed to bI_{NSCC}

Many kinds of NSCC are also permeable to Ca^{2+} (Birnbaumer, 2009), and therefore we investigated if bI_{NSCC} could also be carried by Ca^{2+} . External Ca^{2+} (2mM) was replaced with equimolar Mn^{2+} . In this solution both components of bI_{NSCC} , STICs and HC, were significantly decreased in human and monkey colonic SMC (Fig. 4A-D). These data suggest that external Ca^{2+} is necessary for

bI_{NSCC} . Inhibition of T-type/low threshold voltage-activated Ca^{2+} channels using nickel (50 μ M) had no significant effect on HC or STICs in human or monkey colonic SMC, thus indicating that they are not a source of Ca^{2+} that contributes to bI_{NSCC} activity (Fig. 4E & F).

2.4.5. Single channel conductances recorded in monkey colonic SMC

Since Cs^+ is reported to be a better charge carrier than Na^+ (Dresviannikov *et al.*, 2006), we used symmetrical Cs^+ (140 mM) with $[Ca^{2+}]_o$ (100nM) for inside-out single channel experiments on monkey colonic SMC. Figure 5A demonstrates a 25pS channel under these conditions and reverses at approximately 0mV. The current-voltage (I-V) relationship was constructed using the all-points amplitude histogram (e.g. -1.5 ± 0.2 pA at -60 mV, n=3). We also recorded a 5pS channel (Fig. 5B) and small conductance (non-measurable) NSCC channels (Fig. 5C). Small conductance NSCC did not exhibit clear channel openings and therefore an amplitude histogram could not be constructed. These conductances may be important contributors to bI_{NSCC} recorded at the whole-cell level in monkey colonic SMC.

2.4.6. TRP channels expressed in human and monkey colonic tissue and SMC

We investigated qualitative transcriptional expression of TRPC, M and V subfamily members in colonic tissue from human and monkey. In figure 6A and B, representative gels show TRP-subfamily member transcripts that are present at the tissue level. In our preliminary experiments, certain TRP members were found at the tissue level and therefore only those known to be expressed were included in the representative gels (see figure 6A, upper gel). Since transcript expression at the tissue level includes expression from multiple cell types (e.g. neurons, ICC, fibroblasts, etc), it was necessary to examine transcriptional expression at the SMC level in order to isolate potential molecular candidates for bI_{NSCC} . Therefore following dispersion of cells from human and monkey colonic tissues, SMC were collected (~100 cells) (see materials and methods). RT-PCR analysis revealed that TRPC7, TRPV1 and TRPV2 transcripts were expressed in isolated human colonic SMC (lower gels, Fig. 6A). In monkey SMC, only TRPC4 and TRPC5 were expressed out of all the TRP-subfamily members present in tissue (lower gels, Fig. 6B). These data indicate that expression levels of TRPC, TRPV and TRPM subfamily members were different between species and in addition there was a clear difference in TRP expression in colonic tissue versus SMC. These TRP channels could be potential molecular candidates for bI_{NSCC} in human and monkey SMC.

2.5. Figures and figure legends

Figure 1: Spontaneous transient inward currents recorded in colonic SMC

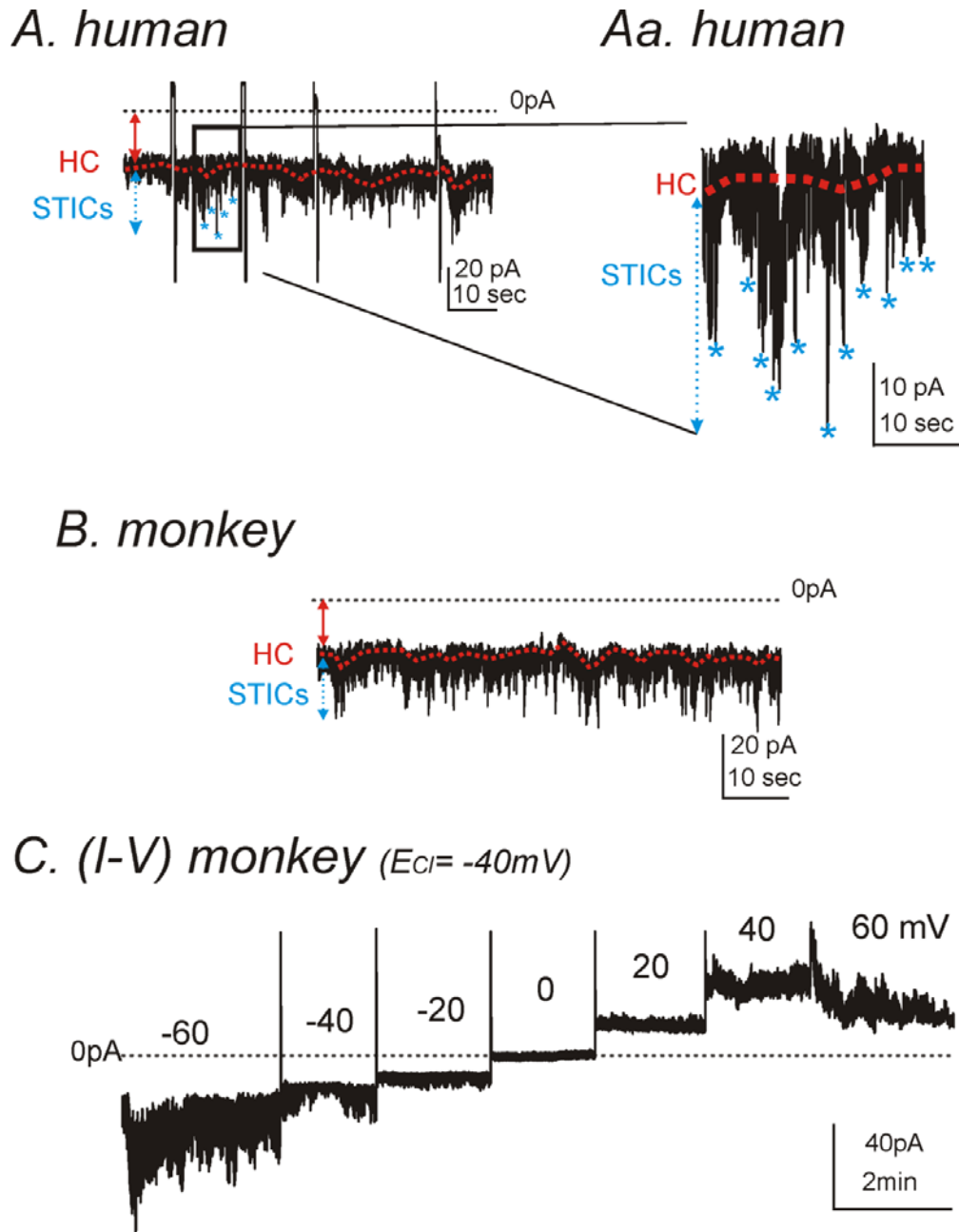


Figure 1: Spontaneous transient inward currents recorded in colonic SMC
(A-C) Under voltage clamp at a holding potential of -80mV, ongoing inward currents were recorded in human and monkey colonic SMC. This activity was divided into two components: holding current (HC, red-dotted line, Fig. 1A & Aa) and spontaneous transient inward currents (STICs, blue dotted arrow and asterix, Fig 1A & Aa). Figure 1Aa illustrates the HC which was the measured current (red arrow) between 0pA and the red-dotted line as an average over a 60 second recording. STICs were measured by taking an average of peak currents (blue asterix, Fig. 1Aa) over a period of 60 seconds from the red-dotted line (which represents 0mV for measuring STIC currents). HC and STICs were collectively termed 'basally activated non-selective cation currents' or bI_{NSCC} . (B) bI_{NSCC} were also recorded in monkey colonic SMC. (C) When E_{Cl} was set to -40mV and the holding potential was changed from -60mV to +60mV in 20mV increments, the STIC activity and HC reversed at approximately 0mV which indicated that Cl^- conductances did not contribute to these currents.

Figure 2: Na^+ contributed to bI_{NSCC} and membrane potential

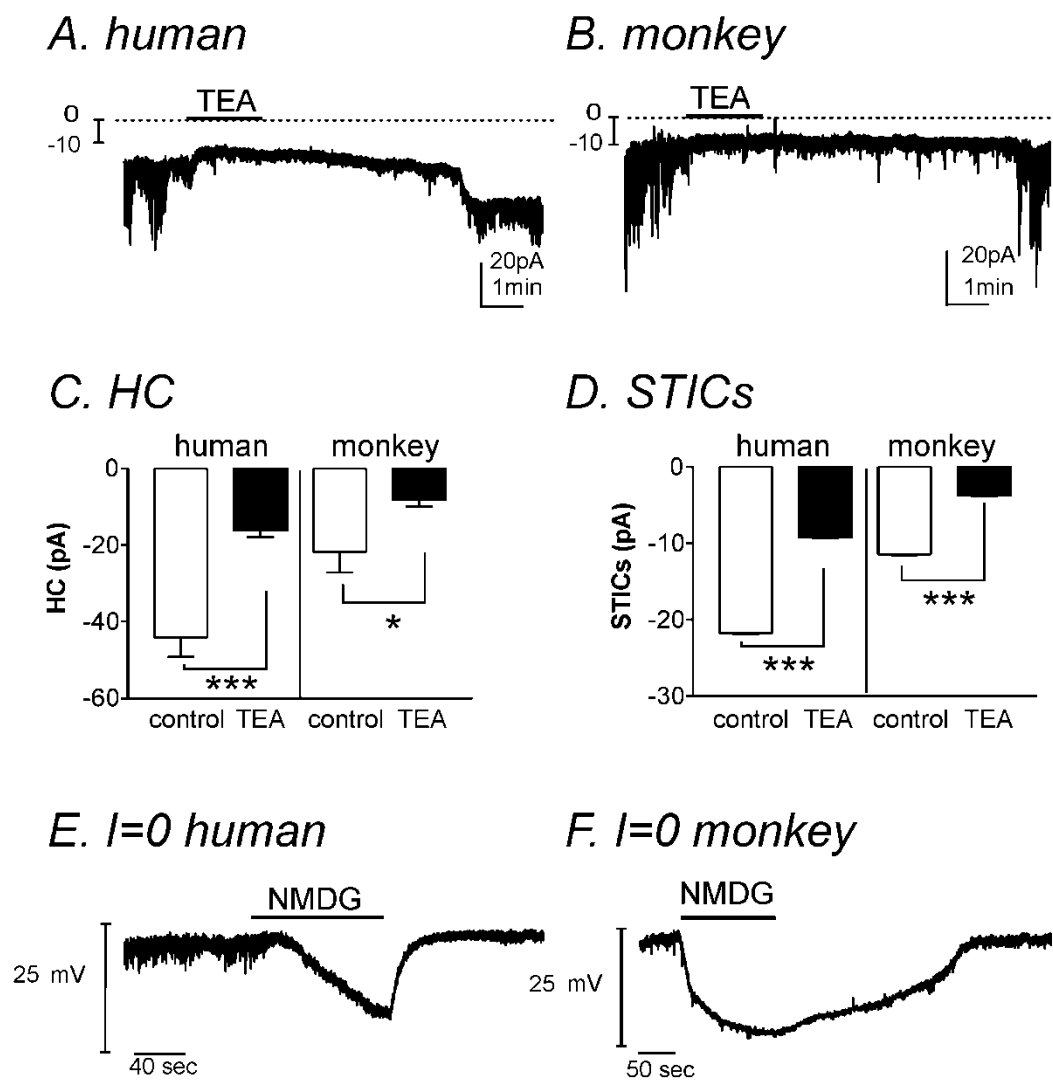
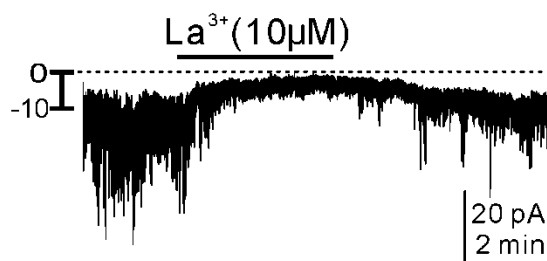


Figure 2: Na⁺ contributed to bI_{NSCC} and membrane potential

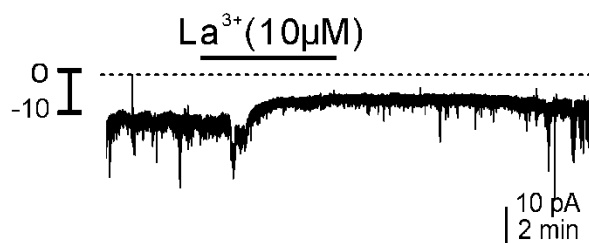
(A and B) Under voltage clamp, replacement of external Na⁺ (135mM) with equimolar TEA significantly reduced HC and STIC activity in human and monkey colonic SMC. (C) Summary of the effect of TEA on HC in human and monkey SMC (human, n=5; monkey, n=6). (D) Summary of the effect of TEA on STICs in human and monkey SMC (human, n=5; monkey, n=5). (E) In current clamp ($I=0$), a reduction in external Na⁺ from 135mM to 5mM (130mM NMDG) induced hyperpolarization in human SMC (n=4, $P<0.001$). (F) A similar effect of reducing external Na⁺ to 5mM (130mM NMDG) was recorded in monkey colonic SMC (n=6, $P<0.001$). * denotes $P<0.05$ and *** denotes $P<0.001$.

Figure 3: NSCC blockers inhibited bI_{NSCC}

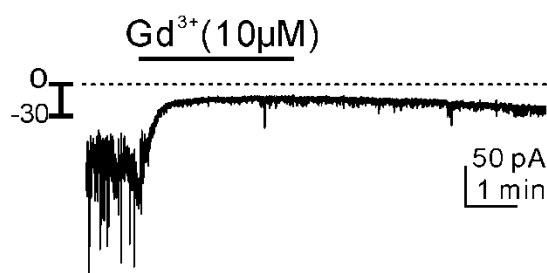
A. human



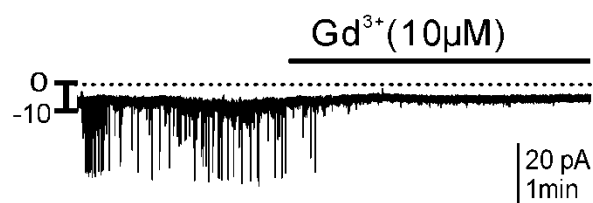
B. monkey



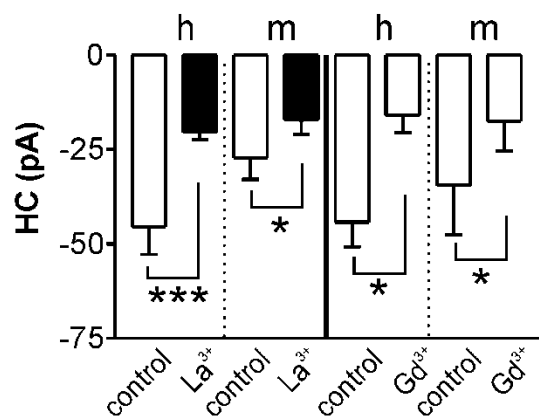
C. human



D. monkey



E. HC



F. STICs

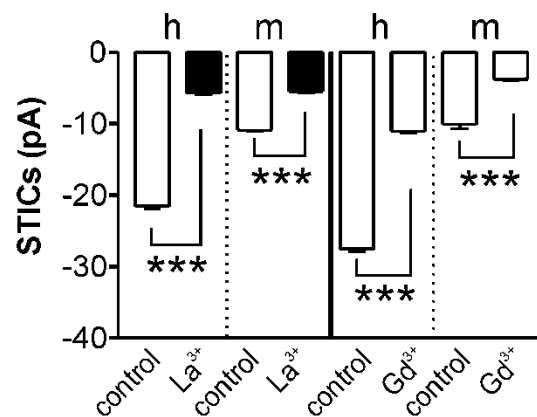


Figure 3: NSCC blockers inhibited bI_{NSCC}

(A and B) Addition of the NSCC blocker La^{3+} (10 μ M), significantly decreased HC and STICs in human and monkey colonic SMC. (C and D) Another NSCC blocker, Gd^{3+} , also significantly decreased HC and STIC in human and monkey colonic SMC. (E) Summary of the effects of La^{3+} and Gd^{3+} on HC in human and monkey colonic SMC (La^{3+} human, n=5; La^{3+} monkey, n=4; Gd^{3+} human, n=4; Gd^{3+} monkey, n=7). (F) Summary of the effect of La^{3+} and Gd^{3+} on STICs from human and monkey colonic SMC (La^{3+} human, n=5; La^{3+} monkey, n=4; Gd^{3+} human, n=4; Gd^{3+} monkey, n=6). * denotes $P<0.05$ and *** denotes $P<0.001$.

Figure 4: Ca^{2+} contributed to bI_{NSCC}

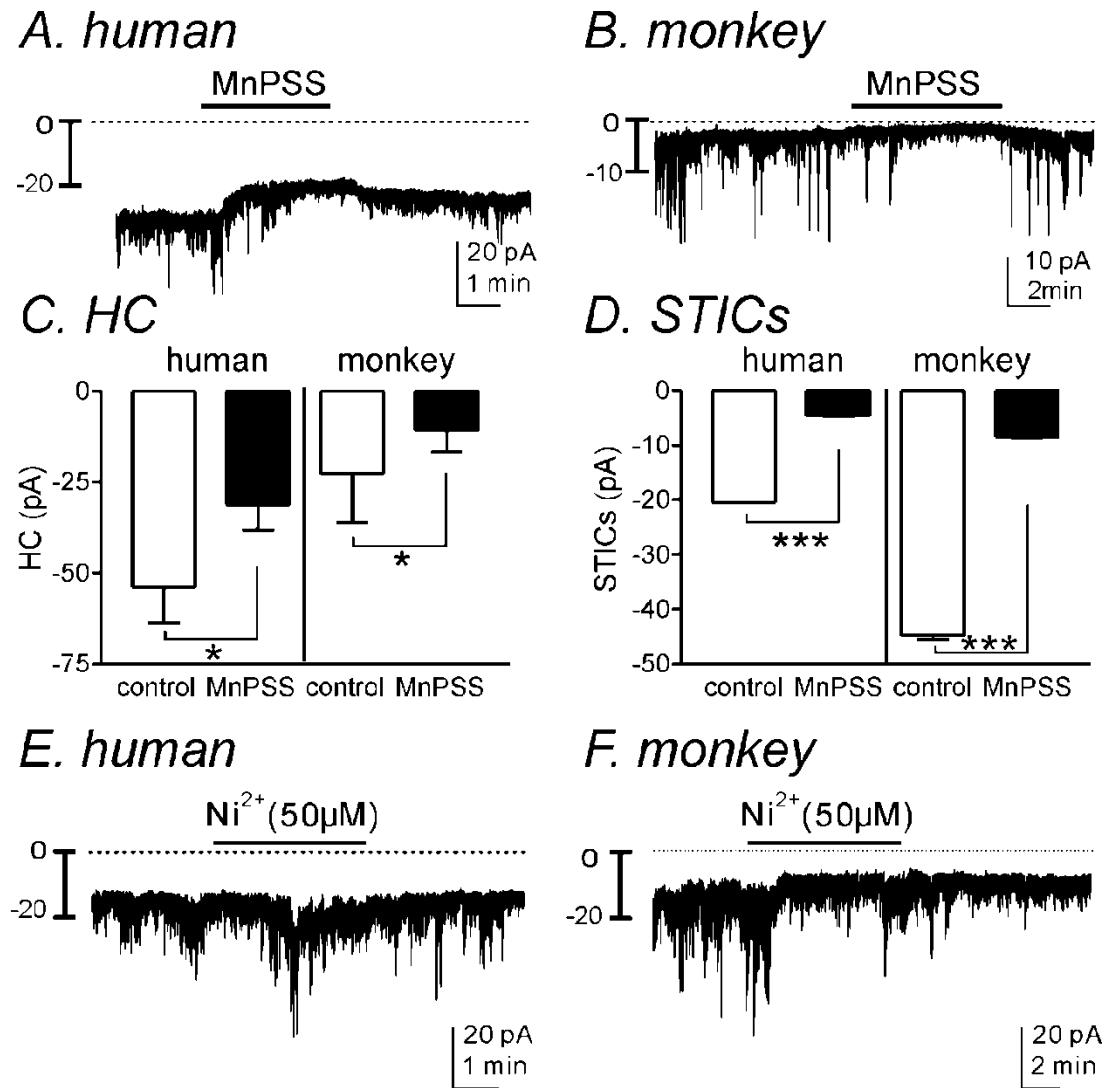


Figure 4: Ca²⁺ contributed to b_{I/NSCC}

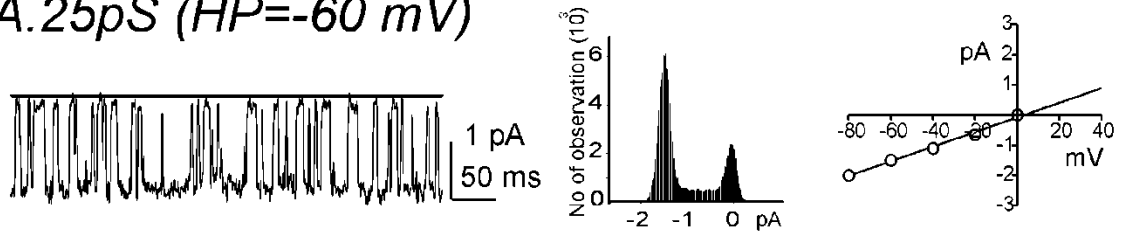
(A and B) Under voltage clamp, replacement of external CaPSS with MnPSS significantly reduced HC and STIC activity in human and monkey colonic SMC.

(C) Summary of the effect of MnPSS on HC in human and monkey SMC (human, n=4; monkey, n=7). (D) Summary of the effect of MnPSS on STICs in human and monkey SMC (human, n=4; monkey, n=4).

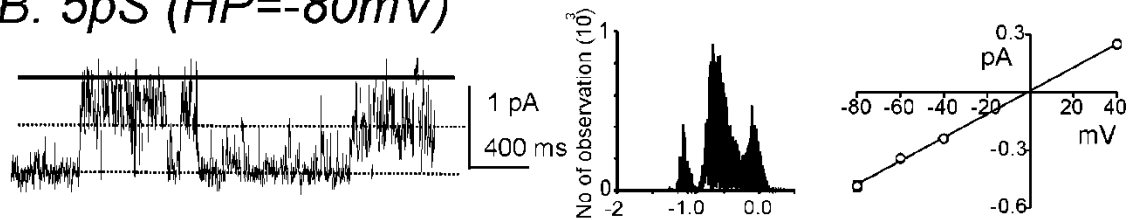
(E & F) Representative traces showing that addition of the T-type Ca²⁺-channel blocker Ni²⁺ (50μM) under voltage clamp conditions had no significant effect on HC and STICs in human and monkey colonic SMC. * denotes $P<0.05$ and *** denotes $P<0.001$

Figure 5: Single channel conductances recorded in monkey colonic SMC

A. 25pS ($HP=-60\text{ mV}$)



B. 5pS ($HP=-80\text{mV}$)



C. $sNSCC$ ($HP=-80\text{mV}$)

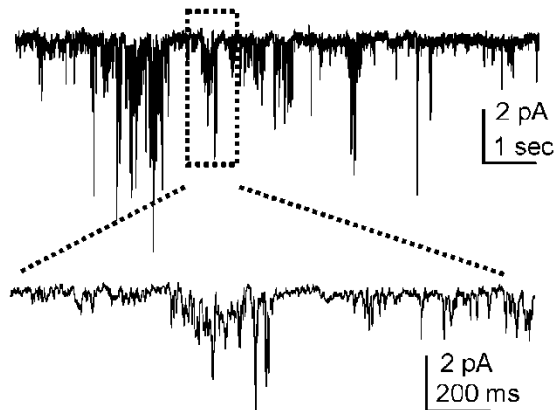
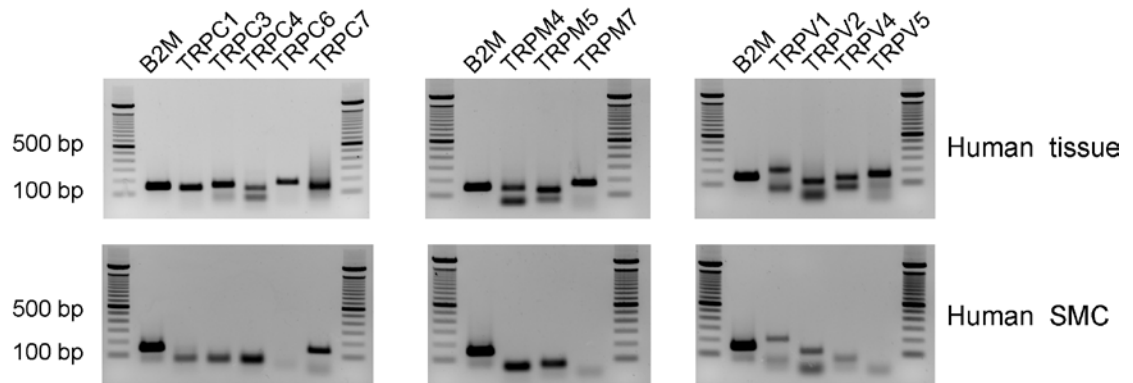


Figure 5: Single channel conductances recorded in monkey colonic SMC

(A-C) Using the inside-out configuration with symmetrical Cs⁺ (140mM), three conductances were recorded in monkey colonic SMC. (A) At a holding potential of -60mV, single channel openings were recorded that were -1.5pA in amplitude (see *single channel trace and all-points amplitude histogram*). A conductance of 25pS was calculated by plotting peak channel amplitude at different voltages and fit with linear regression (see *I-V graph, top right panel*). (B) At a holding potential of -80mV, single channel openings were recorded that had an amplitude of -0.6pA (see *single channel trace and all-points amplitude histogram*). The calculated single conductance was 5pS (see *IV graph, middle right panel*). (C) Small conductance single channel openings (sNSCC) were recorded at a holding potential of -80mV though it was impossible to calculate the conductance since there were no definite open and closed states (see *trace and expanded region*).

Figure 6: TRP channels expressed in human and monkey colonic tissue and SMC

A. HUMAN



B. MONKEY

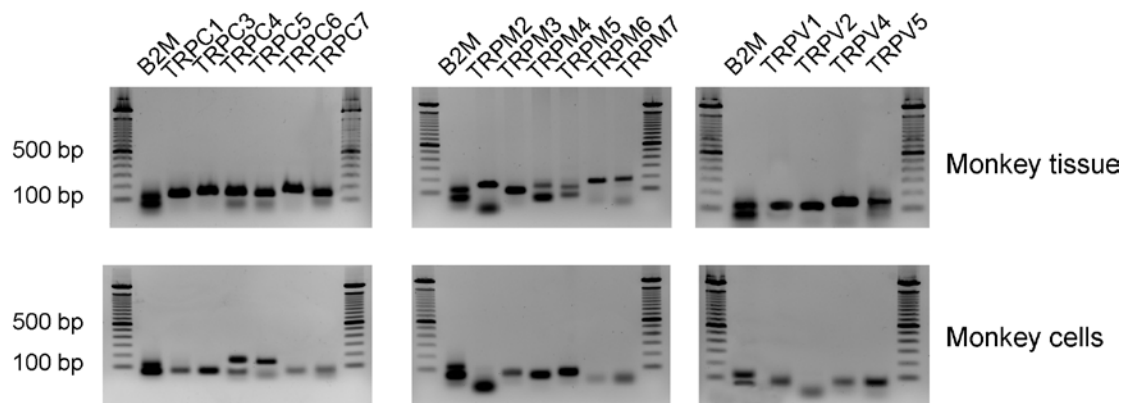


Figure 6: TRP channels expressed in human and monkey colonic tissue and SMC

(A and B) RT-PCR analysis was performed in human and monkey colonic tissue and SMC using TRP isoform specific primers for members of the TRPC, TRPM and TRPV subfamilies. Beta-2-macroglobulin (B2M) was used as a control. (A and B, top gels) Representative agarose gels illustrating TRP transcripts present in human and monkey colonic tissue respectively. (A and B, lower gels) Representative agarose gels showing TRP transcripts expressed in human and monkey colonic SMC respectively. In human colonic tissue, TRP -C1, -C3, -C4, -C6, -C7, -M4, -M5, -M7, -V1, -V2, -V4, -V5 were expressed whereas in colonic SMC, only TRP -C7, -V1 and -V2 transcripts were detected. In monkey colonic tissue, TRP -C1, -C3, -C4, -C5, -C6, -C7, -M2, -M3, -M4, -M5, -M6, -M7, -V1, -V2, -V4, -V5 were expressed whereas in colonic SMC only TRPC4 and TRPC5 transcripts were detected. (Note: other bands on gels are primer dimers).

Table 1. Oligonucleotides used in the TRP channel study

Name	Sequences (5'-3')	T _m	Size(bp)of cDNA	¹ Gene	² Specificity
TRPC1-2	CTGTGGATTATTGGGATGATTTGGTCA	57	138/3611	TRPC1	M/H/MK
TRPC1-2r	CACTTTGAGGGCAAAGGTTGCCAA	57		TRPC1	M/H/MK
TRPC2-1	CTCCTCCTGGCTGGGCTTG	58	159/770	TRPC2	M/H
TRPC2-1r	GGTGAAGCTGAGCATGCTGGTG	59		Trpc2	M/H
TRPC3-2	CAGCATTCTCAATCAGCCAACACG	57	157/13058	TRPC3	M/H/MK
TRPC3-2r	AAGTTCATAACGAAGGCTGGAGATATC	57		TRPC3	M/H/MK
TRPC4-1	CTACCTGATAGCTCCCAAAAGCC	57	152/152	TRPC4	M/H/MK
TRPC4-1r	GACCTTGCCTGTTCAAGTCTGAC	57		TRPC4	M/H/MK
TRPC5-3	CATCTCCCTGGTAGTGCTGCTG	59	134/23393	TRPC5	M/H/MK
TRPC5-3r	CACCTTCATCAAAGTAACTCATCCAGAG	58		TRPC5	M/H/MK
TRPC5-1	GGATTTTGCATGAAGTCCCTCTACC	58	146/5557	TRPC5	M/H
TRPC5-1r	ATGTTGGATATTGCCAAGAGTGCTTC	57		TRPC5	M/H
TRPC6-2	GTGGTCCTTGCTGTTGCCATTG	57	175/9469	TRPC6	M/H/MK
TRPC6-2r	CTTCAAATCTGTCAGCTTCATTGATGAC	58		TRPC6	M/H/MK
TRPC7-2	CTCATAATGAGAATCAAGATGTGCCTC	57	136/1167	TRPC7	M/H/MK
TRPC7-2r	CAGAATTCCTCATGCCAGCCTG	57		TRPC7	M/H/MK
hTRPM1-1	CGTGGATTGAAGCTCTTCCTTAGC	57	185/23243	TRPM1	H/MK
hTRPM1-1r	CTTTCATTGATTTCTTCCAACCTCATTGAC	58		TRPM1	H/MK
hTRPM2-1	CCTGCAGCAAGATCCTGAAGGA	57	155/1574	TRPM2	H/MK
hTRPM2-1r	GAGCAGTTTCTGGGCTCTCTCTTC	59		TRPM2	H/MK
hTRPM3-1	GAAGTGTTCGCGACCAGATAGACC	59	105/37825	TRPM3	H/MK
hTRPM3-1r	CACGATCCAAGCTCCTGTCTTGC	59		TRPM3	H/MK
hTRPM4-1	CTGGATGAGCTGCGTTTGGCTG	59		TRPM4	M/H/MK
hTRPM4-1r	GAATCAGGCCGGTCATTGACGA	59	141/1257	TRPM4	H/MK
TRPM5	CAACTGGAACAAGTGTGACATGGTG	58		TRPM5	M/H/MK
hTRPM5-1r	CAGCGTGAACACCATGAAGTCCATG	59	127/494	TRPM5	H/MK
TRPM6-1	GAATCAACATGCAGGTCCATATGTGAC	58	174/3159	TRPM6	M/H/MK
hTRPM6-1r	TGGCTCAAATACAATATCTCGAGCTAG	57		TRPM6	H/MK
hTRPM7-1	GGTATGTGCGTTTGTAGATTTTCTAGC	58	180/5749	TRPM7	H/MK
hTRPM7-1r	GAGTCCAAGATGGTGTTCATGAG	57		TRPM7	H/MK
TRPM8-1	AAGCTTCTGCTGGAGTGGAAACCAG	59	126/4818	TRPM8	M/H/MK
TRPM8-1r	CTTGGGTCTGTCTTTATGAGAGCC	59		TRPM8	M/H/MK
TRPV1-2	GAGAGCAAGAACATCTGGAAGCTGC	59	204/1502	TRPV1	M/H/MK
TRPV1-2r	GATGATGCCACGTTGGTGTTC	59		TRPV1	M/H/MK
hTRPV2-1	GATCTGGCTGGACTTCCAGATAC	59	110/2460	TRPV2	H/MK
TRPV2-1r	TTCAGCACAGCCTTCATCAGGCAC	59		TRPV2	M/H/MK
hTRPV3-1	GCTGAAGAAGCGCATCTTTGCAGC	59	135/910	TRPV3	H/Mk
TRPV3-1r	GTCAGCTTGTGCATGAGGAAGTCAG	59		TRPV3	M/H/MK
TRPV4-1	GTGCTGGAGATCCTGGTGTACAAC	59	136/2369	TRPV4	M/H/MK
TRPV4-1r	TAGGAGACCACGTTGATGTAGAAGG	58		TRPV4	M/H/MK
hTRPV5-1	CTGCACATCGCTGTTGTGAACCAG	59	159/466	TRPV5	H/MK
TRPV5-1r	CACACAGGCAGCAAAGGACAAAG	57		TRPV5	M/H/MK
TRPV6-1	TGGTGTGGTACCATGGTGATG	59	189/524	TRPV6	M/H/MK
TRPV6-1r	CCATCAGCCAGCAGAATCGCATC	59		TRPV6	M/H/MK
hB2M-1	CTCTTTCTGGCCTGGAGGCTATC	59		B2M	H/MK
hB2M-1r	GAAGTTGACTTACTGAAGAATGGAGAG CTCTCCATTCTTCAGTAAGTCAACTTC	57	152	B2M	H/MK

¹ Reference cDNA sequences for each gene in the NCBI were used to design oligonucleotides. ² M, mouse; H, human; MK, monkey

2.6. Discussion

RMP plays a critical role in determining the excitability of GI smooth muscle since small fluctuations can result in major alterations in electrical activity, Ca^{2+} entry and $[\text{Ca}^{2+}]_i$ levels. Several groups have recognized that in certain cell types such as rabbit coronary artery SMC and pulmonary artery SMC, RMP is less negative than E_k and therefore membrane channels other than those selective for K^+ must contribute (Bae *et al.*, 1999; Terasawa *et al.*, 2002; Albert *et al.*, 2006). In coronary artery SMC, where the membrane potential is $\sim -46\text{mV}$, a background NSCC was shown to contribute to RMP as replacement of extracellular Na^+ with NMDG in current clamp experiments caused significant hyperpolarization (Terasawa *et al.*, 2002). Spontaneous inward currents were recorded in rabbit ear artery myocytes and these constitutively active Ca^{2+} permeable NSCC were suggested to contribute to the RMP (Albert & Large, 2003; Albert *et al.*, 2006). In murine urinary bladder SMC, inhibition of NSCC caused a substantial hyperpolarization from an initial RMP of approximately -40mV and also a decrease in the amplitude of phasic contractions. These data strongly suggested that basal activation of NSCC caused tonic depolarization of bladder SMC (Thorneloe & Nelson., 2004). However no studies have examined how RMP is regulated in GI smooth muscle. Therefore we hypothesized that ongoing regulation of RMP in colonic smooth muscle results from a finely tuned balance between background K^+ channels and constitutive activity of NSCC.

In the present study, basally activated inward currents were recorded at -80mV and reversed at 0mV when the Cl^- equilibrium potential was set at -40mV in human, monkey and murine SMC. These data suggested that these currents were due to basal activation of non-selective cation conductances which we termed bI_{NSCC} . These bI_{NSCC} appeared to be composed of 2 different currents, one a HC and the second composed of STICs. Since these bI_{NSCC} were constitutively active in the resting state, it was possible that continuous influx of cations through these channels could lead to a more positive RMP seen in colonic smooth muscle and thus increase smooth muscle excitability.

In voltage-clamp mode, replacement of external Na^+ with equimolar TEA significantly reduced STICs and HC in human and colonic myocytes suggesting that the major charge carrier for bI_{NSCC} is Na^+ in these species. Thus, bI_{NSCC} raise the net permeability of colonic SMC to Na^+ ions resulting in ongoing Na^+ entry. Ca^{2+} replacement experiments also illustrated that there was a Ca^{2+} permeable component of bI_{NSCC} .

The important contribution of bI_{NSCC} to RMP was further illustrated from current-clamp recordings. Decreasing the influx of Na^+ through bI_{NSCC} by lowering external Na^+ , caused significant hyperpolarization of the RMP in human and monkey SMC. These observations suggest that bI_{NSCC} is a major underlying mechanism that regulates the RMP in human and monkey colonic SMC.

TRP channel proteins are a group of NSCC they are activated by a huge variety of stimuli including voltage, mechanical forces, physical and chemical

factors and intracellular signaling pathways (Venkatachalam & Montell, 2007). Some TRP channels have been proposed to play an important role in the regulation of the RMP. In particular, those TRP channels that exhibit constitutive activity, such as TRPC3, TRPC7 and TRPV2, are thought to allow basal influx of extracellular cations Ca^{2+} and Na^+ that shift the RMP to more positive potentials. TRPC3 is the molecular candidate for constitutively active NSCC proposed to contribute to the resting membrane conductance in rabbit ear artery myocytes (Albert *et al.*, 2006). In the current study qualitative PCR revealed that human and monkey colonic tissue expressed similar TRP channel transcripts (from the three subfamilies tested, TRPC, TRPM and TRPV). However these results reflected TRP channels present in not only SMC but other cell types such as neurons and ICC. Analysis of dispersed human colonic SMC revealed TRPC7, V1 and V2 transcripts which could be molecular candidates for bI_{NSCC} . TRPC7 has a single channel conductance of 25-50pS and is weakly Ca^{2+} selective (Owsianik *et al.*, 2006; Clapham, 2001). Structurally, it is closely related to TRPC3 and most importantly, like TRPC3, it is constitutively active under resting conditions (Trebak *et al.*, 2003). Therefore this channel could be an important component of bI_{NSCC} in human colonic SMC. In relation to TRPV1 and TRPV2 properties, TRPV-subfamily members are classically associated with a role in temperature sensing and nociception and therefore are predominantly expressed in sensory neurons (Caterina *et al.*, 2000). Studies performed in the colon found that TRPV1 is expressed predominantly in the rectum and distal colon and is located in mucosa, submucosa, smooth muscle layers and myenteric plexus.

However since constitutive activity of TRPV1 has not been reported, its potential role in contributing to the RMP in colonic SMC remains to be determined. TRPV2 is constitutively active under resting conditions when expressed in HEK cells and can cause an increase in basal Ca^{2+} levels (Penna *et al.*, 2006). Thus, like TRPC7, it is a possible component of b_{NSCC} .

In monkey SMC, only TRPC4 and TRPC5 were expressed. Reasons for the differences in expression between monkey and human are difficult to interpret although could simply be due to species difference. TRPC5 is reported to be basally active under resting conditions (Schaefer *et al.*, 2000). Thus, TRPC5 conductance may contribute to setting the RMP. In contrast TRPC4 does not appear to play a role in regulating the RMP in the murine small intestine (Tsvilovskyy *et al.*, 2009). However, when the human TRPC4 α (splice variant of TRPC4) is expressed in CHO cells, it forms a constitutively active NSCC (McKay *et al.*, 2000). Therefore, monkey TRPC4 may be structurally and physiologically more similar to human than mouse (which would be expected) and therefore possess higher basal activity.

In conclusion our data suggests that b_{NSCC} contributes to the setting of the RMP and therefore regulates the excitability of colonic smooth muscle.

Chapter 3:

Phospholipase C-independent effects of the phospholipase C agonist, *m*-3M3FBS, in murine colon

3.1. Summary

Since PLC can regulate many ion channels, we initially wanted to examine PLC-dependent regulation of colonic tissue and bI_{NSCC} . However in preliminary studies we found that the PLC agonist, 2, 4, 6-trimethyl-N-(meta-3-trifluoromethyl-phenyl)-benzenesulfonamide (*m*-3M3FBS) had unexpected effects on contractility. Since this drug is commonly used as a PLC-activator, we thought it was necessary to examine the non-specific mode(s) of action of this drug by examining its effects on ion channel activity.

We examined the effects of *m*-3M3FBS and its inactive analog, 2, 4, 6-trimethyl-N-(ortho-3-trifluoromethyl-phenyl)-benzenesulfonamide (*o*-3M3FBS), on murine colonic smooth muscle tissue and SMC by performing conventional microelectrode recordings, isometric force measurements and patch clamp experiments.

Application of *m*-3M3FBS decreased spontaneous contractility in murine colonic smooth muscle without affecting the RMP. Patch clamp studies revealed that delayed rectifier K^+ channels were reversibly inhibited by *m*-3M3FBS and *o*-3M3FBS. The PLC inhibitor, 1-(6-((17 β -3-methoxyestra-1,3,5(10)-trien-17-yl)amino)hexyl)-1H-pyrrole-2,5-dione (U73122), did not prevent this inhibition by

m-3M3FBS. Both *m*-3M3FBS and *o*-3M3FBS decreased two components of delayed rectifier K⁺ currents in the presence of tetraethylammonium chloride or 4-aminopyridine. Ca²⁺ currents were significantly suppressed by *m*-3M3FBS and *o*-3M3FBS with a simultaneous increase in [Ca²⁺]_i. Pretreatment with U73122 did not prevent the decrease in Ca²⁺ currents upon *m*-3M3FBS application.

In conclusion, both *m*-3M3FBS and *o*-3M3FBS inhibited inward and outward currents via mechanisms independent of PLC acting in an antagonistic manner. Paradoxically, both compounds also increased [Ca²⁺]_i in an agonistic manner. From these data we suggest that *m*-3M3FBS is not a specific activator of PLC and *o*-3M3FBS cannot be considered an inactive analogue of *m*-3M3FBS.

3.2. Background and Aims

Phosphoinositide specific phospholipase C (PLC) plays a critical role in multiple signal transduction pathways resulting in various cellular responses (Rebecchi & Pentylala, 2000; Rhee, 2001; Hicks *et al.*, 2008; Suh *et al.*, 2008). Attempts have been made to identify molecules that can directly modulate PLC activity to elucidate PLC-mediated signaling pathways and important physiological reactions. The compound 2, 4, 6-trimethyl-N-(meta-3-trifluoromethyl-phenyl)-benzenesulfonamide (*m*-3M3FBS) stimulated the generation of superoxide in human neutrophils and this stimulation was through direct activation of PLC. 2, 4, 6-trimethyl-N-(ortho-3-trifluoromethyl-phenyl)-benzenesulfonamide (*o*-3M3FBS), which differs from *m*-3M3FBS by the position of the trifluoromethyl-phenyl group, was used as the inactive analog as it did not affect superoxide generation up to 50 μ M (Bae *et al.*, 2003). *m*-3M3FBS caused a transient increase in intracellular Ca²⁺ ([Ca²⁺]_i) in various cell lines including neutrophils, leukocytes and fibroblasts, an effect that was inhibited by the PLC inhibitor, 1-(6-((17 β -3-methoxyestra-1,3,5(10)-trien-17-yl)amino)hexyl)-1H-pyrrole-2,5-dione (U73122). *m*-3M3FBS also stimulated the formation of inositol phosphates (Bae *et al.*, 2003). In addition, it activated three subfamilies of PLC (β , γ and δ) isoforms *in vitro* and thus was concluded to show no isoform-specificity. *o*-3M3FBS did not affect any of these parameters (Bae *et al.*, 2003). However the specificity of *m*-3M3FBS was questioned when changes in Ca²⁺ homeostasis by *m*-3M3FBS were found to be independent of PLC activation

(Krjukova *et al.*, 2004). Unlike in the previous report, *m*-3M3FBS caused a slowly developing Ca^{2+} elevation which reached a plateau within 6 minutes. The measured increase in PLC activity did not coincide with the elevation in $[\text{Ca}^{2+}]_i$ since it took more than 20 minutes for generation of inositol 1,4,5-trisphosphate (IP_3) (Krjukova *et al.*, 2004). This report concluded that *m*-3M3FBS was not a selective PLC activator in these cells and its effects on Ca^{2+} homeostasis were via PLC-independent mechanism(s).

m-3M3FBS has been used to study the role of PLC in the regulation of certain ionic currents. KCNQ2 and 3 currents recorded in transfected tsA cells were suppressed by application of *m*-3M3FBS (50 μM) through activation of PLC whereas *o*-3M3FBS had no effect on these currents. However, this compound was slow to act, had a long latency and also had a varied response that was suggested to be due to multiple actions of *m*-3M3FBS (Horowitz *et al.*, 2005). In contrast, *m*-3M3FBS caused activation of large conductance background-type potassium (LKbg) channels in B lymphocytes under the inside-out configuration suggesting that LKbg channels are regulated by a PLC-dependent mechanism (Nam *et al.*, 2007).

In gastrointestinal smooth muscle, muscarinic receptor agonists produce excitation and contraction of smooth muscle (So & Kim, 2003) via activation of the PLC pathway through coupling between muscarinic receptors and $\text{G}_{q/11}$ proteins (Unno *et al.*, 2003; Unno *et al.*, 2006; Zholos, 2006). Since the specificity of *m*-3M3FBS on membrane excitability has not been studied clearly, we tested

the effects of *m*-3M3FBS on membrane excitability and ionic currents in murine colonic smooth muscle.

3.3. Materials and methods

3.3.1. Animals

SMC were prepared from colons removed from BALB/c mice. Mice were anesthetized with isoflurane and killed by cervical dislocation. Colons were removed from the animals through a midline abdominal incision. The animals were maintained and the experiments performed in accordance with the National Institutes of Health *Guide for the Care and Use of Laboratory Animals*. The Institutional Animal Use and Care Committee at the University of Nevada approved all procedures used.

3.3.2. Mechanical responses

Segments of the proximal colon from 1 cm distal to the ileocecal sphincter were removed through a midline abdominal incision and opened along the mesenteric border. Luminal contents were removed by washing with Krebs–Ringer bicarbonate solution (KRB, see section 3.3.6.), and the cleaned tissue sheets were pinned down onto a Sylgard base with the mucosa facing up. The mucosa was removed leaving the tunica muscularis and remnants of the submucosa.

Mechanical responses were performed using standard organ-bath techniques. Strips of muscle (10 × 5 mm) were cut from the *tunica muscularis* by sharp dissection. The muscles were attached with sutures to a fixed mount within

the organ bath and to an isometric strain gauge (World Precision Instruments, Sarasota, FL, U.S.A.). The muscles were immersed in oxygenated KRB and maintained at $37.5 \pm 0.5^\circ\text{C}$. The muscles were set at resting tension by applying 0.1–0.3 g of basal tension and then allowed to equilibrate for 1–2 hours with constant perfusion with fresh KRB. Contractions of the muscles were monitored, digitized and stored using Axoscope software (Axon Instruments, CA, USA). Contractions were quantified by calculations of area above the baseline using the pClamp software (v8.1, Axon instruments, CA, USA). The area under the curve (AUC) was determined as the integral values above the baseline of a selected area for 5 min recordings ($\text{mN} \cdot \text{min}$). The AUC for the tissues exposed to tested drugs were compared to the AUC for tissues under control conditions during an equivalent period of time. Drugs were diluted to the desired concentrations and applied to the muscles by switching the perfusion to the drug-containing solution.

3.3.3. Intracellular microelectrode recordings

After removing the mucosa, strips of proximal colon (1 cm in length \times 0.5 cm in width) were taken from the region 1–2 cm from the ileocecal sphincter and pinned to a Sylgard (Dow Corning Corp., Midland, MI, USA) elastomer-coated recording chamber with the mucosal side of the circular muscle facing upward. SMC were impaled with glass microelectrodes filled with 3M KCl and having electrical resistances of 80–100 M Ω . Transmembrane potentials were measured with a standard high input impedance amplifier (WPI Duo 773, Sarasota, FL,

USA). Electrical signals were recorded by a PC-style computer running Axoscope data acquisition software (Axon Instruments, CA, USA) and analyzed by Clampfit (v9.02, Axon Instruments, CA, USA). All experiments were performed in the presence of wortmannin (10 μ M) to reduce movement and facilitate impalements of cells for extended periods of time.

3.3.4. Preparation of isolated colonic SMC

Colons were cut open along the longitudinal axis, pinned out in a Sylgard-lined dish, and washed with Ca²⁺-free phosphate-buffered saline containing (mM): 125 NaCl, 5.36 KCl, 15.5 NaHCO₃, 0.336 Na₂HPO₄, 0.44 KH₂PO₄, 10 glucose, 2.9 sucrose, and 11 HEPES and adjusted to pH 7.4 with NaOH. Mucosa and submucosa were removed with fine-tipped forceps. Pieces of muscle were incubated for 30-40 minutes at 37°C in a Ca²⁺-free solution (ml) containing 2 mg collagenase (Worthington Biochemical, Lakewood, NJ), 4 mg trypsin inhibitor, 4 mg fatty acid-free bovine serum albumin, 1 mg papain and 0.3mg dithiothreitol (Sigma-Aldrich, MO, USA). After enzymatic treatment, the muscles were washed with Ca²⁺-free solution and agitated gently to create a cell suspension. Dispersed SMC were stored at 4°C in Ca²⁺-free solution. SMC were transferred from the refrigerator to the recording chamber. Drops of the cell suspensions were placed on the bottom of a 300 μ l chamber mounted on an inverted microscope and allowed to adhere to the bottom of the chamber for 5 minutes before recording.

3.3.5. Voltage-clamp methods

Whole cell voltage-clamp techniques were used to record membrane currents from dissociated SMC. Membrane currents were amplified by an Axopatch 1D (Axon Instruments, Foster City, CA) and digitized with an analog-to-digital converter (Digidata 1200, Axon Instruments). Data were collected at 5 kHz, filtered at 2 kHz via Bessel filter, and digitized online with pCLAMP software. The data were analyzed with the use of Clampfit software (version 9.2, Axon Instruments, CA, USA). Pipette resistances were 1–4 M Ω . The linear leak current was subtracted digitally. Conventional and perforated whole cell patch-clamp techniques were used for recording ionic currents under voltage clamp. For perforated patches, amphotericin B (60 mg/ml) was dissolved in DMSO, sonicated, and diluted in the pipette solution to give a final concentration of 270 μ g/ml. Experiments were performed at room temperature (between 22 and 25°C).

3.3.6. Solutions

For conventional microelectrode and contractile recordings, the strips were exposed to KRB with the following composition (mM): 118.5 NaCl, 4.5 KCl, 1.2 MgCl₂, 23.8 NaHCO₃, 1.2 KH₂PO₄, 11.0 dextrose and 2.4 CaCl₂. In order to measure inward currents, colonic myocytes were bathed in a Ca²⁺-containing physiological salt solution (CaPSS) containing (mM): 135 NaCl, 5 KCl, 2 CaCl₂,

1.2 MgCl₂, 10 glucose, 10 HEPES adjusted to pH 7.4 with Tris. The pipette solution for the study of inward currents contained (in mM): 135 CsCl, 0.1 EGTA, 0.1 Na₂GTP, 3 MgATP, 10 glucose, 2.5 creatine phosphate disodium and 10 HEPES. This solution was adjusted to pH 7.2 with Tris. When studying outward currents, cells were perfused in MnPSS (same as CaPSS except Ca²⁺ was replaced with Mn²⁺ (2 mM)) and the pipette solution contained (in mM): 135 KCl, 10 BAPTA, 0.1 Na₂GTP, 3 MgATP, 10 glucose, 2.5 creatine phosphate disodium and 10 HEPES and was adjusted to pH 7.2 with Tris.

3.3.7. Calcium imaging analysis

A stock solution of Fluo-4 AM (FluoroPure AM; Molecular Probes, Eugene, OR, USA) was dissolved in DMSO (50 µg Fluo-4 AM in 10 µl DMSO). One microlitre of Fluo-4 stock solution (5 µg) was added to dispersed colonic myocytes in 1 ml of Ca²⁺ free solution. Cells were incubated in Fluo-4 for 15 minutes (room temperature) after which they were perfused with CaPSS solution at 24 ± 0.5°C for 10 minutes to allow for de-esterification of the dye. Cells were imaged under an inverted fluorescence microscope (Nikon, TE2000-S; Technical Instruments, Burlingame CA, USA), using excitation and emission suitable for Fluo-4 (excitation 460–490 nm and emission > 515 nm), delivered via a xenon arc from a Lambda DG-5 (Sutter Instruments, Novato, CA, USA). Neutral density filters were used to adjust excitation intensity. Images of Ca²⁺-induced fluorescence changes were recorded at room temperature using a Hamamatsu ORCA digital camera (Bridgewater, NJ, USA) and SIMPLE PCI (version 5.3.1;

Compix Inc. Imaging Systems, PA, USA). Fluorescence images were stored as a time series (one frame per sec). During patch experiments, standard ramp protocols were applied and voltage-dependent changes in $[Ca^{2+}]_i$ recorded. Changes in fluorescence are shown relative to the baseline fluorescence ($\Delta F/F$), where F denotes baseline fluorescence and ΔF is the change in fluorescence in response to stimulation by ramp depolarizations and the compounds *m*-3M3FBS and *o*-3M3FBS.

3.3.8. Statistical analysis

Data are reported as means \pm S.E.M. In describing the intracellular and voltage-clamp results, n is the number of tissues and cells tested respectively. Statistical significance was evaluated by Student's t test. P values less than 0.05 were considered significant.

3.3.9. Chemicals

N-(3-trifluoromethylphenyl)-2,4,6-trimethylbenzenesulfonamide (*m*-3M3FBS) and 1-[6-(((17 β)-3-methoxyestra-1,3,5[10]-trien-17-yl)amino)hexyl]-1*H*-pyrrole-2,5-dione (U-73122) were obtained from Calbiochem (San Diego, CA, USA). 2,4,6-Trimethyl-*N*-[2-(trifluoromethyl)phenyl]benzenesulfonamide (*o*-3M3FBS) was obtained from Tocris Bioscience (Ellisville, MO, USA). 4-

aminopyridine (4-AP), tetraethylammonium chloride (TEA), tetrodotoxin (TTX) and wortmannin were obtained from Sigma (St. Louis, MO, USA).

3.4. Results

3.4.1. *m*-3M3FBS inhibited contractility of murine colonic smooth muscle

We performed isometric force measurements to examine the effects of *m*-3M3FBS on murine colonic smooth muscle. Since excitatory and inhibitory neurotransmitters contribute to spontaneous phasic contractions (Wang *et al.*, 2000b), in all contractile experiments muscle strips were incubated with TTX (1 μ M), which blocks axonal action potential transmission and neurotransmitter release from nerve terminals. Figure 1A shows that after administration of TTX there was a significant increase in the amplitude of the spontaneous phasic contractions, indicating that inhibitory neurotransmitters may be dominant in murine colonic smooth muscle. Although the cellular basis of the rhythmic activities of the colon has not yet been clearly identified, the cyclic depolarizations from pacemaker cells (ICC) may evoke action potentials in SMC and induce spontaneous colonic motility (Alberti *et al.*, 2005).

Contractile responses to *m*-3M3FBS were compared by determining the area under the curve (AUC) (see materials and methods section). The AUC for 5 minute recordings was 526 \pm 62 mN*min in control and 355 \pm 48 mN*min in *m*-3M3FBS (n=10, P <0.001). Increasing the concentration of *m*-3M3FBS to 25 μ M caused a further decrease in AUC to 220 \pm 31 mN*min (n=10, P <0.001 compared to 10 μ M, Fig. 1A). These effects of *m*-3M3FBS were reversible upon washout. Since changes in contractility seen by *m*-3M3FBS could be due to hyperpolarization, we performed membrane potential measurements using

conventional microelectrode recordings. The application of *m*-3M3FBS (10 and 25 μ M) had no significant effect on membrane potential (n=5, Fig. 1B). We also examined the effect of the inactive analog, *o*-3M3FBS, on contractility of colonic smooth muscle. *o*-3M3FBS (10 μ M) decreased AUC from 1058 \pm 189 mN*min in control (in the presence of TTX) to 840 \pm 134 mN*min (n=4, P <0.05). A higher concentration of *o*-3M3FBS (25 μ M) further decreased AUC to 457 \pm 59 mN*min (n=4, P <0.001 compared to 10 μ M, Fig. 1C). These data suggest that *o*-3M3FBS may act on colonic smooth muscle as a partial antagonist. Therefore we performed patch clamp experiments to understand the mechanisms of the electrical and contractile responses seen by application of *m*-3M3FBS and *o*-3M3FBS.

3.4.2. m-3M3FBS inhibited delayed rectifier K⁺ currents in a PLC-independent manner

Since both *m*-3M3FBS and *o*-3M3FBS decreased contractility, we investigated PLC-dependent mechanisms on outward and inward currents. Firstly, we performed conventional dialyzed whole cell experiments to examine direct effects of these drugs on ionic currents. The external solution was MnPSS and cells were dialyzed with K⁺-rich solution containing 10mM BAPTA. Ca²⁺ was replaced with Mn²⁺ (2mM) externally and the Ca²⁺ concentration was decreased using a high concentration of BAPTA internally to minimize contamination by large-conductance Ca²⁺-activated K⁺ currents (BK). *m*-3M3FBS (10 μ M)

significantly decreased net delayed rectifier K^+ currents (I_{DR}) during step depolarizations from -80mV to +30mV at a holding potential of -80mV (Fig. 2A & B). The averaged currents before and after *m*-3M3FBS (10 μ M) application at +20mV were 1327 ± 460 pA and 508 ± 256 pA, respectively ($n=4$, $P<0.05$). Figure 2C shows the normalized current-voltage (*I-V*) relationship with peak currents at +30mV. Peak I_{DR} currents were significantly reduced at potentials positive to -20 mV ($n=4$, $P<0.05$). When colonic myocytes were repetitively depolarized to 0mV from a holding potential of -80mV every 20 seconds, the effect of *m*-3M3FBS (10 μ M) on I_{DR} was reversible (Fig. 2D). Furthermore we tested the effects of *m*-3M3FBS in the presence of the PLC inhibitor, U73122. Upon ramp depolarizations from -80mV to +80mV, U73122 (2 μ M) itself decreased I_{DR} but not significantly ($n=4$, $P=0.4$, Fig. 2E). Additional application of *m*-3M3FBS (10 μ M) in the presence of U-73122 further decreased I_{DR} from 591 ± 83 pA to 244 ± 100 pA ($n=4$, $P<0.05$, Fig. 2F). These data suggested that the effect of *m*-3M3FBS on I_{DR} may not act through PLC activation.

Therefore, we examined effects of *o*-3M3FBS on I_{DR} . There was a significant decrease in the averaged currents before and after *o*-3M3FBS (10 μ M) at +20mV (784 ± 126 pA and 505 ± 115 pA, respectively ($n=7$, $P<0.05$, data not shown). At +20mV, there was a 69 ± 9 % reduction in I_{DR} in the presence of *m*-3M3FBS (10 μ M, $n=4$) and a 36 ± 9 % reduction in I_{DR} in the presence of *o*-3M3FBS (10 μ M, $n=7$). At the same concentration, *m*-3M3FBS was significantly more effective at reducing I_{DR} than *o*-3M3FBS ($P<0.05$).

In a previous report, we found that I_{DR} consists of two types of currents: A-type K^+ currents (I_A) and slowly-activating delayed rectifier K^+ currents (I_{DRS}) in murine colonic myocytes and these currents can be isolated pharmacologically (Koh *et al.*, 1999b). In order to isolate I_A , we added TEA (10mM) externally which inhibits I_{DRS} (Koh *et al.*, 1999b). Figure 3A shows representative traces of I_A in the presence of TEA using the same protocol described previously. The application of *m*-3M3FBS (10 μ M) decreased I_A (Fig. 3A & B). The normalized I - V relationship is shown in figure 3C with peak currents at +40 mV. The effects on I_A were statistically significant at potentials positive to -20mV ($n=4$, $P<0.05$, Fig. 3C). *o*-3M3FBS (10 μ M) also decreased I_A ($n=4$ Fig. 3D-F). At 0mV, there was a 57 ± 10 % reduction in I_A in the presence of *m*-3M3FBS (10 μ M, $n=4$) and a 29 ± 2 % reduction in I_A in the presence of *o*-3M3FBS (10 μ M, $n=4$). *m*-3M3FBS was significantly more effective than *o*-3M3FBS in reducing I_A ($n=4$, $P<0.05$). Both compounds did not affect the voltage dependence of activation (e.g. $V_{1/2} = -5.8\pm 0.9$ mV in control, 2.1 ± 3.2 mV in the presence of *m*-3M3FBS). However, the time constant of inactivation at +20mV in the presence of TEA was 166 ± 61 ms with a single exponential fit. The application of *m*-3M3FBS (10 μ M) induced fast inactivation ($\tau_f=11\pm 2$ and $\tau_s=54\pm 12$ ms) with double exponential fit (see inset in Fig. 3A & B). *o*-3M3FBS (10 μ M) also significantly increased the rate of the fast component of inactivation from $\tau = 83\pm 6$ ms in control (presence of TEA) to $\tau_f = 12\pm 2$ ms and $\tau_s=70\pm 17$ ms at +20mV (see inset in Fig. 3D & E).

In order to confirm the effects of *m*-3M3FBS on I_{DRS} , we performed experiments in the presence of 4-AP (5mM) which inhibits A-type currents (Koh *et al.*, 1999b). Figure 4A shows representative control traces of I_{DRS} in the presence of 4-AP in the bath solution using the same protocol as previously described. Application of *m*-3M3FBS (10 μ M) decreased I_{DRS} (Fig. 4A & B). The peak current in control and in the presence of *m*-3M3FBS was 334 ± 86 pA and 67 ± 20 pA at 0mV respectively ($n=4$, $P<0.05$). The normalized I - V relationship is shown in figure 4C. *o*-3M3FBS (10 μ M) also caused a significant decrease in I_{DRS} from 431 ± 52 to 293 ± 127 pA at 0mV ($n=6$, $P<0.05$, Fig. 4D-4F). There was $81\pm 3\%$ reduction of I_{DRS} by *m*-3M3FBS compared with a $38\pm 11\%$ reduction by *o*-3M3FBS. *m*-3M3FBS was significantly more effective than *o*-3M3FBS at reducing I_{DRS} ($n=4$, $P<0.05$).

3.4.3. *m*-3M3FBS and *o*-3M3FBS inhibited inward currents

The inhibition of I_{DR} should increase the contractile response with membrane depolarization since I_A regulates the RMP. However *m*-3M3FBS decreased the contractile response without affecting the RMP. Therefore we examined the potential non-specific effects of *m*-3M3FBS on inward currents. The perforated configuration of the patch-clamp technique was used on freshly dispersed colonic SMC in order to prevent run-down and preserve intracellular signaling pathways. In the pipette solution, KCl (140mM) was replaced with equimolar CsCl in order to isolate inward currents (see materials

and methods). In a previous report, two types of inward currents have been identified in murine colonic SMC, which are a low threshold voltage-activated Ca^{2+} -current (I_{LVA}) and a high threshold voltage-activated Ca^{2+} current (I_L ; L-type) (Koh *et al.*, 2001). *m*-3M3FBS (10 μ M) significantly decreased inward currents during step depolarizations from -80mV to +50mV from a holding potential of -80mV (Fig. 5A & B). During ramp depolarizations from -80mV to +80mV over 500ms every 1 minute, two distinct components of the Ca^{2+} current were observed: I_{LVA} peaked at \sim -40mV (-27 ± 10 pA, $n=5$, see dashed line in Fig. 5C) and I_L was recorded which peaked at approximately 0mV (195 ± 30 pA, see solid line in Fig. 5C). Inhibition of I_{LVA} and I_L by *m*-3M3FBS was partially reversible upon washout (Fig. 5C). The averaged *I-V* relationship is shown in figure 5D. *m*-3M3FBS (10 μ M) reduced I_{LVA} from -37 ± 10 pA to -18 ± 7 pA at -40mV but not significantly ($n=7$, $P=0.1$). I_L was significantly reduced from -332 ± 53 pA in control to -71 ± 10 pA in the presence of *m*-3M3FBS at 0mV ($n=7$, $P<0.001$, Fig. 5D). There was no significant difference in half activation and inactivation voltages before and during *m*-3M3FBS application (data not shown).

o-3M3FBS (10 μ M) significantly decreased I_L during step depolarizations from -80mV to +40mV at a holding potential of -80mV (Fig. 6A & B). The averaged currents before and during *o*-3M3FBS (10 μ M) application at 0mV were -297 ± 50 pA and -82 ± 26 pA, respectively ($n=7$, $P<0.001$). Figure 6C shows the summarized *I-V* relationship with peak currents at 0mV ($n=7$). Analysis of the half activation and inactivation voltages before and during *o*-3M3FBS application

revealed no significant differences (data not shown). At 0mV, there was a 77 ± 3 % reduction in I_L in the presence of *m*-3M3FBS (10 μ M, n=7) and a 70 ± 8 % reduction in I_L in the presence of *o*-3M3FBS (10 μ M, n=7). There was no significant difference between the percent reductions of I_L by these two compounds.

3.4.4. The effect of *m*-3M3FBS on I_L was PLC-independent

Since *o*-3M3FBS suppressed I_L , this suggests that both *m*-3M3FBS and *o*-3M3FBS act in a PLC-independent manner. In order to further elucidate if the effects of *m*-3M3FBS were PLC-independent, cells were pretreated with the PLC inhibitor U73122 (1 μ M). U73122 significantly decreased peak I_L from -113 ± 24 pA to -59 ± 10 pA at approximately 0mV (n=7, $P<0.05$, Fig. 7A-C). *m*-3M3FBS (10 μ M) caused a further decrease in I_L from -59 ± 10 pA in the presence of U73122 (1 μ M) to -3 ± 4 pA at 0mV (n=7, $P<0.001$, Fig. 7A-C) therefore suggesting a PLC-independent mode of inhibition of I_L by *m*-3M3FBS.

3.4.5. *m*-3M3FBS and *o*-3M3FBS stimulated $[Ca^{2+}]_i$

Previous reports have found that *m*-3M3FBS can cause an increase in $[Ca^{2+}]_i$ in a number of different cell types (Bae *et al.*, 2003; Krjukova *et al.*, 2004). To determine if *m*-3M3FBS could evoke a similar response in murine colonic SMC, we measured intracellular Ca^{2+} transients in conjunction with the patch

clamp technique to analyze changes in $[Ca^{2+}]_i$ along with simultaneous changes in inward currents. The application of *m*-3M3FBS (10-25 μ M) gradually increased $[Ca^{2+}]_i$ over a 10 minute period (n=7, Fig. 8A, Bc & Bd) and simultaneously decreased I_L (n=7, Fig. 8D). *o*-3M3FBS (10-25 μ M) also caused an increase in $[Ca^{2+}]_i$ as well as simultaneously decreased I_L (n=4, Fig. 8A, Ba & Bb, C).

3.5. Figures and figure legends

Figure 1: *m*-3M3FBS and *o*-3M3FBS decreased colonic smooth muscle contractility

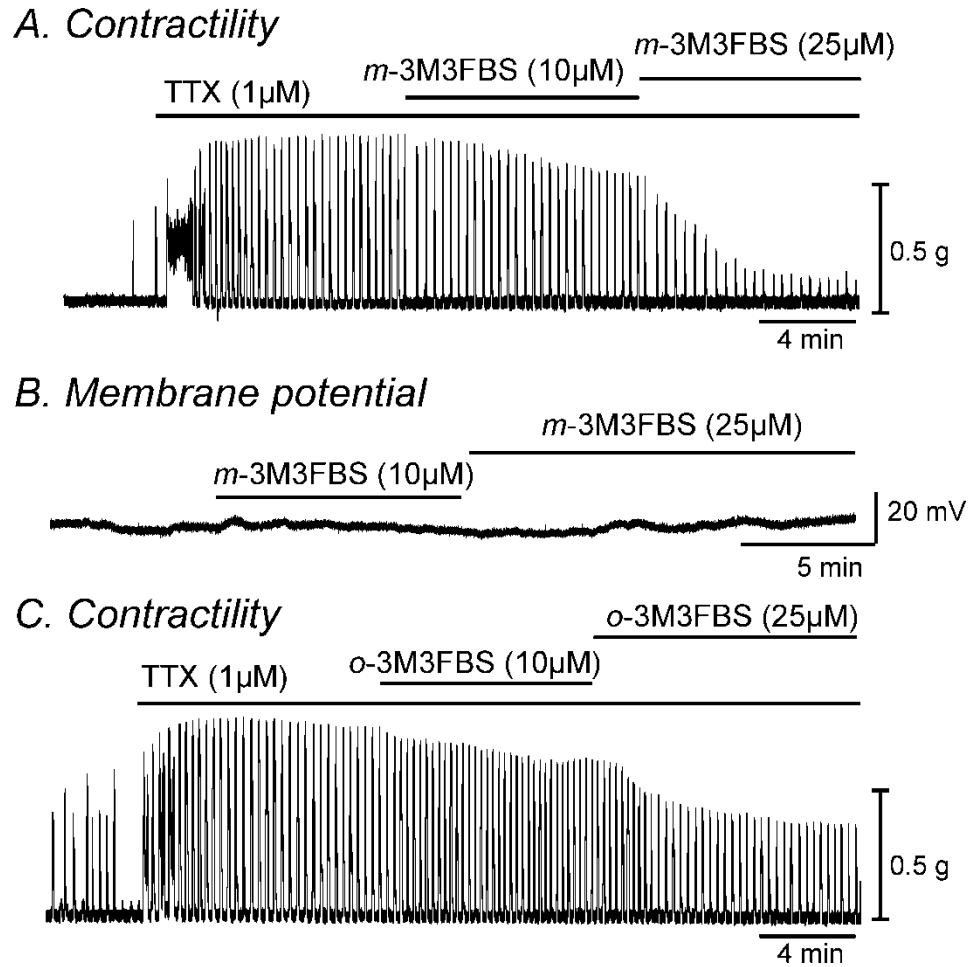


Figure 1: *m*-3M3FBS and *o*-3M3FBS decreased colonic smooth muscle contractility

(A & C) Representative mechanical traces show that exposure to increasing concentrations of *m*-3M3FBS and *o*-3M3FBS (10 and 25 μ M) decreased the contractile responses in colonic smooth muscle in the presence of TTX (1 μ M).

(B) Representative trace illustrating the lack of effect of *m*-3M3FBS (10 and 25 μ M) on membrane potential of intact murine colonic smooth muscle.

Figure 2: *m*-3M3FBS caused a PLC-independent decrease in I_{DR}

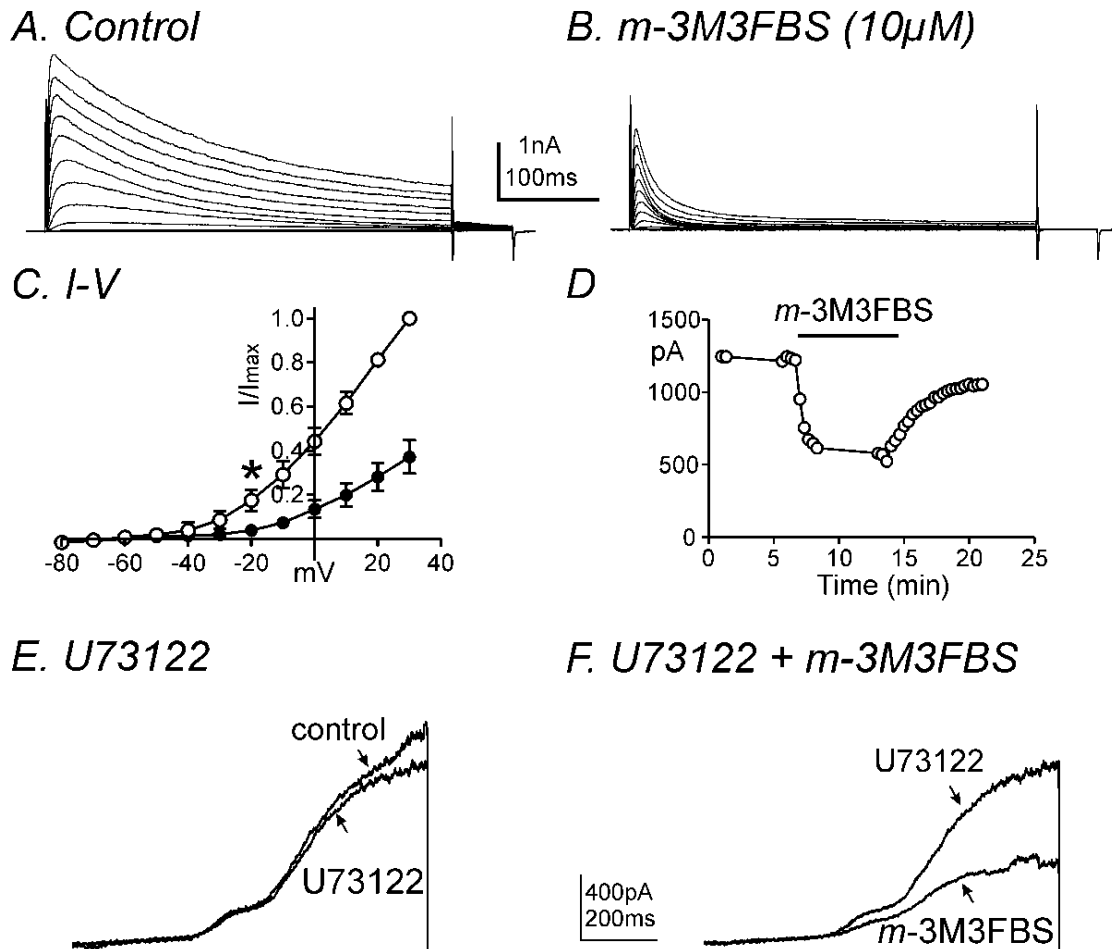


Figure 2: *m*-3M3FBS caused a PLC-independent decrease in I_{DR}

Membrane potential was stepped from -80 to +30mV in 10mV increments from a holding potential of -80mV in (A) control conditions and (B) in the presence of *m*-3M3FBS. (C) Summary of normalized *I-V* relationships in control (□) and *m*-3M3FBS (●). Peak currents (*I*) were normalized with the peak current at +30mV (I_{max}). *m*-3M3FBS (10μM) significantly decreased I_{DR} (n=4, * denotes $P<0.05$ at -20mV). All tested potentials positive to -20mV were significant. (D) Time course of inhibition of I_{DR} generated by repetitive step depolarizations to 0mV from a holding potential of -80mV every 20 seconds before and after *m*-3M3FBS (10μM) application. (E & F) Representative current traces are shown of ramp depolarizations stepping from -80mV to +80mV every 30 seconds in the presence of (E) U73122 (2μM) and (F) U73122 (2μM) and *m*-3M3FBS (10μM). *m*-3M3FBS decreased I_{DR} in the presence of U73122.

Figure 3: *m*-3M3FBS inhibited I_A

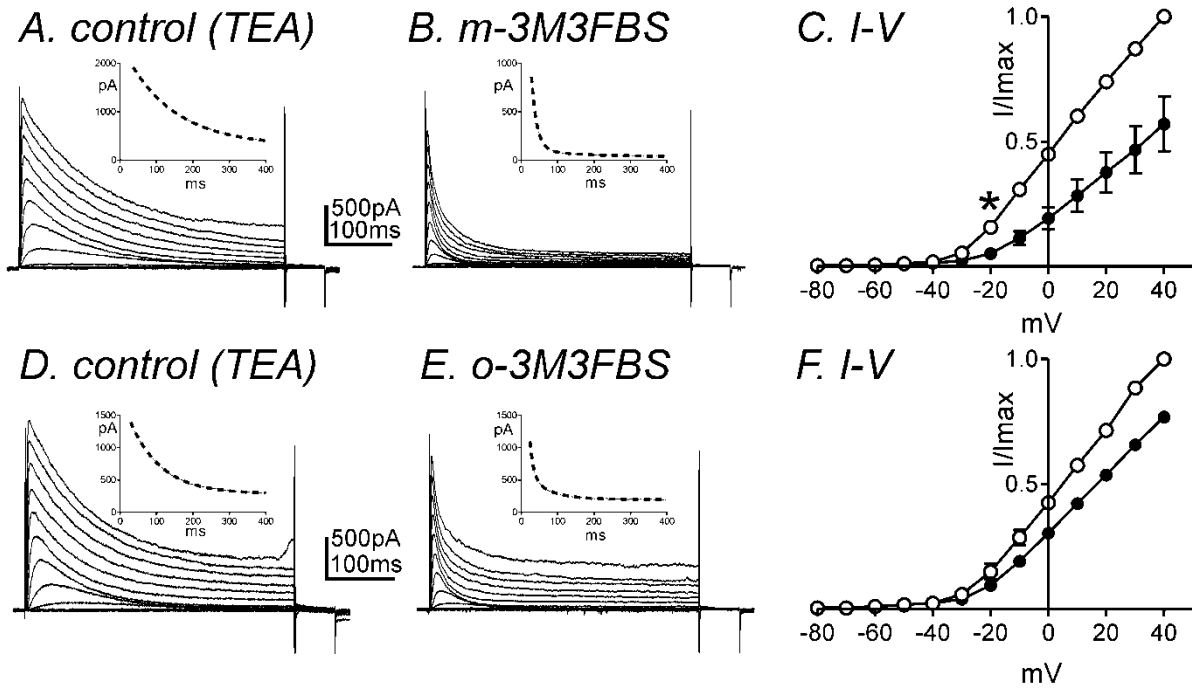


Figure 3: *m*-3M3FBS inhibited I_A

Membrane potential was stepped from -80 to +40mV in 10mV increments from a holding potential of -80mV (A) in the presence of TEA (10mM, control) and (B) in the presence of *m*-3M3FBS (10 μ M) in TEA. (C) Normalized *I-V* relationships in control (○) and in the presence of *m*-3M3FBS (●). Peak currents (*I*) were normalized with the peak current at +40mV (I_{max}). *m*-3M3FBS (10 μ M) significantly decreased I_A (n=4, * denotes $P<0.05$ at -20mV). All tested potentials positive to -20mV were significant. (D-F) *o*-3M3FBS also significantly decreased I_A (n=4). Insets illustrate the time constant of inactivation with single exponential fit (panel A & C, dotted line) and double exponential fit (panel B & E, dotted line) at +20 mV.

Figure 4: *m*-3M3FBS decreased I_{DRS}

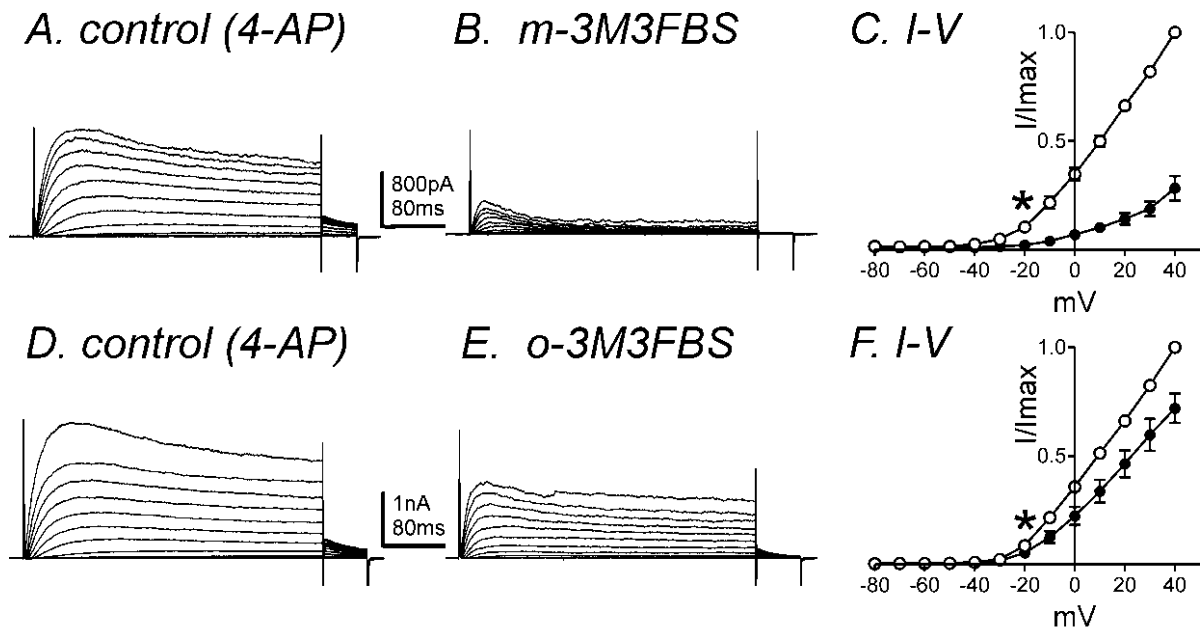


Figure 4: *m*-3M3FBS decreased I_{DRS}

Membrane potential was stepped from -80 to +40mV in 10mV increments from a holding potential of -80mV (A) in the presence of 4-AP (5mM, control) and (B) in the presence of *m*-3M3FBS (10 μ M) in 4-AP. (C) Normalized *I-V* relationships in control (○) and in the presence of *m*-3M3FBS (●). Peak currents (*I*) were normalized with the peak current at +40mV (I_{max}). *m*-3M3FBS (10 μ M) significantly reduced I_{DRS} (n=4, * denotes $P<0.05$ at -20mV). (D-F) *o*-3M3FBS also decreased I_{DRS} (n=6, * denotes $P<0.05$ at -20mV). All tested potentials positive to -20mV were significant.

Figure 5: *m*-3M3FBS decreased I_L

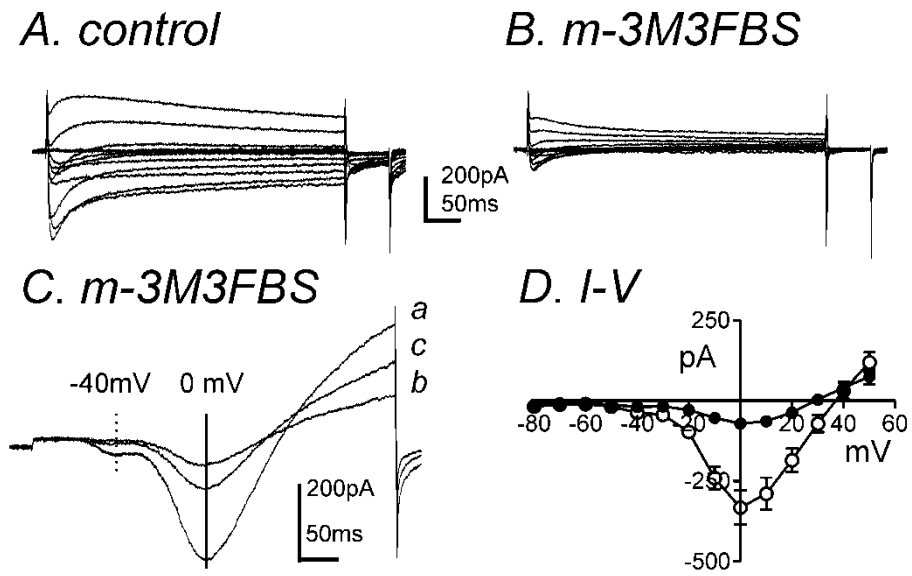


Figure 5: *m*-3M3FBS decreased I_L

Membrane potential was stepped from -80 to +50mV in 10mV increments from a holding potential of -80mV in (A) control and (B) in the presence of *m*-3M3FBS (10 μ M). (C) Representative traces where ramp depolarizations were applied from -80mV to +80mV over 500ms every 1 minute in (a) control, (b) *m*-3M3FBS, and (c) washout. *m*-3M3FBS decreased peak I_{LVA} (dashed line at -40mV) and I_L (vertical solid line at 0mV). (D) Summary of I - V relationship in control (\circ) and in the presence of *m*-3M3FBS (\bullet). *m*-3M3FBS (10 μ M) significantly decreased I_L (n=7) but not I_{LVA} .

Figure 6: *o*-3M3FBS decreased I_L

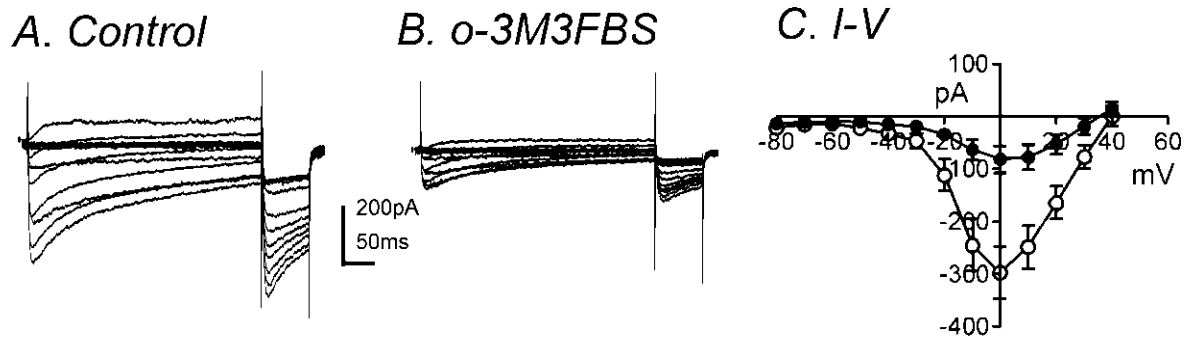
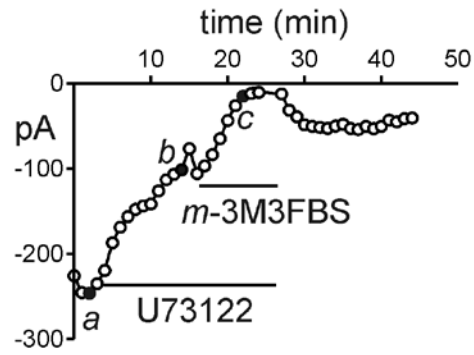


Figure 6: α -3M3FBS decreased I_L

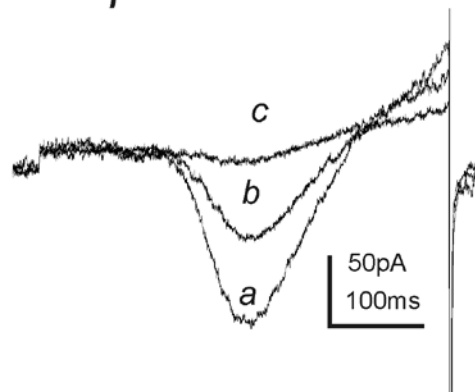
Membrane potential was stepped from -80 to +50mV in 10mV increments from a holding potential of -80mV (A) in control and (B) in the presence of α -3M3FBS (10 μ M). (C) Summarized I - V relationship show significant inhibition by α -3M3FBS on I_L (n=7). (\circ) and (\bullet) denote control and in the presence of α -3M3FBS respectively.

Figure 7: *m*-3M3FBS caused PLC-independent inhibition of I_L

A. I_L



B. Ramp



C. Summary

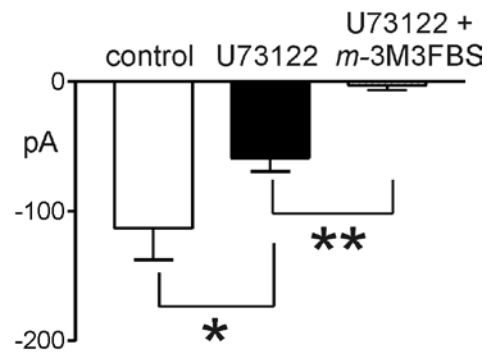


Figure 7: *m*-3M3FBS caused PLC-independent inhibition of I_L

(A) Peak I_L by U73122 (1 μ M) and both U73122 (1 μ M) and *m*-3M3FBS (10 μ M) was plotted as a function of time. (B) Representative traces where ramp depolarizations were applied from -80mV to +80mV over 500ms every 1 minute in (a) control, (b) in the presence of U73122 and (c) in the presence of U73122 and *m*-3M3FBS. (C) Summary of peak I_L at 0 mV by U73122 (1 μ M) and both U73122 (1 μ M) and *m*-3M3FBS (10 μ M) (n=7). * and ** denote $P<0.05$ and $P<0.001$, respectively.

Figure 8: *m*-3M3FBS and *o*-3M3FBS increased $[Ca^{2+}]_i$ and simultaneously decreased I_L

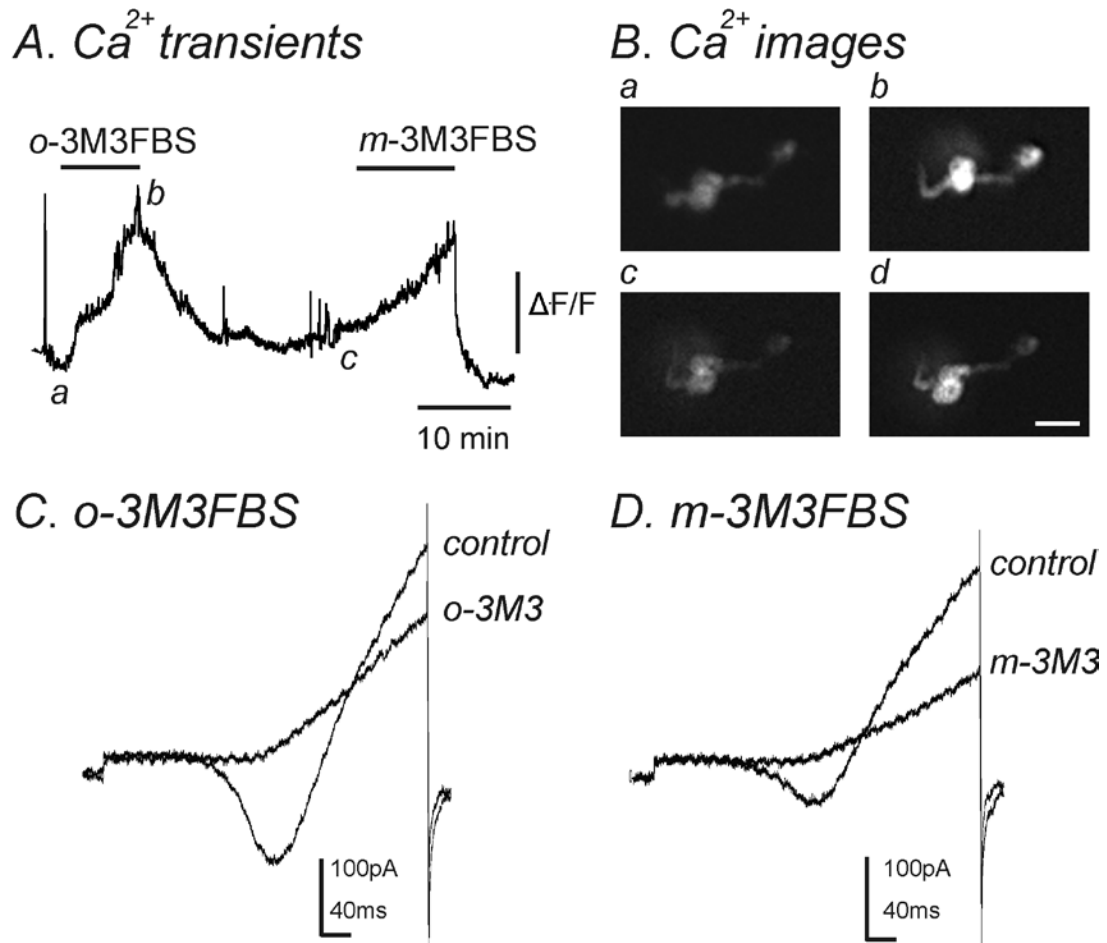


Figure 8: *m*-3M3FBS and *o*-3M3FBS increased $[Ca^{2+}]_i$ and simultaneously decreased I_L

(A) Representative trace showing an increase in $[Ca^{2+}]_i$ upon application of *o*-3M3FBS (10 μ M) which was reversible upon washout. Addition of *m*-3M3FBS (10 μ M) to the same cell also increased $[Ca^{2+}]_i$ which was reversible. (B) Images of a single smooth muscle cell loaded with Fluo-4AM. These images correspond to $[Ca^{2+}]_i$ measurements shown in panel A during (a) control conditions, (b) in the presence of *o*-3M3FBS (10 μ M), (c) after washout of *o*-3M3FBS and (d) in the presence of *m*-3M3FBS (10 μ M). Scale bar= 20 μ m. (C & D) During $[Ca^{2+}]_i$ measurements, a single ramp depolarization was applied from -80mV to +80mV over 500ms in (C) control conditions and in the presence of *o*-3M3FBS (10 μ M) and (D) after washout of *o*-3M3FBS and in the presence of *m*-3M3FBS (10 μ M). Both *o*-3M3FBS (n=4) and *m*-3M3FBS (n=7) inhibited I_L .

3.6. Discussion

Many studies have implicated PLC as a vital component in carrying out important cellular functions such as apoptosis, proliferation and differentiation (Rebecchi & Pentylala, 2000; Rhee, 2001; Hicks *et al.*, 2008; Suh *et al.*, 2008). The identification of a novel PLC agonist, *m*-3M3FBS was an exciting finding since it could be used in a direct way to ascertain the exact roles of PLC in contractility and ion channel regulation. *m*-3M3FBS induces the formation of inositol phosphates in U937 cells thus suggesting stimulation of PLC activity since these effects were not seen using the inactive form, *o*-3M3FBS (Bae *et al.*, 2003).

In gastrointestinal smooth muscle, acetylcholine and carbachol produce excitation and contraction of smooth muscle via stimulation of muscarinic receptors that are coupled to $G_{q/11}$ proteins resulting in activation of PLC- β (Unno *et al.*, 2003; Unno *et al.*, 2006; Zholos, 2006). The important role of PLC in this pathway has been illustrated as application of the PLC-blocker, U73122 prevents cation currents activated by carbachol that are essential to cause depolarization, subsequent activation of voltage-dependent Ca^{2+} channels resulting in contraction (Okamoto *et al.*, 2004). Since carbachol activates the PLC pathway, direct PLC activation using *m*-3M3FBS would be expected to cause a similar depolarization and contraction. However we found *m*-3M3FBS and *o*-3M3FBS actually decreased colonic contractility. A possible explanation could be through activation of K^+ channels and/or inhibition of Ca^{2+} influx through NSCC or Ca^{2+} channels thus causing hyperpolarization of RMP and decreased contractility.

However *m*-3M3FBS did not significantly change the membrane potential. Since none of the tissue experiments could explain the PLC-mediated effects of *m*-3M3FBS, it was essential to examine what channels were affected by *m*-3M3FBS through patch clamp studies.

Many studies have examined the role of PLC and PIP₂ in ion channel regulation. KCNQ currents are known to require PIP₂ for activation since PIP₂ depletion by the muscarinic receptor agonist oxotremorine-M and *m*-3M3FBS caused inhibition of these currents (Horowitz *et al.*, 2005). Menthol-evoked TRPM8 (Transient receptor potential cation channel, subfamily M, member 8) currents were reduced in HEK293T cells by *m*-3M3FBS (Daniels *et al.*, 2009). On the other hand, stretch-activated PLC can cause large conductance background-type potassium (LKbg) channel activation through degradation of PIP₂. This effect was mimicked by application of *m*-3M3FBS (Nam *et al.*, 2007). TRPA1 (Transient receptor potential cation channel, subfamily A, member 1) currents were potentiated by *m*-3M3FBS in dorsal root ganglia neurons (Wang *et al.*, 2008). In general there are no critical experiments that have examined potential PLC-independent effects of *m*-3M3FBS on native ion channels.

Firstly, we examined the effects of *m*-3M3FBS and *o*-3M3FBS on I_{DR} in murine colonic SMC and found that both compounds decreased I_{DR} . *m*-3M3FBS was significantly more effective at reducing I_{DR} than *o*-3M3FBS. This difference could be due to slight structural variation between these two compounds. It has previously been reported that I_{DR} is not affected by U73122 in murine atrial

myocytes (Cho *et al.*, 2001). We found that U73122 did not significantly decrease I_{DR} in colonic SMC. However, preincubation with this PLC inhibitor did not prevent inhibition of I_{DR} by *m*-3M3FBS. Since the PLC-pathway is not expected to be conserved in dialyzed whole cell configurations, this suggests the effects of *m*-3M3FBS on I_{DR} could be non-specific.

I_{DR} are composed of I_{DRS} and I_A (Koh *et al.*, 1999b). I_A are resistant to TEA and I_{DRS} are resistant to 4-AP. Therefore, we isolated I_A with treatment of TEA (10mM). *m*-3M3FBS decreased I_A with induction of fast inactivation. In previous reports, Ca^{2+} -calmodulin-dependent protein kinase II (CaMKII) regulated the inactivation kinetics of I_A . CaMKII inhibitors increased the rate of inactivation whereas increasing $[Ca^{2+}]_i$ decreased the rate of inactivation (Koh *et al.*, 1999a; Amberg *et al.*, 2001; Sergeant *et al.*, 2004). Our findings and previous reports (Bae *et al.*, 2003; Krjukova *et al.*, 2004; Roedding *et al.*, 2006) demonstrated that *m*-3M3FBS increased $[Ca^{2+}]_i$. An increase in $[Ca^{2+}]_i$ would be expected to decrease the rate of inactivation of I_A . However *m*-3M3FBS and *o*-3M3FBS increased the rate of inactivation of I_A suggesting these compounds may have unspecific effects on the inactivation kinetics of I_A .

Inhibition of I_{DRS} increases the amplitude of spike action potentials in murine colon (Koh *et al.*, 1999b). Therefore, we expect an increase in contractility upon treatment of both *m*-3M3FBS and *o*-3M3FBS since both drugs inhibit I_{DRS} . However the contractility was decreased by these agents. In addition, a previous study showed that I_A is involved in the regulation of the RMP and inhibition of this

conductance induces depolarization with continuous spike activity in murine colon (Koh *et al.*, 1999b). Since the RMP was not changed by *m*-3M3FBS, further experiments were needed to elucidate how membrane potential was not changed by application of *m*-3M3FBS to colonic smooth muscle.

In a previous report, two types of inward currents (I_{LVA} and I_L) were identified in murine colonic SMC (Koh *et al.*, 2001). Our studies revealed that *m*-3M3FBS significantly decreased I_L but not I_{LVA} . The decreased contraction seen upon its application to colonic smooth muscle could be explained through inhibition of I_L as this is the major source of Ca^{2+} required for contraction (Wegener *et al.*, 2006). These effects could be via a PLC-dependent mechanism. However *o*-3M3FBS also showed similar results as *m*-3M3FBS suggesting that the effect on I_L could be PLC-independent. These data suggest that the common structures shared by both compounds can directly bind and inhibit these channels in a non-specific manner. However, further experiments need to be performed to identify the specific mechanisms of inhibition of these compounds on these channels.

In ion channel studies, the selectivity of the PLC inhibitor U73122 has been disputed (Mogami *et al.*, 1997; Walker *et al.*, 1998; Hughes *et al.*, 2000; Horowitz *et al.*, 2005; Takenouchi *et al.*, 2005; Sickmann *et al.*, 2008; Klose *et al.*, 2008). It has been shown that U73122 revealed PLC-independent suppression of G protein-coupled inward rectifier K^+ channels (Sickmann *et al.*, 2008) and BK (Klose *et al.*, 2008). Furthermore, U73122 caused a slow rise in

$[Ca^{2+}]_i$ and a total block of L-type Ca^{2+} channels in NG108-15 cells (Jin *et al.*, 1994). Our data also supports PLC-independent effects of U73122 since its application significantly decreased I_L . In addition, pre-incubation with U73122 did not prevent a further reduction in I_L by *m*-3M3FBS. Since *o*-3M3FBS proved to be as efficient as *m*-3M3FBS in decreasing I_L , this data strongly suggests that the actions of *m*-3M3FBS are not attributable to its expected PLC-activation. The similar effects of *m*-3M3FBS and *o*-3M3FBS on I_L suggest that the common structure they share can directly bind and inhibit these channels in an antagonistic manner.

Upon application of *m*-3M3FBS, an increase in $[Ca^{2+}]_i$ has been a common finding in various cell lines (Bae *et al.*, 2003; Krjukova *et al.*, 2004; Roedding *et al.*, 2006). For example, a gradual increase in $[Ca^{2+}]_i$ was recorded after application of *m*-3M3FBS in human neuroblastoma cells and this increase was proposed to be due to mechanisms other than IP_3 (Krjukova *et al.*, 2004). Our studies showed that *m*-3M3FBS gradually increased $[Ca^{2+}]_i$ but simultaneously inhibited I_L . Since this trend was also found with application of *o*-3M3FBS, this suggests a PLC-independent mechanism of action causing this increase $[Ca^{2+}]_i$ in an agonistic manner. These findings were different from the effects on the ionic currents in colonic smooth muscle which revealed antagonistic effects by both compounds. The increase in $[Ca^{2+}]_i$ by these compounds would be expected to increase murine colonic contractility. However, we found that contractility was decreased in colonic strips. Therefore, the

inhibition of I_L by *m*-3M3FBS and *o*-3M3FBS could explain the reduction in contractile responses and thus may be the dominant source of $[Ca^{2+}]_i$ required for contraction.

In conclusion, our studies report the novel and unexpected finding that *m*-3M3FBS and *o*-3M3FBS caused a decrease in contractility in murine colonic muscle. Both compounds acted as antagonists as they inhibited I_L and I_{DR} via mechanisms independent of PLC. Conversely, both compounds revealed agonist-like activities as they caused an increase in $[Ca^{2+}]_i$. Therefore *m*-3M3FBS is not a specific activator of PLC and *o*-3M3FBS cannot be considered as an inactive analogue of *m*-3M3FBS. Caution must be employed when interpreting their effects at the tissue and cellular level.

Chaper 4:

Contribution of Rho-kinase to colonic excitability in murine colonic smooth muscle

4.1. Summary

Ca²⁺ sensitization is an important process that increases myosin light chain (MLC) phosphorylation and force of contractions. This contribution of the RhoA/Rho-kinase pathway in agonist-induced contractions has been shown in several smooth muscle preparations including intestine, urinary bladder and uterus. There is also accumulating evidence that Rho-kinase is involved in modulating other cellular processes such ion channel regulation. In this study we examined the involvement of Rho-kinase in smooth muscle excitability including non-selective channel activity.

We used Rho-kinase inhibitors Y-27632, H-1152 and HA-1077 and recorded their effects on colonic excitability by performing conventional microelectrode recordings, isometric force measurements and patch clamp experiments

Both Y-27632 and H-1152 caused a significant decrease in nerve-stimulated on- and off- contractions elicited at increasing frequencies and durations. Spontaneous and carbachol (CCh) -induced contractions were significantly decreased independent of neuronal influences suggesting Y-27632 acts directly on smooth muscle. CCh-induced depolarization was significantly

reduced by Rho-kinase inhibitors which could not be explained by inhibition of Rho-kinase/ Ca^{2+} sensitization pathway only. KCl-evoked contractions were not influenced by Y-27632 indicating L-type Ca^{2+} channels were not affected by this compound. Patch-clamp experiments revealed that Rho-kinase inhibitors did not affect L-type Ca^{2+} currents and bI_{NSCC} . However, GTP γ S-activated currents were inhibited by Y-27632.

In summary, inhibition of Rho-kinase decreased nerve-stimulated contractility and CCh-induced depolarization suggesting that these effects are due to inhibition of both the Ca^{2+} -sensitization pathway and CCh-sensitive non-selective cation currents.

4.2. Background and Aims

Smooth muscle contraction is primarily regulated by 20-kDa myosin regulatory light chain (MLC₂₀) phosphorylation. The degree of phosphorylation is dependent on the balance between myosin light chain kinase (MLCK) and myosin light chain phosphatase (MLCP) activity. Recent studies have revealed the importance of the small GTP-binding protein, Rho-A and RhoA-dependent serine-threonine kinase, Rho-kinase, in regulating the activity of MLCP and increasing the sensitivity of the contractile machinery (Ohama *et al.*, 2003; Somlyo & Somlyo, 2003; Rattan & Patel, 2008). Stimulation of receptors coupled to heteromeric G proteins results in activation of Rho-A which in turn stimulates Rho-kinase. The non-catalytic subunit of MLCP is phosphorylated by Rho-kinase thus inactivating it. Therefore MLCK phosphorylation of MLC₂₀ is augmented leading to a greater force of contractions at a certain level of $[Ca^{2+}]_i$ (Ohama *et al.*, 2003; Somlyo & Somlyo, 2003; Ohama *et al.*, 2007; Ratten & Patel, 2008).

Several studies have examined the contribution of Rho-kinase in agonist-induced contractions and/or basal tone in different smooth muscle preparations using Rho-kinase inhibitors such as Y-27632, H-1152 and HA-1077 (Jarajapu & Knot, 2005; Rattan & Patal, 2008). The selectivity of these inhibitors has been examined through their inhibitory effects on not only Rho-kinase but other enzymes such as PKC and MLCK (Eto *et al.*, 2001; Rattan & Patel, 2008).

The contribution of the RhoA/Rho-kinase pathway in agonist-induced contractions has been demonstrated in several smooth muscle preparations

including intestine, urinary bladder and uterus (Schneider *et al.*, 2004; Friel *et al.*, 2005; Al-Jarallah *et al.*, 2008; Ratten & Patel, 2008). In the colon, carbachol (CCh)-induced contractions are significantly reduced by pretreatment with Rho-kinase inhibitors such as Y27632 suggesting an important contribution of Ca^{2+} sensitization to agonist-induced contractions (Al-Jarallah *et al.*, 2008).

In addition to its role in Ca^{2+} sensitization in agonist-induced contraction, there is accumulating evidence that Rho-kinase may be involved in the regulation of certain ion channels (Pochynyuk *et al.*, 2006; Villalba *et al.*, 2008). Activation of Rho-kinase by RhoA can stimulate phosphatidylinositol-4-phosphate 5-kinase leading to increases in PIP_2 levels that promotes insertion of epithelial Na^+ channels into the plasma membrane (Pochynyuk *et al.*, 2006). In rat penile arteries, nifedipine-resistant Ca^{2+} influx evoked by phenylalanine was inhibited by Y27632. This influx was proposed to be via NSCC that were somehow regulated by Rho-kinase (Villalba *et al.*, 2008).

However the contribution of Rho-kinase in colonic spontaneous contractions and also nerve-stimulated contractions has not been investigated. Furthermore no studies have clearly investigated the potential involvement of Rho-kinase in ion channel activity that could account for changes in agonist-induced contractions. In this study we aimed to dissect the involvement of Rho-kinase in nerve-stimulated, CCh-induced and spontaneous contractions at the neuronal, smooth muscle and ion channel level.

4.3. Materials and methods

4.3.1. Animals

SMC were prepared from colons removed from BALB/c mice. Mice were anesthetized with isoflurane and killed by cervical dislocation. Colons were removed from the animals through a midline abdominal incision. The animals were maintained and the experiments performed in accordance with the National Institutes of Health Guide for the Care and Use of Laboratory Animals. The Institutional Animal Use and Care Committee at the University of Nevada approved all procedures used.

4.3.2. Mechanical responses and nerve stimulation

Segments of the proximal colon from 1 cm distal to the ileocecal sphincter were removed through a midline abdominal incision and opened along the mesenteric border. Luminal contents were removed by washing with Krebs–Ringer bicarbonate solution (KRB, see section 4.3.6.), and the cleaned tissue sheets were pinned down onto a Sylgard base with the mucosa facing up. The mucosa was removed leaving the tunica muscularis and remnants of the submucosa.

Mechanical responses were performed using standard organ-bath techniques. Strips of muscle (10 × 5 mm) were cut from the tunica muscularis by sharp dissection. The muscles were attached with sutures to a fixed mount within

the organ bath and to an isometric strain gauge (World Precision Instruments, Sarasota, FL, U.S.A.). The muscles were immersed in oxygenated KRB and maintained at $37.5 \pm 0.5^\circ\text{C}$. The muscles were set at resting tension by applying 0.1–0.3 g of basal tension and then allowed to equilibrate for 1–2 hours with constant perfusion with fresh KRB. Contractions of the muscles were monitored, digitized and stored using Axoscope software (Axon Instruments, CA, USA). Contractions were quantified by calculations of area above the baseline using the pClamp software (v8.1, Axon instruments, CA, USA). For electrical field stimulation (EFS) experiments, parameters were 150V and 0.3ms with various stimulation frequencies and durations. The area under the curve (AUC) was determined as the integral values above the baseline of a selected area for 5 min recordings (mN*min). The AUC for the tissues exposed to tested drugs were compared to the AUC for tissues under control conditions during an equivalent period of time. Drugs were diluted to the desired concentrations and applied to the muscles by switching the perfusion to the drug-containing solution.

4.3.3. Intracellular microelectrode recordings

After removing the mucosa, strips of proximal colon (1 cm in length \times 0.5 cm in width) were taken from the region 1–2 cm from the ileocecal sphincter and pinned to a Sylgard (Dow Corning Corp., Midland, MI, USA) elastomer-coated recording chamber with the mucosal side of the circular muscle facing upward. SMC were impaled with glass microelectrodes filled with 3M KCl and had

electrical resistances of 80–100 M Ω . Transmembrane potentials were measured with a standard high input impedance amplifier (WPI Duo 773, Sarasota, FL, USA). Electrical signals were recorded by computer running AxoScope data acquisition software (Axon Instruments, CA, USA) and analyzed by Clampfit (v9.02, Axon Instruments, CA, USA). All experiments were performed in the presence of wortmannin (10 μ M) to reduce movement and facilitate impalements of cells for extended periods of time.

4.3.4. Preparation of isolated colonic SMC

Colons were cut open along the longitudinal axis, pinned out in a Sylgard-lined dish, and washed with Ca²⁺-free phosphate-buffered saline containing (mM): 125 NaCl, 5.36 KCl, 15.5 NaHCO₃, 0.336 Na₂HPO₄, 0.44 KH₂PO₄, 10 glucose, 2.9 sucrose, and 11 HEPES and adjusted to pH 7.4 with NaOH. The mucosa and submucosa were removed with fine-tipped forceps. Pieces of muscle were incubated for 30-40 minutes at 37°C in a Ca²⁺-free solution (ml) containing 2 mg collagenase (Worthington Biochemical, Lakewood, NJ), 4 mg trypsin inhibitor, 4 mg fatty acid-free bovine serum albumin, 1 mg papain and 0.3mg dithiothreitol (Sigma-Aldrich, MO, USA). After enzymatic treatment, the muscles were washed with Ca²⁺-free solution and agitated gently to create a cell suspension. Dispersed SMC were stored at 4°C in Ca²⁺-free solution. Cells were transferred from the refrigerator to the recording chamber. Drops of the cell suspensions were placed on the bottom of a 300 μ l chamber mounted on an

inverted microscope and allowed to adhere to the bottom of the chamber for 5 minutes before recording.

4.3.5. Voltage-clamp methods

Whole cell voltage-clamp techniques were used to record membrane currents from dissociated SMC. Membrane currents were amplified by an Axopatch 1D (Axon Instruments, Foster City, CA) and digitized with an analog-to-digital converter (Digidata 1200, Axon Instruments). Data were collected at 5 kHz, filtered at 2 kHz via Bessel filter, and digitized online with pCLAMP software. The data were analyzed with the use of Clampfit software (version 9.2, Axon Instruments, CA, USA). Pipette resistances were 1–4 M Ω . The linear leak current was subtracted digitally. Conventional and perforated whole cell patch-clamp techniques were used for recording ionic currents under voltage clamp. For perforated patches, amphotericin B (60 mg/ml) was dissolved in DMSO, sonicated, and diluted in the pipette solution to give a final concentration of 270 μ g/ml. Experiments were performed at room temperature (between 22 and 25°C).

4.3.6. Solutions

For contractile and conventional microelectrode recordings, the strips were exposed to KRB with the following composition (mM): 118.5 NaCl, 4.5 KCl, 1.2 MgCl₂, 23.8 NaHCO₃, 1.2 KH₂PO₄, 11.0 dextrose and 2.4 CaCl₂. In order to

measure inward currents, colonic SMC were bathed in a Ca^{2+} -containing physiological salt solution (CaPSS) containing (mm): 135 NaCl, 5 KCl, 2 CaCl_2 , 1.2 MgCl_2 , 10 glucose, 10 HEPES adjusted to pH 7.4 with Tris. The pipette solution for patch-clamp experiments contained (in mM): 135 CsCl, 0.1 EGTA, 0.1 Na_2GTP , 3 MgATP, 10 glucose, 2.5 creatine phosphate disodium and 10 HEPES. This solution was adjusted to pH 7.2 with Tris.

4.3.7. Chemicals

Y-27632[(R)-(+)-trans-*N*-(4-pyridyl)-4-(1-aminoethyl) cyclohexanecarboxanecarb-oxamide, 2HCl], H-1152 [(S)-(+)-(2-methyl-5-isoquinoliny) sulfonylhomopiperazine, 2HCl] and HA-1077 [(5-isoquinolinesulfonyl)homopiperazine, 2HCl] were obtained from Calbiochem (San Diego, CA, USA). Tetrodotoxin (TTX), guanosine 5'-3'-O-(thio)triphosphate (GTP γ S) and wortmannin were obtained from Sigma (St. Louis, MO, USA).

4.3.8. Statistical analysis

Data are reported as means \pm S.E.M. *n* is the number of tissues or cells in patch-clamp experiments tested. Statistical significance was evaluated by Student's *t* test. *P* values less than 0.05 were considered significant.

4.4. Results

4.4.1. Y-27632 reduced nerve-stimulated and CCh-induced contractions in colonic smooth muscle

We performed isometric force measurements to examine the effects of Y27632 on nerve-stimulated contractions in murine colonic smooth muscle. Increasing the frequency of EFS at a fixed duration (from 5 to 30Hz, duration 30sec) increased the amplitude of on-contractions which reached a plateau/peak during EFS (Fig.1A and 1D). On-contractions are the result of cholinergic neurotransmitter release from nerve terminals at the beginning of the EFS, as they can be blocked by atropine (Komori & Suzuki, 1986). Off-contractions evoked after cessation of EFS also increased in amplitude with increased frequency of EFS (Fig. 1A and 1E). Mechanisms underlying off-contractions are not clearly understood though it has been suggested they are due to release of non-cholinergic excitatory peptides such as substance P and neurokinin A (Shuttleworth *et al.*, 1993). Pretreatment with the Rho-kinase inhibitor Y27632 (1 μ M) caused a significant decrease in the amplitudes of nerve-stimulated on- and off-contractions (Fig.1B). A further increase in the concentration of Y27632 to 10 μ M totally abolished on-contractions and significantly reduced off-contractions elicited by EFS at all frequencies (Fig.1C-E). Under control conditions, application of the muscarinic receptor agonist, CCh (1 μ M), induced a prolonged contraction which slowly declined over 5 minutes (Fig. 1A).

Pretreatment with Y27632 caused a dose-dependent decrease in the amplitude of CCh-induced contractions (Fig.1B and C).

We also tested the effect of EFS duration on contractility before and after Y-27632 since EFS duration can also affect transmitter release. Figure 2A illustrates that under control conditions, an increase in the duration (1, 5, 10 and 20 sec) of EFS at a fixed frequency (5Hz) caused an increase in the amplitude of on- and off- contractions in colonic smooth muscle. However, pretreatment with Y-27632 (5 μ M) significantly reduced the amplitude of both types of contraction (Fig. 1B-D). These data suggest that Rho-kinase inhibition may be affecting smooth muscle contraction through impeding excitatory neurotransmitter release pre-synaptically and/or inhibiting Rho-kinase sensitive pathways in smooth muscle. Therefore we performed contractile experiments in the presence of TTX which blocks axonal action potential transmission and neurotransmitter release by inhibiting fast Na⁺ channels. After administration of TTX (1 μ M), there was a significant increase in the amplitude of spontaneous phasic contractions as measured by AUC suggesting that inhibitory neurotransmitters play a dominant role in murine colonic smooth muscle (Fig.3A-D). Application of Y27632 (10 μ M) in the presence of TTX (1 μ M) caused a significant decrease in the AUC following application of CCh (1 μ M) (Fig. 3B and 3C, n=4, *P*<0.05). Furthermore the peak-amplitude of CCh-induced contractions were significantly reduced in the presence of Y27632 and TTX suggesting that this compound may act directly on smooth muscle contractile elements and/or other cellular mechanisms (Fig. 3B

and 3D, $n=4$, $P<0.05$). Since the decrease in CCh-induced contractions by Y27632 could be due to effects on membrane potential, conventional microelectrode recordings were performed.

Figure 4A shows a typical CCh-induced depolarization in murine colonic smooth muscle (Fig. 4A and 4C, $n=7$). Pretreatment with Y27632 (10 μ M) significantly reduced the CCh-induced depolarization (Fig. 4B & C, control conditions, 16.4 ± 1.3 mV; in presence of Y27632 (10 μ M), 6.9 ± 1.0 mV, $n=7$, $P<0.001$). However RMP was not significantly changed in the presence of Y-27632.

4.4.2. H-1152 reduced nerve-stimulated and CCh-induced contractions in colonic smooth muscle

There are several different Rho-kinase inhibitors presently available that are reported to have different selectivities and potencies (Rattan & Patel, 2008). For example in the rat internal anal sphincter, the Rho-kinase inhibitor H-1152 was found to be most potent followed by Y27632 whereas HA-1077 and ROCK II inhibitor were significantly less potent. Therefore we examined if H-1152 and HA-1077 had similar effects on nerve- and agonist-induced contractility and excitability as Y27632. Isometric force measurements revealed that the amplitudes of on-contractions evoked by EFS at increasing frequencies (from 5 to 30Hz, duration 30sec) were significantly reduced in the presence of H-1152

(10 μ M) (Fig. 5A-C, n=6). Similarly the amplitudes of the off-contractions were significantly reduced by treatment with this compound (Fig. 5B and 5D, n=6). In addition CCh-induced contractions were suppressed by H-1152 (Fig. 5B compared with 5A).

Sharp-electrode recordings revealed a similar effect of HA-1077 on CCh-induced depolarization as Y27632 (see Fig. 4). Pretreatment with HA-1077 (10 μ M) significantly reduced the depolarizing effect of CCh (10 μ M) from 22.4 \pm 1.6mV in control compared with 9.0 \pm 0.5 mV in the presence of this Rho-kinase inhibitor (Fig. 6A-C, n=6).

4.4.3. Y27632 did not significantly effect KCl-induced contractions and L-type Ca²⁺ currents

The present studies revealed that Y27632 and H-1152 had marked inhibitory effects on spontaneous and CCh-induced contractions. A possible explanation for these findings could be direct inhibition of voltage-dependent Ca²⁺ channels (VDCC) by these compounds. In order to address this possibility, contractile measurements were performed where the external KCl concentration was periodically increased, which is a classical stimulus for activation of VDCC. If Y27632 was acting on VDCC, we expected that the amplitude of KCl-induced contractions would be significantly reduced from controls. However, we found that in the presence of 20, 40 and 60mM KCl, the contractions following

pretreatment with Y27632 (10 μ M) were not significantly different from those in control (Fig. 7A & B, n=6). These data suggest that the effects of Y27632 on spontaneous and CCh-induced contractions are not through inhibition of VDCC.

Contractile experiments revealed that Y27632 was not having any effect on VDCC. In order to confirm these findings we performed perforated patch clamp experiments to examine any effects of Y27632 on L-type Ca²⁺ channel activity, which is the major VDCC. In the pipette solution, KCl (140mM) was replaced with equimolar CsCl in order to isolate inward currents (see materials and methods). During ramp depolarizations from -80mV to +80mV over 500ms every 1 minute to evoke inward currents, application of Y27632 (5 μ M) had no effect on peak L-type Ca²⁺ currents (Fig. 7C, n=10 out of 11 cells). In a few experiments application of H-1152 caused an inhibition of peak L-type Ca²⁺ current (H-1152, n=2 out of 5 cells; Y-27632, n=1 out of 11 cells) (Fig. 7D).

4.4.4. Y27632 reduced GTP γ S evoked currents

Since bI_{NSCC} may contribute to the RMP of colonic SMC (see Chapter 2), we examined the potential effects of Rho-kinase inhibitors on this activity. In order to preserve intracellular signaling mechanisms, the perforated whole-cell configuration was used. The external solution was CaPSS and internal solution was high Cs solution (see methods section). bI_{NSCC} were not affected by either Y-27632 (1-10 μ M) or H-1152 (5 μ M) (Fig. 8A and B). These data were consistent

with the lack of effect of Rho-kinase inhibitors on RMP colonic smooth muscle. In order to explain the mechanism of decreased CCh-induced depolarization by Rho-kinase inhibitors, we examined CCh-activated NSCC.

Muscarinic-stimulated NSCC result from activation of GTP-binding protein mediated signal transduction. Therefore analogues of GTP that are resistant to hydrolysis such as GTP γ S are often used to mimick these CCh-activated NSCC (Kim *et al.*, 2007). At a holding potential of -80mV, dialysis of GTP γ S activated a slowly developing 'noisy' inward current (Fig. 8C). Application of Y-27632 (5 μ M) significantly reduced the GTP γ S evoked current (Fig. 8D). These data suggest that CCh-activated NSCC may be regulated by Rho-kinase and inhibition of these NSCC by Y-27632 may account for the decrease in CCh-induced depolarization.

4.5. Figures and figure legends

Figure 1: Y-27632 reduced the amplitude of nerve-stimulated on- and off-contractions

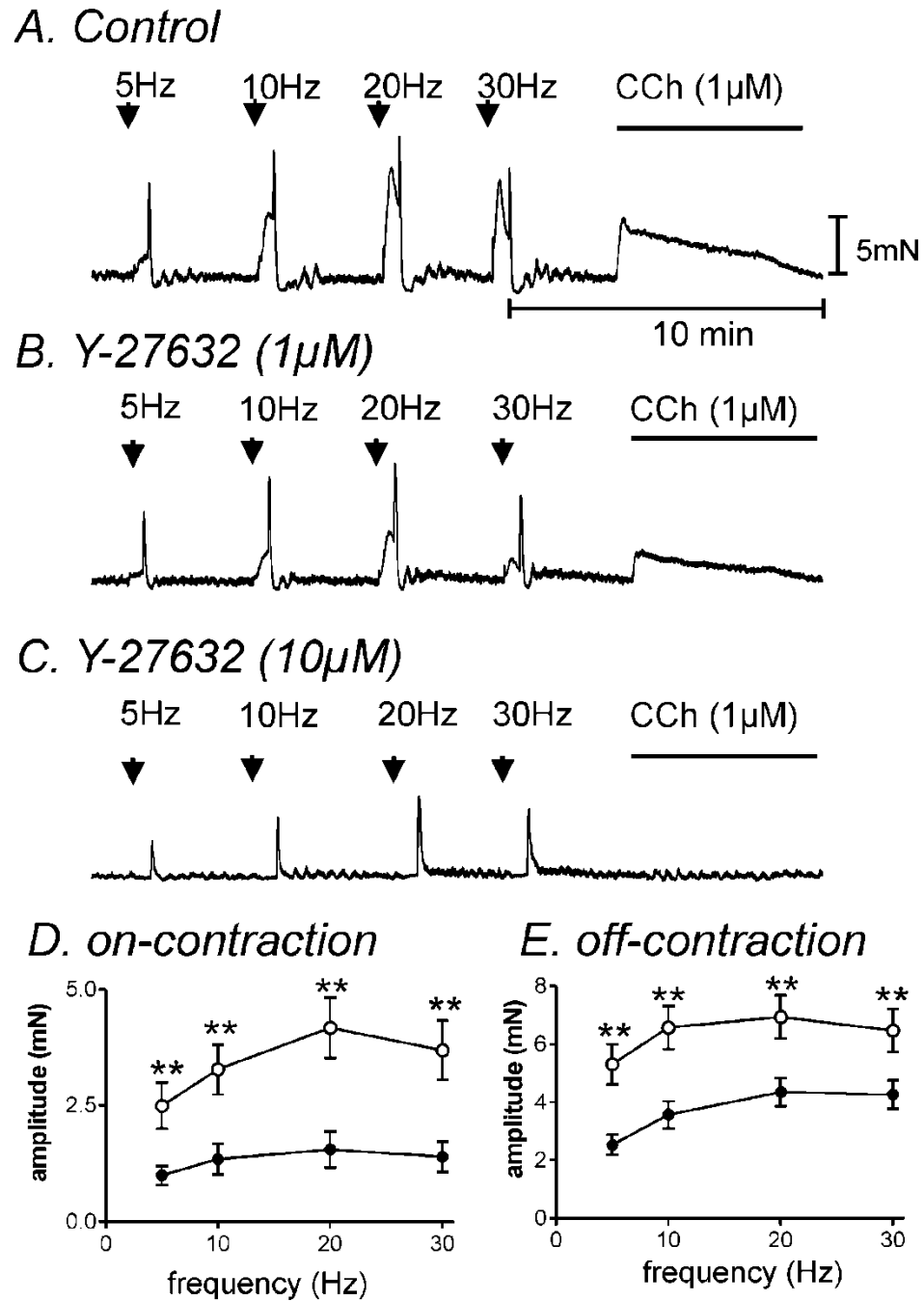


Figure 1: Y-27632 reduced the amplitude of nerve-stimulated on- and off-contractions

(A) Under control conditions, increasing the frequency of EFS (5, 10, 20 and 30Hz for 30 sec) increased the amplitude of on- and off- contractions in colonic smooth muscle. Pretreatment with Y27632 at (B) 1 μ M or (C) 10 μ M significantly decreased or abolished on-contractions respectively. Off-contraction amplitude was significantly decreased at both concentrations of Y27632. (D) Graph summarizing the effect of Y-27632 (10 μ M) on on-contractions evoked at different frequencies (n=13). (E) Graph summarizing the effect of Y-27632 (10 μ M) on off-contractions evoked at different frequencies (n=13). \circ control; \bullet in presence of Y-27632 (10 μ M). ** denotes $P < 0.005$.

Figure 2: Y-27632 reduced the amplitude of nerve-stimulated on- and off-contractions evoked at increasing durations

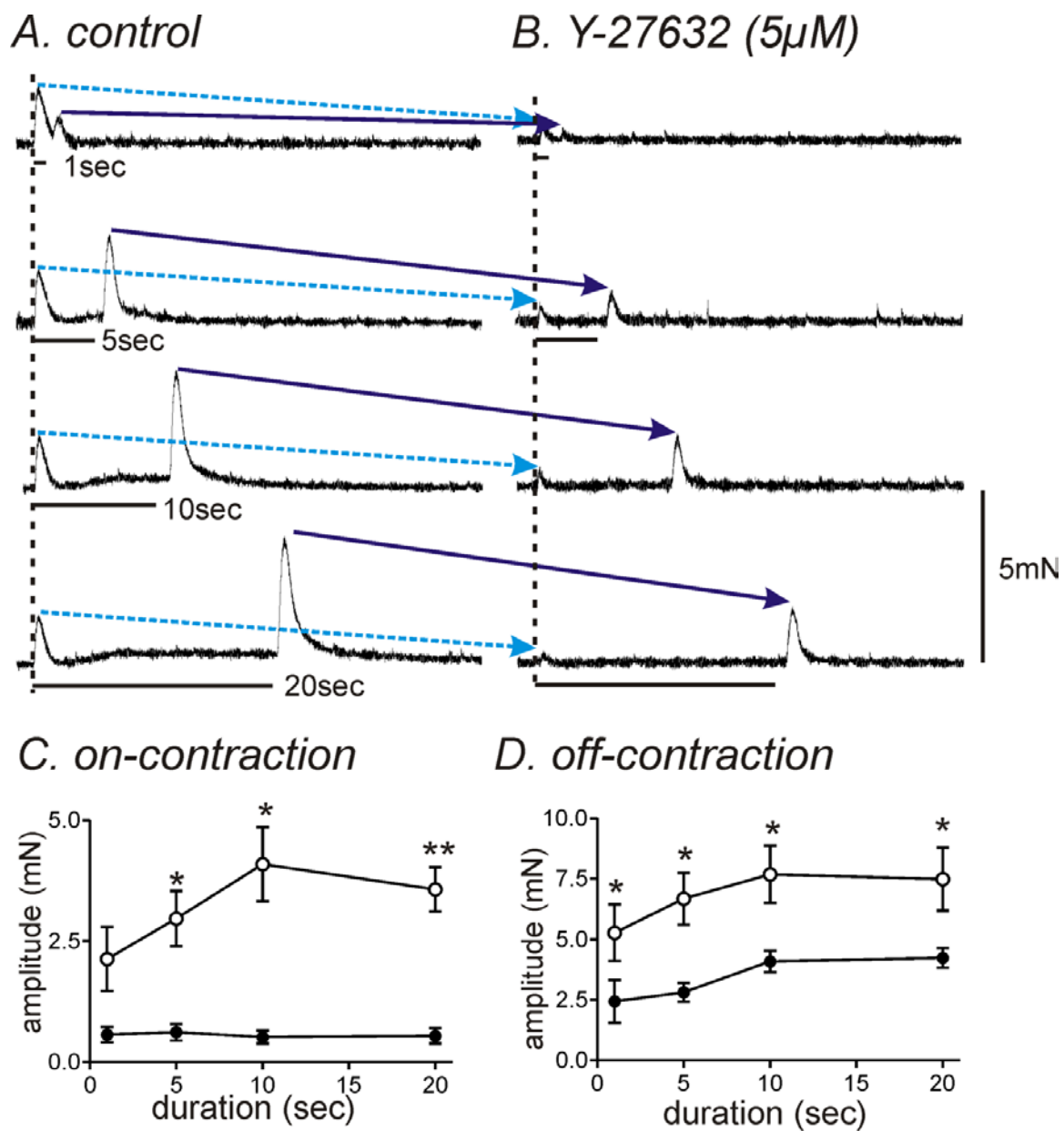


Figure 2: Y-27632 reduced the amplitude of nerve-stimulated on- and off-contractions evoked at increasing durations

(A) Under control conditions, duration of EFS at a fixed frequency (1, 5, 10 and 20 sec at 5Hz) increased the amplitude of on- and off- contractions in colonic smooth muscle. (B) Pretreatment with Y-27632 (5 μ M) significantly reduced the amplitude of both on- and off- contractions. (C) Graph summarizing the effect of Y-27632 (5 μ M) on the amplitude of on-contractions evoked at increasing durations of EFS compared with control (n=4, * P <0.05, ** P <.005). (D) Graph summarizing the effect of Y-27632 on off-contractions evoked following the cessation of EFS at increasing durations (n=4, * P < 0.05). \circ control; \bullet in presence of Y-27632.

Figure 3: Y27632 reduced colonic contractility independent of neuronal influences

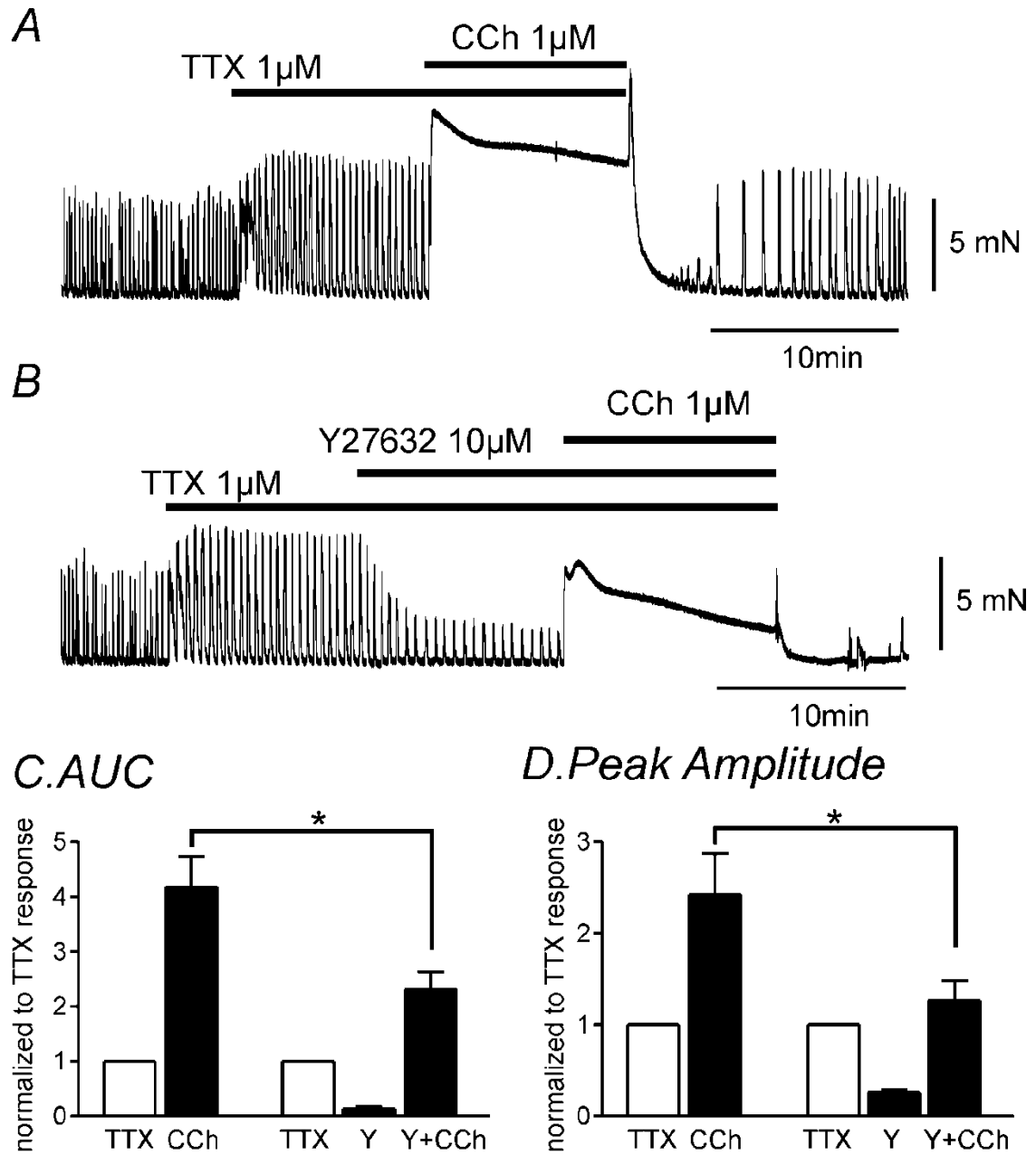
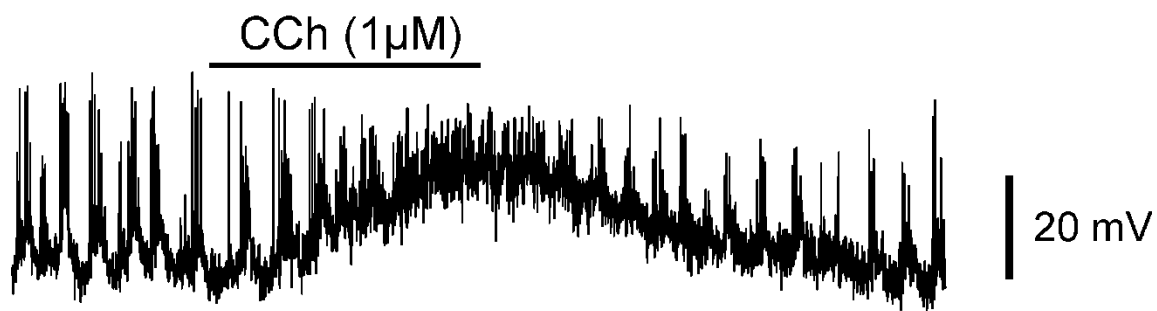


Figure 3: Y27632 reduced colonic contractility independent of neuronal influences

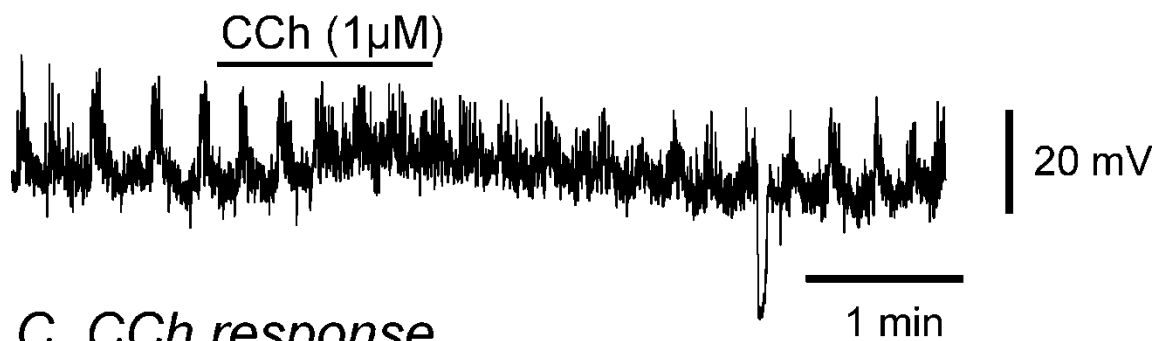
(A) Representative mechanical trace illustrating that in the presence of TTX ($1\mu\text{M}$), exposure to CCh ($1\mu\text{M}$) resulted in an increase in contractility in monkey colonic smooth muscle. (B) Representative trace illustrating how application of Y27632 ($10\mu\text{M}$) caused a decrease in the CCh-evoked contraction in murine colonic smooth muscle. (C) Graph summarizing the significant decrease in AUC following treatment with CCh ($1\mu\text{M}$) in the presence of Y-27632 ($10\mu\text{M}$) normalized to TTX response ($n=4$, * $P<0.05$). (D) Graph summarizing a significant decrease in the peak amplitude of CCh-induced contraction in the presence of Y-27632 ($1\mu\text{M}$) normalized to TTX response ($n=4$, * $P<0.05$).

Figure 4: Y-27632 pretreatment reduced CCh-induced depolarization in murine colonic smooth muscle

A. Control



B. Y-27623 (10 μ M)



C. CCh response

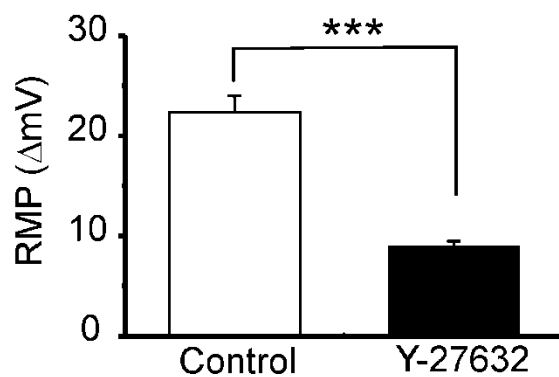
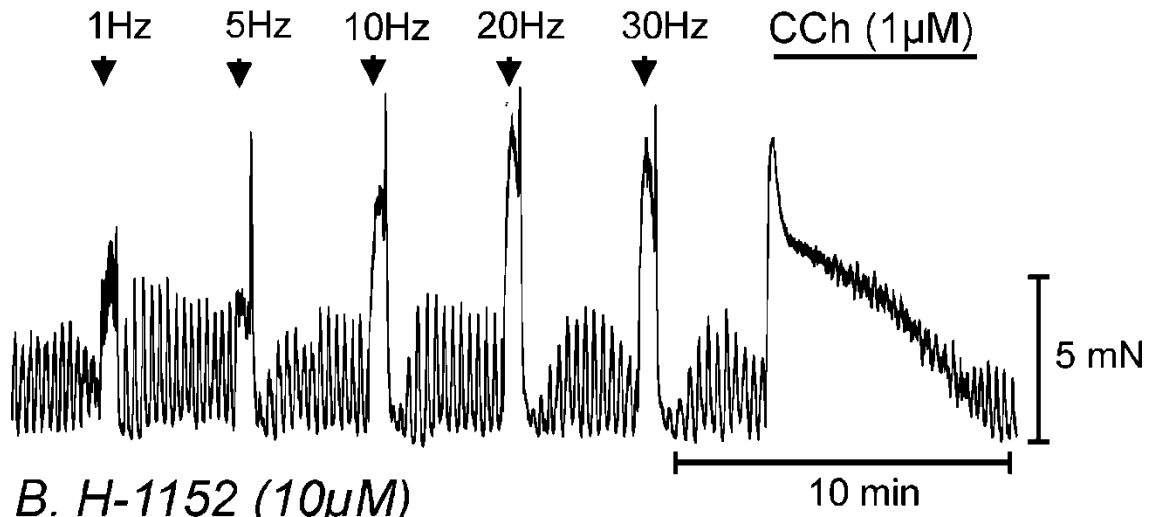


Figure 4: Y-27632 pretreatment reduced CCh-induced depolarization in murine colonic smooth muscle

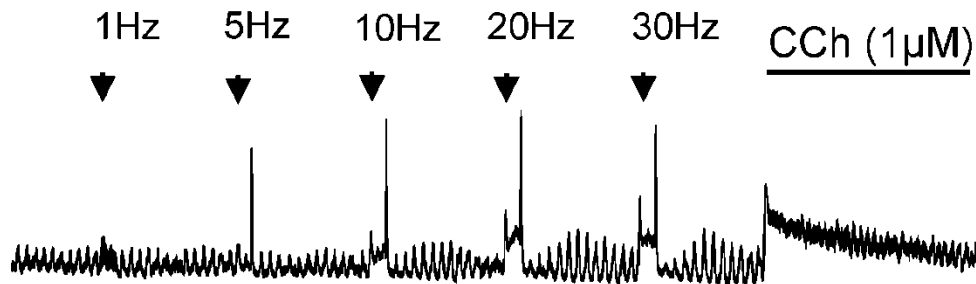
(A) Representative trace illustrating a typical CCh-induced depolarization in colonic smooth muscle. (B) Pretreatment with Y27632 (10 μ M) suppressed the CCh-induced depolarization (1 μ M). (C) Graph summarizing a significant decrease in RMP change upon CCh (1 μ M) treatment when colonic smooth muscle was pretreated with Y-27632 (10 μ M) (n=7, *** $P<0.001$).

Figure 5: H-1152 reduced the amplitude of nerve-stimulated on- and off-contractions

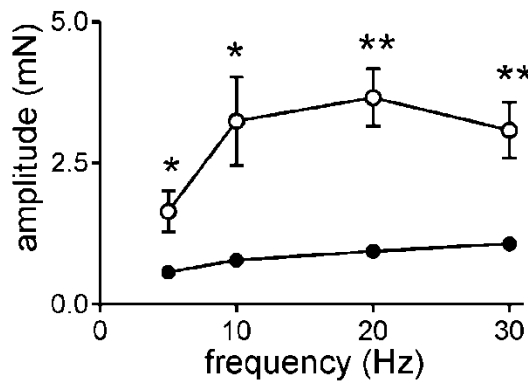
A. Control



B. H-1152 (10 μ M)



C. on-contraction



D. off-contraction

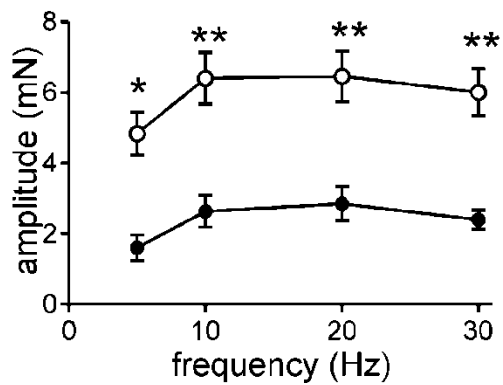
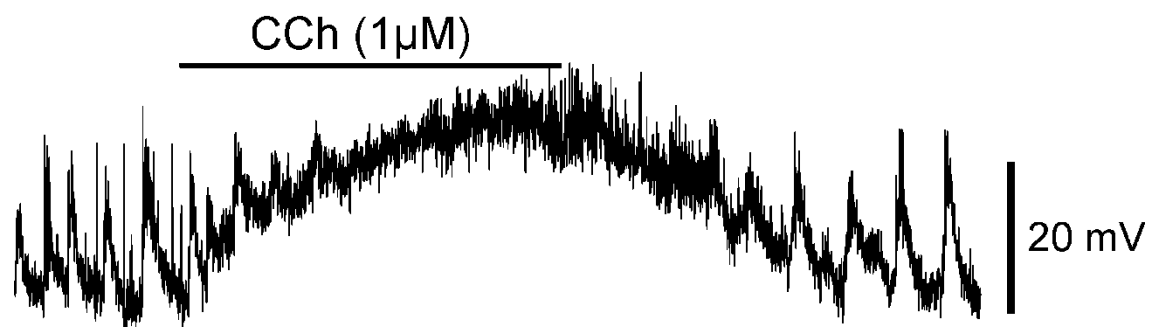


Figure 5: H-1152 reduced the amplitude of nerve-stimulated on- and off-contractions

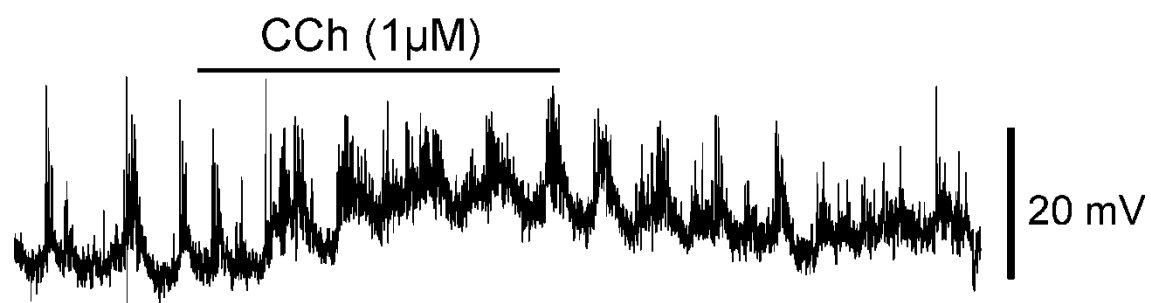
(A) Under control conditions, increasing the frequency of EFS (5, 10, 20 and 30Hz for 30 sec) increased the amplitude of on- and off- contractions in colonic smooth muscle. (B) Pretreatment with H-1152 (10 μ M) significantly decreased on- and off- contractile amplitude. (C) Graph summarizing the effect of H-1152 on nerve-stimulated on-contractions at increasing frequencies (n=6, * $P<0.05$, ** $P<0.005$). (D) Graph summarizing the effect of H-1152 on nerve-stimulated off-contractions at increasing frequencies (n=6, * $P<0.05$, ** $P<0.005$). \circ control; \bullet in presence of H-1152 (10 μ M).

Figure 6: HA-1077 pretreatment inhibited CCh-induced depolarization in murine colonic smooth muscle

A. Control



B. HA-1077 (10 μ M)



C. CCh response

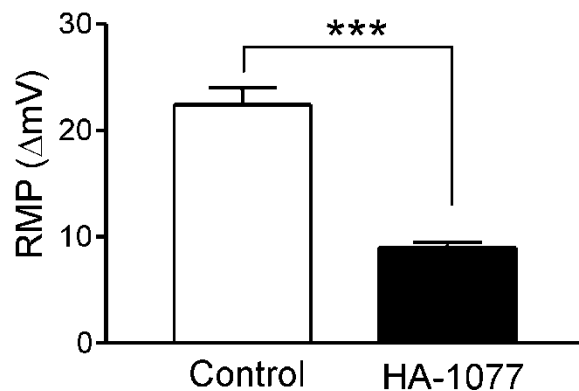
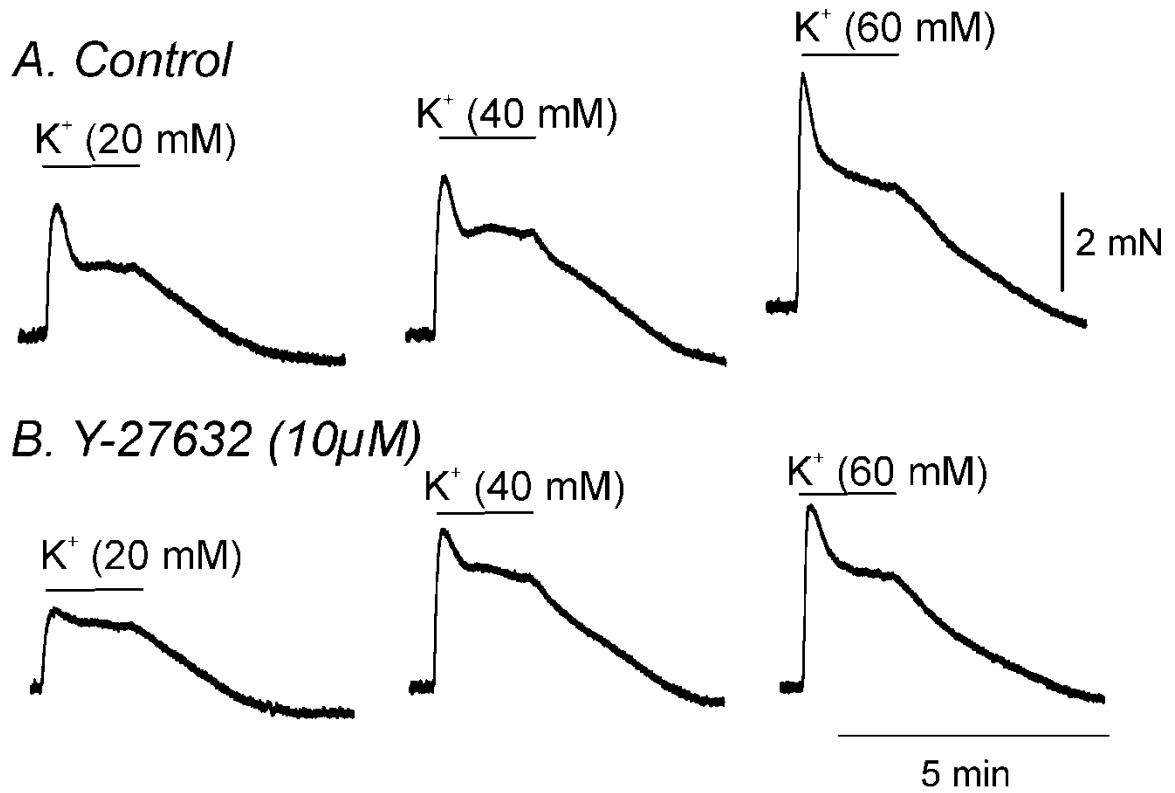


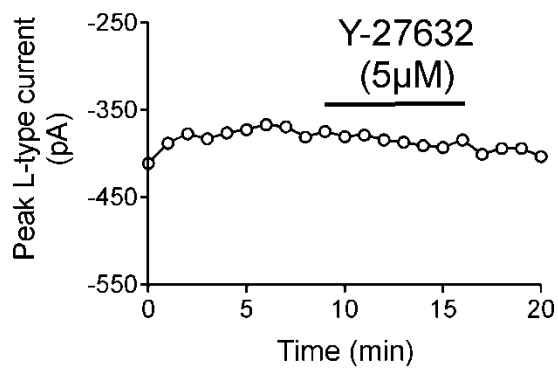
Figure 6: HA-1077 pretreatment inhibited CCh-induced depolarization in murine colonic smooth muscle

(A) Representative trace illustrating a typical CCh-induced depolarization in colonic smooth muscle (1 μ M). (B) Pretreatment with HA-1077 (10 μ M) suppressed the CCh-induced depolarization (1 μ M). (C) Graph summarizing a significant decrease in RMP change upon application of CCh (1 μ M) following pretreatment with HA-1077 (10 μ M) (n=6, *** P <0.001).

Figure 7: Y-27632 pretreatment did not effect KCl evoked contractions in colonic smooth muscle



C. Y-27632 & L-type



D. H-1152 & L-type

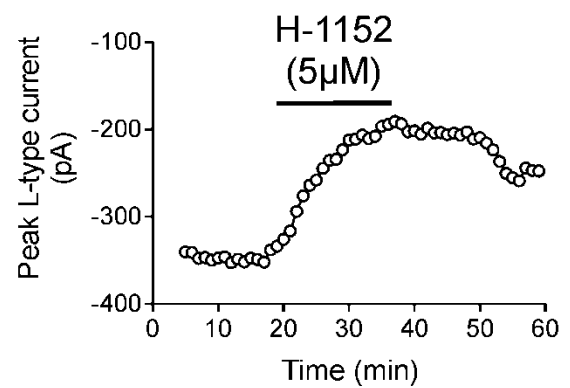


Figure 7: Y-27632 pretreatment did not effect KCl evoked contractions in colonic smooth muscle

(A) Under control conditions, increasing the external concentration of KCl from 5mM to 20, 40 and 60mM for 2mins, which is a classical stimulus for activation of L-type Ca^{2+} channels, evoked an increasing amplitude of contractions in colonic smooth muscle. (B) Pretreatment with Y-27632 (10 μM) had no significant effect on KCl-evoked contractions (n=6). (C) Time course of peak L-type Ca^{2+} currents evoked by step depolarizations to 0mV from a holding potential of -80mV every 1 minute illustrating no effect by application of Y-27632 (5 μM) (n=10 out of 11 cells). (D) In a few of cells, application of H-1152 (5 μM) caused a decrease in peak L-type Ca^{2+} current amplitude that was partially reversible upon washout (n=2 out of 5 cells).

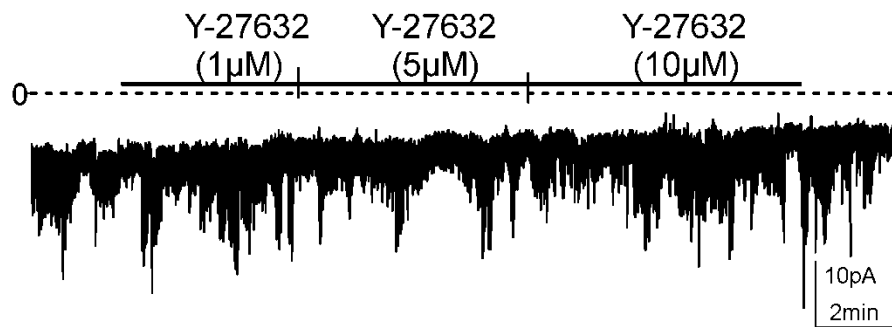
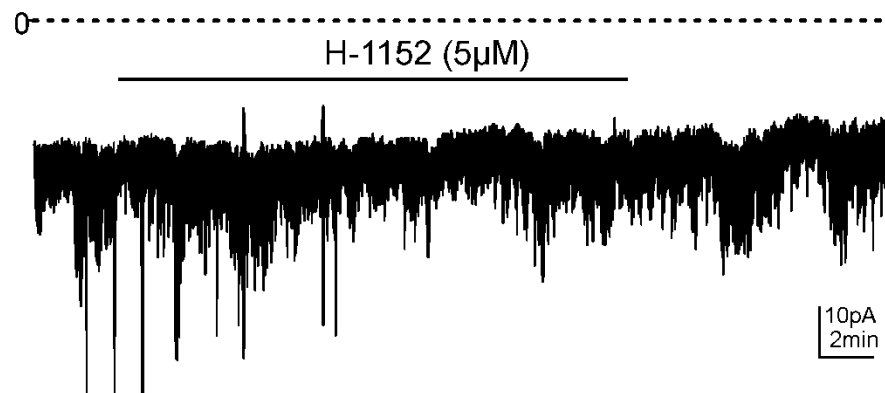
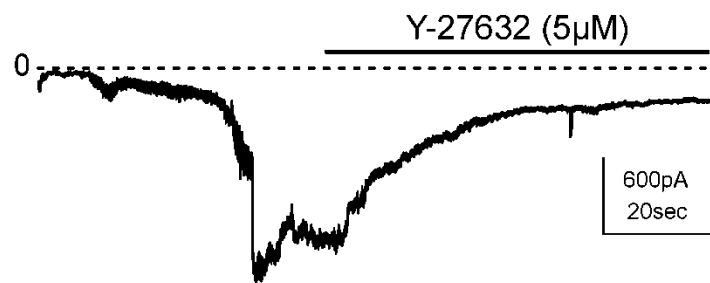
Figure 8: Y-27632 reduced GTP γ S activated NSCC**A. *bInscC* and Y-27632****B. *bInscC* and H-1152****C. GTP γ S evoked current****D. GTP γ S evoked current and Y-27632**

Figure 8: Y-27632 reduced GTP γ S activated NSCC

(A) Under voltage clamp at a holding potential of -80mV, bI_{NSCC} were recorded in murine colonic SMC. Application of Y-27632 at increasing concentrations (1, 5 and 10 μ M) had no effect on bI_{NSCC} (n=12). (B) Under the same recording conditions, exposure to H-1152 (5 μ M) had no effect on bI_{NSCC} (n=5). (C) When whole-cell configuration was achieved using a pipette solution containing GTP γ S (0.5mM), a 'noisy' inward current was gradually activated over 2-4min. (D) The GTP γ S evoked current was significantly reduced by Y-27632 (5 μ M) (n=3).

4.6. Discussion

It has previously been documented that in colonic smooth muscle, Rho-kinase plays an important role in CCh-induced contractions (Al-Jarallah *et al.*, 2008). This study demonstrated that the amplitude of contractions was significantly reduced following Rho-kinase inhibition. Interpretation of these effects was a decrease in Ca^{2+} sensitization through decreased MLCP inhibition.

In the present study the amplitude of on-contractions evoked by increased frequency and duration of EFS were significantly decreased by pretreatment with Rho-kinase inhibitors Y-27632 and H-1152. These effects could be interpreted in a number of ways; 1) the Rho-kinase inhibitors may be acting pre-synaptically to reduce excitatory neurotransmitter release from neurons, 2) they could be acting post-synaptically via direct action on smooth muscle through the Rho-kinase pathway, and 3) Rho-kinase affects the activity of ion channels.

In several smooth muscle preparations Y27632 significantly reduced EFS-induced nerve-stimulated contractions (Büyükaşar & Levent, 2003; Wibberley *et al.*, 2003; Fernandes *et al.*, 2006). In the murine gastric fundus, Y-27632 (100 μ M) reduced neurotransmitter release and caused a simultaneous relaxation (Büyükaşar & Levent, 2003). In another study, murine and guinea-pig tracheal preparations were loaded with [3 H]-choline. Exposure to Y-27632 (10 μ M) significantly increased the outflow of radioactivity following EFS-stimulation compared with controls suggesting this compound increased neurotransmitter release. Despite this finding, the overall effect of Y-27632 was an inhibition of

CCh- and nerve-induced contractions suggesting a dominant post-junctional effect (Fernandes *et al.*, 2006). Therefore in this study TTX was used to examine if the inhibitory effect of Rho-kinase on smooth muscle contractility could still be induced independent of nerves. Y-27632 suppressed CCh-induced contractions in the presence of TTX suggesting that this compound was acting directly on smooth muscle. Inhibition of Rho-kinase and increased MLCP activity could explain this decrease in contractile amplitude.

Contractile experiments also revealed that spontaneous phasic contractions were totally abolished in the presence of Y-27632 (10 μ M). These data suggest that this spontaneous activity is totally dependent on Rho-kinase/Rho-kinase sensitive pathways. However this interpretation is difficult to accept since previous studies have found that the major component required for spontaneous contractions is L-type Ca²⁺ channel activity (Wegener *et al.*, 2006). Application of the L-type Ca²⁺ channel blocker nifedipine can totally inhibit this spontaneous activity (similar to the effect of Y-27632 and H-1152 in the present study). This raised the possibility that Y27632 and/or H-1152 may be directly inhibiting L-type Ca²⁺ channels since non-specific effects of Rho-kinase inhibitors have been reported. For example, in an *in vitro* study in pig aorta smooth muscle, Y-27632 (10 μ M) caused inhibition of PKC (Eto *et al.*, 2001). In the present study, KCl-evoked contractions, which require activation of L-type Ca²⁺ channels, were not affected by pretreatment with Y-27632. To confirm these findings the effects of Y-27632 on L-type Ca²⁺ channels were examined using the perforated-patch

configuration. These studies found no effect of Rho-kinase inhibition on L-type current amplitude. Therefore these results suggest that the suppression of spontaneous phasic contractions is not due to unspecific effects on L-type Ca^{2+} channels. This lead us to consider the possibility that Rho-kinase may regulate activation of NSCC that are required for the initial phase of depolarization.

Recent studies have reported that Rho-kinase may regulate the activity of specific NSCC channels. For example in rat penile arteries, Ca^{2+} influx evoked by phenylalanine, that was insensitive to nifedipine, could be blocked by Y-27632. It was proposed that Rho-kinase may regulate Ca^{2+} influx through cation channels in these arteries (Villalba *et al.*, 2008). Activation of NSCC following muscarinic stimulation by agonists such as CCh play an essential role in smooth muscle depolarization and contraction in the intestine (So & Kim, 2003; Unno *et al.*, 2003; Tsvilovskyy *et al.*, 2009). In the present study, Rho-kinase inhibitors decreased the CCh-induced depolarization which could be due to inhibition of CCh-activated NSCC conductance(s). Dialysis with GTP γ S stimulates CCh-like NSCC through activation of multiple G-proteins (Helliwell & Large, 1997; Dresviannikov *et al.*, 2006). In the present study these GTP γ S currents were inhibited by Y-27632 thus suggesting that decreased depolarization by CCh following pretreatment with Y-27632 was due inhibition of agonist-sensitive NSCC.

Unlike the on-contractions elicited by nerve-stimulation, little research has examined the underlying mechanism(s) responsible for off-contractions. It has been suggested that release of eicosanoids may be involved as non-steroidal

anti-inflammatory drugs such as indomethacin can suppress rebound excitation (Ward *et al.*, 1992). However indomethacin can also inhibit L-type Ca^{2+} channels and therefore this effect must be considered when interpreting the involvement of eicosanoids in rebound excitation using this drug (Sawdy *et al.*, 1998). Our present study showed that off-contractions were also suppressed by Rho-kinase inhibitors although the extent of this inhibition was significantly less than for on-contractions. These findings could be due to inhibition of substance-P activated NSCC (D'Antonio *et al.*, 2009). However further studies are required to understand the mechanism of Rho-kinase inhibition on off-contractions.

In summary, on-contractions which are activated by acetylcholine release by EFS, CCh-induced contractions in the presence of TTX and CCh-induced depolarization were reduced by Rho-kinase inhibitors. Furthermore CCh-activated NSCC were attenuated by Y-27632. Therefore Rho-kinase may be involved in not only the Rho-kinase/MLCP pathway contributing to Ca^{2+} sensitization but also direct regulation of NSCC.

Chapter 5

This chapter is focused on the effect of inflammation on colonic excitability. It has been divided into two sections:

5.1. Identification of histamine receptors and effects of histamine on murine and monkey colonic excitability

5.2. Effect of DSS-induced colitis on contractility and RMP

Section A is an extensive study where one particular inflammatory mediator, histamine, its receptor expression and function were compared in two different species. Section B is an ongoing study that focuses on changes in RMP and contractility following inflammation induced using a DSS-model of colitis.

5.1. Identification of histamine receptors and effects of histamine on murine and monkey colonic excitability

5.1.1. Summary

Histamine is a major mediator in many inflammatory and allergic reactions and is primarily stored in mast cells. Upon its release, histamine modulates many critical functions such as cell migration, motility and chemotaxis. The diverse effects of histamine are exerted through activation of different histamine (H) receptors, H1, H2, H3 and H4. Each receptor is coupled to specific G-protein(s) that activate different signaling pathways resulting in diverse cellular effects. In the human colon, H1, H2 and H4 receptors are expressed. However it is not known which H receptors are expressed in monkey and murine colon and if physiological effects of histamine on colonic excitability in these species can be justly used to predict effects in human colon.

The expression of H receptors and electro-mechanical responses of histamine and various H receptor specific agonists in monkey and mouse colon were examined using molecular techniques, isometric force measurements, conventional microelectrode recordings and patch clamp techniques.

Mast cells were located in colonic smooth muscle layers from untreated monkey and DSS-treated mice therefore supporting a possible direct action of histamine on smooth muscle. H1, H2 and H4 receptor transcripts were expressed at similar levels in monkey colonic tissue whereas only the H2 receptor transcript was detected in murine colonic tissue. Since there was a difference in the

expression of H receptors in these two species, we hypothesized that histamine would have different effects on colonic excitability and contractility.

In monkey colonic tissue, histamine caused substantial depolarization and contraction in the presence of TTX whereas in murine colonic tissue it caused hyperpolarization and transient relaxation in the presence of TTX. H1 and H4 receptor agonists caused depolarization and contraction whereas the H2 receptor agonist caused hyperpolarization and a decrease in contractility in monkey colonic tissue. The open probability of a 5pS channel in monkey colonic SMC was increased by histamine which could contribute to the histamine-induced depolarization and contraction seen in monkey colonic tissue.

In murine colonic tissue, hyperpolarization caused by histamine was prevented by pretreatment with the K_{ATP} blocker, glibenclamide. This suggested that histamine caused relaxation in murine colonic tissue by activation of H2/ G_s /cAMP/PKA pathway resulting in activation of K_{ATP} channels. Perforated-patch clamp experiments further supported these findings as histamine activated a K_{ATP} -sensitive current.

These data suggest that H receptor expression and histamine effects on colonic motility and membrane potential are different between mouse and monkey. Since H receptor expression in monkey colonic tissue is identical to that reported in human colon, we propose that monkey colon is an ideal model to predict the effects of this inflammatory mediator on colonic motility in human inflammatory conditions.

5.1.2. Background and Aims

Histamine is a biogenic amine synthesized from the basic amino acid histidine and is a major mediator in many inflammatory and allergic reactions (Dy & Schneider, 2004). The main sources of histamine are from mast cells, basophils, enterochromaffin-like cells and nerves in the gastrointestinal (GI) tract. Mast cells, derived from hematopoietic progenitor cells in the bone marrow, are widely distributed throughout the GI tract. Many stimuli including allergens, neuropeptides and stress, can activate mast cells resulting in histamine release (Zampeli & Tiligada, 2009). There are four histamine (H) receptors, H1, H2, H3 and H4, through which histamine can exert its effects.

H1 receptors are widely expressed in enterocytes, muscle layer, blood vessels, immune cells and ganglion cells of the myenteric plexus in the human GI tract (Sander *et al.* 2006). H2 receptors are located on parietal cells in the fundic mucosa, intestinal epithelium, immune cells and myenteric ganglia in humans (Sander *et al.*, 2006; Diaz *et al.*, 1994). A number of studies found that H3 receptor mRNA expression could not be detected in the human GI tract, though one report by Heron *et al.* found H3 expression in the mucosa of the rat GI tract (Heron *et al.*, 2001). Transcriptional expression of the H4 receptor is reported to be lower than H1 and H2 in human stomach, small intestine and colon and found to be mainly expressed in leucocytes in mucosa and submucosal blood vessels in the colon (Oda *et al.*, 2000; Liu *et al.*, 2001b; Sander *et al.*, 2006).

There are many functional effects of histamine including gastric acid production, intestinal motility, bronchoconstriction and mucosal ion secretion (Bolton *et al.*, 1981; Kelly *et al.*, 1995; Tanaka *et al.*, 2002; Zampeli & Tiligada, 2009). The diverse effects of histamine in different tissues may be due to differences in the expression pattern of H receptor types since they are coupled to different G-proteins that activate different signaling pathways. H receptor specific agonists and antagonists have been used to try and dissect the role of specific receptors in different tissues (Rossignoli *et al.*, 2008; Santos-Silva *et al.*, 2009).

Surprisingly only a few studies have examined the effect of histamine on GI motility. One study in human colon revealed that histamine caused both contraction and relaxation and these effects were not affected by pretreatment with hyoscine (a ganglion blocker) or anti-adrenaline drugs. The authors concluded that histamine release was not associated with nervous activity and acts directly on the muscle (Bennett & Whitney, 1966). Bolton *et al* demonstrated that in guinea-pig ileum smooth muscle, histamine caused depolarization of the membrane potential and increased action potential discharge (Bolton *et al.*, 1981). Since histamine may play a role in dysmotility seen in inflammatory conditions such as colitis, it is surprising that so few studies have examined this potential role. In addition no studies have examined if H receptor expression in mouse and monkey is similar to humans in order to justify extrapolation of results from studies in these animals to humans. In this study, we report the different

expression of H receptors and electro-mechanical responses of histamine and various H receptor specific agonists in monkey and mouse colon.

5.1.3. Materials and methods

5.1.3.1. Animals.

Male BALB/c mice (10-12 weeks old) were used for electro-mechanical experiments in this study. These mice were killed by inhalation of isoflurane (Baxter Healthcare, Deerfield, IL, USA) followed by cervical dislocation. Colons were removed from abdominal incision and rinsed with Krebs–Ringer bicarbonate buffer (KRB, see section 5.1.3.9.). *Cynomolgus monkeys* of either sex (13 monkeys, 2.5–7 years of age) were donated by Charles River Laboratories (Preclinical Services, Sparks, NV, USA). The animals used were maintained in accordance with the NIH Guide for the Care and Use of Laboratory Animals. All experiments performed and protocols were approved by the Institutional Animal Use and Care Committee at the University of Nevada, Reno.

5.1.3.2. Inducing dextran sulphate sodium (DSS)-colitis in C57BL/6 mice

C57Bl/6 mice of either sex (6- to 8-weeks old, Charles River Laboratories, Wilmington, MA, USA) were administered 5% w/v DSS (MW = 36 000–50 000 Da, MP Biomedicals LLC, Solon, OH, USA) *ad libitum* in the drinking water for 7 days. Mice exhibited typical physical characteristics of DSS-colitis including significant weight loss and bloody stool. Colons were utilized 4 days post-DSS treatment. Mice were maintained and experiments were carried out in accordance with the National Institutes of Health Guide for the Care and Use of

Laboratory Animals. All protocols were approved by the University of Nevada, Reno Institutional Animal Care and Use Committee.

5.1.3.3. Immunohistochemical studies of mast cell infiltration

Tissues were fixed in acetone (4°C; 10 min for murine tissues and 30 min for monkey tissues). Following fixation, tissues were washed overnight in phosphate-buffered saline (PBS; 0.01 M, pH 7.2) and rewashed with fresh PBS the following day for 4 h with a change of PBS every hour. Tissues were subsequently incubated in bovine serum albumin (BSA; 1%; 1 h at room temperature) to reduce non-specific antibody binding. For whole mount preparations, some acetone-fixed tissues were incubated singularly or sequentially in a combination of primary antibodies. The first incubation was carried out for 48 h at 4°C. The tissues were subsequently washed in PBS before being incubated in the second primary antibody for an additional 48 h at 4°C. The combination of antibodies used was a goat monoclonal antibody (hSCF-R; diluted 1: 500 in 0.5% Triton-X 100; R&D Systems Inc., Minneapolis, MN, USA) to identify Kit-positive cells. Following incubation in primary antibodies, immunoreactivity was detected via sequential incubation in Alexa fluor 594-coupled donkey anti-goat secondary antibodies (Molecular Probes, Eugene, OR, USA; 1: 500 in PBS; 1 h, room temperature). Control tissues were prepared by omitting either primary or secondary antibodies from the incubation solution. After incubation in secondary antibodies, tissues were washed with PBS (overnight at 4°C) and mounted on glass slides using Aqua-Mount (Lerner Laboratories,

Pittsburgh, PA, USA). Tissues were examined with a Zeiss LSM 510 Meta confocal microscope (Zeiss, Germany) with an excitation wavelength appropriate for Alexa fluor 594. Confocal micrographs were digital composites of Z-series scans of 10–100 optical sections through a depth of 4–100 μm . Final images were constructed using Zeiss LSM 5 Image Examiner software and converted to Tiff files for final processing in Adobe Photoshop 7.0 (Adobe Co., Mountain View, CA, USA) and Corel Draw X3 (Corel Corp., Ontario, Canada).

5.1.3.4. Molecular Studies

Total RNA isolation and cDNA preparation and amplification of monkey and murine colonic muscle strips (mucosa and submucosa removed) were performed as previously reported (Amberg *et al.*, 2002). Briefly, RNA was prepared using SNAP Total RNA isolation kit (Invitrogen, San Diego, CA) as per the manufacturer's instructions. RNA was treated with Rnase-free Dnase I (2 units) at 37°C (New England Biolabs) prior to cDNA preparation. First strand cDNA was synthesized from each RNA using Superscript II Reverse Transcriptase with 500 $\mu\text{g}/\mu\text{l}$ of oligo dT primers cDNA. To investigate the expression of H receptors the following PCR primers designed against murine sequences were used (genebank accession number is given in parenthesis for the reference nucleotide sequence used): H1 (NM_008285), H2 (NM_008286), H3 (NM_133849), H4 (NM_153087). Similarly, primers were designed against the following human and monkey sequences: H1 (NM_000861 and

XM_001088286), H2 (NM_022304 and XM_001082927), H3 (NM_007232 and NM_001032898), H4 (NM_021624 and XM_001096657). The relative expression levels of H receptors in monkey colons was determined by real-time quantitative PCR performed on a ABI PrismM 7000 sequence detector using SYBR[®] Green chemistry (Applied Biosystems, CA). Standard curves were generated for each receptor and the constitutively expressed GAPDH from regression analysis of the mean values of RT-PCRs for the log₁₀ diluted cDNA. Unknown quantities relative to the standard curve for the H receptor primers were calculated, yielding transcriptional quantization of H receptor cDNA relative to the endogenous standard GAPDH. Each cDNA sample was tested in triplicate and cDNA was obtained from 4 different monkey colons. The reproducibility of the assay was tested by analysis of variance comparing repeat runs of samples, and the mean values generated at individual time points were compared by Student's *t* test.

5.1.3.5. Isometric Force Measurements

Standard organ bath techniques were employed to measure the changes in force generated by murine and monkey smooth muscle strips. One end of a smooth muscle strip was attached to a fixed mount and the opposite end to an isometric strain gauge (Fort 10, WPI, Sarasota, FL, USA) in oxygenated KRB solution maintained at 37.5±0.5°C. A resting force of 500 mg (murine colon) and 1g (monkey colon) was applied to set the muscles at optimum length, and the muscles were allowed to equilibrate for 1-2 h with constant perfusion with KRB

solution. Mechanical responses were recorded on a computer running Axoscope (Axon instrument, Foster City, CA, USA) and measurements of the area under the curve (AUC) obtained. The AUC was determined as the integral values above the baseline of selected area for 5 min recordings (mN*min). The AUC for the tissues exposed to tested drugs were compared to the AUC for tissues under control conditions, during an equivalent period of time. Bathing solutions were exchanged by switching the perfusion to the drug-containing solution.

5.1.3.6. Intracellular Microelectrode Recordings

After preparing the tissue, impalements of cells were made with glass microelectrodes having resistances of 80–120 M Ω . Transmembrane potentials were recorded with a standard electrometer (Duo 773; WPI, Sarasota, FL, USA). Data were recorded using Axoscope (Axon instrument, Foster City, CA, USA).

5.1.3.7. Isolation of SMC

Monkey colon segments were placed in KRB (see section 5.1.3.9.). Each segment was opened and pinned to the base of a dissecting dish coated with Sylgard elastomer (Dow Corning Corp., Miland, MI, USA) and the adhering mucosa and submucosa were removed. Freshly dispersed colonic SMC were prepared from colonic muscle strips using Ca²⁺-free Hank's solution containing (mM): 125 NaCl, 5.36 KCl, 15.5 NaOH, 0.336 Na₂HPO₄, 0.44 KH₂PO₄, 10 glucose, 2.9 sucrose and 11 Hepes, adjusted to pH 7.4 with Tris. Pieces of

muscle were incubated for 50-55 minutes at 37°C in a Ca²⁺-free solution (2 ml) containing collagenase (4 mg/mL, Worthington Biochemical, Lakewood, NJ), trypsin inhibitor (8 mg/mL), fatty acid-free bovine serum albumin (8 mg/mL), papain (2 mg/mL), and L-dithiothreitol (LDTT, 0.3 mg/mL, Sigma-Aldrich, MO, USA). Tissue pieces were washed with Ca²⁺-free solution and then gently agitated to create a cell suspension. Dispersed SMC were stored at 4°C in Ca²⁺-free solution. Drops of the cell suspensions were placed on the bottom of a 300 µl chamber mounted on an inverted microscope and allowed to adhere to the bottom of the chamber for 5 minutes before recording.

Colons from BALB/c mice were dissected in the same fashion as monkey colons. Pieces of muscle were incubated for 35-40 minutes at 37°C in a Ca²⁺-free solution (2 ml) containing collagenase (2 mg/mL, Worthington Biochemical, Lakewood, NJ), trypsin inhibitor (4 mg/mL), fatty acid-free bovine serum albumin (4 mg/mL), papain (1 mg/mL) and LDTT (0.3 mg/mL).

5.1.3.8. Patch Clamp Experiments

The whole-cell voltage clamp technique was used to record membrane currents from dissociated colonic SMC. Currents were amplified with an Axopatch 200B (Axon Instruments). Data were digitized with 16-bit analogue to digital converter (Digidata 1322A, Axon instruments, Foster City, CA, USA). Data were stored directly and digitized online using pClamp software (version 9.0,

Axon instrument, Foster City, CA, USA). The data were sampled at 5 KHz with low pass filtered at 2 KHz using an eight-pole Bessel filter. Conventional and perforated whole cell patch-clamp techniques were used for recording ionic currents under voltage clamp. For perforated patches, amphotericin B (60 mg/ml) was dissolved in DMSO, sonicated, and diluted in the pipette solution to give a final concentration of 270 $\mu\text{g/ml}$. Experiments were performed at room temperature (between 22 and 25°C).

5.1.3.9. Solutions and Drugs

In intracellular microelectrode recordings and mechanical experiments, the tissue chamber housing muscles was constantly perfused with oxygenated KRB of the following composition (mM): NaCl 118.5; KCl 4.5; MgCl_2 1.2; NaHCO_3 23.8; KH_2PO_4 1.2; dextrose 11.0; CaCl_2 2.4. The pH of the KRB was 7.3–7.4 when bubbled with 97% O_2 –3% CO_2 at $37.0 \pm 0.5^\circ\text{C}$. In order to measure inward currents, colonic SMC were bathed in a Ca^{2+} -containing physiological salt solution (CaPSS) containing (mM): 135 NaCl, 5 KCl, 2 CaCl_2 , 1.2 MgCl_2 , 10 glucose, 10 HEPES adjusted to pH 7.4 with Tris. The pipette solution for the study of inward currents contained (in mM): 135 CsCl, 0.1 EGTA, 0.1 Na_2GTP , 3 MgATP, 10 glucose, 2.5 creatine phosphate disodium and 10 HEPES. This solution was adjusted to pH 7.2 with Tris. In some experiments, cells were perfused in High K^+ -containing solution (135 mM Na^+ was replaced with equimolar K^+) and the pipette solution contained (in mM): 135 KCl, 10 BAPTA,

0.1 Na₂GTP, 3 MgATP, 10 glucose, 2.5 creatine phosphate disodium and 10 HEPES and was adjusted to pH 7.2 with Tris. H1 agonist (histamine-trifluoromethyl-toluidine, HTMT), H2 agonist (Dimaprit) and H4 agonist (4-methylhistamine dihydrochloride, MHDC) were purchased from Tocris (Park Ellisville, MO, USA). Histamine, glibenclamide (GBC) and tetrodotoxin (TTX) were obtained from Sigma Chemical Co (St Louis, MO, USA).

5.1.3.10. Statistical Analysis

Data are expressed as means \pm S.E.M. The Student's t-test was used where appropriate to evaluate differences in the data. *P*-values less than 0.05 were taken as statistically significant differences. *n* values refer to the number of recordings from muscle strips in electro-mechanical experiments or from cells in patch clamp experiments.

5.1.4. Results

5.1.4.1. Mast cells were located in monkey and inflamed murine colonic smooth muscle

Histamine is neither expressed by enteric neurons nor acts as a neurotransmitter (Wood, 2006). Instead it is stored mainly in mast cells and acts in a paracrine fashion. Firstly, we examined the infiltration of mast cells in murine and monkey smooth muscles to examine the effects of histamine directly on smooth muscle excitability. In normal untreated monkey colon, staining of mast cells using ACK-2 antibody revealed rounded Kit⁺ cells within the circular muscle layer (Fig. 1A). In normal untreated mice, few if any mast cells were found in the muscle layer of the colon (data not shown). However in DSS-treated mice, regions of smooth muscle were stained heavily for ACK-2 positive cells (Fig. 1B). Interestingly in these regions where there were high levels of mast cells, the morphology of interstitial cells of Cajal (ICC) (that are also stained with the ACK-2 antibody) were distorted. In other areas where ICC structure was normal, no mast cells were found. These data suggest that mast cells/ or release of their mediators may damage ICC. These results support the likely hood that histamine can directly act on smooth muscle by its release from mast cells within the smooth muscle layer. Therefore we tested the functional role of histamine on smooth muscle contractility.

5.1.4.2. Transcriptional expression of histamine receptors was different in murine and monkey colonic tissue

Firstly we investigated the transcriptional expression of H receptor isoforms by performing RT-PCR on colonic muscle from monkey and mouse. Detectable amplicons for H1, H2 and H4 were revealed in monkey colonic muscle (Fig. 2A). This finding is very similar to H receptor expression in human colon (Sander *et al.*, 2006). Only the H2 receptor was detected in murine colonic muscle (Fig. 2B). Quantitative analysis of H1, H2 and H4 receptors in monkey colonic tissue revealed that there was no significant difference in expression levels of these receptors (Fig. 2C).

5.1.4.3. Histamine had opposite effects on spontaneous contractility in monkey and murine colonic smooth muscle

Since the expression of H receptors was different in monkey versus mouse colonic tissue, we wanted to compare the effects of histamine on colonic contractility in these two species. The 'contractility' was determined from averaged area under the contraction curve (AUC) for a 5-min recording period (see materials and methods section). In monkey colonic muscle, application of histamine (10 μ M) increased the AUC from 14.0 \pm 3.4 to 157.4 \pm 54.8 mN*min (Fig 3A and C, n=4, P <0.05). In contrast, in murine colonic smooth muscle, application of histamine (10 μ M) caused a transient decrease in contractility, but

the calculated AUC for initial 5min after histamine was not significant (31.0 ± 2.1 to 30.3 ± 3.4 mN*min) (Fig. 3B and 3C; n=15).

5.1.4.4. Effects of histamine on monkey and murine colonic contractility were TTX-insensitive

Since neuronal cells may also express H receptors and therefore the effects of histamine may have been through neurotransmitter release from enteric neurons acting on the colonic smooth muscle, we pretreated the tissue with tetrodotoxin (TTX, 1 μ M). In monkey smooth muscle, histamine (10 μ M) still induced significant contraction (AUC from 45.2 ± 21.3 to 260.9 ± 56 mN*min) following pretreatment with TTX (Fig. 4A & 4C; n=9, $P < 0.005$). In murine colon, transient relaxation caused by histamine was not affected by pretreatment with TTX (AUC from 74.1 ± 10.4 to 63.5 ± 10.8 mN*min; Fig. 4B & 4D; n=11, $P < 0.005$). These results suggest that histamine acts directly on H receptors on monkey smooth muscle to stimulate a response independent of any neuronal influences.

5.1.4.5. Histamine had opposite effects on membrane potential in monkey and murine colonic smooth muscle

We also performed intracellular microelectrode recordings on monkey and murine colonic muscle to examine the effects of histamine on membrane potential. In monkey, application of histamine (10 μ M) caused a sustained depolarization that was reversible upon washout (Fig. 5A, n=6, $P < 0.005$). A

similar effect of histamine was found in the presence of TTX (1 μ M) (Fig. 5B, n=4). In contrast, in murine colonic muscle, addition of histamine (10 μ M) hyperpolarized colonic muscles from -45.5 ± 0.6 mV to -50.6 ± 1.8 mV (Fig. 5C, n=9; $P<0.05$). A similar effect was found in the presence of TTX (1 μ M) (Fig. 5D, n=11, $P<0.005$). Since murine colonic smooth muscle expresses H₂ receptors exclusively, which are coupled to G_s-proteins, we hypothesized that hyperpolarization may be the result of activation of K_{ATP} channels by PKA following activation of the H₂/G_s pathway. To investigate this, we pretreated murine colonic muscle with the K_{ATP} blocker glibenclamide (GBC) and found that histamine did not change the membrane potential (Fig. 5E, n=4). These data suggest that in murine colonic muscle, histamine causes hyperpolarization and decreased contractility via activation of the H₂-cAMP-PKA-K_{ATP} pathway.

5.1.4.6. Histamine receptor agonists affected monkey colonic contractility

Since H₁, H₂ and H₄ receptors are expressed in monkey colonic tissue, we investigated the effects of specific H receptor agonists on contractility. Application of the H₁ agonist, HTMT (100 μ M), caused a significant increase in contractility in the presence of TTX (1 μ M) (Fig. 6A & B, n=4, $P<0.05$). The amplitude of contractions was transiently decreased upon addition of the H₂ receptor agonist dimaprit (500 μ M) (Fig. 6C & D, n=4, $P<0.05$). Finally the H₄ agonist, MHDC (500 μ M), significantly increased the AUC with a dramatic

increase in the amplitude of spontaneous contractions though frequency was decreased (Fig. 6E & F, $n=4$, $P<0.05$).

5.1.4.7. Histamine receptor agonists affected monkey colonic membrane potential

Following the results from contractility experiments, we examined the effects of H receptor-specific agonists on membrane potential. HTMT (100 μ M) caused a significant depolarization in membrane potential (Fig. 7A and B, -53.9 ± 0.1 to -47.8 ± 0.2 mV, $n=4$, $P<0.05$). Application of the H₂ receptor agonist dimaprit (500 μ M), resulted in transient hyperpolarization (Fig. 7C and D, $n=4$). Finally, MHDC (500 μ M) induced a significant transient depolarization (Fig. 7E and F, $n=4$, $P<0.05$).

5.1.4.8. Histamine increased the open probability of 5pS NSCC in monkey colonic SMC

The overall depolarization and contraction caused by histamine in monkey colonic tissue could be through activation of NSCC. In order to examine this hypothesis, cell-attached single channel experiments were performed using symmetrical Cs/Cs (140mM). At a holding potential of -80mV, application of histamine (10 μ M) increased NP_o (N =number of channel, P_o =open probability) of 5pS NSCC channel (Fig. 8A). 25pS channels were not affected by histamine

(10 μ M) (Fig. 8B). Therefore activation of the 5pS NSCC may contribute to depolarization and contraction caused by histamine in monkey colonic tissue.

5.1.4.9. Histamine activated K_{ATP} whole-cell currents in murine colonic SMC

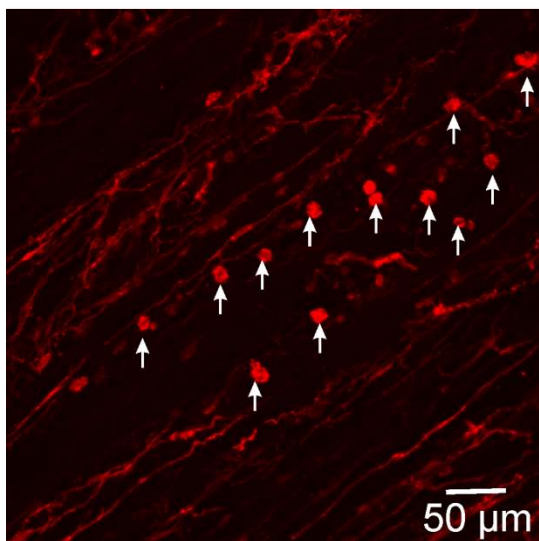
Histamine induced hyperpolarization in murine colonic smooth muscle which could be due to activation of K^+ conductance(s) or inhibition of NSCC through H2 activation. Since the K_{ATP} channel blocker, glibenclamide, prevented histamine-induced hyperpolarization (Fig. 5E), we examined the effect of histamine on these particular K^+ channels. Using the perforated whole-cell patch clamp technique at a holding potential of -80mV, the external solution (CaPSS) was replaced with high K^+ solution (HK; 140mM K^+ , see Materials and methods section) which activated inward currents. Application of histamine under these conditions further activated inward currents. Since the inward currents could be activation of NSCC, we tested the effects of the NSCC blocker Gd^{3+} (10 μ M) during histamine treatment. Gd^{3+} had no effect on the inward currents activated by histamine (Fig. 9A, n=3). These data suggested that it was not NSCC that were activated by histamine but potentially K^+ channels. Therefore we examined the SK blocker, apamin and K_{ATP} blocker, glibenclamide, on histamine-activated inward currents. Application of apamin (300nM) during treatment with histamine did not affect the histamine effects (Fig. 9B, n=3). However, application of glibenclamide (10 μ M) reduced histamine-activated currents (Fig. 9C, n=3). These data suggest that K_{ATP} channel activation by histamine could be

responsible for histamine-induced hyperpolarization and decreased contractility in murine colonic tissue. Since PKA can affect L-type Ca^{2+} channels (Keef *et al.*, 2001) we examined if activation of the H2 receptor pathway by histamine altered L-type Ca^{2+} currents. However, using the perforated patch configuration, histamine had no effect on L-type Ca^{2+} currents (Fig. 9D, n=4).

5.1.5. Figures and figure legends

Figure 1: Mast cells were located in monkey and inflamed murine colonic smooth muscle

A. Monkey



B. Mouse

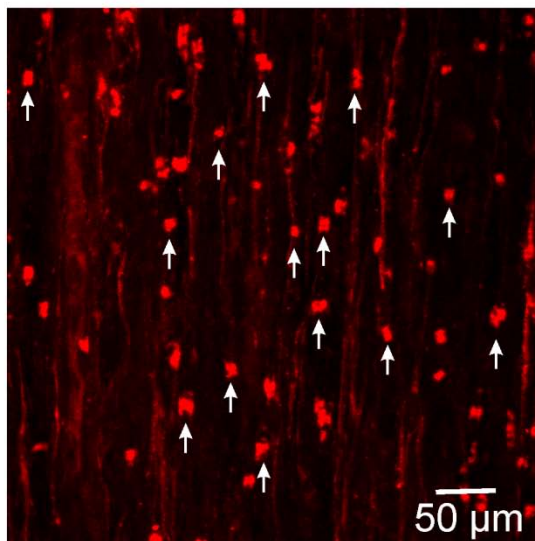
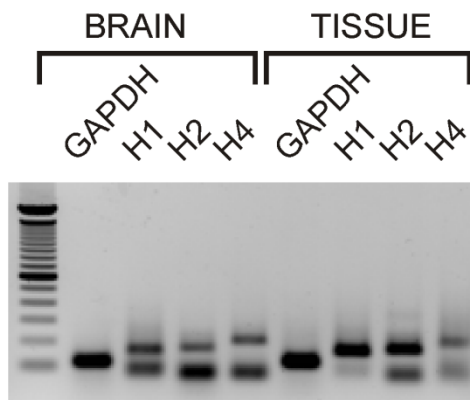


Figure 1: Mast cells were located in monkey and inflamed murine colonic smooth muscle

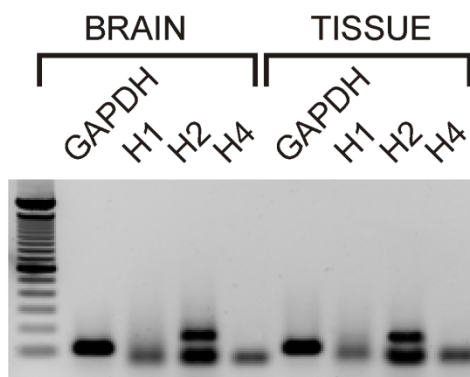
(A) Confocal reconstruction of mast cells within the monkey tunica muscularis. Rounded Kit⁺ cells within the circular muscle layer (arrows) are mast cells. Spindle-shaped cells are Kit⁺ ICC. (B) Confocal image showing mast cells (white arrows) detected within the smooth muscle layers of the colon from a mouse that had been treated with DSS.

Figure 2: H receptor expression was different in monkey and murine colonic tissue

A. MONKEY



B. MOUSE



C. MONKEY- qPCR

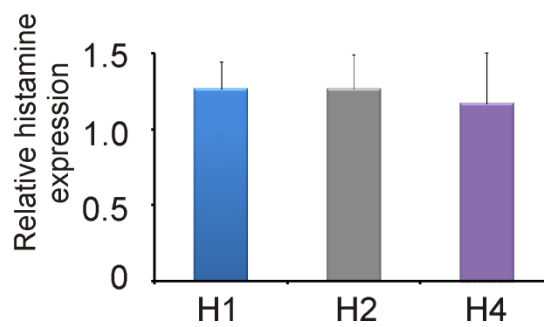


Figure 2: H receptor expression was different in monkey and murine colonic tissue

Representative agarose gels of RT-PCR products of H1, H2 and H4 receptors in (A) monkey and (B) mouse colonic tissue. RT-PCR was performed with H receptor isoform specific primers. GAPDH was used for control. A 100 bp ladder is shown on the left side of each gel. (C) Summary graph of real-time quantitative PCR (qPCR) analysis of H1, H2 and H4 receptors in monkey colonic tissue. qPCR was performed using Syber Green chemistry. Expression of each H receptor isoform was normalized relative to GAPDH expression. Mean + S.D values are shown for the samples from triplicate cultures.

Figure 3: Histamine altered contractility in monkey and murine colonic smooth muscle

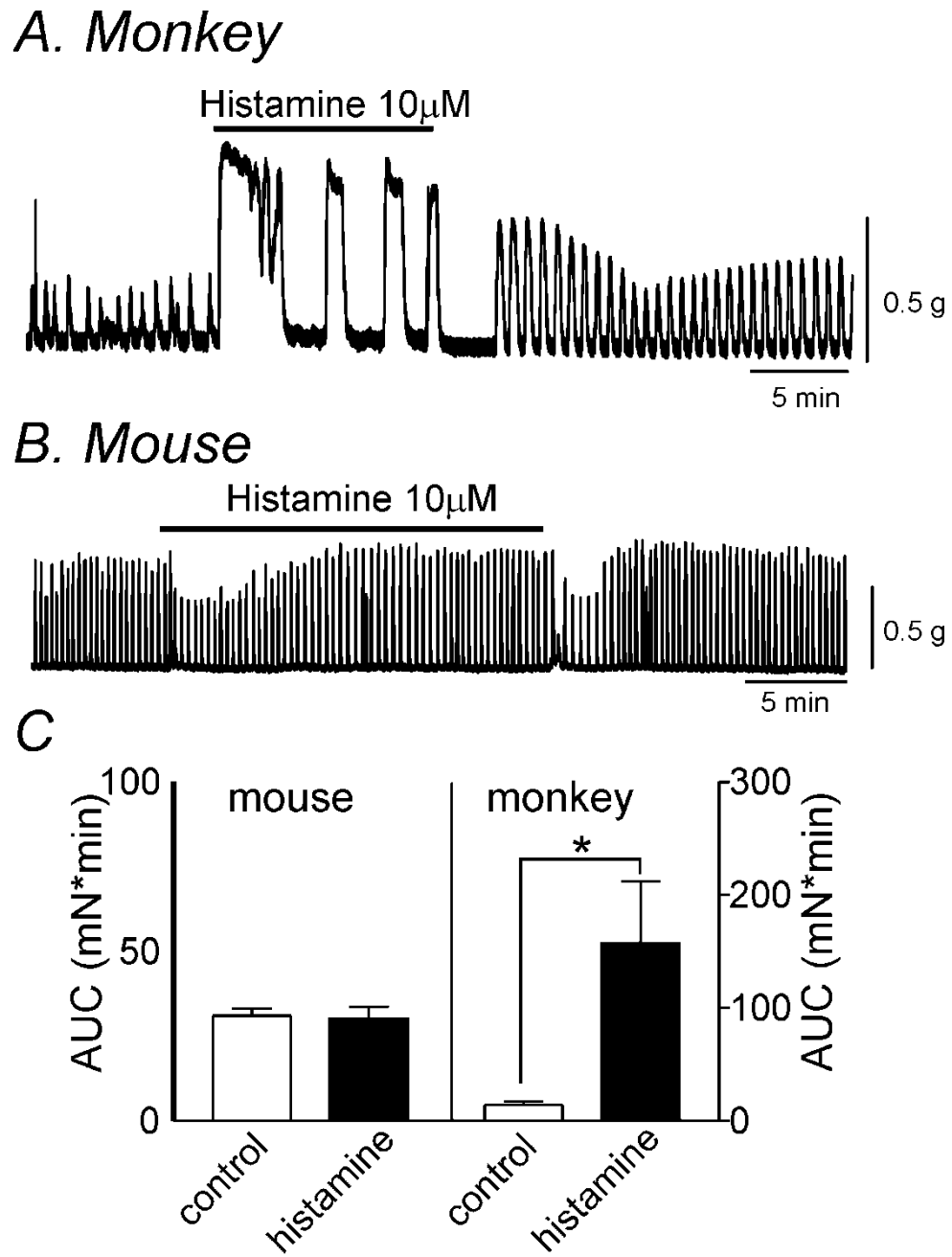
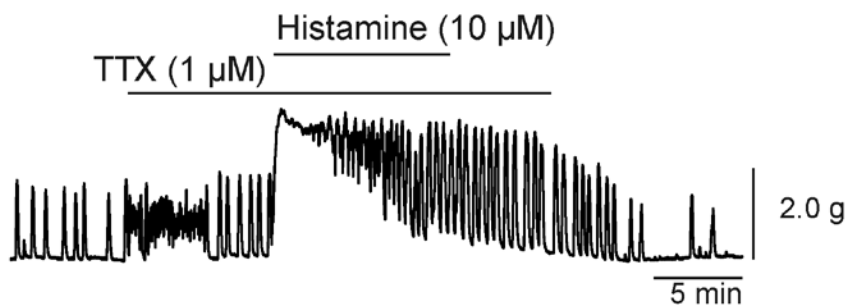


Figure 3: Histamine altered contractility in monkey and murine colonic smooth muscle

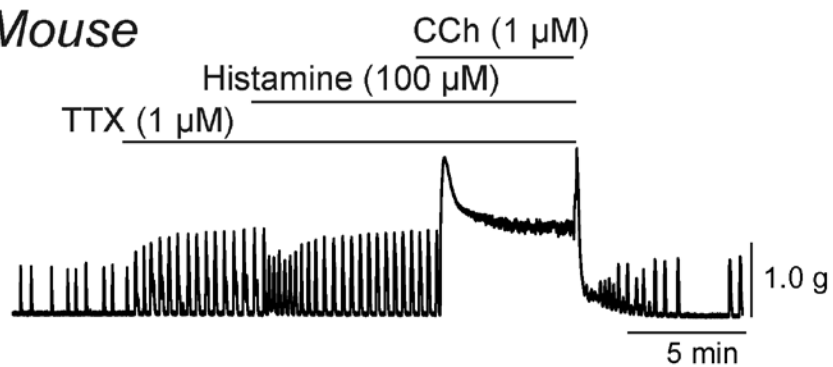
(A) Representative mechanical trace illustrating that histamine (10 μ M) caused an increase in area under the curve (AUC) in monkey colonic smooth muscle. (B) Representative trace illustrating that there was a transient decrease in the amplitude of spontaneous contractions in murine colonic smooth muscle following application of histamine (10 μ M). (C) Summary data of AUC for 5 min recording before and after histamine treatment from murine (n=15) and monkey colonic smooth muscle (n=4, * $P<0.05$).

Figure 4: Histamine-evoked changes in contractility in monkey and murine colonic smooth muscle were TTX-insensitive

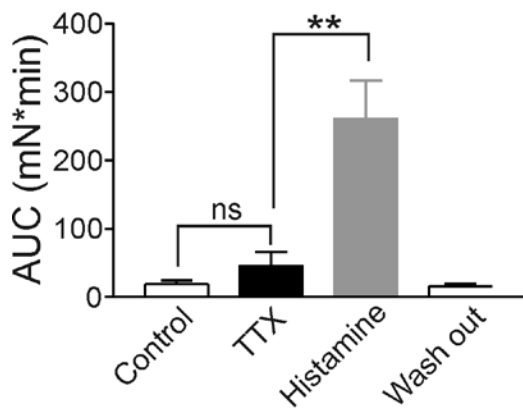
A. Monkey



B. Mouse



C. Monkey



D. Mouse

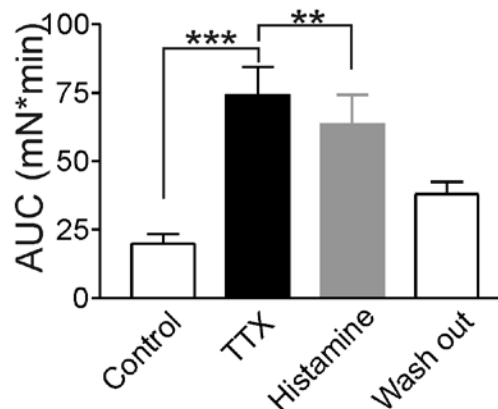


Figure 4: Histamine-evoked changes in contractility in monkey and murine colonic smooth muscle were TTX-insensitive

(A) Representative mechanical trace showing that in the presence of TTX (1 μ M), exposure to histamine (10 μ M) resulted in an increase in contractility in monkey colonic smooth muscle. (B) Representative trace illustrating that histamine caused a transient decrease in amplitude of spontaneous contractions in the presence of TTX (1 μ M) in murine colonic smooth muscle. (C) Graph summarizing the significant increase in AUC by histamine in the presence of TTX in monkey colonic tissue (n=9, ** P <0.005). (D) Graph summarizing the significant decrease in AUC by histamine in the presence of TTX in murine colonic muscle (n=11, ** P <0.005, *** P <0.001).

Figure 5: Histamine altered membrane potential in monkey and murine colonic smooth muscle

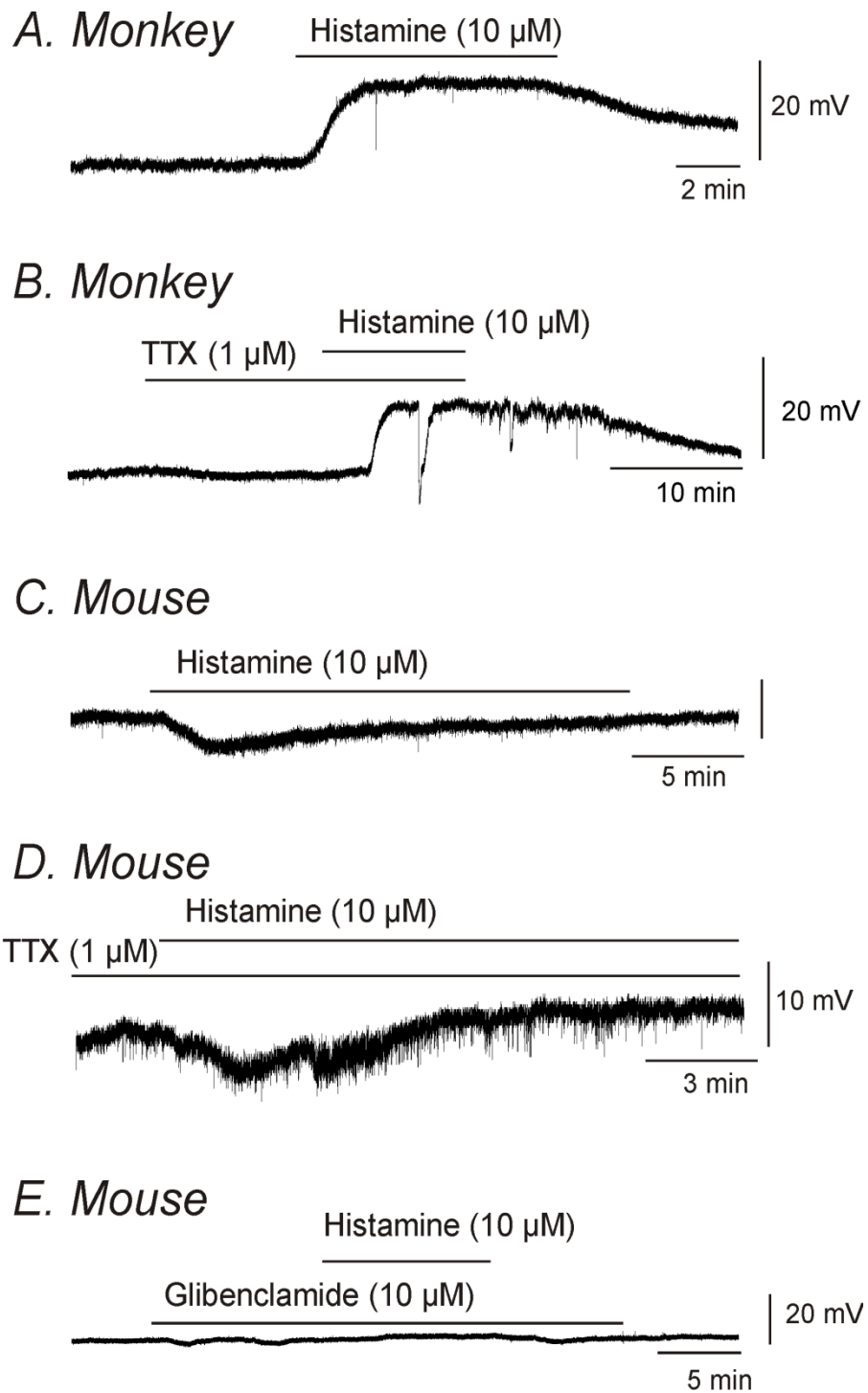
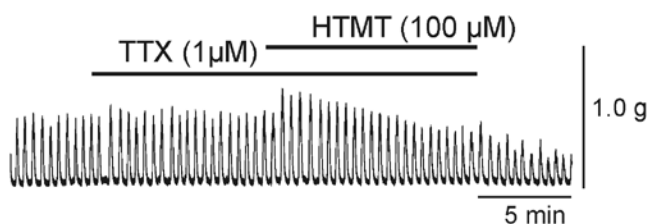


Figure 5: Histamine altered membrane potential in monkey and murine colonic smooth muscle

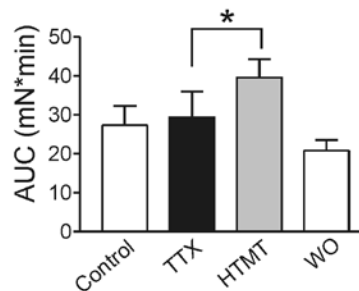
Representative traces illustrating how histamine (10 μ M) caused depolarization in the (A) absence and (B) presence of TTX (1 μ M) in monkey colonic smooth muscle. In contrast, in murine colonic smooth muscle, representative traces show that histamine (10 μ M) induced transient hyperpolarization in the (C) absence and (D) presence of TTX (1 μ M). (E) Pretreatment with the K_{ATP} blocker, glibenclamide (10 μ M), prevented the hyperpolarization caused by histamine (10 μ M) in murine colonic smooth muscle.

Figure 6: Specific H receptor agonists had different effects on contractility in monkey colonic smooth muscle

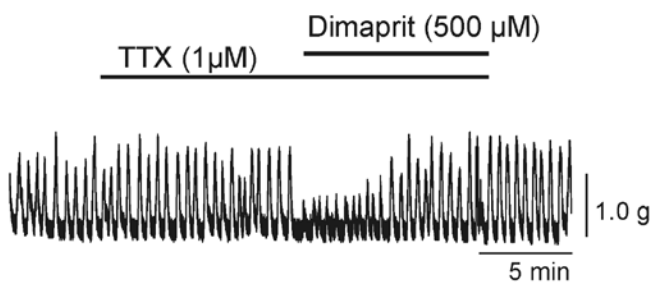
A. H1 agonist



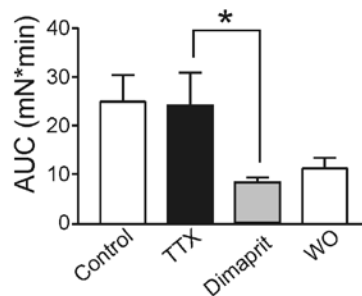
B.



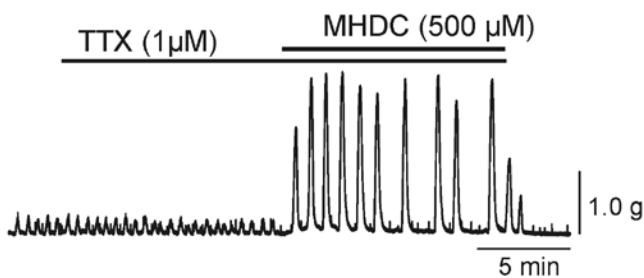
C. H2 agonist



D.



E. H4 agonist



F.

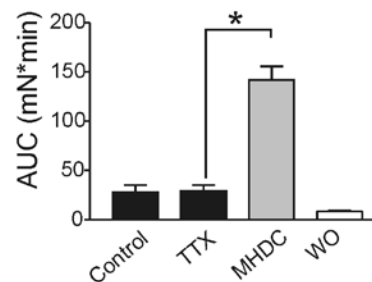


Figure 6: Specific H receptor agonists had different effects on contractility in monkey colonic smooth muscle

(A & B) Application of the H1 agonist, HTMT (100 μ M), caused a transient increase in the amplitude of spontaneous contractions (n=4). (C & D) Dimaprit (500 μ M), a H2 agonist, caused a transient decrease in the amplitude of spontaneous contractions (n=4). (E & F) The H4 agonist, MHDC (500 μ M), evoked an increase in the amplitude of spontaneous contractions but a decrease in frequency (n=4). * denotes $P < 0.05$.

Figure 7: Specific H receptor agonists changed membrane potential in monkey colonic smooth muscle

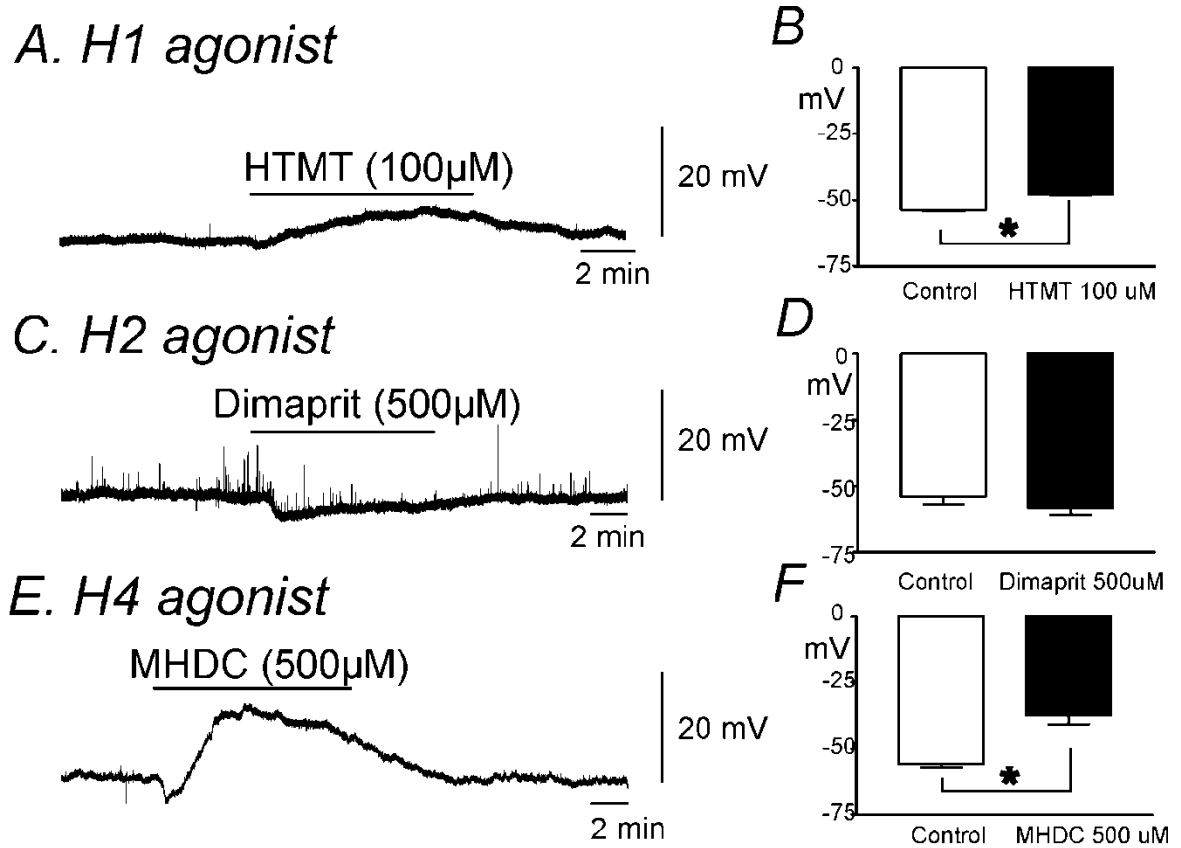


Figure 7: Specific H receptor agonists changed membrane potential in monkey colonic smooth muscle

(A & B) Application of the H1 agonist, HTMT (100 μ M), caused depolarization of the membrane potential in monkey colonic smooth muscle (n=4). (C & D) Dimaprit (500 μ M), H2 agonist, induced transient hyperpolarization (n=4). (E & F) The H4 agonist, MHDC (500 μ M), resulted in a transient depolarization in membrane potential (n=4). * denotes $P < 0.05$.

Figure 8: Histamine increased the open probability of a 5pS NSCC in monkey colonic SMC

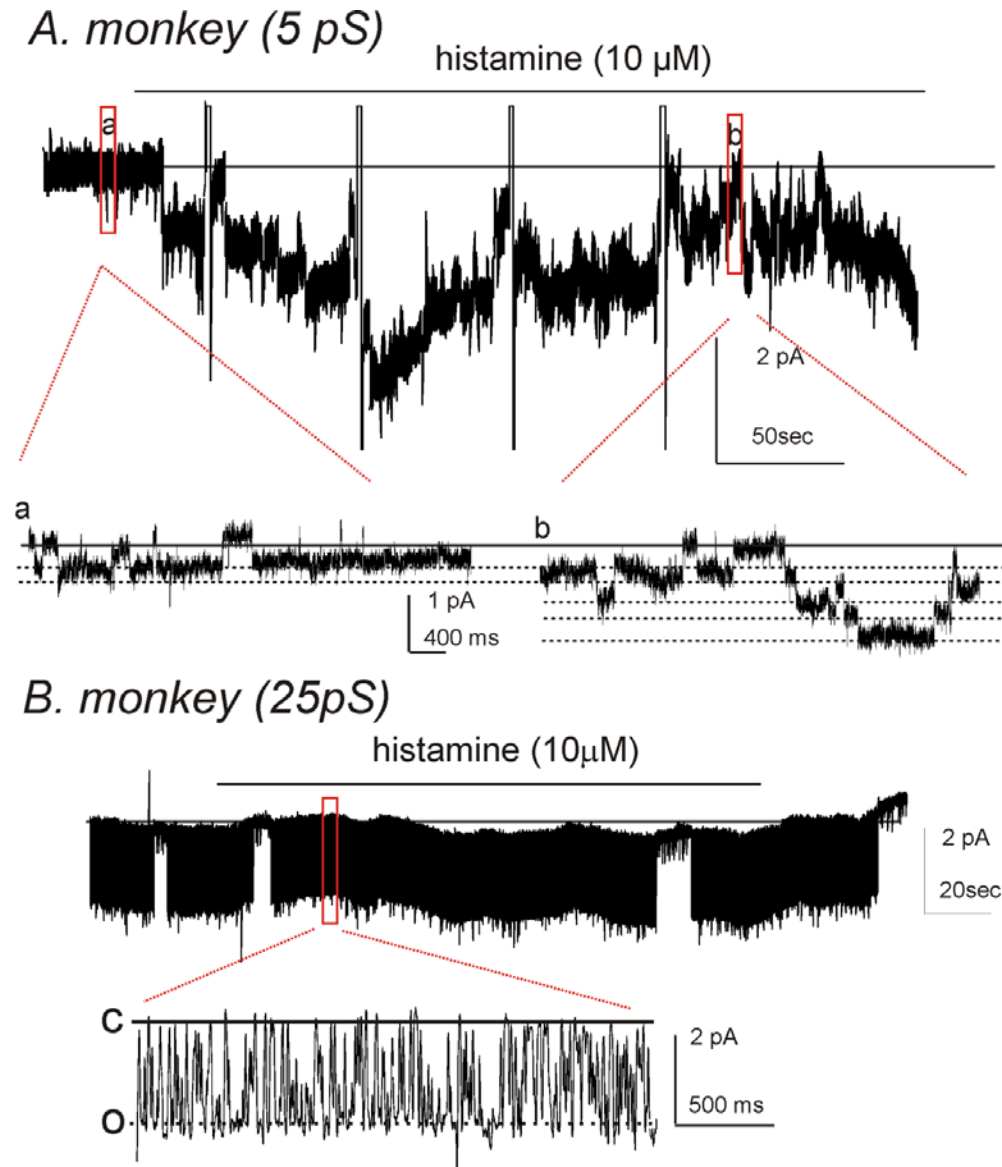


Figure 8: Histamine increased the open probability of a 5pS NSCC in monkey colonic SMC

In monkey colonic SMC, single channel experiments using symmetrical Cs/Cs (140mM) under the cell-attached configuration were performed. Application of histamine (10 μ M) increased NPo (N=number of channel, P_o =open probability) of 5pS NSCC channel at a holding potential of -80 mV. (Aa) Expanded region of (A) before application of histamine. (Ab) Expanded region of (A) during histamine application showing increased single channel openings of the 5pS NSCC. (B) 25pS channel NPo was not affected by application of histamine (10 μ M).

Figure 9: Histamine activated K_{ATP} currents in murine colonic SMC

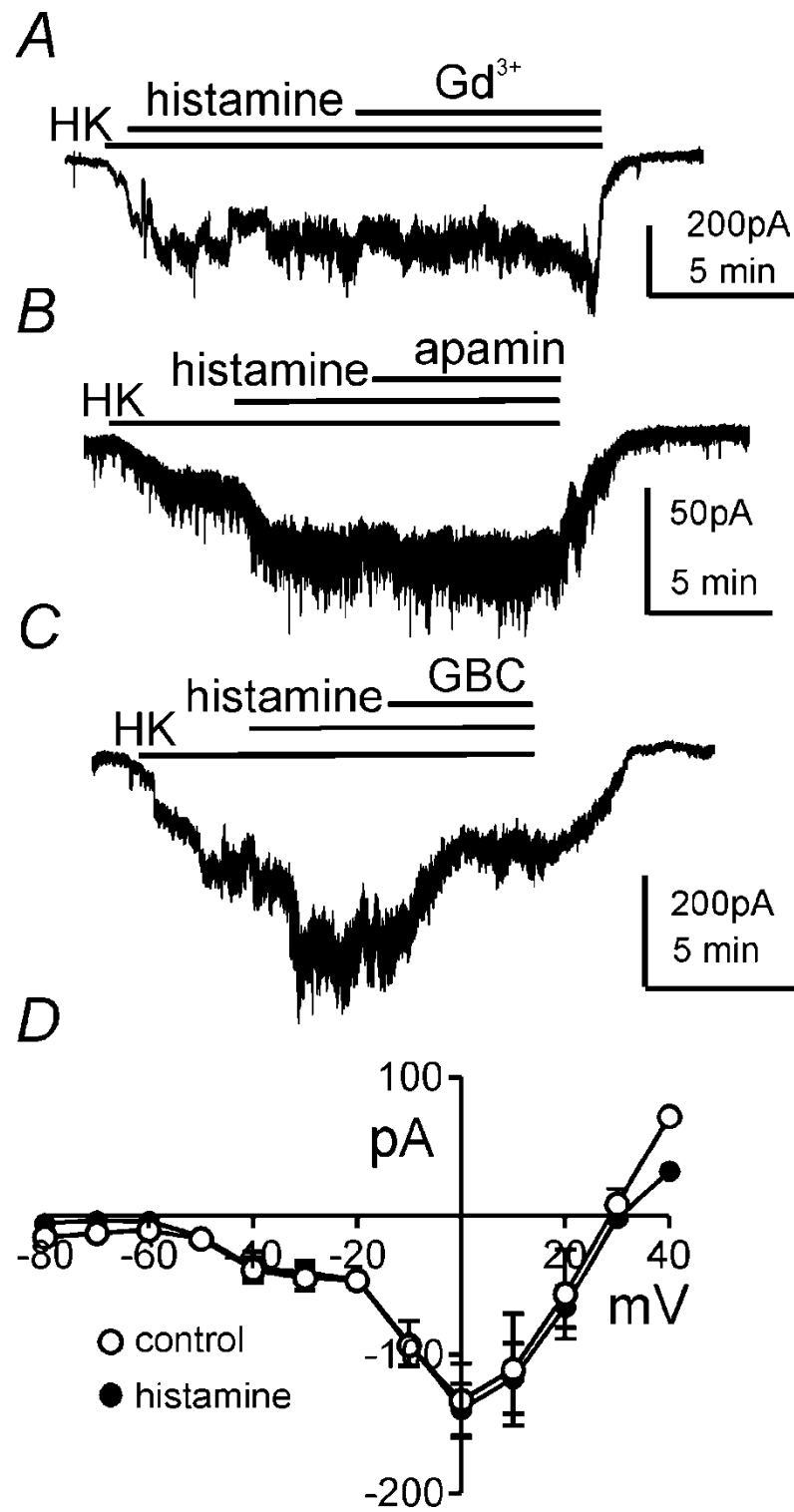


Figure 9: Histamine activated K_{ATP} currents in murine colonic SMC

(A) In order to examine the effects of histamine on K^+ currents in murine colonic SMC, perforated-patch clamp experiments were performed. At a holding potential of -80mV, CaPSS was replaced with high K^+ solution (HK; 140mM K^+ , externally). Exposure to HK solution at -80mV activated inward currents. Application of histamine (10 μ M) activated further inward currents which were not inhibited by the NSCC blocker, Gd^{3+} (10 μ M). (B) Addition of the SK blocker apamin (300nM), did not affect histamine- activated inward currents. (C) However the K_{ATP} channel blocker glibenclamide (GBC, 10 μ M) reduced histamine-activated inward currents. (D) Current-voltage relationship obtained under control conditions (○) (CaPSS) and in the presence of histamine (10 μ M) (●). Histamine had no effect on L-type Ca^{2+} currents (n=4).

5.1.6. Discussion

In IBD, alterations in colonic excitability have been frequently attributed to dysfunction of the enteric and/or central nervous system (Vermillion *et al.*, 1993; Galeazzi *et al.*, 2000; Vrees *et al.*, 2002). In human IBD, marked mast cell accumulation has been reported and this suggests that local paracrine responses may contribute to motility dysfunction in these diseases (Iba *et al.*, 2003). Nolte *et al.* described how mast cell numbers dramatically increase in patients with UC as well as their cellular contents including TNF- α , IL-16, substance P and histamine (Lilja *et al.*, 2000; Middel *et al.*, 2001; Stoyanova & Gulubova, 2002; Rijnierse *et al.*, 2007). In human colitis, mast cell infiltration progresses transmurally to the smooth muscle layers of the colon, thus mast cell mediators may have direct effects on smooth muscle excitability. Controversy surrounds the involvement of mast cells and histamine in animal models of colitis. For example in mast cell deficient *W/W^v* mice, DSS- and TNBS- induced colitis were not affected suggesting that mast cells are not involved in the inflammatory response in these animal models (Chin & Barrett, 1994; Minocha *et al.*, 1995). However a study performed in mast-cell deficient *Ws/Ws* rats found that development of colitis by DSS treatment was significantly attenuated. This study also revealed a positive correlation between development of colitis and mucosal histamine levels (Araki *et al.*, 2000). Furthermore in *HDC^{-/-}* KO mice, the severity of colitis symptoms induced by DSS were significantly reduced (Bene *et al.*, 2004). In the present study, mast cells were located in the circular muscle layer of monkey colon. In untreated/ control mice there were minimal mast cells present in the

smooth muscle layers (data not shown). However, in DSS-treated mice, there were areas within the colonic smooth muscle with substantial accumulation of mast cells. These findings suggest that histamine released from these mast cells located within the muscle layers may act directly on smooth muscle.

In the human GI tract it has been reported that H1, H2 and H4 receptors are present though little is known about the functional role of each H receptor subtype in the colon (Sanders *et al.*, 2006). Also, no reports have examined if the expression of H receptors in monkey and mouse colon are similar to that in humans therefore justifying the extrapolation data from these models to human GI physiology. Therefore, we examined the expression of H receptors in murine and monkey colon using molecular studies and found there were different expression patterns. In monkey colonic tissue, H1, H2 and H4 receptors were detected at similar expression levels whereas only the H2 receptor was found to be expressed in murine colonic tissue.

Histamine can have diverse effects in different tissues due to differential expression of specific H receptors and activation of distinct intracellular pathways (Boer *et al.*, 2008). H1 receptors are coupled to $G_{q/11}$ proteins which activates PLC and the PIP_2 signaling pathway (Bakker *et al.*, 2001). They are also linked to $G_{i/o}$ proteins which results in decreased production of cAMP (Wang *et al.*, 2000a). In contrast, H2 receptors are positively coupled to adenylate cyclase via G_s which is a potent stimulant of cAMP production and results in activation of PKA (Haas *et al.*, 2008). H4 receptors are coupled to pertussis-sensitive $G_{i/o}$ proteins that

inhibit adenylate cyclase activity and therefore decrease cAMP production (Zampeli & Tiligada, 2009). Since there was different expression of these H receptors in monkey versus murine colonic tissue, we hypothesized that histamine would have different effects on colonic excitability by acting through different signaling pathways.

Release of histamine during inflammation can alter intestinal motility (Bennett & Whitney, 1966; Bolton *et al.*, 1981). The acute application of histamine induces depolarization in guinea pig ileum (Leurs *et al.*, 1991). In the present study, different electrical and contractile responses to histamine were observed in mouse and monkey colonic tissue. In murine colon, histamine caused a transient decrease in contractile amplitude whereas in monkey colon it caused a potent contraction. Furthermore, H1 and H4 agonists increased monkey colonic contractility whereas the H2 agonist had the opposite effect.

Since changes in RMP are correlated with changes in colonic contractility, we also examined if histamine and H receptor agonists would affect colonic RMP. In murine colon, histamine induced transient hyperpolarization, an effect that was blocked by pretreatment with the K_{ATP} channel inhibitor glibenclamide. These data suggest that histamine may act through H2 receptor- G_s -cAMP production and finally activation of K_{ATP} channels by PKA phosphorylation. In contrast, histamine induced depolarization in monkey colonic tissue. H1 and H4 receptor agonists caused depolarization whereas H2 agonist induced hyperpolarization in monkey colonic tissue. Since there was no significant difference in expression

levels of H1, H2 and H4 receptors in monkey colonic tissue it is presumed that the depolarization caused by H1 and H4 receptor activation by histamine dominates the H2 induced hyperpolarization.

In order to understand the different responses to contractility and membrane excitability, we tested histamine effects on ion channel activity. It has previously been reported that H1 receptor activation can result in activation of NSCC (Wang & Kotlikoff, 2000a). In the present study, cell-attached patch clamp experiments revealed that histamine increased the open probability of 5pS channel in monkey suggesting this conductance may be activated through $G_{q/11}$ (H1 receptor) and/or $G_{i/o}$ (H4 receptor)-related signaling pathway(s). In murine colonic smooth muscle, histamine caused transient hyperpolarization and relaxation and pretreatment with the K_{ATP} blocker glibenclamide prevented histamine-induced hyperpolarization. Perforated patch clamp experiments revealed that histamine activated K_{ATP} -sensitive currents thus suggesting that histamine can stimulate the H2/ G_s /cAMP pathway resulting in activation of K_{ATP} channels through increases in PKA.

In conclusion, our data demonstrate that the expression of H receptors and responses to histamine in relation to colonic contractility and membrane potential are different between mouse and monkey. These data strongly support that monkey colon is an ideal model to predict the effects of the inflammatory mediator histamine on colonic motility in humans, since H receptor distribution in monkey colon is identical to that reported in human.

5.2. Effect of DSS-induced colitis on RMP and contractility in murine colonic tissue

5.2.1. Summary

Inflammatory bowel disease (IBD) can lead to major alterations in colonic contractility. Numerous studies have revealed that these changes may be attributed to disturbances in smooth muscle contractile mechanisms such as Ca^{2+} sensitization and also ion channel expression and activity. The aim of this study was to examine if inflammation can alter colonic excitability by examining resting membrane potential (RMP) and contractility. The electro-mechanical responses to carbachol in murine colon were examined by performing isometric force measurements and conventional microelectrode recordings. Spontaneous contractility as well as CCh-induced depolarization and contractions were significantly reduced in inflamed colonic smooth muscle. Furthermore, RMP was significantly more negative in DSS-treated colons. This project requires quantitative analysis of TRP channel transcripts in inflamed colon compared with control to confirm functional role of non-selective cation channels (NSCC) in inflammatory conditions that effect colonic excitability.

5.2.2. Background and Aims

Various motility disorders highlight the important role of smooth muscle in maintaining normal colonic contractility. Several animal models of colitis have reported decreased colonic contractility in response to agonists (Myers *et al.*, 1997a; Grossi *et al.*, 1993; Hosseini *et al.*, 1999; Shi & Sarna, 2000; Kinoshita *et al.*, 2003; Natale *et al.*, 2003; Khan *et al.*, 2005). The functional changes of smooth muscle could be attributed to intracellular modifications that directly impair its contractility including changes in the activity of ion channels, muscarinic receptors and Ca^{2+} sensitization mechanisms or extracellular factors such as inflammatory mediators that interact with SMC to modify tissue function (Kawabata *et al.*, 1999; Akbarali *et al.*, 2000; Coruzzi *et al.*, 2001; Liu *et al.*, 2001a; Jin *et al.*, 2004; Ozaki *et al.*, 2005; Ohama *et al.*, 2007; Al-Jarallah *et al.*, 2008; De Schepper *et al.*, 2008). Despite the well documented alterations in agonist-induced contraction of smooth muscle, few studies have examined the effects of colitis on RMP of SMC.

Maintenance of a 'normal' RMP is of critical importance in controlling the excitability of GI smooth muscle. The RMP in the GI tract is less negative than E_{K} , $\sim -50\text{mV}$ and suggests that there is an opposing influx of Na^+ and Ca^{2+} ions through NSCC which drive the RMP to less negative values. This less negative RMP means that only a small degree of depolarization is required to activate L-type Ca^{2+} channels resulting in contraction. The RMP is vital to maintain normal spontaneous contractility of the colon. A shift in the RMP to more negative

values/polarized values, would result in a more quiescent/less-excitabile colon. Therefore changes in ionic mechanisms that maintain a normal RMP may have deleterious effects on colonic motility.

In TRP, subfamily V, member 1 (TRPV1) KO mice treated with DSS to induce inflammation, membrane potential measurements revealed spontaneous atropine insensitive rhythmic action potentials in circular smooth muscle. The investigators suggested that TRPV1 may provide a protective mechanism for maintaining membrane stability during inflammation (Sibaev *et al.*, 2006). Analysis of the RMP in inflamed smooth muscle from the distal colon of formaldehyde treated rabbits revealed a less negative RMP which was suggested to be due to alterations in electrogenic pump mechanisms (Cohen *et al.*, 1986). Conversely in a rat model of colitis using *Trichinella spiralis*, RMP was more hyperpolarized in inflamed circular muscle cells (-57mV) compared with control (-46mV) and suggested to be associated with the decreased contractility seen in inflamed tissue. However the investigators stated that the mechanisms underlying the generation of the RMP are not completely understood and could only speculate underlying reasons for the change in RMP (Na^+ - K^+ pump or ICC) (Aulí & Fernández, 2007).

In this study we examined if DSS-induced colitis affected contractility and if these alterations could be correlated with changes in RMP of inflamed colonic smooth muscle.

5.2.3. Materials and methods

5.2.3.1. Inducing dextran sulphate sodium (DSS) colitis in C57BL/6 mice

C57BL/6 mice of either sex (6- to 8-weeks old, Charles River Laboratories, Wilmington, MA, USA) were administered 5% w/v DSS (MW = 36 000–50 000 Da, MP Biomedicals LLC, Solon, OH, USA) *ad libitum* in the drinking water for 7 days. Mice exhibited typical physical characteristics of DSS-colitis including significant weight loss and bloody stool (data not shown). Colons were utilized 1day post-DSS treatment. Mice were maintained and experiments were carried out in accordance with the National Institutes of Health Guide for the Care and Use of Laboratory Animals. All protocols were approved by the University of Nevada, Reno Institutional Animal Care and Use Committee.

5.2.3.2. Isometric Force Measurements

Standard organ bath techniques were employed to measure the changes in force generated by murine smooth muscle strips. One end of a smooth muscle strip was attached to a fixed mount and the opposite end to an isometric strain gauge (Fort 10, WPI, Sarasota, FL, USA) in oxygenated Krebs–Ringer bicarbonate solution (KRB, see section 5.2.3.4.) maintained at $37.5\pm 0.5^{\circ}\text{C}$. A resting force of 500 mg (murine colon) was applied to set the muscles at optimum length, and the muscles were allowed to equilibrate for 1-2 h with constant perfusion with KRB solution. Mechanical responses were recorded on a

computer running Axoscope (Axon instrument, Foster City, CA, USA) and measurements of the area under the curve (AUC) obtained. The AUC was determined as the integral values above the baseline of selected area for 5 min recordings (mN*min). The AUC for the tissues exposed to tested drugs were compared to the AUC for tissues under control conditions, during an equivalent period of time. Bathing solutions were exchanged by switching the perfusion to the drug-containing solution.

5.2.3.3. Intracellular Microelectrode Recordings

After removing the mucosa, strips of proximal colon (1 cm in length × 0.5 cm in width) were taken from the region 1–2 cm from the ileocecal sphincter and pinned to a Sylgard (Dow Corning Corp., Midland, MI, USA) elastomer-coated recording chamber with the mucosal side of the circular muscle facing upward. SMC were impaled with glass microelectrodes filled with 3M KCl and had electrical resistances of 80–100 MΩ. Transmembrane potentials were measured with a standard high input impedance amplifier (WPI Duo 773, Sarasota, FL, USA). Electrical signals were recorded by a PC-style computer running Axoscope data acquisition software (Axon Instruments, CA, USA) and analyzed by Clampfit (v9.02, Axon Instruments, CA, USA). All experiments were performed in the presence of wortmannin (10μM) to reduce movement and facilitate impalements of cells for extended periods of time.

5.2.3.4. Chemicals and solutions

For contractile and conventional microelectrode recordings, the strips were exposed to KRB with the following composition (mM): 118.5 NaCl, 4.5 KCl, 1.2 MgCl₂, 23.8 NaHCO₃, 1.2 KH₂PO₄, 11.0 dextrose and 2.4 CaCl₂. Tetrodotoxin (TTX) and carbachol (CCh) were obtained from Sigma Chemical Co (St Louis, MO, USA).

5.2.3.5. Statistical Analysis

Data are expressed as means \pm S.E.M. The Student's t-test was used where appropriate to evaluate differences in the data. *P*-values less than 0.05 were taken as statistically significant differences. *n* values refer to the number of recordings from muscle strips.

5.2.4. Results

5.2.4.1. *Clinical symptoms*

Day 1 post-DSS treatment (following 7 days of DSS administration (5%)), bloody stool were observed in cages. There was no mortality among mice treated with 5% DSS for 7 days. Average body weight decreased as treatment commenced. During dissection of colons from DSS-treated mice, bloody stool were observed in the majority of cases. Damage to mucosa, crypts and edema were also observed. Increase in the mRNA expression level of cytokine IL-6 was used as an indicator of inducement of an immune response in these treated mice (data not shown).

5.2.4.2 *RMP and electrical responses to CCh in inflamed colonic smooth muscle were different compared to controls*

As described previously in this thesis, the RMP plays a critical role in determining the excitability of smooth muscle. Therefore we examined if the RMP was changed in colonic smooth muscle from DSS-treated mice. Figure 1A is a representative trace illustrating the typical RMP and CCh (1 μ M) -induced depolarization in untreated murine colonic smooth muscle in the presence of TTX (1 μ M) to exclude neuronal influences. Following DSS treatment for 7 days, sharp electrode recordings revealed a significant change in RMP (Fig. 1A-C). In inflamed colonic smooth muscle, the RMP was -47 ± 3.8 mV compared with -

36±0.6mV in control muscle (Fig. 1C; DSS-treated, n=10; control, n=13, ** $P<0.01$). In addition, the CCh-induced depolarization was significantly decreased in DSS-treated colonic smooth muscle (Fig. 1A & B). In untreated colonic smooth muscle CCh application induced a 19.6±1.8mV depolarization whereas in inflamed tissue, CCh caused a 11.2±1.2mV depolarization (Fig. 1D; control, n=12; DSS-treated, n=10; ** $P<0.01$). These data suggest that smooth muscle mechanisms involved in regulating colonic excitability are disturbed following inflammation induced by treatment with DSS.

5.2.4.3 Contractile responses to CCh were decreased in inflamed colonic smooth muscle compared with controls

In isometric force measurements, spontaneous contractile amplitude and frequency were altered in inflamed colonic smooth muscle (Fig. 2A & B). The amplitude of contraction following application of CCh (1µM) in the presence of TTX (1µM) was significantly smaller in colonic smooth muscle from DSS treated mice compared with controls (Fig. 2C). The calculated AUC following application of CCh (1µM) was 40±6.1 mN*min in control compared with 23±3 mN*min in inflamed colonic smooth muscle (Fig. 2D, control n=5, DSS-treated n=6; * $P<0.05$). These results support findings in Figure 1 that inflammation incurred following DSS-treatment alters the functioning of smooth muscle contractile related mechanisms.

5.2.5. Figures and figure legends

Figure 1: RMP and CCh-induced depolarization were significantly changed in inflamed colonic smooth muscle

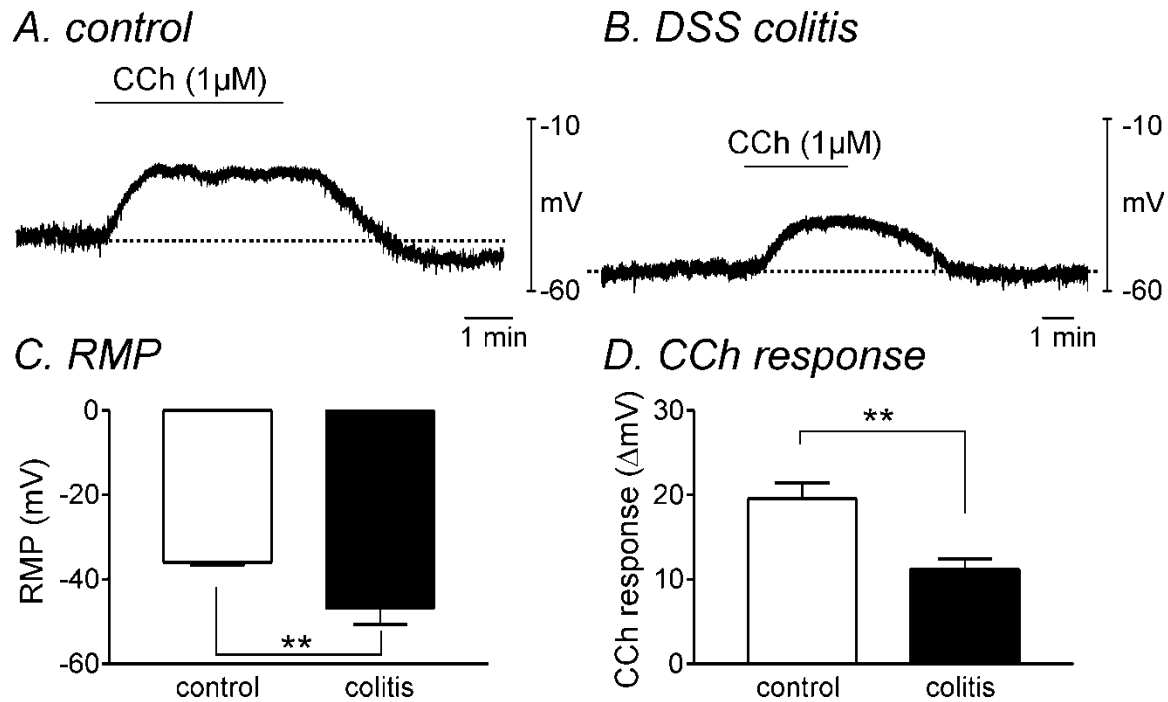


Figure 1: RMP and CCh-induced depolarization were significantly changed in inflamed colonic smooth muscle

(A and B) Representative traces of sharp electrode recordings performed in (A) control and (B) an inflamed colon from a DSS-treated mouse (in the presence of TTX (1 μ M) to block neuronal influences). (C) Summary graph illustrating a significantly more negative RMP in DSS-treated colonic smooth muscle compared with control (control, n=13; DSS-treated, n=10, * P <0.01). (D) Summary graph illustrating a suppressed CCh-induced depolarization in inflamed colonic smooth muscle compared with control (control, n=12; DSS-treated, n=10, * P <0.01).

Figure 2: Spontaneous and CCh-induced contractility were suppressed in inflamed colonic smooth muscle

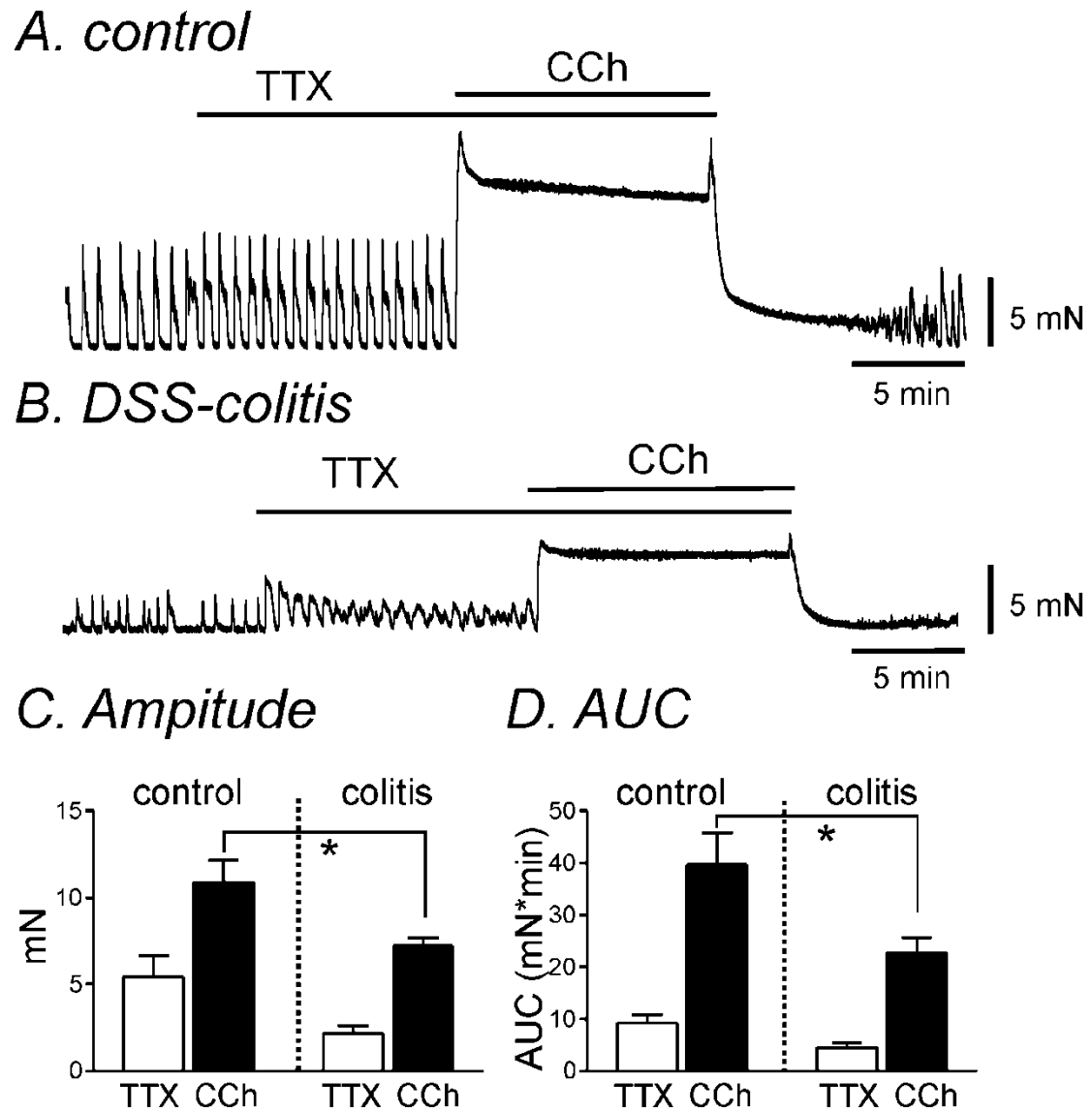


Figure 2: Spontaneous and CCh-induced contractility were suppressed in inflamed colonic smooth muscle

(A) Representative mechanical trace showing that in the presence of TTX (1 μ M), exposure to CCh (1 μ M) resulted in a sustained contraction in untreated colonic smooth muscle. (B) Representative trace illustrating that spontaneous and CCh-induced contractions were significantly reduced in inflamed colonic tissue from DSS-treated mice compared with control. (C) Summarized data of peak amplitude of contractions by CCh (1 μ M) in control (n=5) and in inflamed (n=6) colons in the presence of TTX. (D) Summarized data of AUC before and after application of CCh (1 μ M) in control and inflamed colons from DSS-treated mice in the presence of TTX. * denotes $P < 0.05$.

5.2.6. Discussion

In the GI tract, the RMP plays an essential role in governing the excitability of smooth muscle. Studies of IBD have highlighted how normal excitability and motility are highly dependent on the integrity of smooth muscle. In intestinal inflammation, both hypo- and hyper-contractility have been observed and are thought to reflect changes in smooth muscle and/or the enteric nervous system (Vermillion *et al.*, 1993; Vrees *et al.*, 2002). However the majority of chemically induced experimental models of human IBD including DSS-, TNBS- and acetic acid-induced colitis have found a decrease in contractile activity of smooth muscle in the inflamed colon and/or intestine in response to carbachol or acetylcholine (Grossi *et al.*, 1993; Myers *et al.*, 1997a; Shi & Sarna., 2000; Khan *et al.*, 2005; Kinoshita *et al.*, 2006; Al-Jarallah *et al.*, 2008). These findings suggest that when fundamental smooth muscle mechanisms have been altered in response to carbachol or acetylcholine, motility dysfunction can result.

Several studies have reported changes in RMP in different inflammatory models. For example, in a rat model of colitis using *Trichinella spiralis*, RMP was more hyperpolarized in inflamed circular muscle cells compared with control. These changes in RMP in SMC were suggested to be linked with the decreased contractility seen in the inflamed tissue (Aulí & Fernández, 2007). In TRPV1 KO mice treated with DSS to induce inflammation, membrane potential measurements revealed spontaneous atropine insensitive rhythmic action potentials in circular smooth muscle (Sibaev *et al.*, 2006). In another study,

analysis of the RMP in inflamed smooth muscle from the distal colon of formaldehyde treated rabbits revealed a decreased (more depolarized) RMP which was suggested to be due to alterations in electrogenic pump mechanisms (Cohen *et al.*, 1986).

In the present study, RMP was significantly more negative in DSS-treated colonic smooth muscle compared with controls (Fig. 1). These data suggest that mechanisms involved in regulating RMP may be altered in this inflammatory model. Since we reported in Chapter 2 that b_{MSCC} contributed to the RMP in colonic SMC, we hypothesize that TRP channel expression may be altered by inflammation. In future studies we will examine if specific TRP channels are down-regulated in colonic SMC. A novel approach will be utilized to obtain solely SMC by performing cell sorting of freshly dispersed colonic cells obtained from smooth muscle myosin heavy chain, Cre recombinase, enhanced fluorescent protein (smMHC/Cre/eGFP) transgenic mice. Therefore we will be able to identify if changes seen in smooth muscle excitability can be linked with changes in smooth muscle TRP channel expression. In addition we will treat monkey colonic smooth muscle strips with the major proinflammatory cytokine TNF- α and examine if there are any changes in colonic excitability as well as TRP channel expression in the near future.

In Figure 2, there were diminished responses in contractility to inhibition of neuronal influences by tetrodotoxin as well as CCh-evoked contractions in inflamed colons. In Chapter 4, section A, analysis of smooth muscle layers in

inflamed colons from DSS-treated mice revealed abundant mast cells in certain regions (Fig. 1B). RT-PCR analysis revealed that only the H₂ receptor was expressed in murine colonic tissue. Binding of histamine to this receptor caused hyperpolarization and transient decrease in contractile amplitude through activation K_{ATP} channels (following activation of the H₂/G_s pathway). Therefore release of histamine from mast cells in inflamed colons may activate the H₂ receptor pathway which may contribute to decreased contractile amplitude and a shift in RMP to more negative potentials seen in inflamed colons from DSS-treated mice. Future studies will examine if application of the K_{ATP} blocker, glibenclamide, can restore/ increase excitability in inflamed colons from DSS-treated mice.

Chapter 6

Summary, Discussion and Future Work

6.1. Smooth muscle excitability in colonic SMC

Normal GI function is dependent on a multitude of mechanisms all working in synergy. Dysfunction in any one of these mechanisms can lead to alterations in secretion, sensing and/or motility. The colon is highly innervated by neurons which coordinate the effector systems (including muscle, secretory glands and blood vessels) of the GI tract. In addition, specialized pacemaker cells called ICC are also essential for the rhythmical spontaneous contractions in the muscle layer that are required for propulsion of chyme from the oral to anal end of the GI tract (Wood, 2007). However, regardless of the signals that are directed to smooth muscle from these extrinsic systems, if normal smooth muscle function is disturbed, these input signals will not be translated into the desired responses. Smooth muscle excitability is an important electrical mechanism since it plays a major role in determining the normal contractile patterns and responses of the GI musculature. Hence the mechanisms that modulate smooth muscle excitability are of unequivocal importance since they ultimately determine contractile behavior.

It has been well established that K^+ channels play an important role in regulating colonic excitability through modulating the RMP of SMC. Cells tend to be electrically quiescent when the RMP lies close to E_K . However there are

regions in the GI tract where RMP is substantially more positive than E_K . Surprisingly, the precise mechanisms underlying generation of these more depolarized resting potentials are not understood. Therefore in experiments in Chapter 2, we addressed the hypothesis that influx of Na^+ and Ca^{2+} ions through constitutively active NSCC are responsible for the RMP of the colonic SMC being significantly more positive than E_K . This hypothesis has not been previously addressed and therefore we characterized potential ionic mechanisms that may affect the overall excitability of colonic SMC. Our data revealed that in human and monkey SMC, basally active NSCC (bI_{NSCC}) were recorded under the voltage-clamp configuration and reversed at 0mV when $E_{Cl} = -40\text{mV}$. These data confirmed that these currents were not due to Cl^- conductance but NSCC. When extracellular Na^+ and Ca^{2+} were replaced with equimolar TEA and Mn^{2+} respectively, bI_{NSCC} were inhibited. External application of the trivalent cations, La^{3+} or Gd^{3+} , inhibited bI_{NSCC} . Furthermore in current-clamp experiments, replacement of extracellular Na^+ with NMDG^+ caused hyperpolarization in colonic SMC. These data suggest that continuous influx of Na^+ and Ca^{2+} ions through these channels under resting conditions may be responsible for this shift in RMP to positive values. Molecular analysis for potential candidates for bI_{NSCC} revealed that TRPC7, V1 and V2 were expressed in human SMC whereas TRPC4 and 5 were found in monkey SMC.

The important contribution of bI_{NSCC} to the RMP at the tissue level using pharmacology (e.g. La^{3+} , Gd^{3+}) will be difficult due to penetration problem of such

drugs through the smooth muscle layers. Use of KO mice to determine the contribution of specific TRP channels to the RMP of colonic smooth muscle would be an ideal next step. However this depends on whether the same TRP channels responsible for $b_{I_{NSCC}}$ in murine colon SMC are similar to those in human and/ or monkey. Development of specific agonists and antagonists for each TRP channel will be crucial to understand the physiological role of $b_{I_{NSCC}}$ in human colonic smooth muscle.

6.2. PLC regulation

Since it is well known that many TRP channels are modulated by PLC (Nilius *et al.*, 2007; Abramowitz J & Birnbaumer, 2009), we originally aimed to examine the involvement of PLC in $b_{I_{NSCC}}$ activity using a well-known PLC activator, *m*-3M3FBS. However our preliminary studies at the smooth muscle level revealed unexpected results. Typically, activation of the PLC mediated pathway should result in increased contraction as seen with application of excitatory neurotransmitters such as acetylcholine that activate PLC through stimulation of muscarinic receptors linked to $G_{q/11}$ proteins. However we found a decrease in spontaneous contractile amplitude following application of this drug. Furthermore, its inactive analog, *o*-3M3FBS, also caused a similar decrease in contractility leading us to believe that these drugs were having non-specific effects. Since many studies have reported using these drugs to examine PLC-related mechanisms, we examined the potential non-specific mode(s) of action of

these compounds on ion channel activity and $[Ca^{2+}]_i$. Understanding the mechanisms of non-specificity of these drugs will be beneficial for the interpretation of data in future publications.

6.2.1. Drug non-specificity

In order to understand the cellular mechanisms that underlie the huge array of physiological processes, specific experimental tools are essential. However over the years it is becoming increasingly evident that many of these tools are not specific and can affect other unrelated pathways/ activities therefore obscuring interpretation of their true effects. Clarification of the non-specific effects of these drugs is crucial to highlight the limitations of their use for researchers.

For example it has emerged that the PLC inhibitor, U73122 causes non-specific effects at concentrations required to inhibit PLC. The most significant non-specific effect that has been identified is its ability to cause Ca^{2+} release from intracellular stores. Therefore in experiments where Ca^{2+} release is not seen following receptor activation after pretreatment with U73122, this effect may be wrongly interpreted as a requirement for PLC (De Moel *et al.*, 1995). In addition, this compound can also inhibit many Ca^{2+} entry pathways including capacitative Ca^{2+} entry and L-type Ca^{2+} channels (Berven & Barritt, 1995; Macrez-Lepetre *et al.*, 1996; Wang, 1996). Therefore despite the fact that U73122 may inhibit PLC, its multiple actions on Ca^{2+} stores and entry pathways

would make it extremely difficult to correctly interpret data obtained using this drug (Taylor & Broad, 1998).

Knowledge of the non-specific actions of drugs like U-73122 is essential. Depending on the degree of non-specificity, the researcher may need to use alternative techniques to confirm suspected findings.

6.2.2. *m*-3M3FBS and *o*-3M3FBS

As described earlier, we found unexpected effects of *m*-3M3FBS and *o*-3M3FBS on colonic smooth muscle contractility. In order to explain these effects we performed patch-clamp and Ca^{2+} imaging studies on colonic SMC. Patch clamp studies revealed that delayed rectifier K^+ channels as well as L-type Ca^{2+} currents were reversibly inhibited by *m*-3M3FBS and *o*-3M3FBS. In contrast, $[\text{Ca}^{2+}]_i$ was also increased by *m*-3M3FBS and *o*-3M3FBS whereas contractility decreased which was a paradoxical response to these drugs. We speculated that increases in $[\text{Ca}^{2+}]_i$, possibly through release from IP_3 stores, are not sufficient to cause contraction since L-type Ca^{2+} channels are inhibited simultaneously by these compounds i.e. suggesting that Ca^{2+} influx through L-type channels is the major source of Ca^{2+} for contractions. From these findings we decided not to examine PLC-regulation of bI_{NSCC} using these drugs since their multiple non-specific effects would make it very difficult to interpret the true PLC-contribution to bI_{NSCC} .

For future experiments we will adopt a new approach by performing flash photolysis of caged compounds to examine intracellular regulation of bI_{NSCC} including downstream mediators of PLC activation, DAG and IP_3 and also $[Ca^{2+}]_i$ instead of using pharmacological tools. This powerful tool has many advantages over traditional application of exogenous substances/ drugs. Since the caged compounds are inactive after dialysis or permeation, only a pulse of intense light can activate the targeted substances (caged IP_3 , PKC, DAG etc) (Giovannardi *et al.*, 1998). These experiments will exclude any drug non-specificity on ion channel regulation and signaling pathways.

6.3. Rho-kinase regulation of colonic excitability and ion channel activity

Since Rho-kinase has been implicated in, not only Ca^{2+} sensitization but other cellular processes such as ion channel activity, we examined the contribution of this kinase to colonic excitability as well as ion channel activity in chapter 4. Nerve-evoked contractions were significantly decreased by the Rho-kinase inhibitors, Y-27632 and H-1152. In addition spontaneous and CCh-induced contractions were significantly decreased independent of neuronal influences suggesting Y-27632 acts directly on smooth muscle. Interestingly CCh-induced depolarization was significantly reduced by Rho-kinase inhibitors. Since suppression in Ca^{2+} sensitization could not account for this effect on membrane potential, we considered that Rho-kinase may modulate specific ion channels involved in CCh-induced depolarization. In the majority of colonic SMC,

Y-27632 did not affect L-type Ca^{2+} currents recorded under voltage-clamp conditions. However in a few SMC, H-1152 inhibited L-type Ca^{2+} currents. The discrepancy in these findings is not clear. Potentially, damage to Rho-kinase and/or associated pathways during enzymatic dispersion may affect their potential contribution in L-type Ca^{2+} channel regulation. An interesting observation in this chapter was that GTP γ S-activated currents were inhibited by Y-27632. Dialysis with GTP γ S stimulates CCh-like NSCC through activation of multiple G-proteins. These NSCC are involved in the initial CCh-induced depolarization as influx of Na^+ and Ca^{2+} ions through these channels causes a shift in the membrane potential to values where VDCC are then activated (Helliwell & Large, 1997; Dresviannikov *et al.*, 2006). Overall, the reduction in nerve-stimulated contractility by electrical field stimulation and CCh-induced depolarization by Rho-Kinase inhibitors could be through Ca^{2+} -sensitization as well as regulation of receptor-activated NSCC. The application of constitutively activated Rho-kinase under the inside-out configuration could confirm the regulation of NSCC channels by Rho-kinase in the future. Furthermore, future studies could examine possible phosphorylation sites where Rho-kinase may interact with specific TRP channels using site-directed mutagenesis. We will also examine direct PIP_2 regulation of TRP channels expressed in mammalian cells by deletion of specific regions considered to be potential binding sites.

6.4. Histamine effects on monkey and murine colonic excitability

Chapter 5 of this dissertation focused on the role of inflammation on colonic excitability. In section 1, we examined the effect of histamine since it is a major mediator in many inflammatory and allergic reactions and affects many critical cellular functions (Dy & Schneider, 2004). Review of the literature revealed very few studies that examined the effects of histamine on colonic motility. Since many inflammatory diseases of the colon exhibit dysmotility, we thought it was crucial to examine the effect of this mediator on monkey and murine colonic excitability. Examination of H receptors revealed H1, H2 and H4 transcripts in monkey colonic tissue whereas only the H2 transcript was detected in murine colonic tissue. Therefore we hypothesized that histamine may have different effects on colonic excitability in these two species.

In monkey colonic tissue, histamine caused significant depolarization and increased contractility. A similar effect was seen with application of either H1 or H4 receptor agonists. However the H2 receptor agonist caused hyperpolarization and decreased contractility. Single channel recordings revealed that the open probability of a 5pS channel in monkey colonic SMC was increased by histamine. Therefore this conductance may play an important role in histamine-induced depolarization and contraction seen in monkey colonic tissue. In contrast, in murine colonic tissue, histamine caused hyperpolarization and decreased contractility. This hyperpolarization was prevented by pretreatment with the K_{ATP} blocker, glibenclamide, suggesting activation of these channels through the H2/G_s/cAMP/PKA pathway by histamine. In patch clamp experiments, histamine

activated K_{ATP} currents as they were inhibited by glibenclamide. These studies revealed for the first time the different contractile responses to histamine in two different species. Furthermore, the similar expression of H receptors in monkey with those reported in human (Sanders *et al.*, 2006) suggests that monkey colon is an ideal model to examine effects of histamine. Use of histamine KO mice would be the next step in dissecting the roles of each H receptor to colonic excitability. However, unlike human and monkey colon, the murine colon does not express H1 and H4 receptors and therefore this approach would provide us with limited information.

6.5. DSS-induced colitis results in alterations in colonic excitability

Colonic dysmotility is often observed in inflammatory diseases such as ulcerative colitis and Crohn's disease. Since these changes could be attributed to alterations in colonic excitability, in chapter 5, section 2, we examined this important factor in DSS-induced colitis in mice. Intracellular recordings revealed that RMP was significantly more negative in inflamed colons compared with controls. This effect would render the colonic smooth muscle less excitable than control/untreated colons. Indeed, CCh-induced depolarization and contractile amplitudes were significantly decreased in DSS-treated colonic smooth muscle. In chapter 2, we described how mechanisms of colonic excitability, in particular those contributing to the RMP, are essential for determining the overall colonic motility. Since we have implicated specific TRP channels in regulating the RMP

in colonic SMC, we will examine if the expression of TRP channels is changed in the inflamed colon compared with control at the smooth muscle cellular level using smMHC/Cre/eGFP mice donated by Dr. Kotlikoff. A decreased expression of specific TRP channels at the cellular level would support the hypothesis that TRP channels contribute to the membrane potential and hence excitability of colonic smooth muscle. Their down-regulation may underlie the more negative RMP and decreased excitability seen in inflamed colonic smooth muscle.

6.6. Overall conclusion

The studies in this dissertation addressed for the first time 1) the contribution of non-selective cation channels on resting membrane potential, 2) potential molecular candidates for non-selective cation channels and 3) contribution of non-selective cation channels to colonic excitability in physiological and inflammatory conditions.

References

- Abramowitz J & Birnbaumer L (2009). Physiology and pathophysiology of canonical transient receptor potential channels. *FASEB* 23, 297-328.
- Akbarali HI, Pothoulakis C & Castagliuolo I (2000). Altered Ion Channel Activity in Murine Colonic Smooth Muscle myocytes in an Experimental Colitis Model. *Biochem Biophys Res Commun* 275, 637-642.
- Akdis CA & Simons FE (2006). Histamine receptors are hot in immunopharmacology. *Eur J Pharmacol* 533, 69-76.
- Akiho H, Deng Y, Blennerhassett P, Kanbayashi H & Collins SM (2005). Mechanisms underlying the maintenance of muscle hypercontractility in a model of postinfective gut dysfunction. *Gastroenterol* 129, 131-141.
- Albert AP, Piper AS & Large WA (2005). Role of Phospholipase D and diacylglycerol in activating constitutive TRPC-like cation channels in rabbit ear artery myocytes. *J Physiol* 566, 769-780.
- Albert AP, Piper AS & Large WA (2003). Properties of a constitutively active Ca²⁺-permeable non-selective cation channel in rabbit ear artery myocytes. *J Physiol* 549, 143-156.
- Albert AP, Pucovsky V, Prestwich SA & Large WA (2006). TRPC3 properties of a native constitutively active Ca²⁺-permeable cation channel in rabbit ear artery myocytes. *J Physiol* 571.2, 361-369.
- Albert AP, Saleh SN & Large WA (2008). Inhibition of native TRPC6 channel activity by phosphatidylinositol 4,5-bisphosphate in mesenteric artery myocytes. *J Physiol* 586, 3087-3095.
- Alberti E, Mikkelsen HB, Larsen Jo & Jimenez M (2005). Motility patterns and distribution of interstitial cells of Cajal and nitrergic neurons in the proximal, mid- and distal-colon of the rat. *Neurogastroenterol Motil* 17: 133–147.
- Alex P, Zachos NC, Nguyen T, Gonzales L, Chen T-E, Conklin LS, Centola M & Li X (2009). Distinct Cytokine Patterns Identified from Multiplex Profiles of Murine DSS and TNBS-induced Colitis. *Inflamm Bowel Dis* 15, 341-352.
- Al-Jarallah A, Khan I & Oriowo MA (2008). Role of Ca²⁺-sensitization in attenuated carbachol-induced contraction of the colon in a rat model of colitis. *Eur J Pharm* 579, 365-373.
- Amberg GC, Koh SD, Hatton WJ, Murray KJ, Monaghan K, Horowitz B & Sanders KM (2002). Contribution of Kv4 channels toward the A-type potassium current in murine colonic myocytes. *J Physiol* 544.2, 403-415.
- Amberg GC, Koh SD, Imaizumi Y, Ohya S & Sanders KM (2003). A-type potassium currents in smooth muscle. *Am J Physiol* 284, C583-C595.

- Amberg, GC, Koh SD, Perrino BA, Hatton WJ & Sanders KM (2001). Regulation of A-type potassium channels in murine colonic myocytes by phosphatase activity. *Am J Physiol Cell Physiol* 281, C2020-2028.
- Andersson DA, Chase HW & Bevan S (2004). TRPM8 activation by menthol, icilin and cold is differentially modulated by intracellular pH. *J Neuroscience* 24, 5364-5369.
- Araki Y, Andoh A, Fujiyama Y & Bamba T (2000). Development of dextran sulphate sodium-induced experimental colitis is suppressed in genetically mast cell-deficient Ws/Ws rats. *Clin Exp Immunol* 119, 264-269.
- Arrang JM, Garbarg M & Schwartz JC (1983). Auto-inhibition of brain histamine release mediated by a novel class (H3) of histamine receptor. *Nature* 302, 832-837.
- Ashcroft FM & Kakei M (1989). ATP-sensitive K⁺ channels in rat pancreatic β -cell: modulation by ATP and Mg²⁺ ions. *J Physiol* 416, 349-367.
- Aulí M & Fernández E (2007). Time course of neural and contractile disturbances in a rat model of colitis induced by *Trinchinella spiralis*. *Life Sciences* 81, 1117-1129.
- Bae YS, Lee TG, Park JC, Hur JH, Kim Y, Heo K, Kwak JY, Suh PG & Ryu SH (2003). Identification of a Compound That Directly Stimulates Phospholipase C Activity. *Mol Pharmacol* 63, 1043-1050.
- Bae YM, Park MK, Lee SH, Ho WK & Ye E (1999). Contribution of Ca²⁺-activated K⁺ channels and non-selective cation channels to membrane potential of pulmonary arterial smooth muscle cells of the rabbit. *J Physiol* 514, 747-758.
- Bakker RA, Schoonus SBJ, Smit MJ, Timmerman H & Leurs R (2001). Histamine H1-Receptor Activation of Nuclear Factor- κ B: Roles for G $\beta\gamma$ - and G $\alpha_q/11$ -Subunits in Constitutive and Agonist-Mediated Signaling. *Mol Pharmacol* 60, 1133-1142.
- Barnard R, Barnard A, Salmon G, Liu W & Sreckovic S (2008). Histamine-induced actin polymerization in human eosinophils: an imaging approach for histamine H4 receptor. *Cytometry A* 73, 299-304.
- Baumgart DC (2009). The diagnosis and treatment of Crohn's disease and ulcerative colitis. *Dtsch Arztebl Int* 106(8), 123-133.
- Bayguinov O, Hagen B, Kenyon J & Sanders KM (2001). Coupling strength between localized Ca²⁺ transients and K⁺ channels is regulated by protein kinase C. *Am J Physiol Cell Physiol* 281, C1512- C1523.
- Beck B, Zholos A, Sydorenko V, Roudbaraki M, Lehen'kyi V, Bordat P, Prevarskaya N & Skryma R (2006). TRPC7 is a receptor-operated DAG-activated channel in human keratinocytes. *J Invest Dermatol* 126, 1982-1993.
- Bene L, Sápi Z, Bajtai A, Buzás E, Szentmihályi A, Arató A, Tulassay Z & Falus A (2004). Partial Protection against Dextran Sodium Sulphate Induced Colitis in Histamine-Deficient, Histidine Decarboxylase Knockout Mice. *JPGN* 39, 171-176.

Benham CD, Bolton TB & Lang RJ (1985). Acetylcholine activates an inward current in single mammalian smooth muscle cells. *Nature* 316, 345-347.

Bennett A & Whitney B (1966). A pharmacological study of the motility of the human gastrointestinal tract. *Gut* 7, 307-316.

Berg DJ, Davidson N, Kühn R, Müller W, Menon S, Holland G, Thompson-Snipes L, Leach MW & Rennick D (1996). Enterocolitis and colon cancer in interleukin-10-deficient mice are associated with aberrant cytokine production and CD4⁺ Th-1 like responses. *J Clin Invest* 98, 1010-1020.

Berven LA & Barritt GJ (1995). Evidence obtained using single hepatocytes for inhibition by the phospholipase C inhibitor U73122 of store-operated Ca²⁺ inflow. *Biochem Pharmacol* 49, 1373-1379.

Bianco SD, Peng JB, Takanaga H, Suzuki Y, Crescenzi A, Kos CH, Zhuang L, Freeman MR, Gouveia CH, Wu J, Luo H, Mauro T, Brown EM & Hediger MA (2007). Marked disturbance of calcium homeostasis in mice with targeted disruption of the Trpv6 calcium channel gene. *J Bone Miner Res* 22, 274-285.

Birnbaumer L (2009). The TRPC class of ion channels: a critical review of their roles in slow, sustained increases in intracellular (Ca²⁺) concentrations. *Annu Rev Pharmacol Toxicol* 49, 395-426.

Blair NT, Kaczmarek & Clapham DE (2009). Intracellular calcium strongly potentiates agonist-activated TRPC5 channels. *J Gen Physiol* 133, 525-546.

Blandizzi C, Tognetti M & Colucci R (2001). H3 receptor-mediated inhibition of intestinal acetylcholine release: pharmacological characterization of signal transduction. *Naunyn Schmiedebergs Arch Pharmacol* 363, 193-202.

Blennerhassett MG, Vignjevic P, Vermillion DL & Collins SM (1992). Inflammation causes hyperplasia and hypertrophy in smooth muscle of rat small intestine. *Am J Physiol* 262, G1041-1046.

Boer K, Helinger E, Helinger A, Pocza P, Pos Z, Demeter P, Baranyai Z, Dede K, Darvas Z & Falus A (2008). Decreased expression of histamine H1 and H4 receptors suggests disturbance of local regulation in human colorectal tumors by histamine. *Eur J Cell Biol* 87, 227-236.

Boirivant M, Fuss IJ, Chu A & Strober W (1998). Oxazolone colitis: A murine model of T helper cell type 2 colitis treatable with antibodies to interleukin 4. *J Exp Med* 188, 1929-1939.

Boismenu R & Chen Y (2000). Insights from mouse models of colitis. *J Leukocyte Biol* 67, 267- 278.

Boissé L, Chisholm SP, Lukewich MK & Lomax AE (2009). Clinical and experimental evidence of sympathetic neural dysfunction during inflammatory bowel disease. *Clin Exp Pharm Physiol* [Epub ahead of print].

- Bolton T (2006). Calcium events in smooth muscles and their interstitial cells; physiological roles of sparks. *J Physiol* 570, 5-11.
- Bolton TB, Clark JP, Kitamura & Lang RJ (1981). Evidence that histamine and carbachol may open the same ion channels in longitudinal smooth muscle of guinea-pig ileum. *J Physiol* 320, 363-379.
- Borjesson L, Nordgren S & Delbro DS (1999). K⁺-induced neurogenic relaxation of rat distal colon. *J Pharmal Exp Ther* 291, 717-724.
- Bosma GC, Custer RP & Bosma MJ (1983). A severe combined immunodeficiency mutation in the mouse. *Nature* 300, 527-530.
- Boulay G (2002). Ca²⁺-calmodulin regulates receptor-operated Ca²⁺ entry activity of TRPC6 in HEK-293 cells. *Cell Calcium* 320, 201-207.
- Brading AF & Sneddon P (1980). Evidence for multiple sources of calcium for activation of the contractile mechanism of guinea-pig taenia coli on stimulation with carbachol. *Br J Pharmacol* 70, 229-240.
- Buelens C, Verhasselt V, De Groote D, Thielemans K, Goldman M & Willems F (1997). Human dendritic cell responses to lipopolysaccharide and CD40 ligation are differentially regulated by interleukin-10. *Eur J Immunol* 27, 1848-1852.
- Burdyga T, Mitchell RW, Ragozzino JR & Ford LE (2003). Force and myosin light chain phosphorylation in dog airway smooth muscle activated in different ways. *Respir Physiol Neurobiol* 137, 141-149.
- Büyükaşar K & Levent A (2003). Involvement of Rho/Rho-kinase signaling in the contractile activity and acetylcholine release in the mouse gastric fundus. *Biochem Biophys Res Commun* 303(3), 777-781.
- Camello-Almaraz C, Macias B, Gomez-Pinilla PJ, Alcon S, Martin-Cano FE, Baba A, Matsuda T, Camello PJ & Pozo MJ (2009). Developmental changes in Ca²⁺ homeostasis and contractility in gallbladder smooth muscle. *Am J Physiol Cell Physiol* 296, C783-C791.
- Cao G, van der Wijst J, van der Kemp A, van Zeeland F, Bindels RJ & Hoenderop JG (2009). Regulation of the Epithelial Mg²⁺ Channel TRPM6 by Estrogen and the Associated Repressor Protein of Estrogen Receptor Activity (REA). *J Biol Chem* 284, 14788-14795.
- Caprioli F, Pallone F & Monteleone G (2008). Th17 immune response in IBD: A new pathogenic mechanism. *J Crohns* 2, 291-295.
- Carl A, Lee HK & Sanders KM (1996). Regulation of ion channels in smooth muscles by calcium. *Am J Physiol Cell Physiol* 271, C9-C34.

Caterina MJ, Leffler A, Malmberg AB, Martin WJ, Trafton J, Petersen-Zeitz KR, Koltzenburg M, Basbaum AI & Julius D (2000). Impaired nociception and pain sensation in mice lacking the capsaicin receptor. *Science* 288, 306-313.

Caterina MJ, Rosen TA, Tominaga M, Brake AJ & Julius D (1999). A capsaicin-receptor homologue with a high threshold for noxious heat. *Nature* 398, 436-441.

Cenac N, Altier C, Chapman K, Liedtke W, Zamponi G & Vergnolle N (2008). Transient receptor potential vanilloid-4 has a major role in visceral hypersensitivity symptoms. *Gastroenterol* 135, 937-946.

Chin KW & Barrett KE (1994). Mast cells are not essential to inflammation in murine model of colitis. *Dig Dis Sci* 39, 513-525.

Cho HJ (2008). The genetics and immunopathogenesis of inflammatory bowel disease. *Nature Reviews Immunology* 8, 458-466.

Cho HJ (2003). Significant role of genetics in IBD: the NOD2 gene. *Rev Gastroenterol Disord* 3 (suppl 1), S18-22.

Cho SY, Beckett EA, Baker SA, Han I, Park KJ, Monaghan K, Ward SM, Sanders KM & Koh SD (2005). A pH-sensitive potassium conductance (TASK) and its function in the murine gastrointestinal tract. *J Physiol* 565, 243-259.

Cho H, Youm JB, Ryu SY, Earm YE & Ho WK (2001). Inhibition of acetylcholine-activated K⁺ currents by U73122 is mediated by the inhibition of PIP₂-channel interaction. *Br J Pharmacol* 134, 1066-1072.

Chomarat P & Banchereu J (1998). Interleukin-4 and interleukin-13: their similarities and discrepancies. *Int Rev Immunol* 17, 1-52.

Claesson MH, Rudolphi A, Kofoed S, Poulsen S & Reimann J (2003). CD4⁺ T lymphocytes injected into severe combined immunodeficient (SCID) mice lead to an inflammatory and lethal bowel disease. *Clin Exper Immunol* 104, 491-500.

Clapham DE (2003). TRP channels as cellular sensors. *Nature* 426, 517-524.

Clapham DE, Runnels LW & Strubing C (2001). The TRP ion channel family. *Nat Rev Neurosci* 2, 387-396.

Cohen JD, Kao HW, Tan ST, Lechago J & Snape WJ Jr (1986). Effect of acute experimental colitis on rabbit colonic smooth muscle. *Am J Physiol Gastrointest Liver Physiol* 251, G538-G545.

Conway SJ (2008). TRPping the switch on pain: an introduction to the chemistry and biology of capsaicin and TRPV1. *Chem Soc Rev* 37, 1530-1545.

Coruzzi G, Morini G, Adami M & Grandi D (2001). Role of histamine H3 receptors in the regulation of gastric functions. *J Physiol Pharmacol* 52, 539-553.

Craven M, Sergeant GP, Hollywood MA, McHale NG & Thornbury KD (2004). Modulation of spontaneous Ca²⁺-activated Cl⁻ currents in the rabbit corpus cavernosum by the nitric oxide-cGMP pathway. *J Physiol* 15, 495-506.

Damaj BB, Becerra CB, Esber HJ, Wen Y & Maghazachi AA (2007). Functional expression of H4 histamine receptor in human natural killer cells, monocytes, and dendritic cells. *J Immunol* 179, 7907-7915.

Damak S, Rong M, Yasumatsu K, Kokrashvili Z, Pérez CA, Shigemura N, Yoshida R, Mosinger B Jr, Glendinning JI, Ninomiya Y & Margolskee RF (2006). Trpm5 null mice respond to bitter, sweet, and umami compounds. *Chem Sens* 31, 253-264.

Damann N, Voets T & Nilius B (2008). TRPs in our senses. *Curr Biol* 23, R880-889.

Daniels RL, Takashima Y, McKemy DD (2009). Activity of the Neuronal Cold Sensor TRPM8 Is Regulated by Phospholipase C via the Phospholipid Phosphoinositol 4,5 Bisphosphate. *J Biol Chem* 284, 1570-1582.

D'antonio C, Wang B, McKay C & Huizinga JD (2009). Substance P activates a non-selective cation channel in murine pacemaker ICC. *Neurogastroenterol Motil* 21, 985-e79.

De Moel MP, Van De Put FHMM, Vermegen TMJA, De pont JHHM & Willems PHGM (1995). Effect of the aminosteroid, U73122, on Ca²⁺ uptake and release properties of rat liver microsomes. *Eur J Biochem* 234, 626-631.

De Schepper HU, De Man JG, Moreels TG, Pelckmans PA & De Winter BY (2008). Review article: gastrointestinal sensory and motor disturbances in inflammatory bowel disease - clinical relevance and pathophysiological mechanisms. *Aliment Pharmacol Ther* 27, 621-637.

Der T, Bercik P, Donnelly G, Jackson T, Berezin I, Collins SM & Huizinga JD (2000). Interstitial cells of cajal and inflammation-induced motor dysfunction in the mouse small intestine. *Gastroenterol* 119, 1590-1599.

Devi S, Kedlaya R, Maddodi N, Bhat KMR, Weber CS, Valdivia H & Setaluri V (2009). Calcium Homeostasis in Human Melanocytes: Role of Transient Receptor Potential Melastatin 1 (TRPM1) and its Regulation by Ultraviolet Light. *Am J Physiol Cell Physiol* 297, 679-687.

Diaz J, Vizuete ML, Traiffort E, Arrang JM, Ruat M & Schwartz JC (1994). Localization of the histamine H2 receptor and gene transcripts in rat stomach: back to parietal cells. *Biochem Biophys Res Commun* 198, 1195-1202.

Dietrich A, Kalwa H, Storch U, Schnitzler M, Salanova B, Pinkenburg O, Dubrovskaja G, Essin K, Gollasch M, Birnbaumer L & Gudermann T (2007). Pressure-induced and store-operated cation influx in vascular smooth muscle cells is independent of TRPC1. *Pflugers Arch* 455, 465-477.

Dietrich A, Mederos Y, Schnitzler M, Gollasch M, Gross V, Storch U, Dubrovskaja G, Obst M, Yildirim E, Salanova B, Kalwa H, Essin K, Pinkenburg O, Luft FC, Gudermann T & Birnbaumer L (2005a). Increased vascular smooth muscle contractility in TRPC6^{-/-} mice. *Mol Cell Biol* 16, 6980-6989.

Dietrich A, Schnitzler M, Kalwa H, Storch U & Gudermann T (2005b). Functional characterization and physiological relevance of the TRPC3/6/7 subfamily of cation channels. *Naunyn Schmiedeberg's Arch Pharmacol* 371, 257-265.

Dhaka A, Murray AN, Mathur J, Earley TJ, Petrus MJ & Patapoutian A (2007). TRPM8 is required for cold sensation in mice. *Neuron* 54, 371-378.

Dresviannikov AV, Bolton TB & Zholos AV (2006). Muscarinic receptor-activated cationic channels in murine ileal myocytes. *Br J Pharmacol* 149 (2), 179-187.

Durlu-Kandilci NT & Brading AF (2006). Involvement of Rho kinase and protein kinase C in carbachol-induced calcium sensitization in beta-escin skinned rat and guinea-pig bladders. *Br J Pharmacol* 148(3), 376-384.

Dy M & Schneider E (2004). Histamine-cytokine connection in immunity and hematopoiesis. *Cytokine Growth Factor Rev* 15, 393-410.

Earley S, Waldron BJ & Brayden JE (2004). Critical role for transient receptor potential TRPM4 in myogenic constriction of cerebral arteries. *Cir Res* 95, 922-929.

Eisfeld J & Lückhoff A (2007). TRPM2. *Handb Exp Pharmacol* 179, 237-252.

Eto M, Kitazawa T, Yazawa A, Mukai H, Ono Y & Brautigan DL (2001). Histamine-induced vasoconstriction involves phosphorylation of a specific inhibitor protein for myosin phosphatase by protein kinase C alpha and delta isoforms. *J Biol Chem* 276, 29072-29078.

Elble RC, Ji G, Nehrke K, DeBiasio J, Kingsley PD, Kotlikoff MI & Pauli BU (2002). Molecular and Functional Characterization of a Murine Calcium-activated Chloride Channel Expressed in Smooth Muscle. *J Biol Chem* 277, 18586-18591.

Fang YC, Kuo DH, Shieh P, Chen FA, Kuo CC & Jan CR (2009). Effect of m-3M3FBS on Ca²⁺ movement in Madin-Darby canine renal tubular cells. *Hum Exp Toxicol* [Epub ahead of print].

Farrugia G (2008). Role of interstitial cells of Cajal in health and disease. *Neurogastroenterol Motil* 20 (Suppl.1), 54-63.

Faussone-Pellegrini MS, Gay J, Vannucchi MG, Corsani L & Fioramonti J (2002). Alterations of neurokinin receptors and interstitial cells of cajal during and after jejunal inflammation induced by nippostrongylus brasiliensis in the rat. *Neurogastroenterol Motil* 14, 83-95.

Fernandes L, D'Aprile A, Self G, McGuire M, Sew T, Henry P & Goldie R (2006). A Rho-kinase inhibitor, Y-27632, reduces cholinergic contraction but not neurotransmitter release. *Eur J Pharmacol* 550, 155-161.

Fioretti B, Catacuzzeno L, Sforna L, Aiello F, Francesca P, Ragozzino D, Castigli E & Franciolini F (2009). Histamine hyperpolarizes human glioblastoma cells by activating the intermediate-conductance Ca^{2+} -activated K^+ channel. *Am J Physiol Cell Physiol* 297, C102- C110.

Fleig A & Penner R (2004). The TRPM ion channel subfamily: molecular, biophysical and functional features. *Trends Pharmacol Sci* 25, 633-639.

Flynn ER, McManus CA, Bradley KK, Koh SD, Hegarty TM, Horowitz B & Sanders KM (1999). Inward rectifier potassium conductance regulates membrane potential of canine colonic smooth muscle. *J Physiol* 518.1, 247-256.

Fort MM, Lesley R, Davidson NJ, Menon S, Brombacher F, Leach MW & Rennick DM (2001). IL-4 Exacerbates Disease in a Th1 Cell Transfer Model of Colitis. *J Immuno* 166, 2793-2800.

Franks NP & Honore E (2004). The TREK K2P channels and their role in general anaesthesia and neuroprotection. *Trends Pharmacol Sci* 25, 601-608.

Freichel M, Suh SH, Pfeifer A, Schweig U, Trost C, Weißgerber P, Biel M, Philipp S, Freise D, Droogmans G, Hofmann F, Flockerzi V & Nilius B (2001). Lack of an endothelial store-operated Ca^{2+} current impairs agonist-dependent vasorelaxation in $\text{TRP4}^{-/-}$ mice. *Nat Cell Biol* 3, 121-127.

Friel AM, Curley M, Ravikumar N, Smith TJ & Morrison JJ (2005). RhoA/Rho kinase mRNA and protein levels in human myometrium during pregnancy and labor. *J Soc Gynecol Investig* 12, 20-27.

Fujino S, Andoh A & Bamba S (2003). Increased expression of interleukin 17 in inflammatory bowel disease. *Gut* 52, 65-70.

Fuss I J, Neurath M, Boirivant M, Klein JS, de la Motte C, Strong SA, Fiocchi C & Strober W (1996). Disparate CD4^+ lamina propria (LP) lymphokine secretion profiles in inflammatory bowel disease. Crohn's disease LP cells manifest increased secretion of IFN-gamma, whereas ulcerative colitis LP cells manifest increased secretion of IL-5. *J Immunol* 157, 1261-1270.

Galeazzi F, Haapala EM, Rooijen NV, Vallance BA & Collins SM (2000). Inflammation-induced impairment of enteric nerve function in nematode-infected mice is macrophage dependent. *Am J Physiol Liver Physiol* 278, G259-265.

Giovannardi S, Landò L & Peres A (1998). Flash photolysis of Caged Compounds: Casting Light on Physiological Processes. *News Physiol Sci* 13, 251-255.

Gkika D & Prevarskaya N (2009). Molecular mechanisms of TRP regulation in tumor growth and metastasis. *Biochimica et Biophysica Acta* 1793, 953-958.

Golovina VA, Platoshyn O, Bailey CL, Wang J, Limsuwan A, Sweeney M, Rubin LJ & Yuan JX (2001). Upregulated TRP and enhanced capacitative Ca(2+) entry in human pulmonary artery myocytes during proliferation. *Am J Physiol Heart Circ Physiol* 280, H746-755.

Gor DO, Rose NR & Greenspan NS (2003). TH1-TH2: a procrustean paradigm. *Nat Immunol* 4, 503-505.

Gordienko DV & Zholos (2003). Modulation of muscarinic cation current by intracellular Ca²⁺ release: a central role of the inositol 1, 4, 5-triphosphate receptors. *Neurophysiol* 35, 320.

Gordienko DV, Zholos AV, Shuba MF & Bolton TB (2004). Mechanisms of Ca²⁺ signaling in smooth muscle cells explored with fluorescence confocal imaging. *Neurophysiol* 36, 455-465.

Gosens R, Schaafsma D, Grootte Bromhaar MM, Vrugt B, Zaagsma J, Meurs H & Nelemans SA (2004). Growth factor-induced contraction of human bronchial smooth muscle is Rho-kinase-dependent. *Eur J Pharmacol* 494, 73-76.

Gottlieb P, Folgering J, Maroto R, Raso A, Wodd TG, Kurosky A, Bowman C, Bichet D, Patel A, Sachs F, Martinac B, Hamill OP & Honoré E (2008). Revisiting TRPC1 and TRPC6 mechanosensitivity. *Pflugers Arch* 455, 1097-1103.

Grimm C, Kraft R, Sauerbruch S, Schultz G & Harteneck C (2003). Molecular and functional characterization of the melastatin-related cation channel TRPM3. *J Biol Chem* 278, 21493-21501.

Grossi L, McHugh K & Collins SM (1993). On the specificity of altered muscle function in experimental colitis in rats. *Gastroenterol* 104, 1049-1056.

Guarner F & Malagelada JR (2003). Role of bacteria in experimental colitis. *Best Pract Res Clin Gastroenterol* 17, 793-804.

Haas HL, Sergeeva OA & Selbach O (2008). Histamine in the nervous system. *Physiol Rev* 88, 1183-1241.

Hagar HH, El Medany A, El Eter E & Arafa M (2007). Ameliorative effect of pyrrolidinedithiocarbamate on acetic acid-induced colitis in rats. *Eur J Pharmacol* 554, 69-77.

Halaszovich CR, Zitt C, Jüngling E & Lückhoff A (2000). Inhibition of TRP3 channels by lanthanides. *J Biol Chem* 275, 37423-37428.

Hanano T, Hara Y, Shi J, Morita H, Umebayashi C, Mori E, Sumimoto H, Ito Y, Mori Y, & Inoue R (2004). Involvement of TRPM7 in cell growth as a spontaneously activated Ca^{2+} entry pathway in human retinoblastoma cells. *J Pharmacol Sci* 95, 403-419.

Hashimoto K, Peebles RS, Sheller JR, Jarzecka K, Furlong J, Mitchell DB, Hartert DB & Graham BS (2002). Suppression of airway hyperresponsiveness induced by ovalbumin and RSV infection with Y-27632, a Rho kinase inhibitor. *Thorax* 57, 524-527.

Hartmann J, Dragicevic E, Adelsberger H, Henning HA, Sumser M, Abramowitz J, Blum R, Dietrich A, Freichel M, Flockerzi V, Birnbaumer L & Konnerth (2008). TRPC3 Channels Are Required for Synaptic Transmission and Motor Coordination. *Neuron* 59, 392-398.

He Y, Yao G, Savoia C & Touyz RM (2005). Transient receptor potential melastatin 7 ion channels regulate magnesium homeostasis in vascular smooth muscle cells: role of angiotensin II. *Circ Res* 96, 207-215.

Heller F, Florian P, Bojarski C, Richter J, Christ M, Hillenbrand B, Mankertz J, Gitter A H, Bürgel N, Fromm M, Zeitz M, Fuss I, Strober W & Schulzke JD (2005). Interleukin-13 Is the Key Effector Th2 Cytokine in Ulcerative Colitis That Affects Epithelial Tight Junctions, Apoptosis, and Cell Restitution. *Gastroenterology* 129, 550-564.

Helliwell RM & Large WA (1997). A1-Adrenoceptor activation of a non-selective cation current in rabbit portal vein by 1,2-diacyl-*sn*-glycerol. *J Physiol* 499.2, 417-428.

Héron A, Rouleau A, Cochois V, Pillot C, Schwartz JC & Arrang JM (2001). Expression analysis of the histamine H(3) receptor in developing rat tissues. *Mech Dev* 105, 167-173.

Hibi T & Ogata H (2006). Novel pathophysiological concepts of inflammatory bowel disease. *J Gastroenterol* 41, 10-16.

Hicks SN, Jezyk MR, Gershburg S, Seifert JP, Harden K & Sondek J (2008). General and Versatile Autoinhibition of PLC Isozymes. *Mol Cell* 31, 383-394.

Hille B (2001). *Ion Channels of Excitable Membranes*, 3rd ed. Sinauer, Associates, Inc., Sunderland.

Hoenderop JG, Hartog A, Stuiver M, Doucet A, Willems PH & Bindels RJ (2000). Localization of the epithelial Ca^{2+} channel in rabbit kidney and intestine. *J Am Soc Nephrol* 11, 1171-1178.

Hoenderop JG, van Leeuwen JP, van der Eerden BC, Kersten FF, van der Kemp AW, Merillat AM, Waarsing JH, Rossier BC, Vallon V, Hummler E & Bindels RJ (2003). Renal Ca^{2+} wasting, hyperabsorption, and reduced bone thickness in mice lacking TRPV5. *J Clin Invest* 112, 1906-1914.

Hofmann T, Obukhov AG, Schaefer M, Harteneck C, Gudermann T & Schultz G (1999). Direct activation of human TRPC6 and TRPC3 channels by diacylglycerol. *Nature* 397, 259-263.

Hogaboam CM, Vallance BA, Kumar A, Addison CL, Graham FL, Gaudie J & Collins SM (1997). Therapeutic effects of interleukin-4 gene transfer in experimental inflammatory bowel disease. *J Clin Invest* 100, 2766.

Horowitz LF, Hirdes W, Suh BC, Hilgemann DW, Mackie K & Hille B (2005). Phospholipase C in living cells: activation, inhibition, Ca²⁺ requirement, and regulation of M current. *J Gen Physiol* 126, 243-262.

Horowitz B, Ward SM & Sanders KM (1999). Cellular and molecular basis for electrical rhythmicity in gastrointestinal muscles. *Annu Rev Physiol* 61, 19-43.

Hosseini JM, Goldhill JM, Bossone C, Pineiro-Carrero V & Shea-Donohue T (1999). Progressive alterations in circular smooth muscle contractility in TNBS-induced colitis in rats. *Neurogastroenterol Motil* 11, 347-356.

Hughes SA, Gibson WJ & Young JM (2000). The interaction of U-73122 with the histamine H1 receptor: implications for the use of U-73122 in defining H1 receptor-coupled signalling pathways. *Naunyn Schmiedebergs Arch Pharmacol* 362, 555-558.

Hurst SM & Collins SM (1994). Mechanism underlying tumor necrosis factor- α suppression of norepinephrine release from rat myenteric plexus. *Am J Physiol Gastrointest Liver Physiol* 266, G1123-G1129.

Iba Y, Sugimoto Y, Kamei C & Masukawa T (2003). Possible role of mucosal mast cells in the recovery process of colitis induced by dextran sulfate sodium in rats. *International Immunopharmacology* 3, 485-491.

Ihara E, Beck PL, Chappellaz M, Wong J, Medlicott SA & MacDonald JA (2009). Mitogen-Activated Protein Kinase Pathways Contribute to Hypercontractility and Increased Ca²⁺ Sensitization in Murine Experimental Colitis. *Mol Pharmacol* 75, 1031-1041.

Ihle JN (1995). Cytokine receptor signaling. *Nature* 377, 591-594.

Inoue R & Isenberg G (1990). Acetylcholine activates non-selective cation channels in guinea pig ileum through a G protein. *Am J Physiol* 258, C1173-1178.

Inoue R, Okada T, Onoue H, Hara Y, Shimizu S, Naitoh S, Ito Y & Mori Y (2001). The transient receptor potential protein homologue TRP6 is the essential component of vascular $\alpha(1)$ -adrenoceptor-activated Ca²⁺-permeable cation channel. *Circ Res* 88, 325-332.

Ishizaki T, Uehata M, Tamechika I, Keel J, Nonomura K, Maekawa M & Narumiya S (2000). Pharmacological Properties of Y-27632, a Specific Inhibitor of Rho-Associated Kinases. *Mol Pharmacol* 57, 976-983.

Janssen LJ & Sims SM (1993). Histamine activates Cl^- and K^+ currents in guinea-pig tracheal myocytes: convergence with muscarinic signalling pathway. *J Physiol* 465, 661-677.

Jarajapu YPR & Knot HJ (2005). Relative contribution of Rho kinase and protein kinase C to myogenic tone in rat cerebral arteries in hypertension. *Am J Physiol Heart Circ Physiol* 289, H1917-H1922.

Jin J, Desai BN, Navarro B, Donovan A, Andrews NC & Clapham (2008). Deletion of *Trpm7* disrupts embryonic development and thymopoiesis without altering Mg^{2+} homeostasis. *Sci* 322, 756-760.

Jin W, Lo TM, Loh HH & Thayer SA (1994). U73122 inhibits phospholipase C-dependent calcium mobilization in neuronal cells. *Brain Res* 642, 237-243.

Jin X, Malykhina AP, Lupu F & Akbarali HI (2004). Altered gene expression and increased bursting activity of colonic smooth muscle ATP-sensitive K^+ channels in experimental colitis. *Am J Physiol Gastrointest Liver Physiol* 287, G274-285.

Jung S, Muhle A, Schaefer M, Strotmann R, Schultz G & Plant TD (2003). Lanthanides potentiate TRPC5 currents by an action at extracellular sites close to the pore mouth. *J Biol Chem* 278, 3562-3571.

Jung S, Strotmann R, Schultz G & Plant TD (2002). TRPC6 is a candidate channel involved in receptor-stimulated cation currents in A7r5 smooth muscle cells. *Am J Physiol Cell Physiol* 282, C347-359.

Kamei K, Nabata H & Kuriyama H (1994). Effects of KC 399, a novel ATP-sensitive K^+ channel opener, on electrical and mechanical responses in dog tracheal smooth muscle. *J Pharmacol Exp Ther* 268, 319-327.

Kamouchi M & Kitamura K (1994). Regulation of ATP-sensitive K^+ channels by ATP and nucleotide diphosphate in rabbit portal vein. *Am J Physiol* 266, H1687-1698.

Kanai T, Watanabe M, Okazawa A, Sato T, Yamazaki M, Okamoto S, Ishii H, Totsuka T, Iiyama R, Okamoto R, Ikeda M, Kurimoto M, Takeda K, Akira S & Hibi T (2001). Macrophage-derived IL-18-mediated intestinal inflammation in the murine model of Crohn's disease. *Gastroenterol* 121, 875-888.

Kanauchi O, Serizawa I, Araki Y, Suzuki A, Andoh A, Fujiyama Y, Mitsuyama K, Takaki K, Toyonaga A, Sata M & Bamba T (2003). Germinated barley foodstuff, a prebiotic product, ameliorates inflammation of colitis through modulation of the enteric environment. *J Gastroenterol* 38, 134-141.

Kang TM, Kim YC, Sim JH, Rhee JC, Kim SJ, Uhm DY, So I & Kim KW (2001). The Properties of Carbachol-activated Nonselective Cation Channels at the Single Channel Level in Guinea Pig Gastric Myocytes. *Jpn J Pharm* 85, 291-298.

Kang M, Morsy N, Jin X, Lupu F & Akbarali HI (2004). Protein and gene expression of Ca^{2+} channel isoforms in murine colon: effect of inflammation. *Pflugers Arch-Eur J Physiol* 449, 288-297.

Kanki H, Kinoshita M, Akaike A, Satoh M, Mori Y & Kaneko S (2001). Activation of inositol 1,4,5-trisphosphate receptor is essential for opening of mouse TRP5 channels. *Mol Pharmacology* 60, 989-998.

Kawada M, Arihiro A & Mizoguchi E (2007). Insights from advances in research of chemically induced experimental models of human inflammatory bowel disease. *World J Gastroenterol* 13, 5581-5593.

Kawabata A, Kuroda R, Nishikawa H & Kawai K (1999). Modulation by protease-activated receptors of the rat duodenal motility in vitro: possible mechanisms underlying the evoked contraction and relaxation. *Br J Pharmacol* 128, 865-872.

Keef KD, Hume JR & Zhong J (2001). Regulation of cardiac and smooth muscle Ca^{2+} channels ($\text{Ca}_v1.2a,b$) by protein kinases. *Am J Physiol Cell Physiol* 281, C1743-C1756,

Kelly SJ, Stack WA, O'Donoghue DP & Baird AW (1995). Regulation of ion transport by histamine in the human colon. *Eur J Pharmacol* 12, 203-209.

Kennedy RJ, Hoper M, Deodhar K, Erwin PJ, Kirk SJ & Gardiner KR (2000). Interleukin 10-deficient colitis: new similarities to human inflammatory bowel disease. *B J Surgery* 87, 1346-1351.

Khan WI, Blennerhassett PA, Varghese AK, Chowdhury SK, Omsted P, Deng Y & Collins SM (2002). Intestinal Nematode Infection Ameliorates Experimental Colitis in Mice. *Infection and Immunity* 70, 5931-5937.

Khan I, Oriowo MA & Anim JT (2005). Amelioration of experimental colitis by Na-H exchanger-1 inhibitoramiloride is associated with reversal of IL-1 β and ERK mitogen-activated protein kinase. *Scan J Gastroenterol* 40, 578-585.

Khan WI & Collins SM (2004). Immune-mediated alteration in gut physiology and its role in host defense in nematode infection. *Parasite Immunology* 26, 319-326.

Khan I & Collins SM (1994). Expression of cytokines in the longitudinal muscle of myenteric plexus of the inflamed intestine of rat. *Gastroenterol* 107, 691-700.

Kim BJ, Jeon JH, Kim SJ & So Insuk (2007). Role of calmodulin and myosin light chain kinase in the activation of carbachol-activated cationic current in murine ileal myocytes. *Can J Physiol Pharmacol* 85, 1254-1262.

Kim BJ, So I & Kim KW (2006). The relationship of TRP channels to the pacemaker activity of interstitial cells of Cajal in the gastrointestinal tract. *J Smooth Muscle Res* 42, 1-7.

Kinoshita K, Hori M, Fujisawa M, Sato K, Ohama T, Momotani E & Osaki H (2006). Role of TNF- α in muscularis inflammation and motility disorder in a TNBS-induced colitis model: clues from TNF- α -deficient mice. *Neurogastroenterol Motil* 18, 578-588.

Kinoshita K, Sato K, Hori M, Ozaki H & Karaki H (2003). Decrease in activity of smooth muscle L-type Ca²⁺ channels and its reversal by NF- κ B inhibitors in Crohn's colitis model. *Am J Physiol* 285, G483-G493.

Kitajima S, Takuma S & Morimoto M (1999). Changes in colonic mucosal permeability in mouse colitis induced with dextran sulfate sodium. *Exp Anim* 48, 137-143.

Klose A, Huth T & Alzheimer C (2008). 1-[6-[[[(17 β)-3-Methoxyestra-1,3,5(10)-trien-17-yl]amino]hexyl]-1H-pyrrole-2,5-dione (U73122) Selectively Inhibits Kir3 and BK Channels in a Phospholipase C-Independent Fashion. *Mol Pharmacol* 74, 1203-1214.

Knutson L, Ahrenstedt O, Odland B & Hallgren R (1990). The jejunal secretion of histamine is increased in active Crohn's disease. *Gastroenterol* 98, 849-854.

Kobayashi T, Tonai S, Ishihara Y, Koga R, Okabe S & Watanabe T (2000). Abnormal functional and morphological regulation of the gastric mucosa in histamine H2 receptor-deficient mice. *J Clin Invest* 105, 1741-1749.

Koch TR, Carney JA, Go VL & Szurszewski JH (1988). Spontaneous contractions and some electrophysiologic properties of circular muscle from normal sigmoid colon and ulcerative colitis. *Gastroenterol* 95 (1), 77-84.

Koh SD, Bradley KK, Rae MG, Keef KD, Horowitz B & Sanders KM (1998). Basal activation of ATP-sensitive potassium channels in murine colonic smooth muscle cell. *Biophys J* 75(4), 1793-1800.

Koh SD, Dick GM & Sanders KM (1997). Small-conductance Ca²⁺-dependent K⁺ channels activated by ATP in murine colonic smooth muscle. *Am J Physiol* 273, C2010-C2021.

Koh SD, Monaghan K, Ro S, Mason HS, Kenyon JL & Sanders KM (2001). Novel voltage-dependent non-selective cation conductance in murine colonic myocytes. *J Physiol* 533, 341-355.

Koh SD, Perrino BA, Hatton WJ, Kenyon JL & Sanders KM (1999a). Novel regulation of the A-type K⁺ current in murine proximal colon by calcium-calmodulin-dependent protein kinase II. *J Physiol* 517, 75-84.

Koh, SD, Ward, SM, Dick GM, Epperson A., Bonner, HP, Sanders KM, Horowitz B & Kenyon JL (1999b). Contribution of delayed rectifier potassium currents to the electrical activity of murine colonic smooth muscle. *J Physiol* 515.2, 475-487.

Komori S, Kawai M, Pacaud P, Ohashi H & Bolton TB (1993). Oscillations of receptor-operated cationic current and internal calcium in single guinea-pig ileal smooth muscle cells. *Pflugers Arch* 424, 431-438.

Komori K & Suzuki H (1986). Distribution and properties of excitatory and inhibitory junction potentials in circular muscle of the guinea-pig stomach. *J Physiol* 370, 339-355.

Kong D, Koh SD & Sanders KM (2000). Purinergic activation of spontaneous transient outward currents in guinea pig taenia colonic myocytes. *Am J Physiol Cell Physiol* 278, C352-C362.

Krjukova J, Holmqvist T, Danis AS, Akerman KE & Kukkonen JP (2004). Phospholipase C activator *m*-3M3FBS affects Ca^{2+} homeostasis independently of phospholipase C activation. *Br J Pharmacol* 143, 3-7.

Kuhn R, Lohler J, Rennick D, Rajewsky K & Müller W (1993). Interleukin-10-deficient mice develop chronic enterocolitis. *Cell* 75, 263-274.

Lange I, Yamamoto S, Partida-Sanchez S, Mori Y, Fleig A & Penner R (2009). TRPM2 functions as a lysosomal Ca^{2+} -release channel in beta cells. *Sci Signal* 19, ra23.

Langeslag M, Clark K, Moolenaar WH, van Leeuwen FN & Jalink K (2007). Activation of TRPM7 channels by phospholipase C-coupled receptor agonists. *J Biol Chem* 282, 232-239.

Launay P, Fleig A, Perraud AL, Scharenberg AM, Penner R & Kinet JP (2002). TRPM4 is a Ca^{2+} -activated nonselective cation channel mediating cell membrane depolarization. *Cell* 109, 397-407.

Lee KP, Jun JY, Chang IY, Suh SH, So I, & Kim KW (2005). TRPC4 is an essential component of the nonselective cation channel activated by muscarinic stimulation in mouse visceral smooth muscle cells. *Mol Cells* 20, 435-441.

Lemonnier L, Trebak M, Lievreumont JP, Bird GS & Putney JW Jr (2006). Protection of TRPC7 cation channels from calcium inhibition by closely associated SERCA pumps. *FASEB J* 20, 503-505.

Lemonnier L, Trebak M & Putney JW Jr (2008). Complex regulation of the TRPC3, 6 and 7 channel subfamily by diacylglycerol and phosphatidylinositol-4,5-bisphosphate. *Cell Calcium* 43, 506-514.

Leurs R, Brozius MM, Smit MJ, Bast A & Timmerman H (1991). Effects of histamine H1-, H2- and H3- receptor selective drugs on the mechanical activity of guinea pig small and large intestine. *Br J Pharmacol* 102, 179-185.

Lewinter RD, Skinner K, Julius D & Basbaum AI (2004). Immunoreactive TRPV-2 (VRL-1), capsaicin receptor homolog, in the spinal cord of the rat. *J Comp Neurol* 470, 400-408.

Li L, Matsuoka I, Suzuki Y, Watanabe Y, Ishibashi T, Yokoyama K, Maruyama Y & Kimura J (2002). Inhibitory effect of fluvastatin on lysophosphatidylcholine-induced

nonselective cation current in guinea pig ventricular myocytes. *Mol Pharmacol* 62, 602-607.

Lilja I, Gustafson-Svard C, Franzen L & Sjudahl R (2000). Tumor necrosis factor-alpha in ileal mast cells in patients with Crohn's disease. *Digestion* 61, 68-76.

Lindsay J, van Montfrans C, Brennan F, van Deventer S, Drillenburger P, Hodgson H, te Velde A & Pena MSR (2002). IL-10 gene therapy prevents TNBS-induced colitis. *Gene Therapy* 9, 1715-1721.

Liu X, Rusch NJ, Striessnig J & Sarna SK (2001a). Down-regulation of L-type calcium channels in inflamed circular smooth muscle cells of the canine colon. *Gastroenterol* 120, 480-489.

Liu C, Wilson SJ, Kuei C & Lovenberg TW (2001b). Comparison of human, mouse and guinea pig histamine H4 receptors reveals substantial pharmacological species variation. *J Pharmacol Exp Ther* 299, 121-130.

Lu G, Qian X, Berezin I, Telford GL, Huizinga JD & Sarna SK (1997). Inflammation modulates in vitro colonic myoelectric and contractile activity and interstitial cells of cajal. *Am J Physiol Gastrointest Liver Physiol* 36, G1233-1245.

MacGlashan D (2003). Histamine: A mediator of inflammation. *J Allerg Clin Immunol* 112, S53-S59.

MacPherson BR & Pfeiffer CJ (1978). Experimental production of diffuse colitis in rats. *Digestion* 17, 135-150.

Macrez-Leprêtre N, Morel JL & Mironneau J (1996). Effects of phospholipase C inhibitors on Ca^{2+} channel stimulation and Ca^{2+} release from intracellular stores evoked by alpha 1A- and alpha 2A- adrenoceptors in rat portal vein myocytes. *Biochem Biophys Res Commun* 218, 30-34.

Main C, Blennerhassett PA & Collins SM (1993). Human recombinant interleukin 1 β suppresses acetylcholine release from rat myenteric plexus. *Gastroenterol* 104, 1648-1654.

Marigo V, Courville K, Hsu WH, Feng JM & Cheng H (2009). TRPM4 impacts on Ca^{2+} signals during agonist-induced insulin secretion in pancreatic β -cells. *Mol Cell Endo* 299, 194-203.

Maroto R, Raso A, Wood TG, Kurosky A, Martinac B & Hamill OP (2005). TRPC1 forms the stretch-activated cation channel in vertebrate cells. *Nat Cell Biol* 7, 179-185.

Matsumoto K, Kurosawa E, Terui H, Hosoya T, Tashima K, Murayama T, Priestley JV & Horie S (2009). Localization of TRPV1 and contractile effect of capsaicin in mouse large intestine: high abundance and sensitivity in rectum and distal colon. *Am J Physiol Gastrointest Liver Physiol* 297, G348-G360.

McKay RR, Szymeczek-Seay CL, Lievremont JP, Bird GS, Zitt C, Jüngling E, Lückhoff A & Putney JW Jr (2000). Cloning and expression of the human transient receptor potential 4 (TRP4) gene: localization and functional expression of human TRP4 and TRP3. *Biochem J* 351(3), 735-746.

Melgar S, Karlsson A & Michaëlsson E (2005). Acute colitis induced by dextran sulfate sodium progresses to chronicity in C57BL/6 but not in BALB/c mice: correlation between symptoms and inflammation. *Am J Physiol Gastrointest Liver Physiol* 288, G1328-1338.

Mesenkamp AR, Hoenderop JG & Bindels RJ (2007). TRPV5, the gateway to Ca^{2+} homeostasis. *Handb Exp Pharmacol* 179, 207-220.

Middel P, Reich K, Polzien F, Blaschke V, Hemmerlein B, Herms J, Korabiowska M & Radzun H (2001). Interleukin 16 expression and phenotype of interleukin 16 producing cells in Crohn's disease. *Gut* 49, 795-803.

Minocha A, Thomas C & Omar R (1995). Lack of crucial role of mast cells in pathogenesis of experimental colitis in mice. *Dig Dis Sci* 40, 1757-1762.

Miyamoto K, Iwase M, Nyui M, Arata S, Sakai Y, Gabazza EC, Kimura H & Homma I (2006). Histamine Type 1 Receptor Deficiency Reduces Airway Inflammation in a Murine Asthma Model. *Int Arch Allergy Immunol* 140, 215-222.

Mizoguchi E, Xavier RJ, Reinecker HC, Uchino H, Bhan AK, Podolsky DK & Mizoguchi A (2003). Colonic epithelial functional phenotype varies with type and phase of experimental colitis. *Gastroenterol* 125, 148-161.

Mogami H, Mills CL & Gallacher DV (1997). Phospholipase C inhibitor, U73122, releases intracellular Ca^{2+} , potentiates $\text{Ins}(1,4,5)\text{P}_3$ -mediated Ca^{2+} release and directly activates ion channels in mouse pancreatic acinar cells. *Biochem J* 324, 645-651.

Montell C (2005). The TRP superfamily of cation channels. *Sci STKE* 272, re3.

Montell C (2003). Mg^{2+} homeostasis: the Mg^{2+} -sensitive TRPM channels. *Curr Biol* 13, R799-R801.

Moore KW, de Waal Malefyt R, Coffman RL & O'Garra A (2001). Interleukin-10 and the interleukin-10 receptor. *Annu Rev Immunol* 19, 683-765.

Moqrich A, Hwang SW, Earley TJ, Petrus MJ, Murray AN, Spencer KS, Andahazy M, Story GM & Patapoutian A (2005). Impaired thermosensation in mice lacking TRPV3, a heat and camphor sensor in the skin. *Science* 307, 1468-1472.

Mori Y, Wakamori M, Miyakawa T, Hermosura M, Hara Y, Nishida M, Hirose K, Mizushima A, Kurosaki M, Mori E, Gotoh K, Okada T, Fleig A, Penner R, Iino M & Kurosaki T (2002). Transient receptor potential 1 regulates capacitative Ca^{2+} entry and Ca^{2+} release from endoplasmic reticulum in B lymphocytes. *J Exp Med* 195, 673-681.

Morrissey PJ, Charrier K, Braddy S, Liggitt D & Watson JD (1993). CD4+ T cells that express high levels of CD45RB induce wasting disease when transferred into congenic severe combined immunodeficient mice. Disease development is prevented by cotransfer of purified CD4+ T cells. *J Exp Med* 178, 237-244.

Murthy KS, Grider JR, Kuemmerle JF & Makhlouf GM (2000). Sustained muscle contraction induced by agonists, growth factors, and Ca²⁺ mediated by distinct PKC isozymes. *Am J Physiol Gastrointest Liver Physiol* 279, G201-G210.

Myers BS, Martin JS, Dempsey DT, Parkman HP, Thomas RM & Ryan JP (1997a). Acute experimental colitis decreases colonic smooth muscle contractility in rats. *Am J Physio- Gastrointestinal and Liver Physiology* 273 (4), G928-936.

Myers BS, Dempsey DT, Yasar S, Martin JS, Parkman HP, Ryan JP (1997b). Acute experimental distal colitis alters colonic transit in rats. *J Surg Res* 69, 107-112.

Nadler MJ, Hermosura MC, Inabe K, Perraud AL, Zhu Q, Stokes AJ, Kurosaki T, Kinet JP, Penner R, Scharenberg AM & Fleig A (2001). LTRPC7 is a Mg.ATP-regulated divalent cation channel required for cell viability. *Nature* 411, 590-595.

Nam JH, Lee HS, Nguyen YH, Kang TM, Lee SW, Kim HY, Kim SJ, Earm, YE & Kim SJ (2007). Mechanosensitive activation of K⁺ channel via Phospholipase C-induced depletion of phosphatidylinositol 4,5-bisphosphate in B lymphocytes. *J Physiol* 582, 977-990.

Natale L, Piepoli AL, De Salvia MA, De Salvatore G, Mitolo CI, Marzullo A, Portincasa P, Moschetta A, Palasciano G & Mitolo-Chieppa D (2003). Interleukins-1 β and 6 induce functional alteration of rat colonic motility: an in vitro study. *Eur J Clin Invest* 33, 704-712.

Neeper MP, Liu Y, Hutchinson TL, Wang Y, Flores CM, & Qin N (2007). Activation properties of heterologously expressed mammalian TRPV2: evidence for species dependence. *J Biol Chem* 282, 15894-15902.

Neurath MF, Fuss I, Kelshall BL, Stuber E & Strober W (1995). Antibodies to interleukin 12 abrogate established experimental colitis in mice. *J Exp Med* 182, 1281-1290.

Nilius B, Owsianik G, Voets T & Peters JA (2007). Transient Receptor Potential Cation Channels in Disease. *Physiol Rev* 87, 165-217.

Nilius B, Vennekens R, Prenen J, Hoenderop JG, Droogmans G & Bindels RJ (2001). The single pore residue D542 determines Ca²⁺ permeation and Mg²⁺ block of the epithelial Ca²⁺ channel. *J Biol Chem* 276, 1020-1025.

Noma A (1983). ATP-regulated K⁺ channels in cardiac muscle. *Nature* 305, 147-148.

Oancea E, Vriens J, Brauchi S, Jun J, Splawski I, Clapham DE (2009). TRPM1 forms ion channels associated with melanin content in melanocytes. *Sci Signal* 12, ra21.

Oda T, Morikawa N, Saito Y, Masuho Y & Matsumoto S (2000). Molecular cloning and characterization of a novel type of histamine receptor preferentially expressed in leukocytes. *J Biol Chem* 275, 36781-36786.

O'Gara A & Murphy K (1994). Role of cytokines in determining T-lymphocyte function. *Curr Opin Immunol* 6, 459.

Ogura Y, Bonen DK, Inohara N, Nicolae DL, Chen FF, Ramos R, Britton H, Moran T, Karaliuskas R, Duerr RH, Achkar JP, Brant SR, Bayless TM, Kirschner BS, Hanauer S B, Nunez G & Cho JH (2001). A frameshift mutation in NOD2 associated with susceptibility to Crohn's disease. *Nature* 411, 603-606.

Ohama T, Masatoshi H & Ozaki H (2007). Mechanism of abnormal intestinal motility in inflammatory bowel disease: how much smooth muscle contraction is reduced? *J Smooth Muscle Res* 43, 43-54.

Ohama T, Hori M, Sato K, Ozaki H & Karaki H (2003). Chronic Treatment with Interleukin-1 β Attenuates Contractions by Decreasing the Activities of CPI-17 and MYPT-1 in Intestinal Smooth Muscle. *J Biol Chem* 278, 48794-48804.

Okada T, Inoue R, Yamazaki K, Maeda A, Kurosaki T, Yamakuni T, Tanaka I, Shimizu S, Ikenaka K, Imoto K & Mori Y (1999). Molecular and functional characterization of a novel mouse transient receptor potential protein homologue TRP7. Ca²⁺-permeable cation channel that is constitutively activated and enhanced by stimulation of G protein-coupled receptor. *J Biol Chem* 274, 27359-27370.

Okamoto H, Unno T, Arima D, Suzuki M, Yan H-D, Matsuyama H, Nishimura M & Komori S (2004). Phospholipase C Involvement in Activation of the Muscarinic Receptor-Operated Cationic Current in Guinea Pig Ileal Smooth Muscle Cells. *J Pharmacol Sci* 95, 203-213.

Okayasu I, Hatakeyama S, Yamada M, Ohkusa T, Inagaki Y & Nakaya R (1990). A novel method in the induction of reliable experimental acute and ulcerative colitis in mice. *Gastroenterol* 98, 694-702.

O'Shea JJ & Murray PJ (2008). Cytokine signaling modules in inflammatory responses. *Immunity* 28, 477-487.

Oosterhout AJM & Motta AC (2005). Th1/Th2 paradigm: not seeing the forest for the trees? *Eur Respir J* 25, 591-593.

Otsuguro KI, Tang O, Tang Y, Xiao R, Freichel M, Tsvilovskyy V, Ito S, Flockerzi V, Zhu M & Zholos AV (2008). Isoform-specific Inhibition of TRPC4 Channel by Phosphatidylinositol 4,5-Bisphosphate. *J Biol Chem* 283, 10026-10036.

- Owczarek D, Cibor D, Szczepanek M & Mach T (2009). Biological therapy of inflammatory bowel disease. *Pol Arch Med Wewn* 119, 1-2.
- Owsianik G, Talavera K, Voets T & Nilius B (2006). Permeation and selectivity of TRP channels. *Annu Rev Physiol* 68, 685-717.
- Ozaki H, Hori M, Kinoshita K & Ohama T (2005). Intestinal dysmotility in inflammatory bowel disease: mechanisms of the reduced activity of smooth muscle contraction. *Inflammopharmacology* 13, 103-111.
- Park U, Vastani N, Guan Y, Raja SN, Koltzenburg M & Caterina MJ (2008). Evaluation of TRPV2 function in mouse thermal nociception. *Abstract, Nociceptor Symposium*.
- Penna A, Juvin V, Chemin J, Compan V, Monet M & Rassendren FA (2006). PI3-kinase promotes TRPV2 activity independently of channel translocation to the plasma membrane. *Cell Calcium* 39, 495-507.
- Pérez CA, Huang L, Rong M, Kozak JA, Preuss AK, Zhang H, Max M & Margolskee RF (2002). A transient receptor potential channel expressed in taste receptor cells. *Nat Neurosci* 5, 1169-1176.
- Perraud AL, Knowles HM & Schmitz C (2004). Novel aspects of signaling and ion-homeostasis regulation in immunocytes. The TRPM ion channels and their potential role in modulating the immune response. *Mol Immunol* 41, 657-673.
- Plant TD & Schaefer M (2005). Receptor-operated cation channels formed by TRPC4 and TRPC5. *Naunyn-Schmiedeberg's Arch Pharmacol* 371, 266-276.
- Pochynyuk O, Medina J, Gamper N, Genth H, Stockand JD & Staruschenko A (2006). Rapid translocation and insertion of the epithelial Na⁺ channel in response to RhoA signaling. *J Biol Chem* 281, 26520-26527.
- Poteser M, Graziani A, Rosker C, Eder P, Derler I, Kahr H, Zhu M X, Romanin C & Groschner K (2006). TRPC3 and TRPC4 Associate to Form a Redox-sensitive Cation Channel. *J Biol Chem* 281, 13588-13595.
- Powrie F, Leach MW, Mauze S, Caddie LB & Coffman RL (1993). Phenotypically distinct subsets of CD4⁺ T cells induce or protect from chronic intestinal inflammation in C.B-17 scid mice. *Int Immunol* 5, 1461-1471.
- Prevarskaya N, Zhang L & Barritt G (2007). TRP channels in cancer. *Biochim Biophys Acta* 1772, 937-946.
- Prinz C, Zanner R & Gratzl M (2003). Physiology of gastric enterochromaffin-like cells. *Annu Rev Physiol* 65, 371-382.
- Rae MG, Fleming N, McGregor DB, Sanders KM & Keef KD (1998). Control of motility patterns in the human colonic circular muscle layer by pacemaker activity. *J Physiol* 510(1), 309-320.

Raingo J, Rebolledo A, Iveli F, Grassi de Gende AO & Milesi V (2004). Non-selective Cationic Channels (NSCC) in Smooth Muscle Cells from Human Umbilical Arteries. *Placenta* 25, 723-729.

Raithel M, Matek M, Baenkler HW, Jorde W & Hahn EG (1995). Mucosal histamine content and histamine secretion in Crohn's disease, ulcerative colitis and allergic enteropathy. *Int Arch Allergy Immunol* 108, 127-133.

Ramsey IS, Delling M & Clapham DE (2006). An introduction to TRP channels. *Annu Rev Physiol* 68, 619-647.

Rattan S & Patel CA (2008). Selectivity of ROCK inhibitors in the spontaneously tonic smooth muscle. *Am J Physiol Gastrointest Liver Physiol* 294, G687-G693.

Reddy SN, Bazzocchi G, Chan S, Akashi K, Villanueva-Meyer J, Yanni G, Mena I & Snape WJ Jr (1991). Colonic motility and transit in health and ulcerative colitis. *Gastroenterol* 101, 1289-1297.

Rebecchi MJ & Pentylala SN (2000). Structure, Function, and Control of Phosphoinositide-Specific Phospholipase C. *Physiol Rev* 80, 1291-1335.

Rhee SG (2001). Regulation of Phosphoinositide-Specific Phospholipase C. *Annu Rev Biochem* 70, 281-312.

Riccio A, II, Moon J, Kim KS, Smith KS, Rudolph U, Gapon S, Yao GL, Tsvetkov E, Rodig SJ, Veer AV, Meloni EG, Carlezon WA, Bolshakov VY & Clapham DE (2009). Essential Role for TRPC5 in Amygdala Function and Fear-Related Behaviour. *Cell* 137, 761-772.

Rijnierse A, Nijkamp FP & Kraneveld AD (2007). Mast cells and nerves tickle in the tummy. Implications for inflammatory bowel disease and irritable bowel syndrome. *Pharmacol Therapeut* 116, 207-235.

Roedding AS, Li PP & Warsh JJ (2006). Characterization of the transient receptor potential channels mediating lysophosphatidic acid-stimulated calcium mobilization in B lymphoblasts. *Life Sci* 80, 89-97.

Rosenthal R, Choritz L, Schlott S, Bechrakis NE, Jaroszewski J, Wiederholt M & Thieme H (2005). Effects of ML-7 and Y-27632 on carbachol- and endothelin-1-induced contraction of bovine trabecular meshwork. *Exp Eye Res* 80(6), 837-845.

Rossignoli Pde S, Rodrigues AD, Tinti T, Pereira OC, Ellinger F & Chies AB (2008). The possible involvement of hyperpolarizing mechanisms in histamine-induced relaxation of the rat portal vein. *J Smooth Muscle Res* 44, 129-141.

Roumestan C, Henriquet C, Gougat C, Michel A, Bichon F, Portet K, Jaffuel D & Mathieu M (2008). Histamine H1-receptor antagonists inhibit nuclear factor-kappaB and activator

protein-1 activities via H1-receptor-dependent and –independent mechanisms. *Clin Exp Allergy* 38, 947-956.

Ruhl A, Hurst S & Collins SM (1994). Synergism between interleukins 1 β and 6 on noradrenergic nerves in rat myenteric plexus. *Gastroenterol* 107, 993-1001.

Runnels LW, Yue L & Clapham DE (2001). TRP-PLIK, a bifunctional protein with kinase and ion channel activities. *Science* 291, 1043-1047.

Sadlack B, Merz H, Schorle H, Schimpl A, Feller AC & Horak I (1993). Ulcerative colitis-like disease in mice with a disrupted interleukin-2 gene. *Cell* 75, 253-261.

Sakamoto N, Kono S, Wakai K, Fukada Y, Satomi M & Shimoyama T (2005). Epidemiology Group of the Research Committee on Inflammatory Bowel Disease in Japan. Dietary risk factors for inflammatory bowel disease: a multicenter case-control study in Japan. *Inflamm Bowel Dis* 11, 154-163.

Sanders KM (2008). Regulation of smooth muscle excitation and contraction. *Neurogastroenterol Motil* 20, 39-53.

Sanders KM & Koh SD (2006). Two-pore-domain potassium channels in smooth muscles: new components of myogenic regulation. *J Physiol* 570, 37-43.

Sander LE, Lorentz A, Sellge G, Coëffier M, Neipp M, Veres T, Frieling T, Meier PN, Manns MP & Bischoff SC (2006). Selective expression of histamine receptors H1R, H2R, and H4R, but not H3R, in the human intestinal tract. *Gut* 55, 498-504.

Santos-Silva AJ, Cairrao E, Marques B & Verde I (2009). Regulation of Human Umbilical Artery Contractility by Different Serotonin and Histamine Receptors. *Reprod Sci* [Epub ahead of print].

Sawdy R, Knock GA, Bennett PR, Poston L & Aaronson PI (1998). Effect of nimesulide and indomethacin on contractility and the Ca²⁺ channel current in myometrial smooth muscle from pregnant women. *Br J Pharmacol* 125, 1212-1217.

Schaefer M, Plant TD, Obukhov AG, Hofmann T, Gudermann T, & Schultz G (2000). Receptor-mediated regulation of the nonselective cation channels TRPC4 and TRPC5. *J Biol Chem* 275, 17517-17526.

Schlicker E, Fink K, Detzner M & Göthert M (1993). Histamine inhibits dopamine release in the mouse striatum via presynaptic H3 receptors. *J Neural Transm Gen Sect* 93, 1-10.

Schlicker E, Fink K, Hinterthaler M & Göthert M (1989). Inhibition of noradrenaline release in the rat brain cortex via presynaptic H3 receptors. *Naunyn-Schneiderberg's Arch Pharmacol* 340, 633-638.

Schneider T, Fetscher C, Krege S & Michel MC (2004). Signal transduction underlying carbachol-induced contraction of human urinary bladder. *J Pharmacol Exp Ther* 309, 1148-1153.

Sergeant GP, Ohya S, Reihill JA, Perrino BA, Amberg GC, Imaizumi Y, Horowitz B, Sanders KM & Koh SD (2004). Regulation of $K_v4.3$ currents by Ca^{2+} /calmodulin-dependent protein kinase II. *Am. J. Physiol. Cell Physiol* 288, C304-C313.

Shi J, Mori E, Mori Y, Mori M, Li J, Ito Y & Inoue R (2004). Multiple regulation by calcium of murine homologues of transient receptor potential proteins TRPC6 and TRPC7 expressed in HEK293 cells. *J Physiol* 561, 415-432.

Shi XZ, Pazdrak K, Saada N, Dai B, Palade P & Sarna SK (2005). Negative transcriptional regulation of human colonic smooth muscle Cav1.2 channels by p50 and p65 subunits of nuclear factor-kappa β . *Gastroenterol* 129, 1518-1532.

Shi XZ & Sarna SK (2000). Impairment of Ca^{2+} mobilization in circular muscle cells of the inflamed colon. *Am J Physiol* 278, G234-242.

Shimizu T, Owsianik G, FreichelM, Flockerzi V, Nilius B & Vennekens R (2009). TRPM4 regulates migration of mast cells in mice. *Cell Calcium* 45, 226-232.

Shuttleworth CW, Sanders KM & Keef KD (1993). Inhibition of nitric oxide synthesis reveals non-cholinergic excitatory neurotransmission in the canine proximal colon. *Br J Pharmacol* 109(3), 739-747.

Sibaev A, Massa F, Yuce B, Marsicano G, Lehr HA, Lutz B, Goke B, Allescher HD & Storr M (2006). CB1 and TRPV1 receptors mediate protective effects on colonic electrophysiological properties in mice. *J Mol Med* 84, 513-520.

Sickmann T, Klose A, Huth T & Alzeheimer C (2008). Unexpected suppression of neuronal G-protein-activated, inwardly rectifying K^+ current by common phospholipase C inhibitor. *Neurosci Lett* 436, 102-106.

Sivakumar PV, Westrich GM, Kanaly S, Garka K, Born TL, Derry JM & Viney JL (2002). Interleukin 18 is a primary mediator of the inflammation associated with dextran sulphate sodium induced colitis: blocking interleukin 18 attenuates intestinal damage. *Gut* 50, 812-820.

Snape Jr WJ, Williams R & Hyman PE (1991). Defect in colonic smooth muscle contraction in patients with ulcerative colitis. *Am J Physiol Gastrointest Liver Physiol* 261, G987-991.

So I & Kim WK (2003). Nonselective Cation Channels Activated by the Stimulation of Muscarinic Receptors in Mammalian Gastric Smooth Muscle. *J Smooth Muscle Res* 39, 231-247.

Somlyo AP & Somlyo AV (2003). Ca^{2+} sensitivity of smooth muscle and non-muscle myosin II: modulated by G proteins, kinases, and myosin phosphatase. *Physiol Rev* 83, 1325-1358.

Sours-Brothers S, Ding M, Graham S & Ma Rong (2009). Interaction Between TRPC1-TRPC4 Assembly and STIM1 Contributes to Store-Operated Ca^{2+} Entry in Mesangial Cells. *Exp Biol Med* 234, 673-682.

Staruschenko A, Nichols A, Medina JL, Camacho P, Zheleznova NN & Stockand JD (2004). Rho Small GTPases Activate the Epithelial Na^+ Channel. *J Biol Chem* 279, 49989-49994.

Steidler L, Hans W, Schotte L, Neiryneck S, Obermeier F, Falk W, Fiers W & Remaut E (2000). Treatment of murine colitis by *Lactococcus lactis* secreting interleukin-10. *Science* 289, 1352-1355.

Steinhoff M & Bíró T (2009). A TR(I)P to pruritusresearch: role of TRPV3 in inflammation and itch. *J Invest Dermatol* 129, 531-535.

Strober W, Kelsall B, Fuss I, Marth T, Ludviksson B & Ehrhardt R (1997). Reciprocal $\text{IFN}\gamma$ and $\text{TGF}\beta$ responses regulate the occurrence of mucosal inflammation. *Immunol Today* 18, 61-64.

Stokes AJ, Shimoda LMN, Kblan-Huberson M, Adra CN & Turner H (2004). A TRPV2-PKA Signalling Module for Transduction of Physical Stimuli in Mast Cells. *JEM* 200, 137-147.

Stoyanova II & Gulubova MV (2002). Mast cells and inflammatory mediators in chronic ulcerative colitis. *Acta Histochem* 104, 185-192.

Strübing C, Krapivinsky G, Krapivinsky L & Clapham D (2003). Formation of Novel TRPC Channels by Complex Subunit Interactions in Embryonic Brain. *J Biol Chem* 278, 39014-39019.

Strübing C, Krapivinsky G, Krapivinsky L & Clapham DE (2001). TRPC1 and TRPC5 form a novel cation channel in mammalian brain. *Neuron* 29, 645-655.

Suh PG, Park JI, Manzoli L, Cocco L., Peak JC, Katan M, Fukami K, Kataoka T, Yun S & Ryu SH (2008). Multiple Roles of Phosphoinositide-specific phospholipase C isozymes. *BMB Rep* 41, 415-434.

Sung TS, Kim MJ, Hong S, Jeon JP, Kim BJ, Jeon JH, Kim SJ & So I (2009). Functional characteristics of TRPC4 channels expressed in HEK 293 cells. *Mol Cells* 27, 167-173.

Takenouchi T, Ogihara K, Sato M & Kitani H (2005). Inhibitory effects of U73122 and U73343 on Ca^{2+} influx and pore formation induced by the activation of P2X7 nucleotide receptors in mouse microglial cell line. *Biochim Biophys Acta* 1726, 177-186.

Takeuchi T, Kushida M, Hirayama N, Kitayama M, Fujita A & Hata F (2004). Mechanisms involved in carbachol-induced Ca^{2+} sensitization of contractile elements in rat proximal and distal colon. *Br J Pharmacol* 142(4), 657-666.

Tanaka S, Hamada K, Yamada N, Sigita Y, Tonai S, Hunyady B, Palkovits M, Falus A, Watanabe T, Okabe S, Ohtsu H, Atsushi I & Nagy A (2002). Gastric acid secretion in L-histidine decarboxylase-deficient mice. *Gastroenterol* 122, 145-155.

Taylor CW & Broad LM (1998). Pharmacological analysis of intracellular Ca²⁺ signaling: problems and pitfalls. *Trends Pharmacol Sci* 19, 370-375.

Terasawa K, Nakajima T, Lida H, Iwasawa K, Oonuma H, Jo T, Morita T, Nakamura F, Fujimori Y, Toyo-oka T & Nagai R (2002). Nonselective cation currents regulate membrane potential of rabbit coronary arterial cell: modulation by lysophosphatidylcholine. *Circulation* 106, 3111-3119.

Thebault S, Cao G, Venselaar H, Xi Q, Bindels RJ & Hoenderop JG (2008). Role of the alpha-kinase domain in transient receptor potential melastatin 6 channel and regulation by intracellular ATP. *J Biol Chem* 283, 19999-20007.

Thorneloe KS & Nelson MT (2004). Properties of a tonically active, sodium-permeable current in mouse urinary bladder smooth muscle. *Am J Physiol Cell Physiol* 286(6), C1246-1257.

Trebak M (2006). Canonical transient receptor potential channels in disease: targets for novel drug therapy? *Drug Discov Today* 11, 924-930.

Trebak M, Vazquez G, Bird GS & Putney JW Jr (2003). The TRPC3/6/7 subfamily of cation channels. *Cell Calcium* 33, 451-461.

Tsavalier L, Shapero MH, Morkowski S & Laus R (2001). Trp-p8, a novel prostate-specific gene, is upregulated in prostate cancer and other malignancies and shares high homology with transient receptor potential calcium channel proteins. *Cancer Res* 61, 3760-3769.

Tsvilovskyy VV, Zholos AV, Aberle T, Philipp SE, Dietrich A, Zhu MX, Birnbaumer L, Freichel M & Flockerzi V (2009). Deletion of TRPC4 and TRPC6 in mice impairs smooth muscle contraction and intestinal motility in vivo. *Gastroenterol* 137, 1415-1424.

Ueda T, Yamada T, Ugawa S, Ishida Y & Shimada S (2009). TRPV3, a thermosensitive channel is expressed in mouse distal colon epithelium. *Biochem Biophys Res Commun* 383, 130-134.

Unno T, Matsuyama H, Okamoto H, Sakamoto T, Yamamoto M, Tanahashi Y, Yan HD & Komori S (2006). Muscarinic cationic current in gastrointestinal smooth muscles: signal transduction and role in contraction. *Auto Autacoid Pharmacol* 26, 203-217.

Unno T, Kwon SC, Okamoto H, Irie Y, Kato Y, Matsuyama H & Komori S (2003). Receptor signaling mechanisms underlying muscarinic agonist-evoked contraction in guinea-pig ileal longitudinal smooth muscle. *Br J Pharmacol* 139, 337-350.

Van Abel M, Hoenderop JGJ & Bindels RJM (2005). The epithelial calcium channels TRPV5 and TRPV6: regulation and implications for disease. *Naunyn-Schmiedeberg's Arch Pharmacol* 371, 295-306.

Vandebrouck C, Martin D, Colson-Van Schoor M, Debaix H & Gailly P (2002). Involvement of TRPC in the abnormal calcium influx observed in dystrophic (mdx) mouse skeletal muscle fibers. *J Cell Biol* 158, 1089-1096.

Vannier B, Peyton M, Boulay G, Brown D, Qin N, Jiang M, Zhu X & Birnbaumer L (1999). Mouse *trp2*, the homologue of the human *trpc2* pseudogene, encodes mTrp2, a store depletion-activated capacitative Ca²⁺ entry channel. *Proc Natl Acad Sci* 96, 2060-2064.

Varga C, Horvath K, Berko A, Thurmond RL, Dunford PJ & Whittle BJR (2005). Inhibitory effects of histamine H4 receptor antagonists on experimental colitis in the rat. *Eur J Pharmacol* 522, 130-138.

Vazquez G, Bird GS, Mori Y & Putney JW Jr. (2006). Native TRPC7 channel activation by an inositol trisphosphate receptor-dependent mechanism. *J Biol Chem* 281, 25250-25258.

Vázquez E & Valverde MA (2006). A review of TRP channels splicing. *Seminars in Cell and Developmental Biology* 17, 607-617.

Vazquez G, Wedel BJ, Aziz O, Trebak M, & Putney JW Jr (2004a). The mammalian TRPC cation channels. *Biochim Biophys Acta* 1742, 21-36.

Vazquez G, Wedel BJ, Kawaski BT, Bird GSJ & Putney Jr W (2004b). Obligatory Role of Src kinase in the Signalling Mechanism for TRPC3 Cation Channels. *J Biol Chem* 279, 40521-40528.

Vennekens R, Hoenderop JG, Prenen J, Stuijver M, Willems PH, Droogmans G, Nilius B & Bindels RJ (2000). Permeation and gating properties of the novel epithelial Ca²⁺ channel. *J Biol Chem* 275, 3963-3969.

Vennekens R, Olausson J, Meissner M, Bloch W, Mathar I, Philipp SE, Schmitz F, Weissgerber P, Nilius B, Flockerzi V & Freichel M (2007). Increased IgE-dependent mast cell activation and anaphylactic responses in mice lacking the calcium-activated nonselective cation channel TRPM4. *Nat Immunol* 8, 312-320.

Venkatachalam K & Montell C (2007). TRP channels. *Annu Rev Biochem* 76, 387-417.

Venkatachalam K, Zheng F & Gill DL (2003). Regulation of canonical transient receptor potential (TRPC) channel function by diacylglycerol and protein kinase C. *J Biol Chem* 278: 29031-29040.

Vermillion DL, Huizinga JD, Riddell RH & Collins SM (1993). Altered small intestinal smooth muscle function in Crohn's disease. *Gastroenterol* 104, 1692-1699.

Vermillion DL & Collins SM (1988). Increased responsiveness of jejunal longitudinal muscle in *Trichinella*-infected rats. *Am J Physiol* 254, G124-129.

Videla S, Vilaseca J, Guarner F, Salas A, Treserra F, Crespo E, Antolín M & Malagelada JR (1994). Role of intestinal microflora in chronic inflammation and ulceration of the rat colon. *Gut* 35, 1090-1097.

Villalba N, Stankevicius E, Simonsen U & Prieto D (2008). Rho-kinase is involved in Ca^{2+} entry of rat penile small arteries. *Am J Physiol Heart Circ Physiol* 294, H1923-H1932.

Voets T, Nilius B, Hoefs S, van der Kemp AW, Droogsmans G, Bindels RJ & Hoenderop JG (2004). TRPM6 forms the Mg^{2+} influx channel involved in intestinal and renal Mg^{2+} absorption. *J Biol Chem* 279, 19-25.

Vrees MD, Pricolo VE, Potenti FM & Cao W (2002). Abnormal Motility in Patients With Ulcerative Colitis. *Arch Surg* 137, 439-436.

Vriens J, Appendino G & Nilius B (2009). Pharmacology of vanilloid transient receptor potential cation channels. *Mol Pharmacol* 75, 1262-1279.

Vriens J, Owsianik G, Voets T, Droogsmans G & Nilius B (2004). Invertebrate TRP proteins as functional models for mammalian channels. *Pflugers Arch* 449, 213-226.

Wagner TFJ, Loch S, Lambert S, Straub I, Mannebach S, Mathar I, Düfer M, Lis A, Flockerzi V, Philipp SE & Oberwinkler J (2008). Transient receptor potential M3 channels are ionotropic steroid receptors in pancreatic β cells. *Nature Cell Biol* 10, 1421-1430.

Walder RY, Yang B, Stokes JB, Kirby PA, Cao X, Shi P, Searby CC, Husted RF & Sheffield VC (2009). Mice defective in *Trpm6* show embryonic mortality and neural tube defects. *Hum Mol Genet* [Epub ahead of print].

Walker EM, Bispham JR & Hill SJ (1998). Nonselective effects of the putative phospholipase C inhibitor, U73122, on adenosine A1 receptor-mediated signal transduction events in Chinese hamster ovary cells. *Biochem Pharmacol* 56, 1455-1462.

Wang JP (1996). U-73122, an aminosteroid phospholipase C inhibitor, may also block Ca^{2+} influx through phospholipase C-independent mechanism in neutrophil activation. *Naunyn-Schmiedeberg's Archives of Pharmacol* 353, 599-605.

Wang YZ, Cooke HJ, Su HC & Fertil R (1990). Histamine augments colonic secretion in guinea pig distal colon. *Am J Physiol* 258, G432-G439.

Wang S, Dai Y, Fukuoka T, Yamanaka H, Kobayashi K, Obata K, Cui X, Tominaga M & Noguchi K (2008). Phospholipase C and protein kinase A mediate bradykinin sensitization of TRPA1: a molecular mechanism of inflammatory pain. *Brain* 131, 1241-1251.

- Wang Q, Hogg RC & Large WA (1992). Properties of spontaneous inward currents recorded in smooth muscle cells isolated from the rabbit portal vein. *J Physiol* 451, 525-537.
- Wang YX & Kotlikoff MI (2000a). Signalling pathway for histamine activation of non-selective cation channels in equine tracheal myocytes. *J Physiol* 523.1, 131-138.
- Wang XY, Sanders KM & Ward SM (2000b). Relationship between interstitial cells of Cajal and enteric motor neurons in the murine proximal colon. *Cell Tissue Res* 302, 331-342.
- Ward SM, Burns AJ, Torihashi S & Sanders KM (1994). Mutation of the proto-oncogene c-kit blocks development of interstitial cells and electrical rhythmicity in murine intestine. *J Physiol* 480, 91-97.
- Ward SM, Dalziel HH, Thornbury KD, Westfall DP & Sanders KM (1992). Nonadrenergic, noncholinergic inhibition and rebound excitation in canine colon depend on nitric oxide. *Am J Physiol* 262, G237-243.
- Wegener JW, Schulla V, Koller A, Klugbauer N, Feil R & Hofmann F (2006). Control of intestinal motility by the Ca_v1.2 L-type calcium channel in mice. *FASEB J* 20, 1260-1262.
- Welsh DG, Morielli AD, Nelson MT & Brayden JE (2002). Transient Receptor Potential Channels Regulate Myogenic Tone of Resistance Arteries. *Circ Res* 90, 248-250.
- Wibberley A, Chen Z, Hu E, Hieble JP & Westfall TD (2003). Expression and functional role of Rho-kinase in rat urinary bladder smooth muscle. *Br J Pharmacol* 138, 757-766.
- Wood JD (2007). Neuropathophysiology of functional gastrointestinal disorders. *World J Gastroenterol* 13(9), 1313-1332.
- Wood JD (2006). Histamine, mast cells, and the enteric nervous system in the irritable bowel syndrome, enteritis, and food allergies. *Gut* 55, 445-447.
- Wood JD, Alpers DH & Andrews PLR (1999). Fundamentals of neurogastroenterology. *Gut* 45 (Suppl. 2), II6-II16.
- Xie H & He SH (2005). Roles of histamine and its receptors in allergic and inflammatory bowel diseases. *World J Gastroenterol* 11, 2851-2857.
- Yamada Y, Marshall S, Specian RD & Grisham MB (1992). A comparative analysis of two models of colitis in rats. *Gastroenterol* 102, 1524-1534.
- Yamamoto-Furusho JK (2007). Insights from advances in research of chemically induced experimental models of human inflammatory bowel disease. *World J Gastroenterol* 14, 5581-5593.
- Yamamoto S, Shimizu S, Klyonaka S, Takahashi N, Wajima T, Hara Y, Negoro T, Hiroi T, Kluchi Y, Okada T, Kaneko s, Lange I, Fleig A, Penner R, Nishi M, Takeshima H &

- Mori Y (2008). TRPM2-mediated Ca^{2+} influx induces chemokine production in monocytes that aggravates inflammatory neutrophil infiltration. *Nature Medicine* 14, 738–747.
- Yildirim E & Birnbaumer L (2007). TRPC2: molecular biology and functional importance. *Handb Exp Pharmacol* 179, 53-75.
- Yoshii A, Iizuka K, Dobashi K, Horie T, Harada T, Nakazawa T & Mori M (1999). Relaxation of Contracted Rabbit Tracheal and Human Bronchial Smooth Muscle by Y-27632 through Inhibition of Ca^{2+} sensitization. *Am J Respir Cell Mol Biol* 20, 1190-1200.
- Yuan XJ (1995). Voltage-Gated K^+ Currents Regulate Resting Membrane Potential and $[\text{Ca}^{2+}]_i$ in Pulmonary Arterial Myocytes. *Circulation* 77, 370-378.
- Zampeli E & Tiligada E (2009). The role of histamine H4 receptor in immune and inflammatory disorders. *Br J Pharmacol* 157, 24-33.
- Zhang Y, Hoon MA, Chandrashekar J, Mueller KL, Cook B, Wu D, Zuker CS & Ryba NJ (2003). Coding of sweet, bitter, and umami tastes: different receptor cells sharing similar signaling pathways. *Cell* 112, 293-301.
- Zhao P, Dong L, Luo JY, Guan HT, Ma H & Wang XQ (2009). Changes of mast cells and gut hormones in rats with TNBS-induced ulcerative colitis. *Nan Fang Yi Ke Da Xue Xue Bao* 29, 1359-1363.
- Zhuang L, Peng JB, Tou L, Takanaga H, Adam RM, Hediger MA & Freeman MR (2002). Calcium-selective ion channel, CaT1, is apically localized in gastrointestinal tract epithelia and is aberrantly expressed in human malignancies. *Lab Invest* 82, 1755-1764.
- Zholos A (2006). Regulation of TRP-like muscarinic cation current in gastrointestinal smooth muscle with special reference to PLC/InsP3/ Ca^{2+} system. *Acta Pharmacol Sin* 27, 833-842.
- Zholos AV & Bolton TB (1995). Effects of divalent cations on muscarinic receptor cationic current in smooth muscle from guinea-pig small intestine. *J Physiol* 486, 67-82.
- Zufall f (2005). The TRPC2 ion channel and pheromone sensing in the accessory olfactory system. *Naunyn-Schmiedeberg's Archives of Pharmacol* 371, 245-250.